Technical Report

TR-13-08

Flow modelling on the repository scale for the safety assessment SR-PSU

Elena Abarca, Andrés Idiart, Luis Manuel de Vries,
Orlando Silva, Jorge Molinero, Amphos[21] Consulting S.L.

Henrik von Schenck, Svensk Kärnbränslehantering AB

December 2013

Svensk Kärnbränslehantering AB
Swedish Nuclear Fuel
and Waste Management Co

Box 250, SE-101 24 Stockholm
Phone +46 8 459 84 00

SKB

ISSN 1404-0344
SKB TR-13-08
ID 1411922

Flow modelling on the repository scale for the safety assessment SR-PSU

Elena Abarca, Andrés Idiart, Luis Manuel de Vries,
Orlando Silva, Jorge Molinero, Amphos[21] Consulting S.L.

Henrik von Schenck, Svensk Kärnbränslehantering AB

December 2013

Summary

The present work is a part of the safety assessment SR-PSU and deals with the future hydrogeological conditions in the near-field of SFR 1 (the existing facility) and SFR3 (the planned extension). The term near-field refers to the rock vaults, their components and barriers, as well as the surrounding rock in the vicinity of the repository.

Three steady-state flow fields have been calculated from the regional hydrogeology model. The flow fields correspond to different positions of the repository relative to the shoreline of the Baltic Sea. At closure, the repository is submerged beneath the sea (shoreline position 1). After a thousand years the shoreline will be located above the repository due to land uplift (shoreline position 2). With the progression of land uplift the shoreline will retreat further and land conditions will dominate (shoreline position 3). The surface conditions above the repository will influence the magnitude and direction of the groundwater flow. The three stationary flow fields provide a representation of the time-evolution hydrogeology in the repository near-field. Additional calculation cases are presented that investigate change in flow through the repository caused by barrier degradation, different closure options, and permafrost. The calculated flow rates through the repository vaults and waste serves as input to the radionuclide transport modelling of the SR-PSU (SKB 2014a).

Sammanfattning

Följande arbete utgör en del av SR-PSU och behandlar framtida hydrogeologiska förhållanden i närfältet av SFR1 (existerande anläggning) och SFR3 (planerad utbyggnad). Med närfältet avses förvarssalarna med dess komponenter och barriärer samt berget i förvarets närhet.

Tre stationära flödesfält har beräknats utifrån den regionala hydrogeologimodellen. Flödesfälten svarar mot olika lägen som förvaret har i förhållande till Östersjöns strandlinje. Vid förslutning ligger förvaret under havet (strandlinje position 1). Efter tusen år ligger strandlinjen över förvaret på grund av landhöjning (strandlinje position 2). Strandlinjen förskjuts med vidare landhöjning så att landförhållanden efterhand blir dominerade (strandlinje position 3). Förhållanden som råder vid ytan ovan förvaret påverkar grundvattenströmningen till storlek och riktning. De tre stationära flödesfälten ger en bild av utvecklingen av hydrogeologin i förvarets närfält över tiden. Ytterligare beräkningsfall redovisas vilka undersöker förändring i flöden genom förvaret orsakat av degraderade barriärer, olika förslutningsalternativ och permafrost. Beräknade vattenflöden i förvarssalar och avfall utgör indata för modellering av radionuklidtransport inom SR-PSU (SKB 2014a).

Contents

1 Introduction and objectives 7

2 Methodology 9
2.1 Chain of models 9
2.1.1 Data handling 10
2.2 Computer codes and model interfaces 11
2.2.1 COMSOL Multiphysics 11
2.2.2 DarcyTools 11
2.2.3 Data Import Interface: iDC 11
2.2.4 Ecolego 11

3 Description of the repository scale model 13
3.1 The SFR 1 and the SFR 3 13
3.2 Representation of rock vaults 16
3.3 Partitioning of vaults for radionuclide transport simulations 19
3.4 Representation of tunnels 21
3.5 Initial state of the repository materials 22
3.6 Representation of the host rock 25
3.7 Overall mass conservation equation 27
3.8 Boundary conditions 27
3.9 Mesh 30

4 Model verification 35
4.1 Determination of the model size 35
4.2 DarcyTools-COMSOL Benchmark 37
4.2.1 Objectives and scope 37
4.2.2 Model set-up 38
4.2.3 Results of the comparison 39
4.2.4 Discussion and conclusions 41

5 Overview of calculation cases 43

6 SFR 1 Calculation cases 47
6.1 Base case: different shoreline positions 47
6.1.1 Shoreline position 1 48
6.1.2 Shoreline position 2 49
6.1.3 Shoreline position 3 50
6.1.4 Total flow through the vaults and waste 50
6.2 Barrier degradation 55
6.2.1 Concrete degradation 55
6.2.2 Plug degradation 62
6.2.3 No barriers 67
6.2.4 Ice lens 69
6.3 Repository closure 71
6.3.1 Effect of extended bentonite sections 71
6.3.2 Abandoned repository 78
6.4 Permafrost 81
6.5 Estimation of uncertainty associated with the geosphere 84
6.6 Summary of calculation cases 93

7 SFR 3 Calculation cases 97
7.1 Base case: different shoreline positions 97
7.1.1 Shoreline position 1 98
7.1.2 Shoreline position 2 98
7.1.3 Shoreline position 3 98
7.1.4 Total flow through the vaults 100

7.2 Barrier degradation 102
7.2.1 Concrete degradation 102
7.2.2 Plug degradation 106
7.2.3 No barriers 108
7.3 Repository closure 110
7.3.1 Abandoned repository 110
7.4 Permafrost 112
7.5 Estimation of uncertainty associated with the geosphere 115
7.6 Summary of calculation cases 120
8 Summary and Conclusions 123
References 127
Appendix A iDC interface 129
Appendix B Figures SFR 1 131
Appendix C Figures SFR 3 145

1 Introduction and objectives

The Swedish Nuclear Fuel and Waste Management Company (SKB) operates the repository for low- and intermediate-level nuclear waste (SFR) located in Forsmark. An extension of the SFR is planned to mainly accommodate waste arising from the decommissioning of Swedish nuclear power plants. The work presented here is a part of the long-term safety assessment for the SFR extension application, and concerns the future hydrogeological conditions in the near-field of the SFR 1 (the existing facility) and the SFR 3 (the planned extension). The term near-field refers to the engineered barrier system (EBS) components that are designed to contain the waste, and the host rock in the vicinity of the repository.

The present study has two main objectives. The first is to estimate groundwater flow rates in the repository under saturated and steady-state conditions. These flow rates serve as input to the radionuclide transport modelling (SKB 2014a), performed to show compliance with radiation safety regulations. The second objective is to deepen the system understanding of the SFR 1 and SFR 3 from a hydrogeological perspective, focusing on the effects of barrier degradation, closure alternatives, and permafrost. The influence of several representations of the rock permeability field on the groundwater flow has also been investigated. Knowledge gained allows for the evaluation of proposed engineering solutions with increased confidence.

The mathematical model, input parameters, and the geometries required to evaluate groundwater flow on repository scale (10^2 m scale) have been implemented and solved in the commercial finite element code COMSOL Multiphysics (COMSOL 2012a). The COMSOL user interface is well suited for working with detailed repository geometries. The software also provides the framework to couple mass transport and other physico-chemical processes to the flow within a single model. The COMSOL repository-scale model reads in the boundary conditions and rock hydraulic properties from the regional hydrogeological model set and solved in DarcyTools (Svensson and Ferry 2010) by means of a dedicated interface.

Once solved, the COMSOL repository-scale model produces tables of groundwater flow rates for specified control volumes representing different parts of the rock vaults and waste. These tables serve as input to the radionuclide transport model that is set up and solved in the commercial software Ecolego (SKB 2014b).

The SFR 1 and SFR 3 have been modeled separately. A base case has been defined for each model considering a reference description of the rock and hydraulic parameters representing the initial state of the repository. Three steady-state flow fields have been calculated from the regional hydrogeology model for each repository-scale model, representing three different positions of the shoreline relative to the repository: a case with the repository being submerged, a case with the shoreline passing over the repository, and a case where the repository footprint is well above the shoreline. In addition to the base case, a set of cases investigating different hydraulic properties of repository components have been simulated to assess the impact on groundwater flow in the repository.

2 Methodology

This work analyzes in a deterministic way the impact of the hydraulic behavior of the engineered barriers on the groundwater flow in the repository. The methodology is based on three dimensional finite element models of both the SFR 1 and SFR 3 facilities. The commercial software COMSOL Multiphysics is used for the simulations. In addition to the geometry of the repository, the models also include a volume of surrounding rock. This volume is chosen such that any change of hydraulic properties of the repository will leave the regional pressure field unaffected. The model for the regional hydrogeology is implemented in the DarcyTools code, which is then connected to the repository-scale model by means of a dedicated interface developed in this work.

The results of the repository-scale model in terms of groundwater flow rates within the repository are then used to calculate radionuclide transport. This is done using the commercial software Ecolego. Therefore, the calculated water flow rates in the COMSOL elements need to be transferred to the Ecolego model. In the following sections, this chain of models approach is described in more detail, together with a brief description of the different codes involved. The results presented in this report only include those obtained from the repository-scale model, i.e. groundwater flow in the near-field. The results from the regional scale model and radionuclide transport are reported in Odén et al. (2014) and SKB (2014a), respectively.

2.1 Chain of models

A schematic representation of the chain of models approach is presented in Figure 2-1. The DarcyTools model for the regional hydrogeology also contains the SFR repository. The COMSOL repository-scale model, however, represents the repository with increased geometric resolution (Figure 2-2) and a more detailed description of the hydraulic properties inside the rock vaults. Therefore, the flow field inside the rock vaults can be calculated in greater detail.

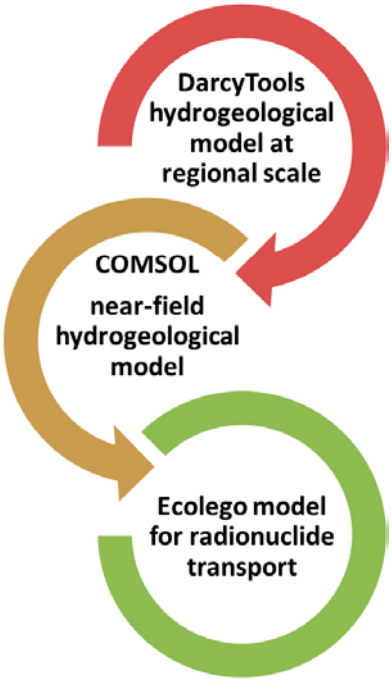

Figure 2-1. *Schematic representation of the chain of models approach.*

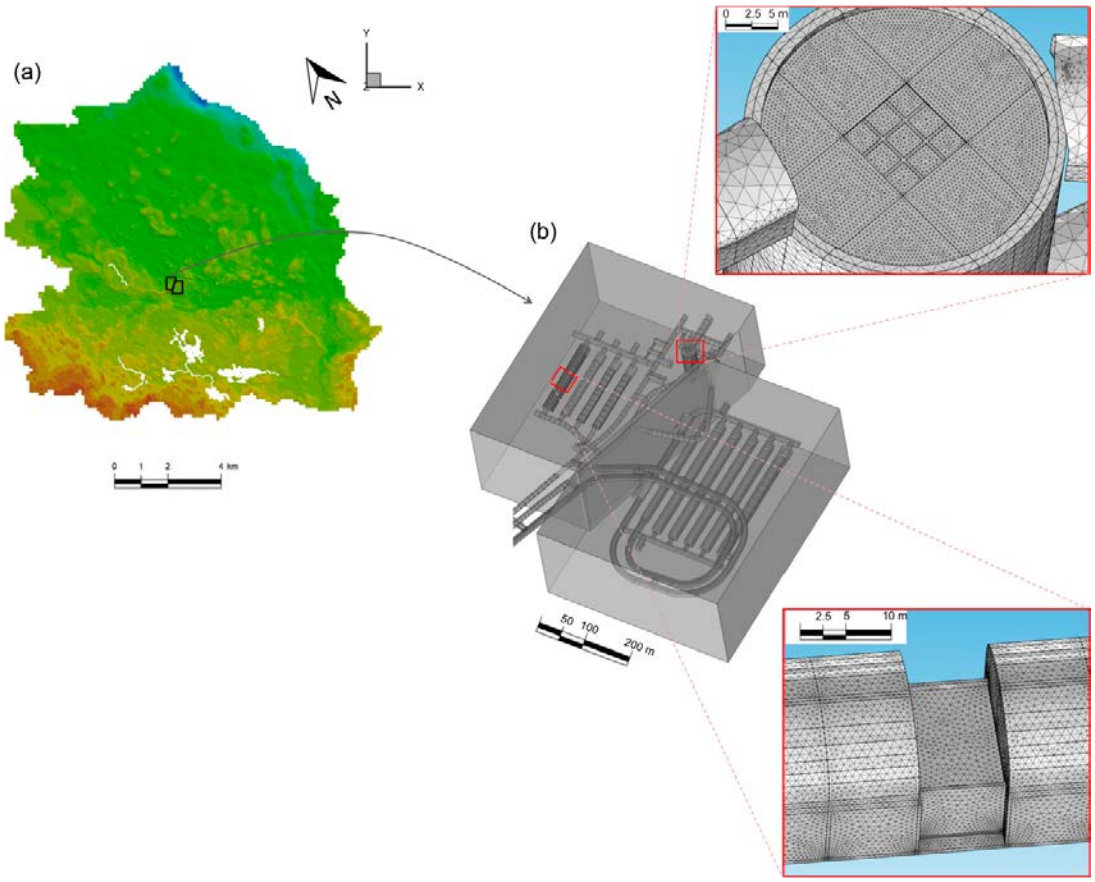

Figure 2-2. *(a) Regional-scale model domain (several km width) in DarcyTools and, in black, location of the repository-scale model domain (b) repository-scale domains (hundred m scale) and details of the meter scale structures within the vaults.*

The first step consists of importing the results of the larger DarcyTools domain into COMSOL. The necessary data for the flow simulations in the repository-scale model comprises driving pressure and flux boundary conditions, as well as the rock permeability field. This is a crucial step since consistency is required between the regional hydrogeology model and the repository scale model. Three states of the regional hydrogeology model, with different top boundary conditions, are selected as inputs to the repository-scale model, to represent the evolution of the near-field hydrology with time using steady-state simulations.

The second step is the simulation of the groundwater flow at the repository-scale using COMSOL. The model generates tables of water flow rates for predefined control volumes as part of the output. The flow rates are exported from COMSOL in a standardized way. Because of the large number of flow rates, files are generated using the COMSOL Java interface. The export files are then post-processed to convert the flow rates to a format suitable for Ecolego.

The last step of the chain of models approach involves the radionuclide transport calculations using the Ecolego code. To this end, Ecolego reads in the flow rate tables generated by the repository-scale model.

2.1.1 Data handling

The step of transferring data from the regional hydrogeological model in DarcyTools and the repository scale model in COMSOL is performed by means of a dedicated interface. The process is described in more detail in Section 2.2.3.

The data transfer from COMSOL to Ecolego is based on commonly defined control volumes. The partitioning of each vault into control volumes for Ecolego is described in detail in Section 3.2.1. This procedure results in a total of 280 control volumes used to calculate groundwater flow rates:

- 233 control volumes for SFR 1
- 47 control volumes for SFR 3

2.2 Computer codes and model interfaces

2.2.1 COMSOL Multiphysics

COMSOL Multiphysics is a powerful finite element software for the modelling and simulation of a large number of physics-based systems based on partial differential equations (PDE) and/or ordinary differential and algebraic equations (COMSOL 2012a). The main advantage over other codes is its ability to account for coupled multi-physics phenomena in a flexible way. The software furthermore offers interfacing to CAD software, technical computing software, and script programming in Java. In this work, the Subsurface Flow Module (COMSOL 2012b) has been used in addition to the base software package.

2.2.2 DarcyTools

DarcyTools (Svensson and Ferry 2010, Svensson 2010) is a computer code for simulation of flow and transport in porous and/or fractured media. In SR-PSU, the code was used to model the regional hydrogeology of the SFR area. The regional hydrogeology model provides boundary conditions as well as the rock permeability field to the repository-scale models. COMSOL accepts these inputs by means of a dedicated interface, developed as part of the present work (see Section 2.2.3).

2.2.3 Data Import Interface: iDC

The program connecting DarcyTools with COMSOL is called *iDC (interface DarcyTools to COMSOL)*. The program reads and interprets the following output files from the regional hydrogeology model:

ROF file

DarcyTools generates a Result Output File called ROF. In a ROF file, all data necessary to restart a computation are stored. Also intermediate data, for example a time series, can be stored.

XYZ file

In addition to the ROF file, a file containing the topological mesh information is needed to retrieve necessary data. This file is by default called xyz and is automatically generated by DarcyTools.

The program extracts the necessary information for the repository-scale model, and writes it to text files. These files can be read by COMSOL and used as interpolation function fields. The flowchart is described in Figure 2-3. For more information about iDC see Appendix A.

2.2.4 Ecolego

Ecolego is a software tool for creating compartment models (see example in Figure 2-4) and performing deterministic and probabilistic simulations, as well as sensitivity analysis. The graphical user interface of Ecolego allows the user to define a model as an interaction matrix in several hierarchical levels, which simplifies the handling of large complex models.

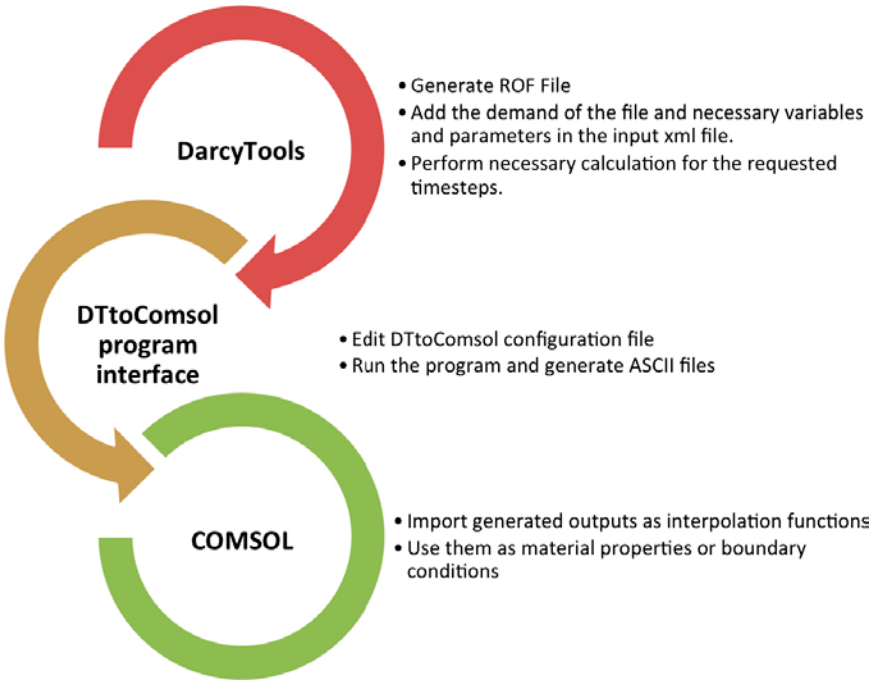

Figure 2-3. *Information flowchart between DarcyTools, iDC, and COMSOL.*

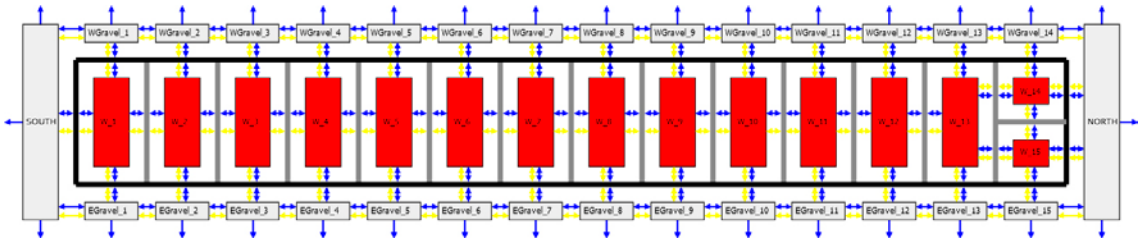

Figure 2-4. *Conceptual representation of the 1BMA vault: boxes represent model compartments and the arrows represent radionuclide fluxes calculated with transfer rate coefficients.*

3 Description of the repository scale model

The Forsmark facility for short-lived low- and intermediate-level nuclear waste, SFR, was commissioned in 1988. The rock vaults of the existing facility, SFR 1, are located around 60 m below the seabed and are accessed via an operational and a construction tunnel. The SFR extension (SFR 3) will be excavated, at a depth of around 120 m. A schematic view of the repository and its extension is shown in Figure 3-1.

3.1 The SFR 1 and the SFR 3

The hydrogeological interaction between the SFR 1 and SFR 3 is modest (SKBdoc 1395217). The two repository parts have therefore been treated in separate models in this work, as shown in Figure 3.3 and Figure 3.4. The rock volume surrounding a repository cavern has been chosen such that any change of hydraulic properties (inside the rock vaults) in the model will leave the regional pressure field unaffected. This is further explained in Section 4.1.

The model geometries are based on CAD data for the SFR 1 (SKBdoc 1428528)[1] and SFR 3 (SKBdoc 1428206, 1428207, 1428208)[2]. Dimensions of the vault structures in the repository are described in the Initial state report (SKB 2014c).

Figure 3-2 shows the CAD geometry imported in COMSOL of the whole repository, comprising SFR 1 (top-right of the figure), SFR 3 (bottom-left of the figure), and the corresponding access tunnels. SFR 1 is composed of four vaults (from top to bottom: 1BMA, 1BLA, 1BTF, and 2BTF) and a Silo. The SFR 3 will be composed of six vaults (from bottom to top): 2BMA, 2BLA, 3BLA, 4BLA, 5BLA, and BRT.

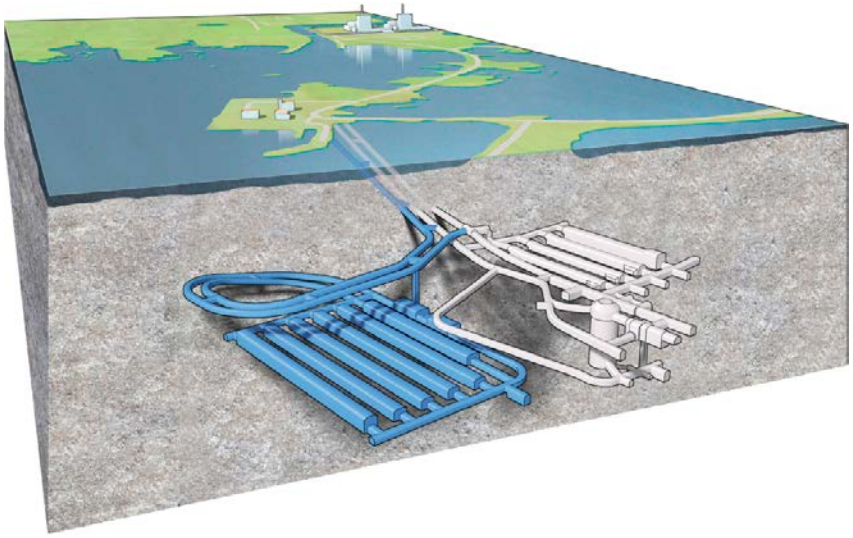

Figure 3-1. *Schematic view of the SFR repository in Forsmark: SFR 1 (gray) and SFR 3 (blue).*

[1] Internal document, Svensk Kärnbränslehantering AB.

[2] Internal document, Svensk Kärnbränslehantering AB.

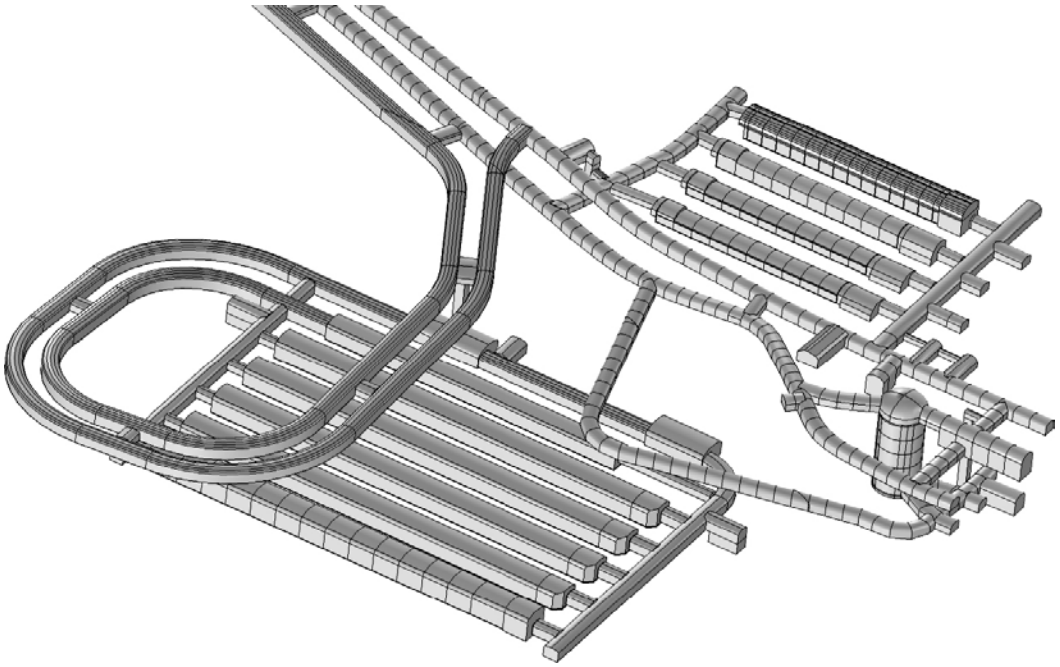

Figure 3-2. *Geometry of SFR 1 (on the right) and SFR 3 (on the left) from the CAD files as imported into COMSOL, and description of the different vaults.*

The dimensions and geometries of the SFR 1 and SFR 3 models are presented in Figure 3-3. The dimensions have been chosen after estimating the hydraulic radius of influence corresponding to extreme permeability changes within the repository (see Section 4.1). Figure 3-4 depicts the subdomains of the regional model that have been finally selected for SFR 1 and SFR 3 models to be implemented in COMSOL. The final SFR 1 repository-scale model domain, defined by the coordinates presented in Table 3-1, represents a repository footprint of 0.1523 km^2 and a volume of 0.03122 km^3. In turn, the SFR 3 model domain, which is defined by the coordinates in Table 3-2, presents a footprint of 0.1839 km^2 and a volume of 0.0377 km^3. The position and orientation are given in the reference coordinate system of the SDM-PSU Forsmark report (SKB 2013).

Table 3-1. Coordinates defining the SFR 1 COMSOL model domain (external box).

X (m)	Y (m)	Z_{max} (m)	Z_{min} (m)
6,625.00	10,335.00	–25	–230
6,625.00	10,271.00	–25	–230
6,496.12	9,850.00	–25	–230
6,255.00	9,850.00	–25	–230
6,255.00	10,335.00	–25	–230

Table 3-2. Coordinates defining the SFR 3 COMSOL model domain (external box).

X (m)	Y (m)	Z_{max} (m)	Z_{min} (m)
6,890.00	9,690.00	–25	–230
6,490.00	9,690.00	–25	–230
6,490.00	9,865.96	–25	–230
6,589.19	10,190.00	–25	–230
6,890.00	10,190.00	–25	–230

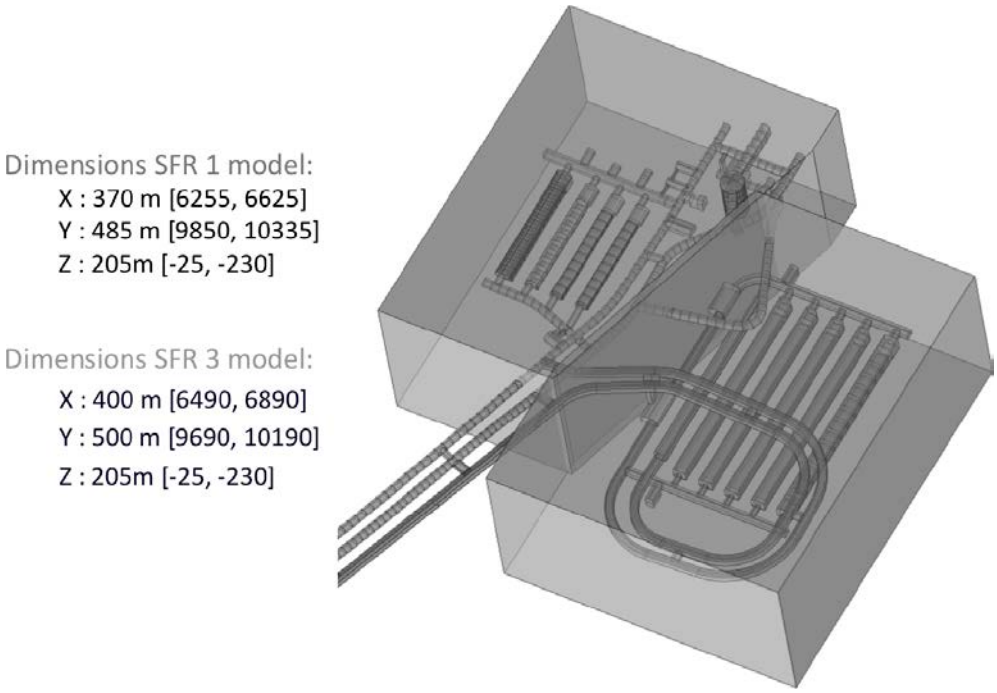

Figure 3-3. *3D view of geometries considered in the COMSOL simulations of the SFR 1 and SFR 3 repositories.*

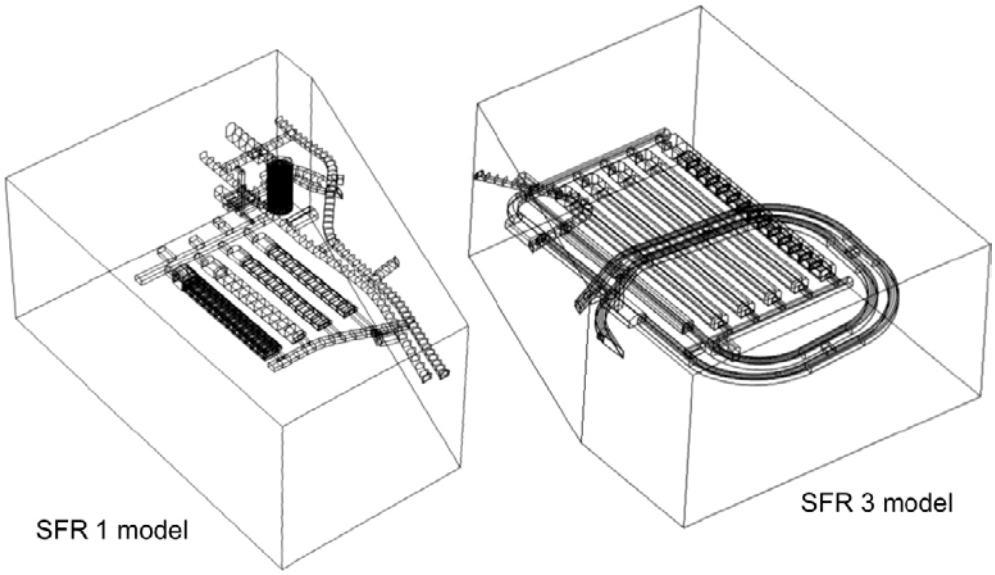

Figure 3-4. *3D view of individual subdomains considered in the simulations in COMSOL of the SFR 1 (left) and SFR 3 (right) repositories.*

The SFR repository receives waste packages from different sources, containing a variety of radioactive materials. Each vault contains different types of waste packages. The waste domain represented in the model geometries is resolved to the compartment level for the 1BMA and 2BMA vaults, and the shaft level for the Silo. In the cases of BTF vaults in SFR 1 and BLA vaults in SFR 1 and SFR 3, the waste domain is treated as homogeneous. The reasons of introducing these simplifications are based on (1) the complexity to implement the wide range of different waste types contained and geometric configuration, and (2) the uncertainty of the hydraulic properties of each waste type and the future evolution of the waste spatial distribution in the repository. This means that the hydraulic properties of a single compartment or shaft are constant. Moreover, it has been assumed that for each vault, all the waste compartments/shafts have the same hydraulic conductivity.

3.2 Representation of rock vaults

1BMA vault (Figure 3-5): The 1BMA is a rock vault for intermediate level waste. Constructed from reinforced concrete, the 1BMA is divided by inner walls into 13 main compartments and two auxiliary compartments. The structure is founded on a base of concrete beams. After the compartments are filled with waste packages, concrete lids are placed on top. At closure, the rock cavern will be filled with permeable backfill material. In the model the waste is treated as a homogeneous block and individual packages are not resolved in the geometry.

Silo (Figure 3-6): The Silo is a vertical deposition tunnel with a cylindrical shape. Inside the tunnel a cylindrical concrete structure is installed (encapsulation) where the waste is stored in vertical shafts. The encapsulation is completely surrounded by a bentonite barrier. The space between the dome ceiling and the bentonite top barrier is filled with a high permeability material.

1BTF and 2BTF vaults (Figure 3-7): The BTF tunnels contain mainly the de-watered low-level ion exchange resin in concrete tanks. A concrete radiation protection lid and a structural concrete lid are placed on top of the tanks. The space between tanks is filled with concrete and the space between the tanks and the rock walls will be filled with concrete backfill. This concrete construction forms the encapsulation of the BTF tunnels. The space above the encapsulation will be filled with gravel.

The two BTF vaults are treated identically in the repository-scale model. The waste domain is modeled as a homogeneous block.

1BLA vault (Figure 3-8): The 1BLA vault contains low level waste in standard steel containers, standing on a concrete floor cast on a layer of crushed rock. The waste is assumed to have the same hydraulic properties as the highly permeable backfill that fills the vault.

BRT vault (Figure 3-9): This vault will contain reactor pressure vessels from the nuclear power plants. The grouted waste of the BRT sits on a concrete floor cast on a layer of crushed rock. A homogeneous waste domain is considered, surrounded by backfill material on top and the sides.

2-5BLA vaults (Figure 3-10): The 2-5BLA vaults will contain low level waste in standard steel containers, standing on a concrete floor cast on a layer of crushed rock. The waste is assumed to have the same hydraulic properties as the highly permeable backfill that fills the vault.

2BMA vault (Figure 3-11): The 2BMA is a vault for intermediate level waste. It consists of fourteen separate concrete compartments placed directly on a floor of crushed rock. A highly permeable backfill completely surrounds each waste compartment. The waste inside each compartment is treated as a homogeneous block.

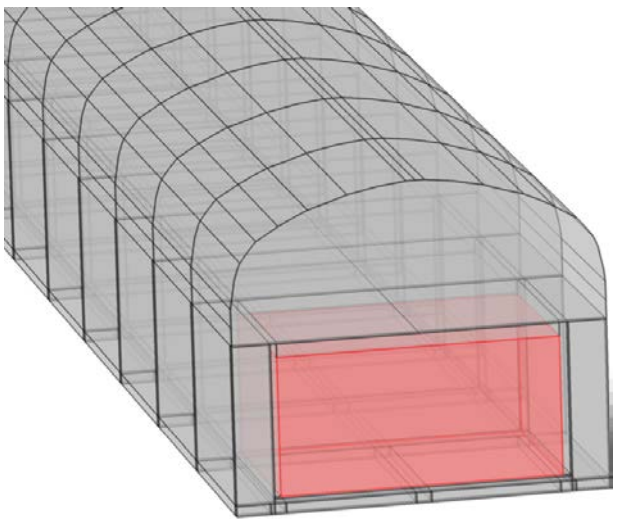

Figure 3-5. *Geometry of the 1BMA vault in the SFR 1 repository as implemented in the repository-scale model. The red volume corresponds to a waste compartment surrounded by concrete walls. The waste compartments are supported by longitudinal and transversal concrete beams embedded in a gravel layer (macadam).*

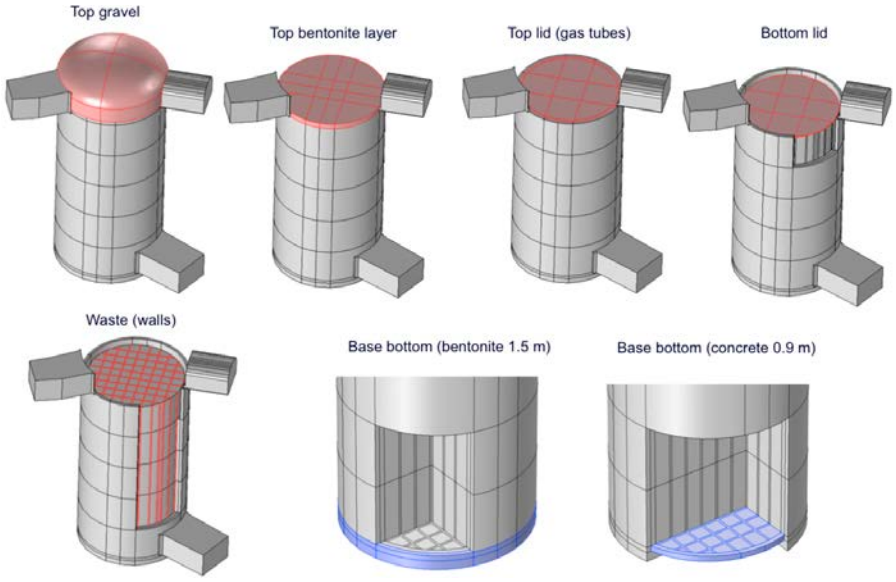

Figure 3-6. *Geometric representation of the different Silo materials in the repository-scale model, highlighted in red and blue.*

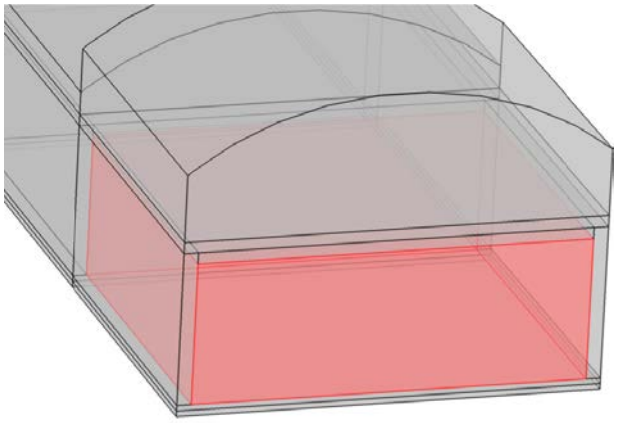

Figure 3-7. *Geometry of the 1BTF and BTF2 vaults in the SFR 1 repository-scale model. The red volume corresponds to the waste domain.*

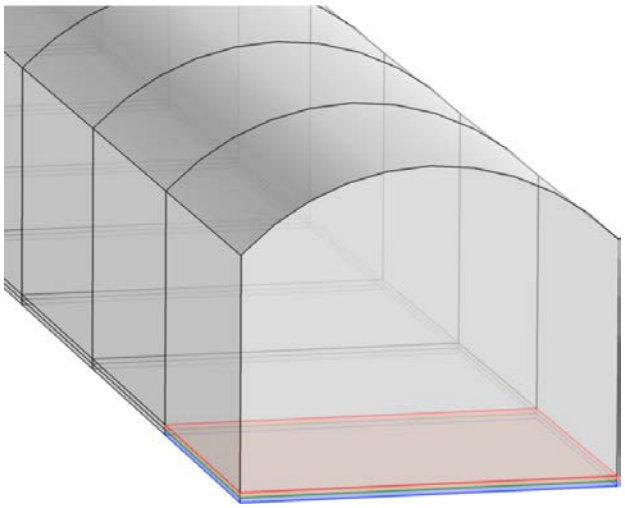

Figure 3-8. *Geometric representation of the 1BLA vaults materials in the repository-scale model showing the concrete floor (in red) and the crushed rock domain (in blue) beneath the waste domain.*

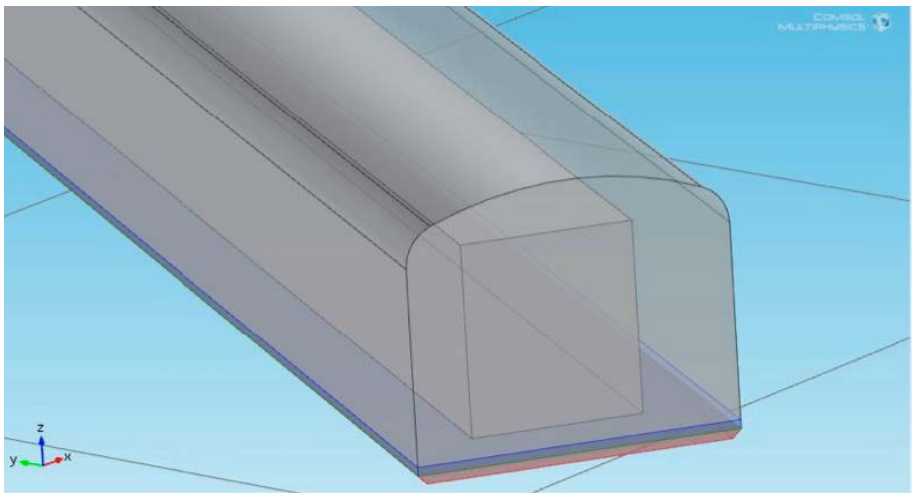

Figure 3-9. *Geometry of the BRT vault in the SFR 3 repository-scale model, showing the concrete floor (in blue) and the crushed rock domain (in red), as well as the waste domain surrounded by backfill.*

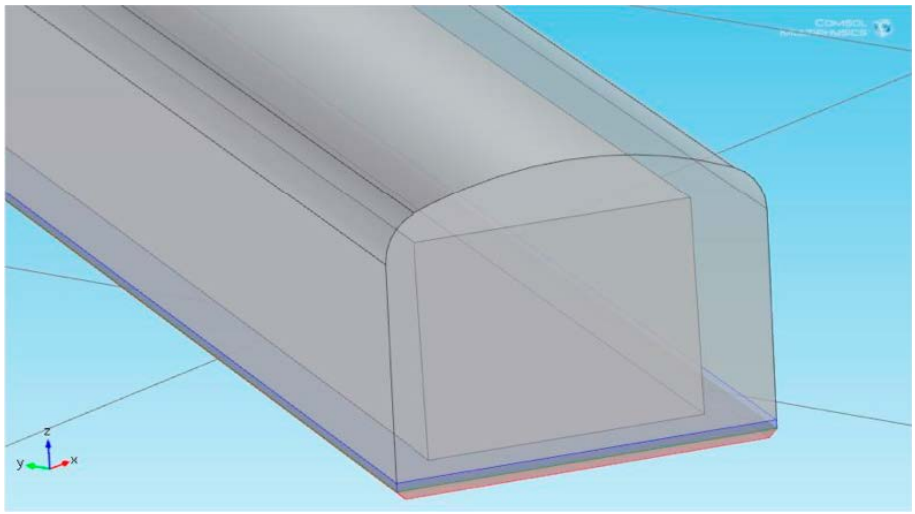

Figure 3-10. *Geometry of the BLA vaults in the SFR 3 repository-scale model.*

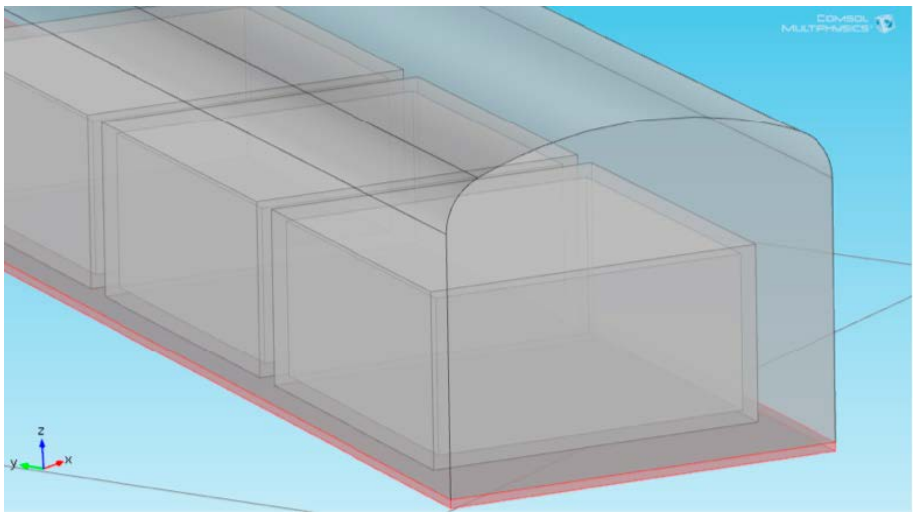

Figure 3-11. *Geometry of the 2BMA vault in the SFR 3 repository-scale model.*

3.3 Partitioning of vaults for radionuclide transport simulations

A shared discretization of the vaults for the groundwater flow and the radionuclide transport models has been used.

The following control volumes were implemented for the SFR 1 repository:

- The SFR 1 vault ends (loading areas) that are not part of the other control volumes are considered as separate control volumes for each tunnel. These control volumes are named south gravel and north gravel.
- 1BMA (see Figure 3-12):
  - Each of the 15 waste compartments is considered a control volume. These control volumes include the surrounding concrete barriers (i.e. concrete floor, walls and lids). Note that where a concrete wall is shared between two compartments, it is considered to be part of the southern control volume.
  - The volumes are numbered from 1 in the south to 15 in the north.
  - Around each waste control volume there are 4 gravel control volumes (top, bottom, east and west), with the exception of compartments 14 and 15 that lie in parallel.
- 1BTF and 2BTF (see Figure 3-13 right):
  - The BTF vaults follow the same control volume system as the 1BMA vault, although in this case there are only 10 waste control volumes in each vault.
  - In the BTF vaults the waste control volumes extend to the cavern wall, so there are no east or west gravel control volumes.
- 1BLA (see Figure 3-13 left):
  - Similar to the BTF vaults, the 1BLA is also divided into 10 control volumes.
  - Note that in the 1BLA vault the waste control volumes extend to the ceiling of the cavern, so that there are no top gravel control volumes.
- Silo (see Figure 3-14)
  - The Silo cylinder is divided into 5 waste sections, numbered from bottom to top. Each waste section is divided into 9 control volumes that group waste shafts (inner, x+, y+, x–, y–, x+y+, x–y–, x+y– and x–y+) (see Figure 3-14, to the right)
  - Under the waste sections there is a bottom bentonite control volume.
  - On top of the waste sections there is a top bentonite control volume.
  - Above the top bentonite control volume there is a top gravel control volume

For SFR 3 repository, the subdivision into control volumes is done in the following way:

- Each of the SFR 3 vault ends to the north are considered as a control volume (loading area)
- BRT (see Figure 3-15):
  - The entire waste storage domain is considered as 1 single control volume
  - Accordingly, the entire tunnel area is considered as 1 single control volume (backfill)
- 2–5BLA (see Figure 3-15):
  - Similar to the BRT the 2–5BLA vaults have 3 control volumes: waste, backfill and loading area.
- 2BMA (see Figure 3-16):
  - Each waste compartment is delimited by a concrete barrier on top, bottom, and lateral sides. These outer concrete walls define the waste control volumes. The waste control volumes are numbered from 1 in the south to 14 in the north.
  - There are also 14 control volumes (backfill) surrounding the waste control volumes. Note that unlike the 1BMA there are no concrete walls between the waste storage sections in this case. The limits of the backfill control volumes are chosen exactly in the middle of the two volumes (see Figure 3-16– on the right side). Because of this the size of backfill control volume 14 is slightly bigger.

The following conventions were agreed upon for naming the flows:

- The flows at the south side of the control volumes are indicated as y+,
- The flows at the north side of the control volumes are indicated as y–
- The flows at the west side of the control volumes are indicated as x+
- The flows at the east side of the control volumes are indicated as x–

Although the control volumes for the Silo do not line up completely with the north-south and east-west axes, the above naming scheme was applied here as well for simplicity.

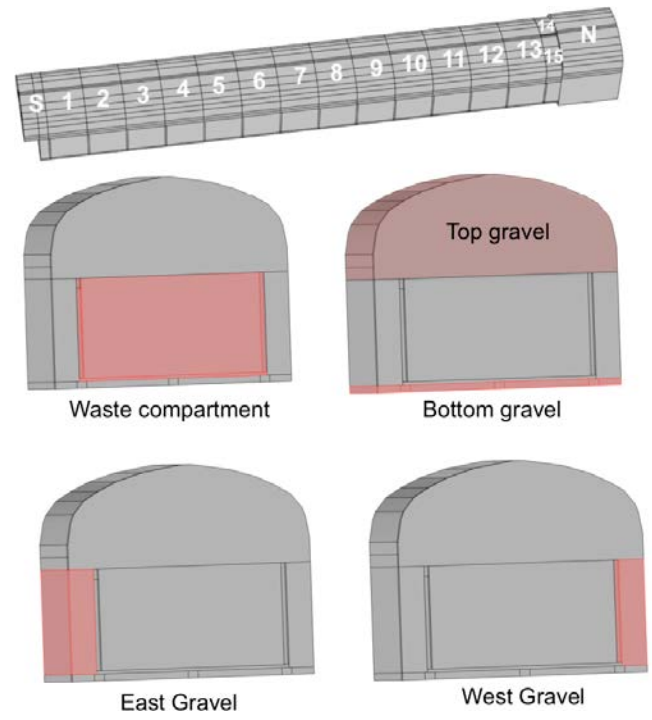

Figure 3-12. *Representation of 1BMA control volumes for Ecolego: slice (bottom) and numbering (top).*

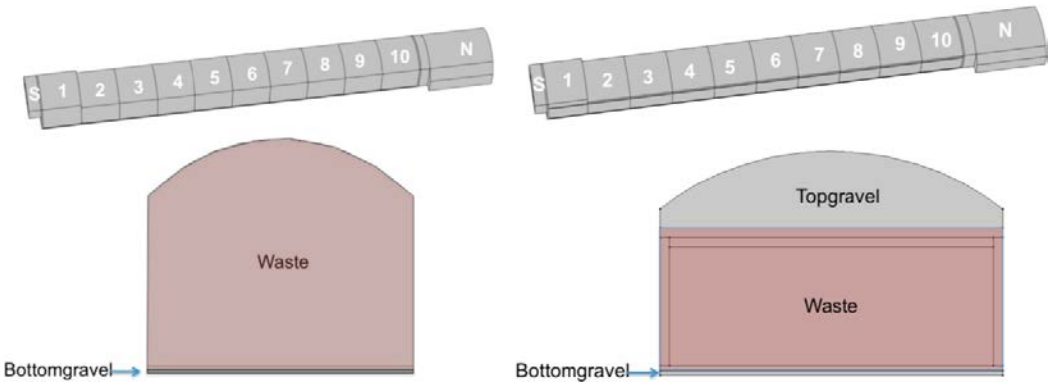

Figure 3-13. *Representation of 1BLA (left) and 1BTF and 2BTF (right) control volumes for Ecolego: cross-section (bottom) and numbering (top).*

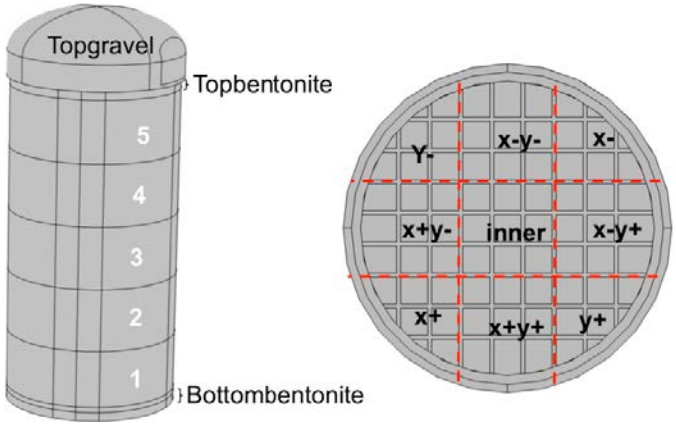

Figure 3-14. *Representation of the Silo control volumes for Ecolego: waste domain sectioning (left) and cross-section showing different control volumes and naming (right).*

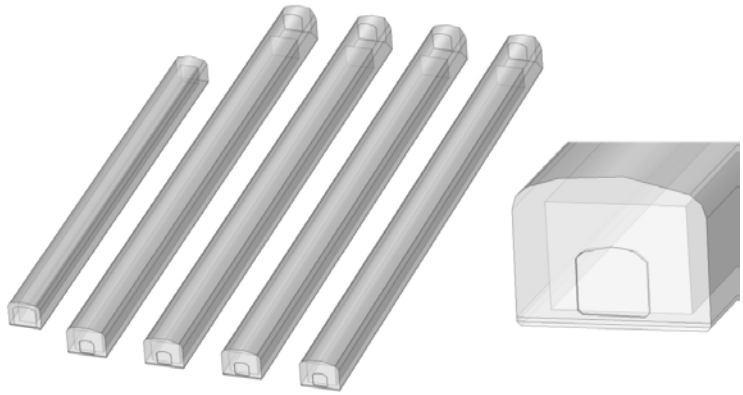

Figure 3-15. *Representation of control volumes of the SFR 3 repository. From felt to right: BRT, 2BLA, 3BLA, 4BLA and 5BLA control volumes for Ecolego, and detail of BLA geometry at the tunnel end.*

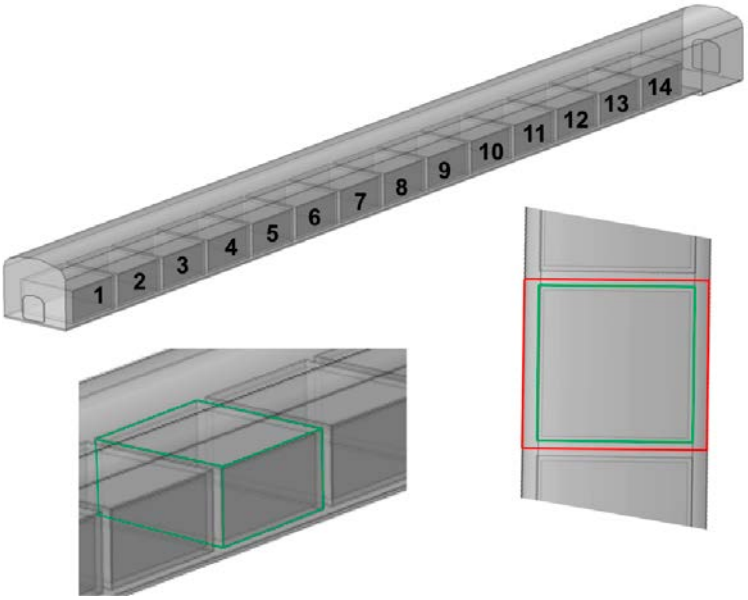

Figure 3-16. *Representation of 2BMA control volumes for Ecolego: numbering (top) and details of control volume definition (bottom). On the right, the green line delineates a waste control volume and the red line a gravel control volume.*

3.4 Representation of tunnels

The access ramps and tunnels were obtained directly from the CAD geometry (SKB 2013b, c). The closure of the repository has been implemented according to Luterkort et al. (2012). The spatial discretization and hydraulic conductivity of the tunnels and plugs for the SFR 1 and SFR 3 models is illustrated in Figure 3-17.

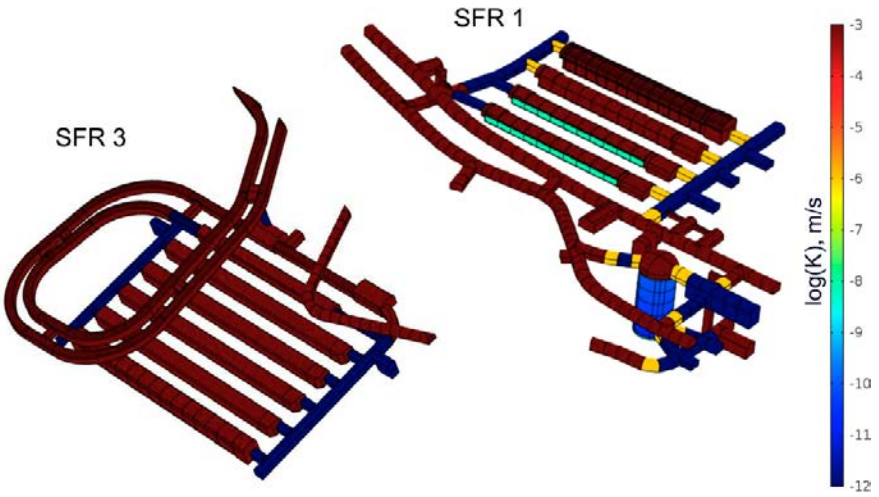

Figure 3-17. *Tunnel and plugs geometries and hydraulic conductivities for the SFR 1 and SFR 3 models.*

3.5 Initial state of the repository materials

The hydraulic conductivity for the materials in the vaults of the SFR 1 and SFR 3 repositories are described in Table 3-3 and Table 3-4, respectively and graphically in Figure 3-18 and Figure 3-19.

The hydraulic conductivity of the waste (K_{waste}, m/s) has been assigned considering the safety functions assumed for the waste packages and concrete structures of the repository. A safety function is a property by means of which a component contributes to the long-term safety of the repository. The concrete structures of the BMA vaults, the concrete tanks of the BTF vault, as well as the bentonite surrounding the silo, are considered to be flow barriers with the safety function to minimize advective flow. This safety function is not assigned to the waste packages, which are therefore not assumed to restrict groundwater flow. To represent these assumptions in the models the hydraulic conductivity of the waste has been set to a value 1,000 times greater than the hydraulic conductivity for the associated concrete structure ($K_{concrete}$, m/s). In the cases when concrete degradation is considered, this permeability ratio is also maintained. However, an upper limit for the hydraulic conductivity of the waste has been set to 1e–3 m/s, such that no hydraulic contrast exists in a vault when the concrete is assumed to be completely degraded.

$K_{waste} = 1E03 \cdot K_{concrete}$, with the constraint $K_{waste} \leq 1E{-}03$ m/s Equation 3-1

This relation is used for the 1BMA, the Silo, and 2BMA. In the case of the 1-2BTF vaults, the waste domain includes not only the waste material but also longitudinal and transverse concrete walls not geometrically discretized in the model. Thus, the hydraulic conductivity of the 1-2BTF waste domain depends on the hydraulic conductivity of both the waste and the concrete. The homogenized values of the hydraulic conductivities along the tunnel and perpendicular to the tunnels for the 1-2BTF waste domains were calculated based on the above assumption (Equation 3-1) and on the homogenization formulation proposed by Holmén and Stigsson (2001). In turn, in the 1BLA vault, a hydraulic conductivity equal to that of the backfill material (1.0E–03 m/s) is considered for the whole waste domain (no flow barriers are assumed for this vault).

For the concrete backfill located in the space between the waste and the rock walls in the 1-2BTF vaults, similarly to Holmén and Stigsson (2001), the following relation has been adopted:

$K_{grout} = 10 \cdot K_{concrete}$, with the constraint $K_{grout} \leq 1E{-}03$ m/s Equation 3-2

In the cases when concrete degradation is considered, this permeability ratio is also maintained.

An upper hydraulic conductivity limit of 1.0E–03 m/s has been adopted in the models. This value is assigned to the backfill domains, as well as for the completely degraded state of the different barriers (concrete, bentonite, etc.). This constraint is also considered in Equations 3-1 and 3-2.

Table 3-3. Hydraulic conductivity values for the materials in the SFR 1 repository considered in the Base Case.

Repository components	Materials		K (m/s)
Tunnels	Backfill		1.00E–03
Vaults	Construction concrete		8.30E–10
	Concrete Backfill (BTF vaults)		8.30E–09
	1BMA concrete beams		8.30E–10
	Waste 1-2BTF vaults	K_x*	3.79E–09
		K_y*	6.65E–09
		K_z*	6.79E–09
	Waste 1BLA		1.00E–03
	Waste (BMA)		8.30E–07
	Sand layer		1.00E–07
Silo	Top layer (90% sand, 10% bentonite)		1.00E–09
	Bottom layer (90% sand, 10% bentonite)		1.00E–09
	Waste		8.30E–07
	Silo concrete lid with gas evacuation pipes	K_x=K_y	8.30E–10
		K_z	3.00E–07
	Silo Bentonite Walls		1.54E–12·z(m) + 2.11E–10
Plugs	Structural plug		1.00E–06
	Sealed hydraulic bentonite section		1.00E–12

* homogenized values calculated with formulation in Appendix B of Holmén and Stigsson (2001), based on vault dimensions, configuration, and waste and concrete material properties

Table 3-4. Hydraulic conductivity values for the materials in the SFR 3 repository.

Materials	K (m/s)
Concrete	8.30E–10
Backfill	1.00E–03
BRT grouted waste	8.30E–09
2BMA waste	8.30E–07
Sand layer	1.00E–07
2BMA gravel layer	1.00E–03

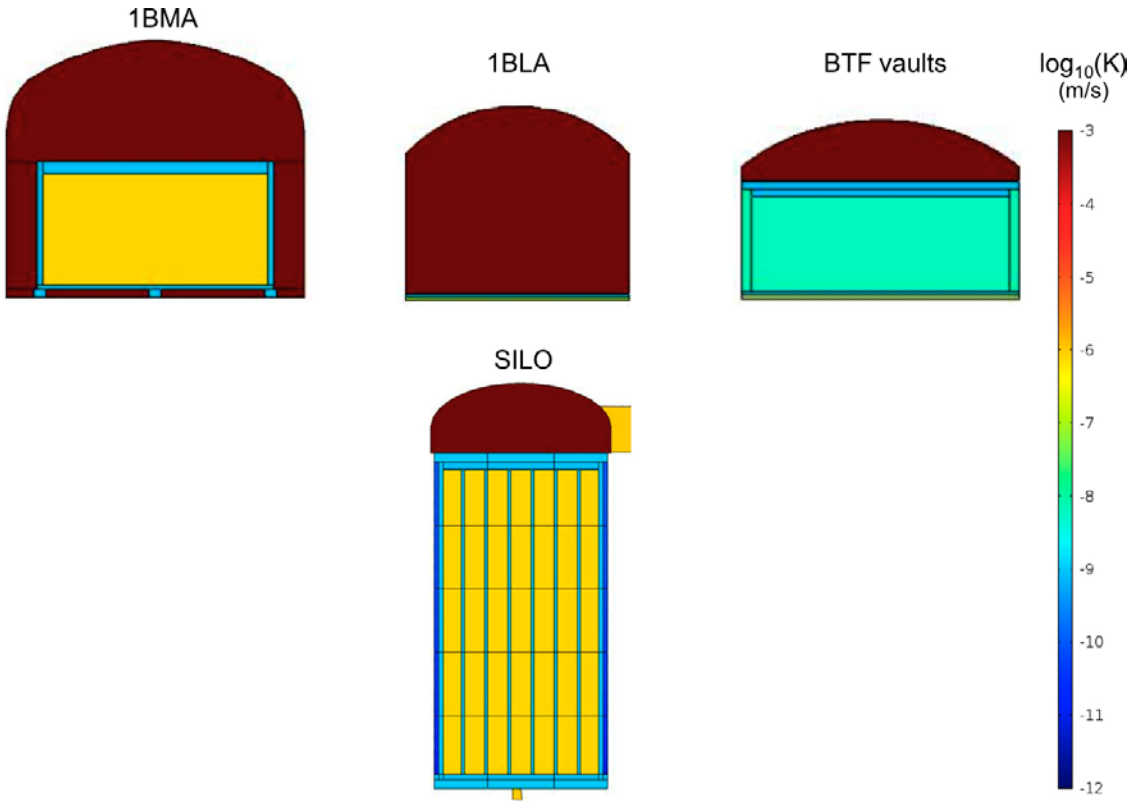

Figure 3-18. *Hydraulic conductivity parameterization for the SFR 1 vaults.*

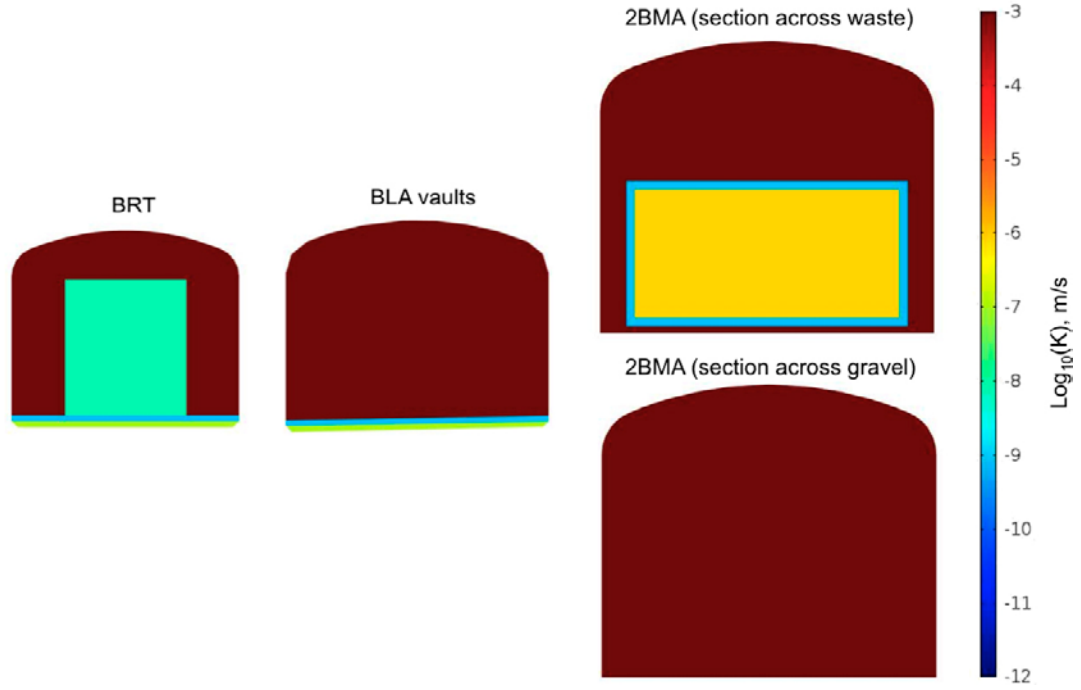

Figure 3-19. *Hydraulic conductivity parameterization for the SFR 3 vaults.*

A concrete lid will be placed on top of the shafts in the Silo. Within this lid, cylindrical gas evacuation pipes filled with sand will be added to facilitate gas release (one gas pipe with a diameter of 10 cm for each waste shaft has been assumed, which leads to a surface area of the pipes that is approximately 0.3% of the lid surface area). The initial state effective conductivity of the concrete lid in the z-direction is thus given by (assuming a conductivity of the sand of 1E–04 m/s)

$$K_z = 3E{-}03 \cdot K_{sand} + K_{concrete} \cong 3.00E{-}07 \qquad \text{Equation 3-3}$$

In the cases where concrete degradation is considered, the value of $K_{concrete}$ in the above expression is changed accordingly.

There is uncertainty associated with the effective permeability of the concrete beams/drainage system beneath the 1BMA concrete floor. The concrete beams can be degraded and the drainage system clogged. We consider, as initial state, a conservative case with a low effective conductivity of the beams/drains system equal to the structural concrete conductivity.

3.6 Representation of the host rock

The SFR repository is located in a fractured crystalline rock mass at Forsmark, Sweden. In this type of rock groundwater flow occurs mainly through a fracture network, with fractures and deformation zones of different size and transmissivity. This complex system determines the heterogeneity and anisotropy of the hydraulic properties of the rock mass. In the DarcyTools model of the geosphere, the implementation is based on the continuum approach. A discrete fracture network (DFN) is first generated taking into account field data. The most important features, such as large fracture zones, are defined deterministically in the model. Thereafter, the hydraulic properties of these structures are mapped onto a continuum representation of the domain. The non-structured grid in DarcyTools depends on the depth and the distance to the repository tunnels. More details on the rock mass representation in DarcyTools can be found in Öhman (2010).

In this work, the rock permeability field is extracted directly from the DarcyTools model for the regional hydrogeology by means of the iDC interface, and is then interpolated with a linear interpolation method in the COMSOL finite element mesh. The simulation data used corresponds to the Case 1 (Base_Case1_DFN_R85), which is presented in more detail in Odén et al. (2014). The hydrogeological model is based on the combined regional and local geological model version 1.0 (Curtis et al. 2011, SKB 2013a), containing all the modeled deformation zones (Figure 3-20). The SFR 1 and SFR 3 repositories are located in a tectonic wedge, denoted the “central block”, delimited by two broad belts of west-northwest (WNW) to north-east (NE) trending deformation zones. The main deformation structures have a WNW to NE trend. Within the model domains lay the vertical deformation zone ZFMNNW1209 (former zone 6), which crosses the SFR 1 repository, and the zones ZFMWNN0835 and ZFMWNW8042, which cross the SFR 3 vaults. Also, a thinner and shorter NE to ENE striking set of brittle deformation zones is present. Among those are the deformation zones ZFMNNE0869 (former Zone 3) and the ZFMNE0870 (former Zone 9) which intersect the model domains. ZFM871 (former Zone H2) is a gently dipping zone that intersects the SFR 1 model domain without reaching the ground surface. In the rock volume for the SFR 3, no sub-horizontal deformation zone is identified.

The anisotropic hydraulic conductivity field of the rock is extracted from the DarcyTools input files before the tunnels are implemented. In this way, the effect on the hydraulic conductivity around the tunnels of any small discrepancy between the discretization of the tunnels in DarcyTools (with cubic finite volumes) and in COMSOL (tetrahedral finite elements adjusting to curved domains) is eliminated. A Java script extracts the hydraulic conductivity field of the rock of a subsection of the DarcyTools model domain. This subsection is slightly larger than the repository-scale model domain to avoid interpolation artifacts at the repository-scale model boundaries. The coordinates in Table 3-5 define the extracted box for the SFR 1 and SFR 3 models. Some characteristic values of the rock conductivity field are presented in Table 3-6. The volume-averaged hydraulic conductivity of the rock is of the order of 1.5E–7 in the three spatial directions.

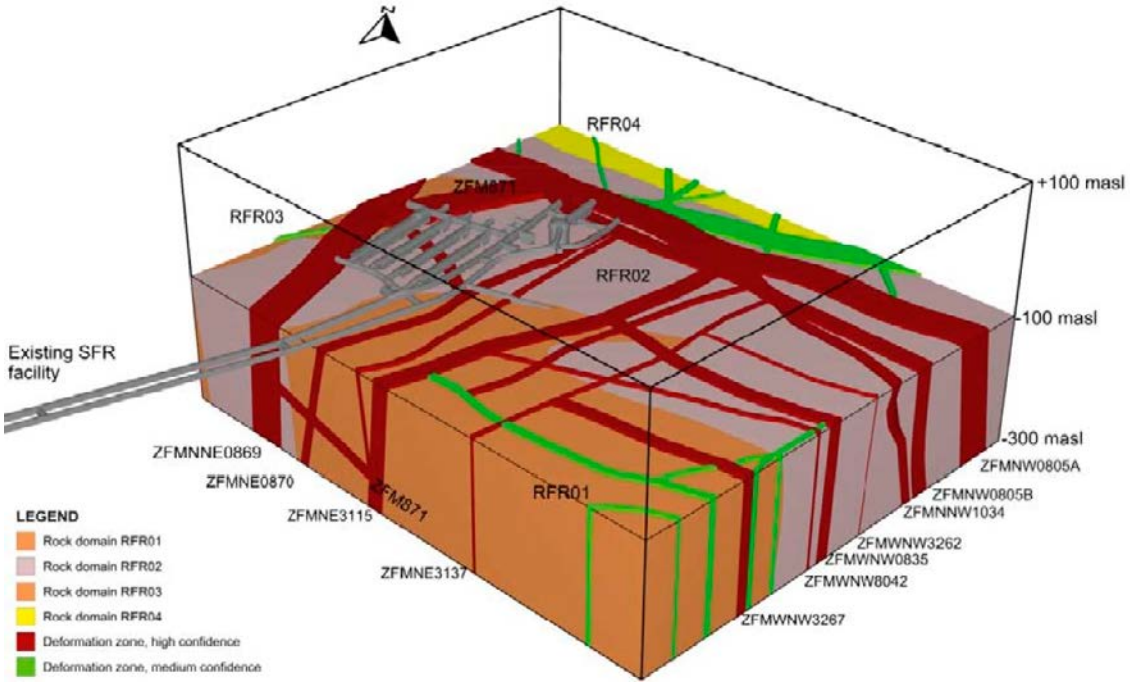

Figure 3-20. *Rock domains and deformation zones included in the SFR local model, version 1.0 Adapted from Curtis et al. (2011).*

Table 3-5. Coordinates of the data extracted from the DarcyTools model for the SFR 1 and SFR 3 repository-scale models. The ranges are slightly larger than the repository-scale model domains to avoid interpolation artifacts at the model boundaries.

	SFR 1		SFR 3	
Coordinate	Minimum (m)	Maximum (m)	Minimum (m)	Maximum (m)
X	6,100	6,700	6,400	7,000
Y	9,800	10,400	9,250	10,250
Z	–250	–20	–250	–20

Table 3-6. Characteristics values of the rock conductivity field (Base_Case1_DFN_R85) within the local model domains.

	Kx (m/s)	Ky (m/s)	Kz (m/s)
Volume averaged	1.57E–07	1.55E–07	1.44E–07
Minimum	3.00E–11	3.00E–11	3.00E–11
Maximum	1.06E–05	1.07E–05	1.06E–05

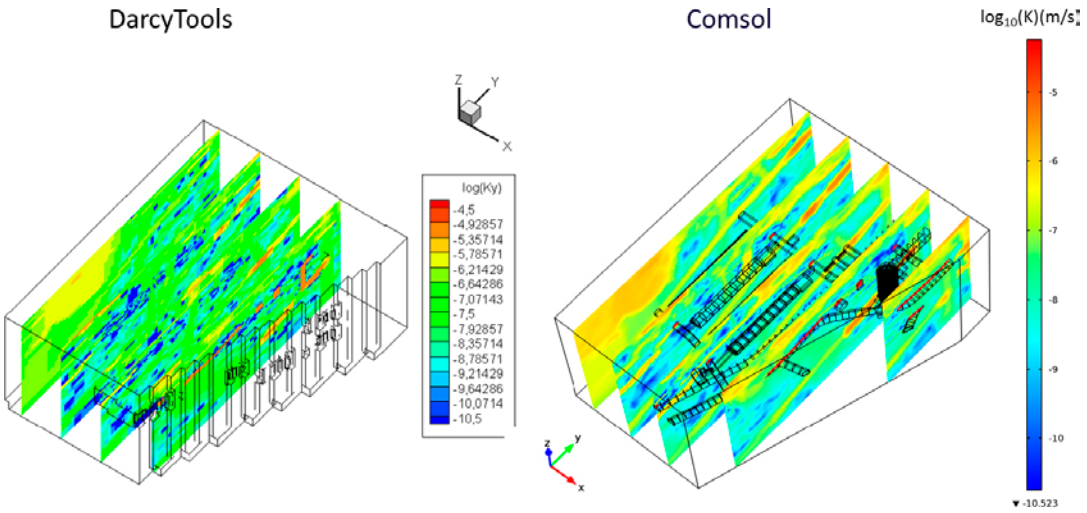

Figure 3-21. *Rock hydraulic conductivity field represented in yz planes in the DarcyTools (left) and the COMSOL (right) models.*

3.7 Overall mass conservation equation

The repository models have been implemented using the Subsurface Flow Module of COMSOL Multiphysics (COMSOL 2012b), which is tailored for modelling groundwater flow in fractured and porous media. The overall conservation of mass constitutes the main governing equation involved in this study, and is given by

$$\partial(\rho\phi)/\partial t = -\nabla\cdot(\rho q) + Q \qquad \text{Equation 3-4}$$

Above, q is the Darcy velocity (m/s), ρ the water density (kg/m^3), ϕ the porosity of the media (–) and Q represents a sink/source term (m^3/s). In turn, the Darcy velocity can be expressed as

$$q = -k/\mu\,(\nabla p) \qquad \text{Equation 3-5}$$

where p is the driving pressure (Pa), defined as the difference between the liquid pressure and the hydrostatic contribution (ρ·g·z, with g = –9.81 m/s^2 and z the elevation (negative in the present model), k is the rock permeability (m^2) and μ the dynamic viscosity (Pa·s).

In this work, all the simulations are performed under steady-state conditions, so that the time derivative is equal to zero. Furthermore, constant water density is assumed and no sink/source terms are expected in the domain. As a result, Equation 3-4 reduces to its divergence free form:

$$\nabla\cdot q = 0 \qquad \text{Equation 3-6}$$

3.8 Boundary conditions

Driving pressure and groundwater velocities from the regional hydrogeological simulations are extracted by means of the iDC interface and used as boundary conditions for the repository-scale model. Again, this box is larger than the repository-scale model domain to avoid interpolation artifacts near the boundaries. A linear interpolation function onto the domain mesh is used to impose the boundary conditions in COMSOL. A combination of boundary conditions was used in both the SFR 1 and SFR 3 models. A pressure field was specified on the surfaces corresponding to rock material. In addition, flux boundary conditions were specified where access tunnels intersect the model boundary. This ensures consistency with the DarcyTools fluxes to the repository when modifying the permeability of the materials filling the access tunnels. Both the pressure field and the Darcy velocity fields used as boundary conditions come from the same solution of the regional-scale model. Therefore, they are consistent in the intersection. The groundwater flow though the access ramp is limited by the groundwater divide upstream of the repository (Holmén and Stigsson 2001). It is not expected to change as function of state of the plugs in the access ramp nor due to changes in the properties of the repository materials.

Three different descriptions of the top boundary in DarcyTools serve as input to produce the boundary conditions for the repository-scale models. These descriptions outline the time-evolution of the groundwater flow and correspond to three different positions of the repository relative to the shoreline of the sea:

- Shoreline position 1 corresponds to a submerged repository.
- Shoreline position 2 corresponds to shoreline dominating conditions above the repository.
- Shoreline position 3 corresponds to land dominating conditions above the repository.

The different shoreline positions are illustrated in Figure 3-22 below, and are further described in the Climate report (SKB 2014d).

In the SFR 1 domain (Figure 3-23), the driving pressure gradient for the shoreline position 1 indicates an upward vertical groundwater flow in the repository area. The driving pressure fields for the shoreline position 2 and shoreline position 3 show a downward vertical flow south of the repository and a vertical upwards flow north of the repository. The recharge area is located above the entire repository. The main difference between shoreline position 2 and shoreline position 3 is that the gradient is larger in the latter. The driving pressure gradient for the shoreline position 1, and therefore the regional groundwater flow, is two orders of magnitude smaller than the other two cases.

The driving pressure at the SFR 3 model boundaries (Figure 3-24) indicates the groundwater flow direction in the SFR 3 surroundings for the three different shoreline positions. Pressure decreases upwards from the bottom south-east corner to top north-west boundary in the shoreline position 1. In the shoreline position 2, the highest pressures occur in the upper boundary over the south-east part of the SFR 3 repository and decrease towards the bottom, north of the repository. In this case, the pressure gradient indicates vertical downward flow affecting the SFR 3 repository. The driving pressure gradient increases for shoreline position 3 and maintains the main downwards component of the groundwater flow.

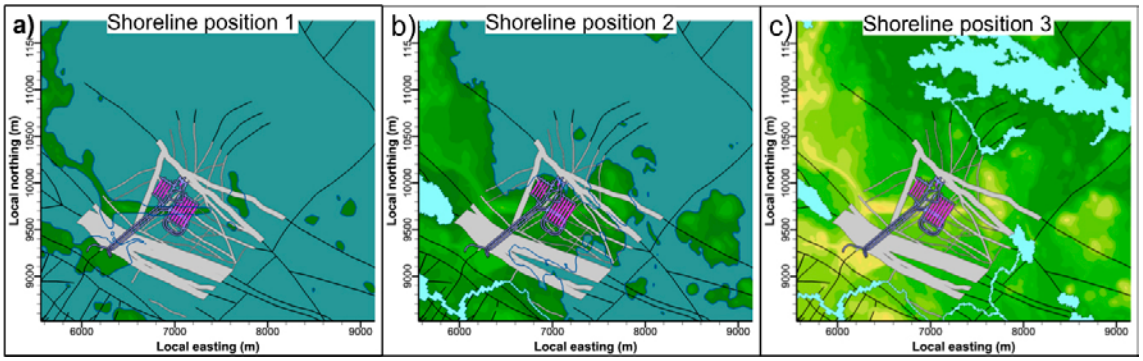

Figure 3-22. *Shoreline positions with respect to the SFR repository used as boundary conditions for the three regional hydrological simulations.*

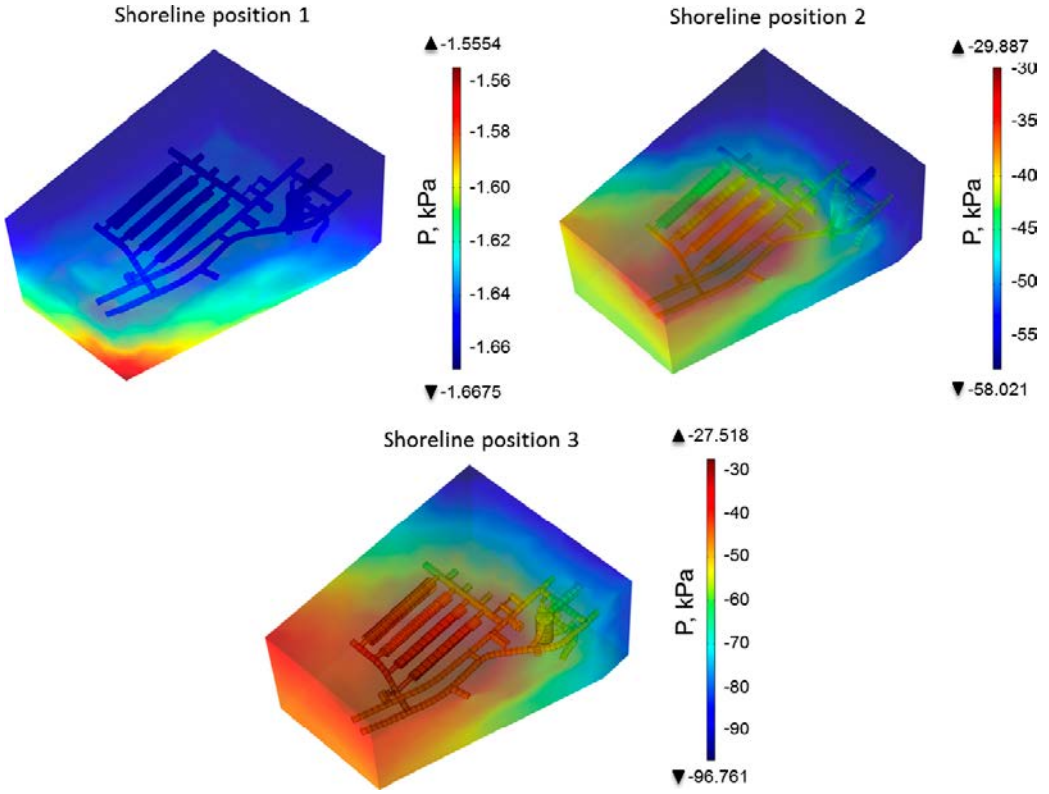

Figure 3-23. *Driving pressure field (P-ρ·g·z) in the repository-scale SFR 1 model for the three shoreline positions for the Base case.*

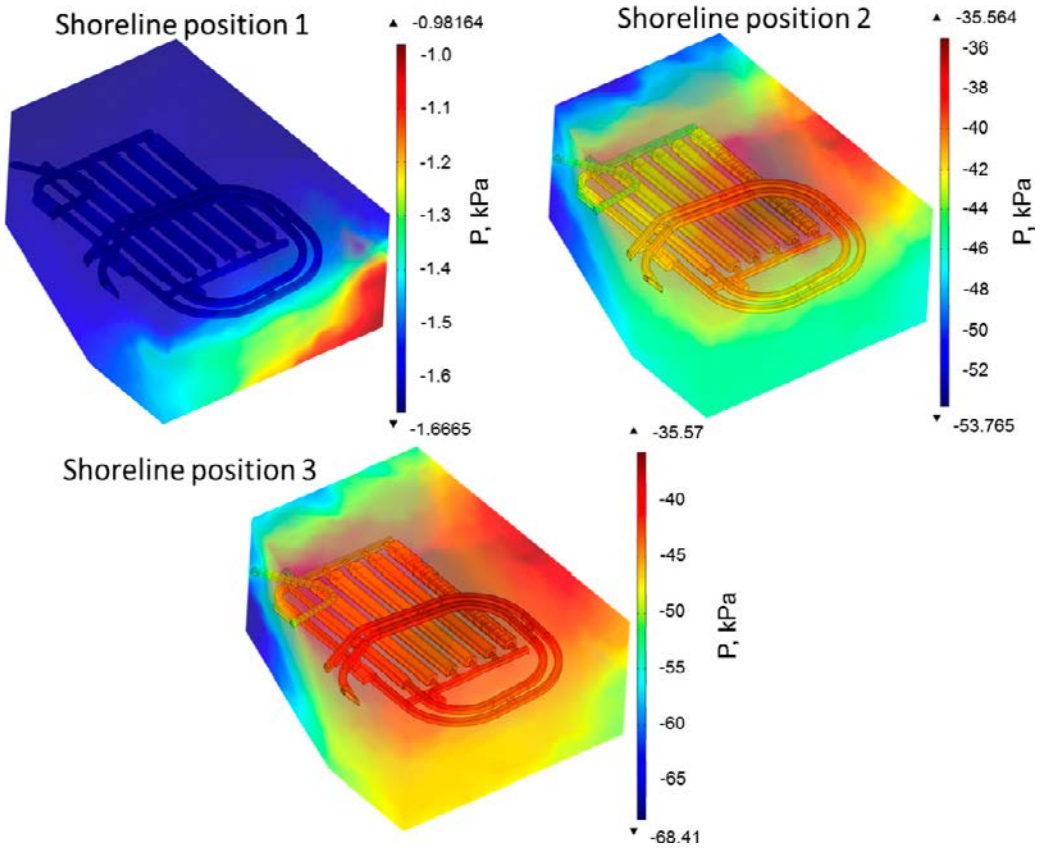

Figure 3-24. *Driving pressure field (P– ρ·g·z) in the repository-scale SFR 3 model for the Base case and the three shoreline positions.*

3.9 Mesh

The SFR 1 domain was discretized into a mesh consisting of 10,748,580 tetrahedral quadratic finite elements (14,380,723 degrees of freedom) whereas the SFR 3 domain is discretized in 11,548,320 tetrahedral quadratic elements (15,435,799 degrees of freedom). The meshes of both models are depicted in Figure 3-25. A detailed view of the mesh of the SFR 1 vaults and access tunnels is presented in Figure 3-26. Zoom-in views of the mesh of the waste compartments of the 1BMA, 1–2BTF vaults and the waste shafts of the Silo are presented in Figure 3-27, Figure 3-28 and Figure 3-29, respectively.

The average grid size of the DarcyTools model and the local model are very similar at the vicinity of local model boundaries where the transfer from the regional model and the local model takes place. There, the DarcyTools grid is $8\times8\times8$ m^3 in average, with larger elements at the bottom boundary ($16\times16\times16$ m^3) and more refined parts near the tunnels ($2\times2\times2$ m^3). The irregular mesh of tetrahedral of the local model has a defined maximum size of 9 m. Therefore, the size of the elements at the boundaries are around 9 m in the least refined areas and very refined near the intersection with the access tunnels.

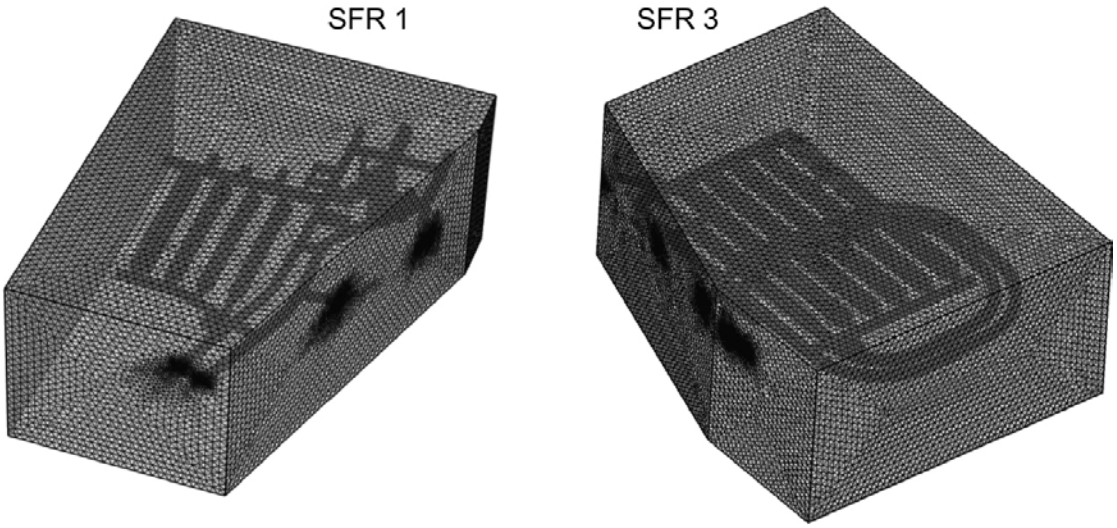

Figure 3-25. *Three-dimensional finite element meshes (tetrahedral) of the SFR 1 (left, 10,748,580 elements) and SFR 3 (right, 11,548,320 elements) repository-scale models.*

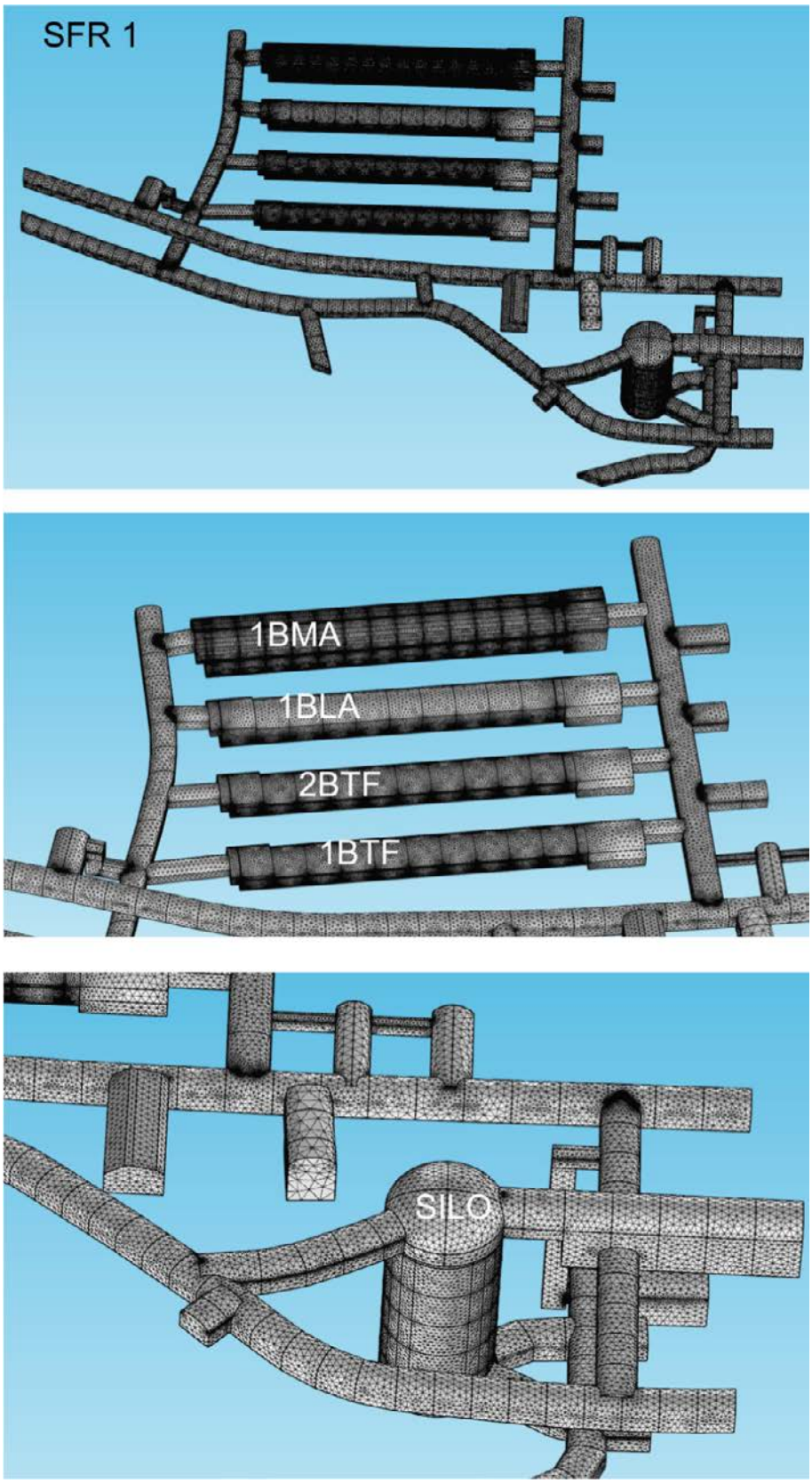

Figure 3-26. *Finite element mesh of the SFR 1 vaults, Silo, and access tunnels.*

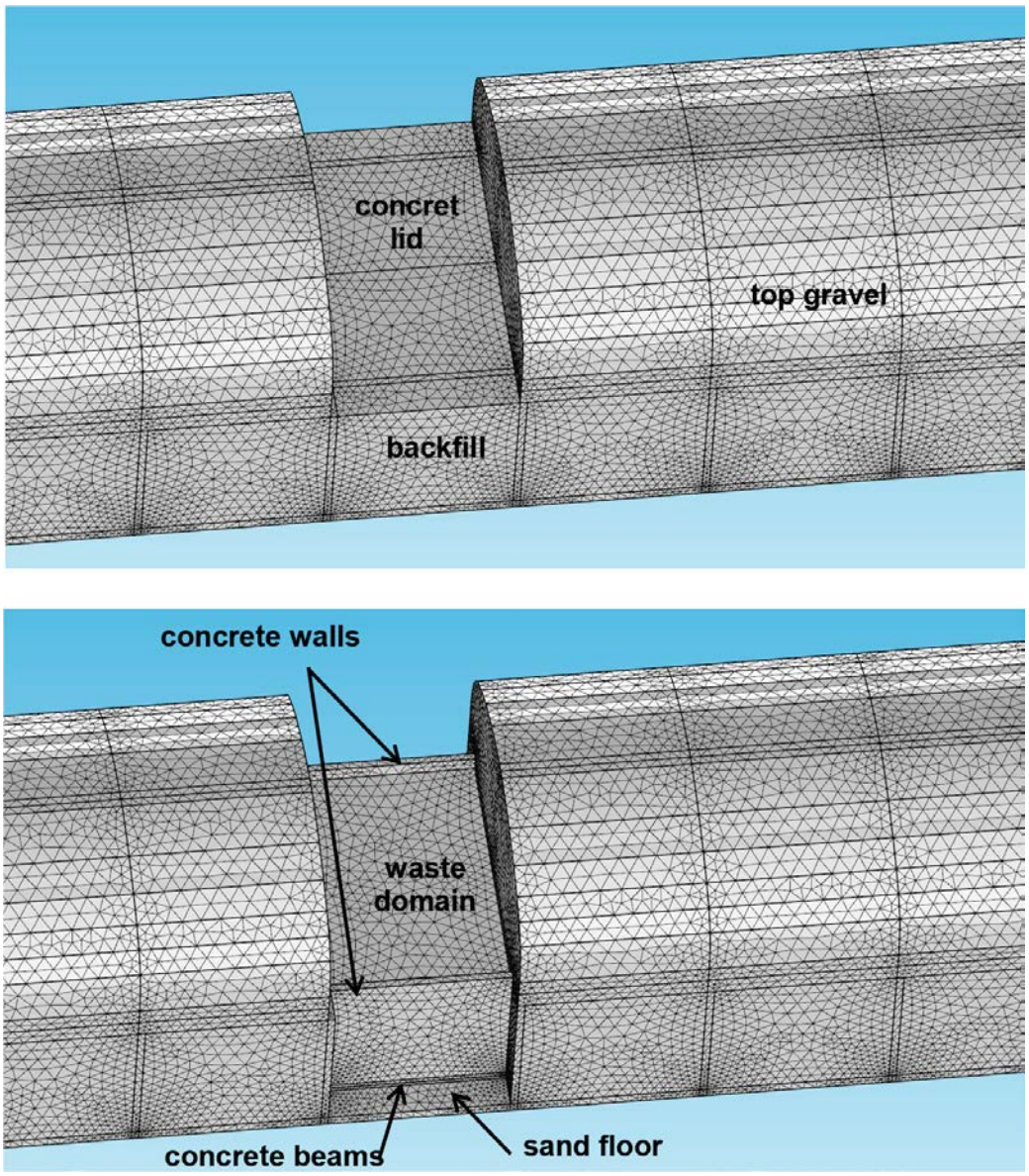

Figure 3-27. *Detailed finite element mesh of the 1BMA compartments.*

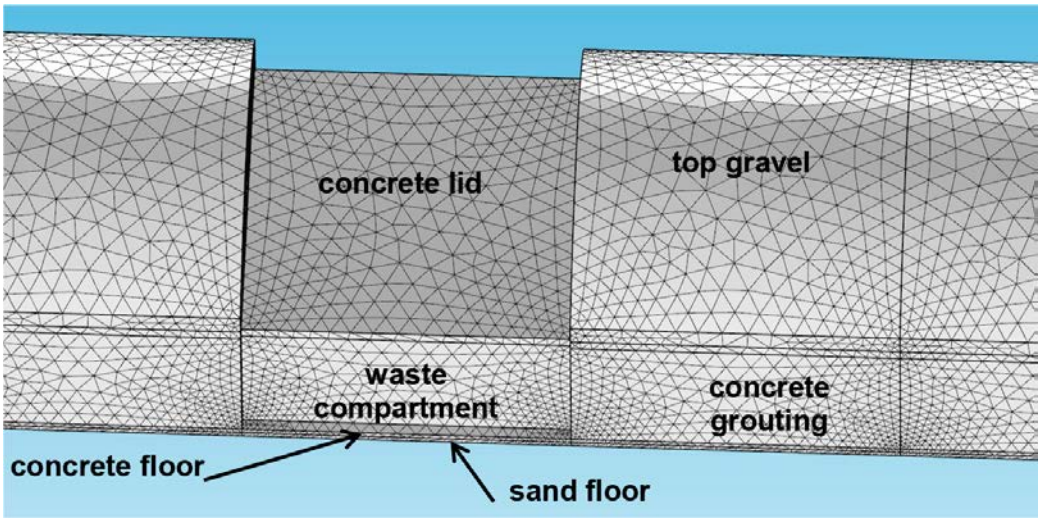

Figure 3-28. *Detailed finite element mesh of the compartments of the 1–2BTF vaults.*

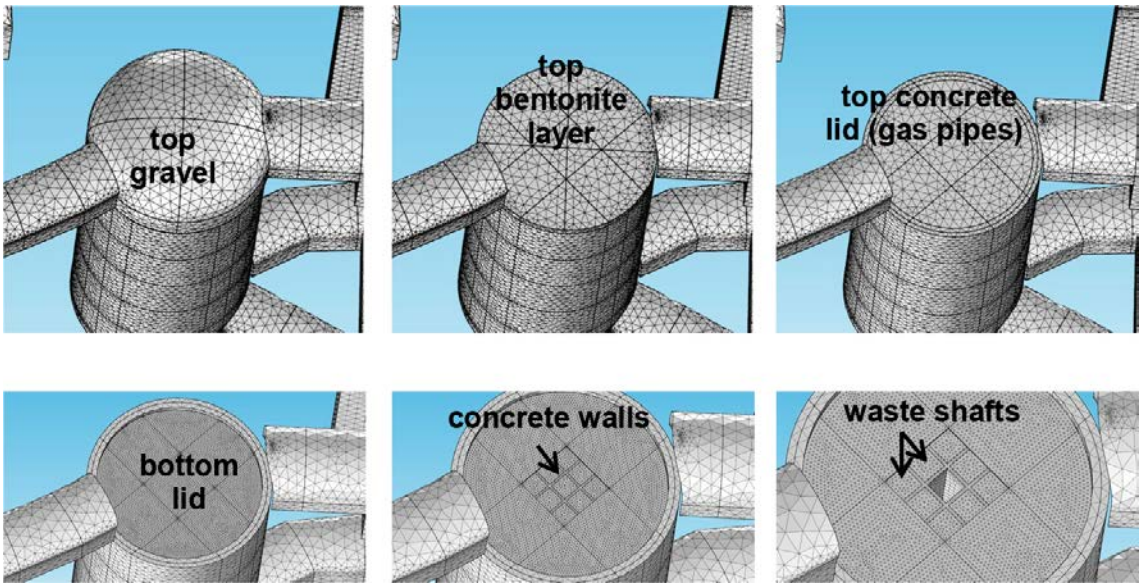

Figure 3-29. *Detailed finite element mesh of the Silo.*

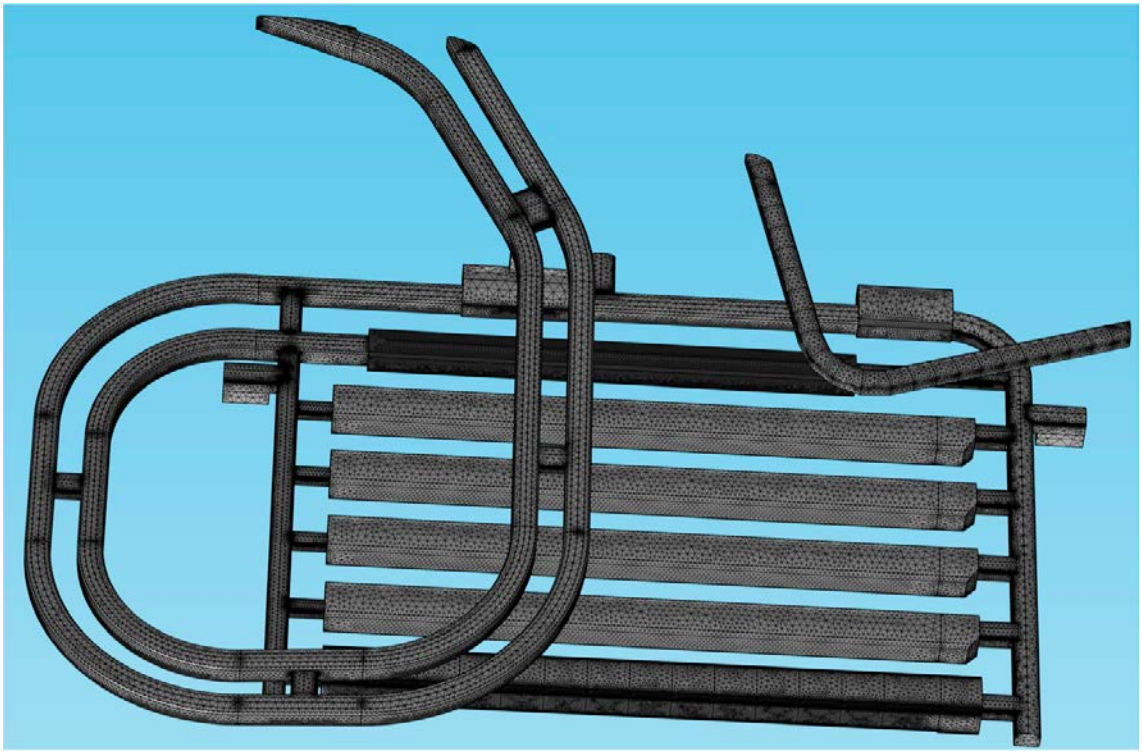

Figure 3-30. *Finite element mesh of the SFR 3 vaults and access tunnels.*

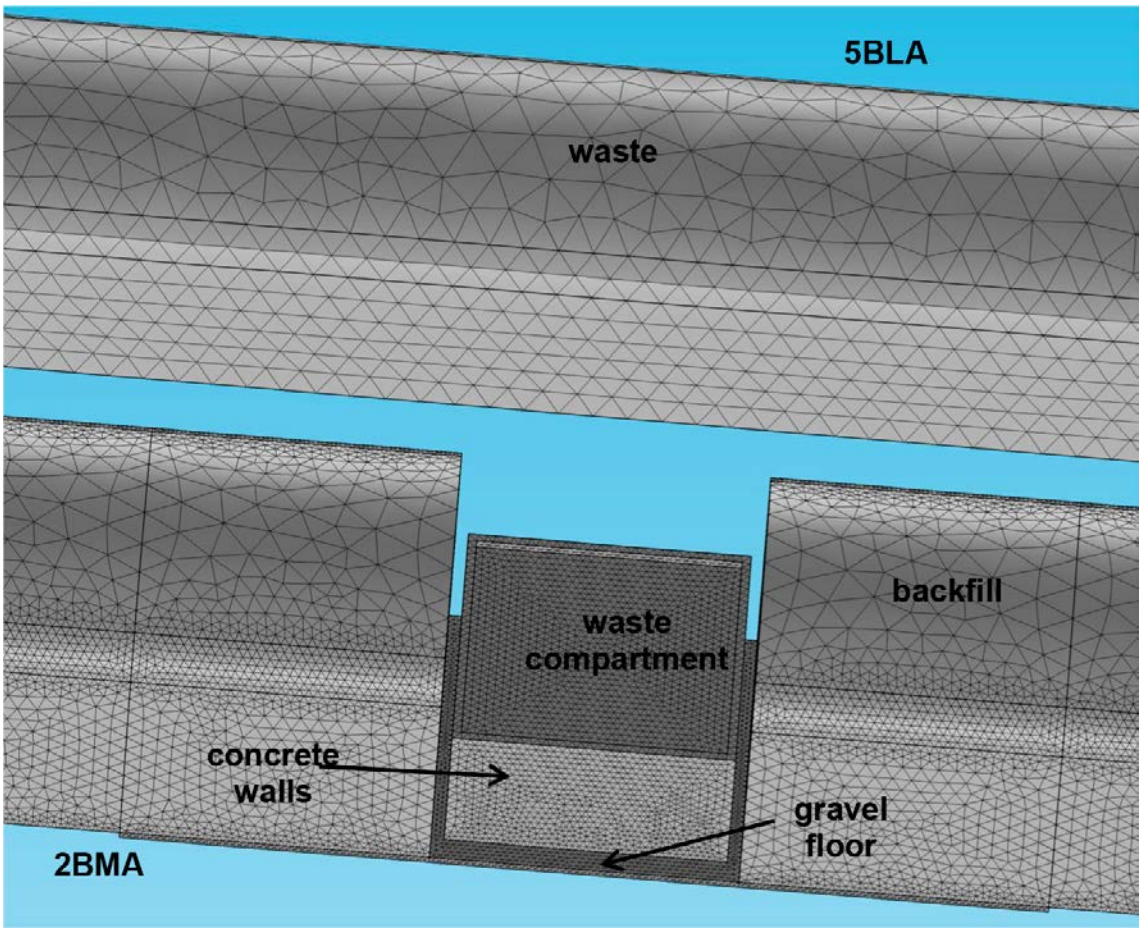

Figure 3-31. *Detailed finite element mesh of the compartments of the 2BMA and the 5BLA vaults.*

4 Model verification

This section presents test cases that were simulated in COMSOL to verify the coupling methodology of DarcyTools and COMSOL by means of the interface presented in Section 2.2.3. In addition, a set of simulations in DarcyTools has been performed to determine the domain size of the repository-scale models.

4.1 Determination of the model size

The domain size of the repository-scale models has been selected based on the prerequisite that any change of hydraulic properties within the repositories should not affect the flow in the regional hydrogeology model. Furthermore, changes in hydraulic properties within one repository model should not affect the flow conditions in the other repository-scale model. To this end, a series of cases were simulated in DarcyTools, and then compared. For the same regional groundwater flow, two extremes in hydraulic conductivity were assigned to the repository:

- with all rock vaults and tunnels homogenously filled with a high permeability material (K=1e–5 m/s)
- with all rock vaults and tunnels homogenously filled with a low permeability material (K=2e–12 m/s)

DarcyTools was run for both cases and a reference case until a new steady-state was reached. The hydraulic properties for the reference case are the same as those used in the DarcyTools model, from which the boundary conditions are obtained (SKBdoc 1395214). The reference case falls in between the two extreme cases with regard to the hydraulic conductivity of the near field materials. Thereafter, the resulting driving pressure fields were compared with the reference case. In this way, the influence of changes within the repository on the flow in the host rock could be determined. This methodology was repeated for two shoreline positions of the TD08a DarcyTools model realization of the repository (SKBdoc 1395214), denoted here as shoreline position X and shoreline position Y (Figure 4-1).

The computed results of the pressure fields are presented in terms of pressure differences calculated as

$$P_{Difference} = Abs\left(\frac{P_{low/high\ permeability} - P_{reference\ case}}{P_{reference\ case}}\right)\cdot 100$$

In this way, different envelopes of pressure differences around the SFR 1 repository were generated with increasing differences in percentage: 1%, 3%, 5%, and 10%. The low permeability case turned out to be the most unfavorable case. Therefore, the results of difference of pressure with the low permeability case were used to define the radius of influence of the permeability changes within the repository. The results of this difference for the shoreline position X are shown in Figure 4-1, and for the shoreline position Y in Figure 4-2.

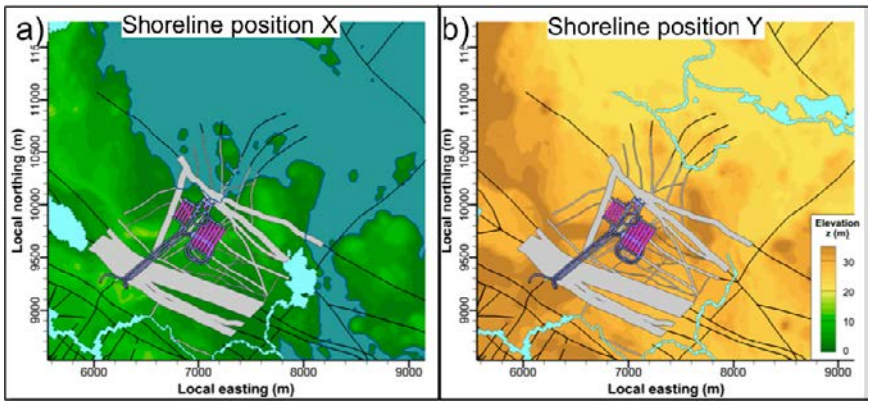

Figure 4-1. Shoreline positions used as boundary conditions for the DarcyTools simulations.

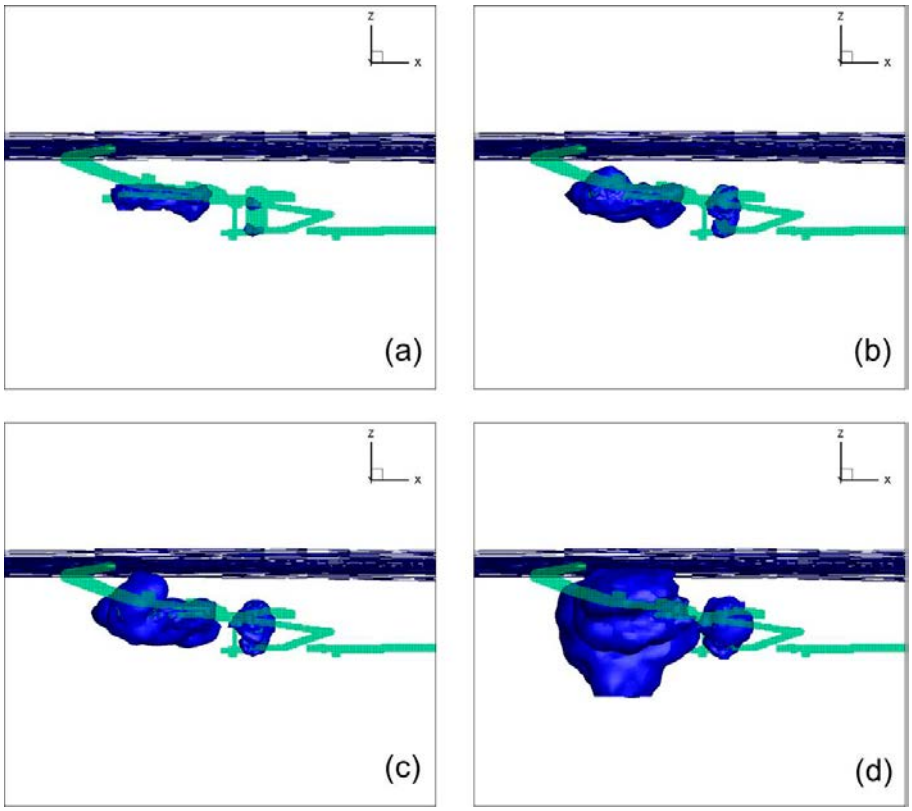

Figure 4-2. *Low Permeability case and shoreline position X. ZX view of the envelope of Pressure Difference around the rock vaults and Silo: (a) > 10%, (b) > 5%, (c) > 3%, (d) > 1%.*

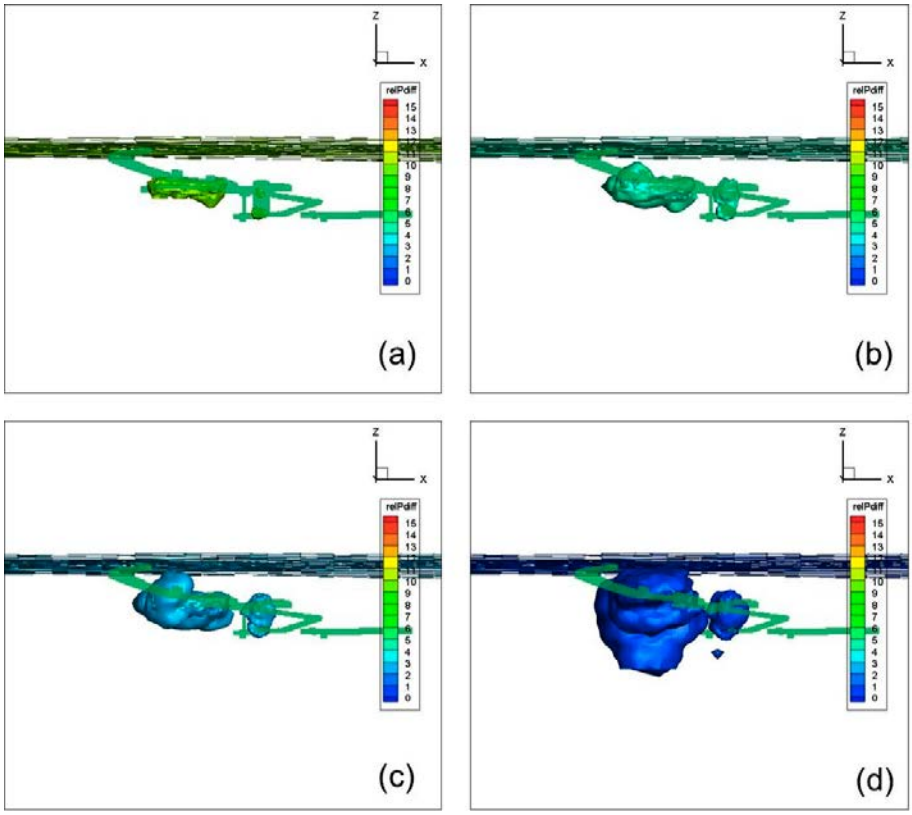

Figure 4-3. *Low Permeability case and shoreline position Y. ZX view of the envelope of Pressure Difference around the SFR 1 vaults and Silo: (a) > 10%, (b) > 5%, (c) > 3%, (d) > 1%.*

It may be observed that for both shoreline positions the differences in the pressure fields do not extend far from the repository domain, even for a large hydraulic conductivity contrast of the whole repository. For instance, a pressure difference of 5% for the shoreline position Y extends 10–15 m South from the bentonite plugs, and around 30 m East from the 1BMA. The differences around the Silo are also quite limited and their extension is smaller than the Silo diameter (i.e., around 20 m). It can also be deduced that the SFR 3 repository is not affected by changes in the SFR 1 permeability field. Based on these results, the boundaries of the domain to be modeled have been selected for the SFR 1 repository model. For the SFR 3 repository model, the exercise has not been repeated. Instead, the observations from SFR 1 model have been transferred, so that the size of the SFR 3 subdomain follows from qualitative conclusions from SFR 1. The dimensions of the SFR 1 and SFR 3 models are the following:

- Dimensions of the SFR 1 model:
  - X : 370 m [6,255 m, 6,625 m]
  - Y : 485 m [9,850 m, 10,335 m]
  - Z : 205m [–25 m, 230 m]
- Dimensions of the SFR 3 model:
  - X : 400 m [6,490 m, 6,890 m]
  - Y : 500 m [9,690 m, 10,190 m]
  - Z : 205m [–25 m, 230 m]

Figure 3-3 and Figure 3-4 depict the final subdomains for SFR 1 and SFR 3 models to be considered.

4.2 DarcyTools-COMSOL Benchmark

4.2.1 Objectives and scope

The repository-scale model for the flow in the repository near-field is connected to a larger model for the regional flow that is set up and solved using the software DarcyTools. The regional flow model supplies (1) driving pressure and/or fluxes boundary conditions to the repository-scale model, as well as (2) the hydraulic conductivity field of the bedrock that is considered in the repository-scale model. To connect the models, an interface between the two codes has been developed, which has been described in Section 2.2.3.

In this section, a benchmark exercise is presented, which has been set up with the following objectives:

- To verify that the interface between DarcyTools and COMSOL works properly
- To verify that the regional-scale model in DarcyTools and the repository-scale model in COMSOL are consistently connected,
- To build confidence in the methodology employed by comparing the results in the common domain

To this end, a test case of the SFR 1 repository has been calculated using DarcyTools (labeled as BASE_CASE1_DFN_R85, see Odén et al. 2014), including both the regional and near-field flow. Thereafter, these results were compared to the results of a repository-scale model of the near-field flow (i.e. a subdomain of the regional scale model) of the exact same problem, in which the boundary conditions and the hydraulic conductivity of the bedrock are extracted using the iDC interface, and the hydraulic properties of the rock vaults, barriers, and tunnels are in complete agreement with the DarcyTools model. Both models have thus identical parameterization regarding hydraulic conductivities of the vaults, tunnels, and bedrock.

As a consequence, differences observed in the comparison between the results of both models will quantify the similarity between the two modelling approaches. Potential sources of discrepancies are the following:

- Interpolation errors: the transfer of information from DarcyTools to COMSOL with the iDC interface developed in this work implies (at least) two interpolation steps, which can result in a smoothing of both the permeability field and the boundary conditions (pressure and Darcy velocity fields).
- Different discretization: COMSOL uses an irregular mesh of tetrahedral finite elements that adapts to the CAD surfaces defining the external geometry of the vaults and tunnels. On the other hand, DarcyTools uses an irregular mesh of cubic volume elements. The refinement of the two meshes is also different.

4.2.2 Model set-up

The parameters of the model domain have been defined according to the parameterization of the BASE_CASE1_DFN_R85 case of the DarcyTools model (Odén et al. 2014). The hydraulic conductivity of the rock is extracted from the DarcyTools input files before the tunnels are implemented (i.e. the undisturbed rock). The hydraulic conductivity values of the materials in the vaults and tunnels of SFR 1 are presented in Table 4-1. The hydraulic conductivity of the bentonite walls surrounding the Silo has been defined in both models by a decreasing function of the conductivity with depth (z). The discretization of the materials in the regional hydrogeology model and the repository-scale model is shown in Figure 4-4.

Table 4-1. Hydraulic conductivity values (K, m/s) for the materials in the vaults and tunnels.

Parameters	K (m/s)
Access tunnels	1.00E–05
Structural plugs	1.00E–06
Plugs	1.00E–10
Vaults	1.00E–05
Silo top layer*	1.00E–09
Silo bottom layer*	1.00E–09
Silo bentonite walls	1.54E–12·z(m)+2.11E–10
Silo dome	1.00E–05
Silo Waste	5.00E–09

* Silo top and bottom layers composed of a sand (90 wt.%) – bentonite (10 wt.%) mixture

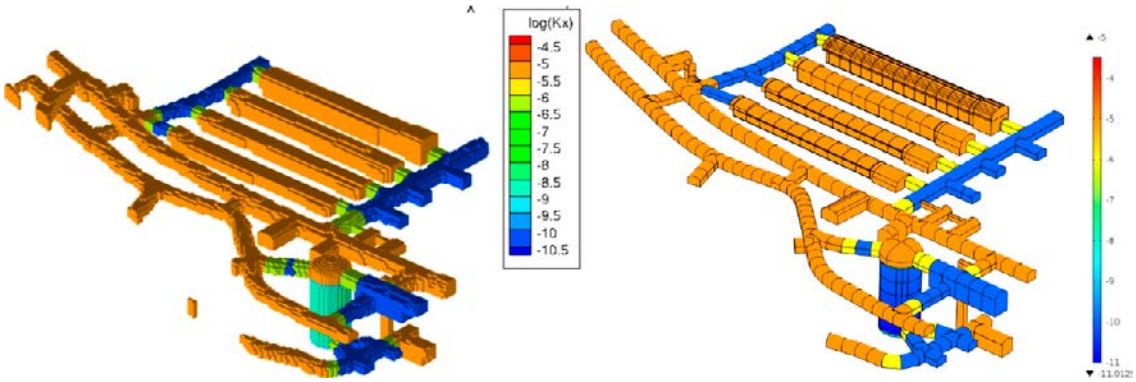

Figure 4-4. Geometry and hydraulic conductivity of the vaults and tunnels in SFR 1: DarcyTools model (left) and COMSOL model (right).

The boundary conditions for the repository-scale model in COMSOL are extracted from the DarcyTools model output through the interface iDC. As described in Section 3.6, two types of boundary conditions were used in the benchmark problem. On the outer surfaces of the SFR 1 model domain corresponding to rock materials, a prescribed driving pressure boundary condition was specified and the corresponding interpolated fields applied. In the intersections of the access tunnels with the model boundaries, a prescribed flux boundary condition was specified.

4.2.3 Results of the comparison

Three simulation cases corresponding to the three shoreline positions under study are compared (see Section 3.6). The comparison is made in terms of flows through different domains in the model as well as driving pressure differences. Three main indicators are defined for flow comparisons in order to quantitatively compare both models computed results:

1. The total groundwater flow (average of the absolute values of inflow and outflow) to the entire repository-scale model domain: this is defined in the boundary of the outer box surrounding the SFR 1 repository model.
2. The total groundwater flow to the repository: this is defined as average of the absolute values of inflow and outflow from each of the vaults in the SFR 1 repository (i.e. 1BMA, 1BLA, 1BTF, 2BTF, and Silo).
3. Volume-averaged pressure difference between the regional-scale and repository-scale models

The results of the groundwater inflow to the entire modeled domain are summarized in Table 4-2. The regional flow field from DarcyTools leads to an increase in the flow through the boundary of the repository-scale model as the shoreline progresses from position 1 towards position 3. The increase is as high as three orders of magnitude, with the change between shoreline positions 1 and 2 being the most pronounced. The comparison of this indicator between COMSOL and DarcyTools models shows a difference of between 15 and 25% (i.e. COMSOL systematically predicts a higher flow). The inflow from the access tunnels (prescribed flux boundary condition) corresponds to the 1%, 1.25% and 1.3% of the total flow through the boundaries in the COMSOL model for shoreline positions 1, 2 and 3, respectively.

The COMSOL computed flow through the repository (total flow in Table 4-3) is 14–18% lower than the flow computed by DarcyTools. The analysis of the inflow per vault (Table 4-3) and Figure 4-5 and Figure 4-6) shows that the repository-scale model consistently predicts lower inflow through the 1BMA, 1BLA and 1BTF and higher flow through the Silo. It is worth noticing that the flow to the Silo have been computed over an inner volume of the vault, which corresponds to the waste compartment in the DarcyTools model but to the waste plus the bentonite walls materials in the repository-scale model. Thus, part of the higher flow estimated in the Silo of the repository-scale model could be attributed to the larger sampled volume.

The fraction of total flow through the repository-scale model domain entering the repository (total flow through vaults/total flow through model domain) is reasonably constant for the three shoreline positions (3%, 5% and 4% for the shoreline positions 1, 2 and 3, respectively).

Table 4-2. Total flow (m^3/year) through the model domain and difference in the total flows (in percentage) estimated by the COMSOL and DarcyTools models (positive values imply higher flow in COMSOL).

Shoreline position	DarcyTools	COMSOL	Difference
1	8.54	9.79	15%
2	2,469.99	2,869.47	16%
3	6,994.94	8,746.16	25%

Table 4-3. Total flow through the vaults (m^3/year) and difference in the total flows through the vaults (in percentage) estimated by the repository-scale and regional-scale models (positive values imply higher flow in COMSOL).

	Shoreline position	1BMA	1BLA	1BTF	2BTF	Silo*	Total vaults
COMSOL	1	0.04	0.13	0.03	0.05	0.0017	0.25
	2	31.39	76.23	11.60	27.61	0.53	147.35
	3	69.39	162.83	28.83	62.65	1.99	325.68
DarcyTools	1	0.05	0.14	0.04	0.07	0.0012	0.30
	2	51.92	89.52	14.82	23.86	0.40	180.52
	3	99.61	187.26	36.19	52.41	1.45	376.92
Difference	1	–10%	–12%	–27%	–25%	39%	–16%
	2	–40%	–15%	–22%	16%	33%	–18%
	3	–30%	–13%	–20%	20%	37%	–14%

* Silo results correspond to the waste domain

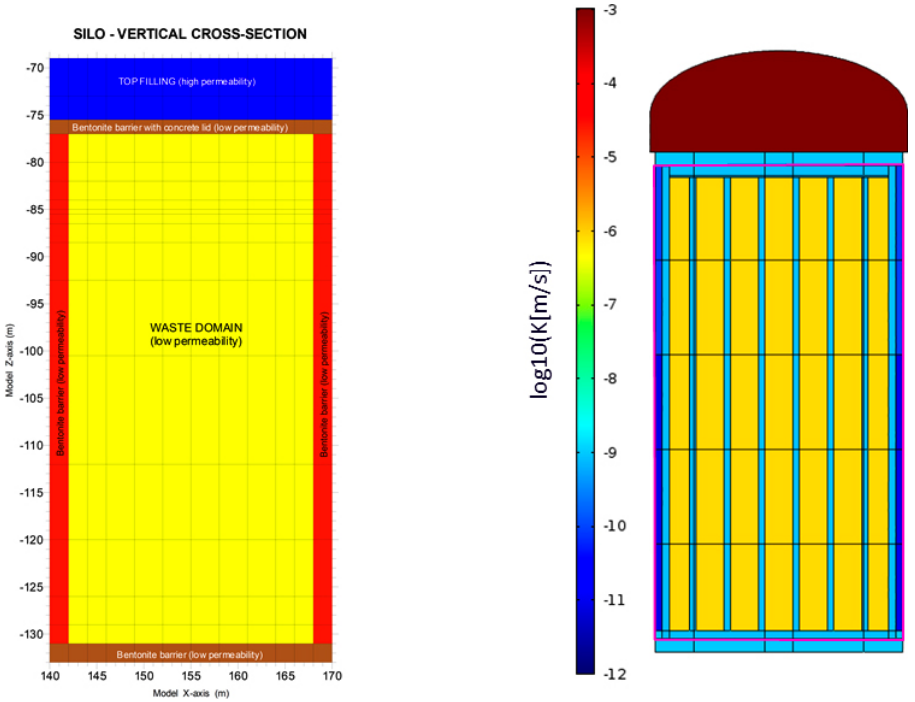

Figure 4-5. *Differences between waste domains in regional-scale (left) and repository-scale models (right, colored by hydraulic conductivity in this case).The flow has been evaluated in the waste domain of the DarcyTools model and in the volume delimited by the pink line in the repository-scale model.*

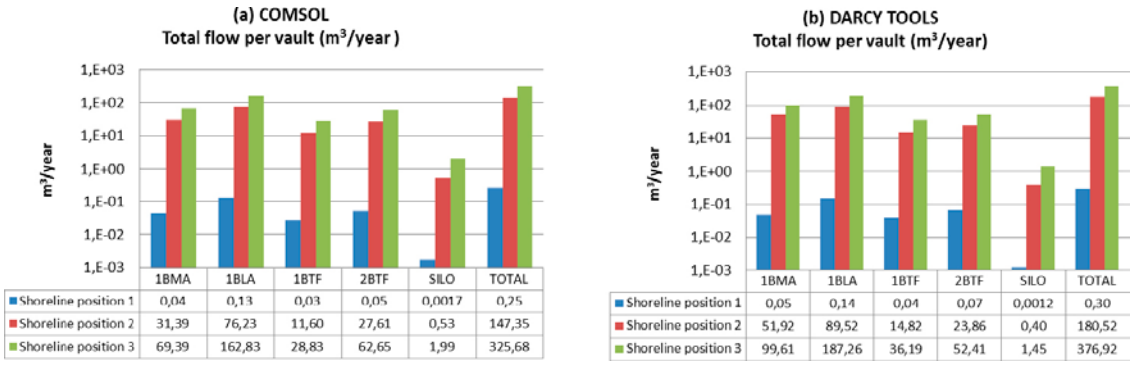

	1BMA	1BLA	1BTF	2BTF	SILO	TOTAL
Shoreline position 1	0,04	0,13	0,03	0,05	0,0017	0,25
Shoreline position 2	31,39	76,23	11,60	27,61	0,53	147,35
Shoreline position 3	69,39	162,83	28,83	62,65	1,99	325,68

	1BMA	1BLA	1BTF	2BTF	SILO	TOTAL
Shoreline position 1	0,05	0,14	0,04	0,07	0,0012	0,30
Shoreline position 2	51,92	89,52	14,82	23,86	0,40	180,52
Shoreline position 3	99,61	187,26	36,19	52,41	1,45	376,92

Figure 4-6. *Total flow per vault from (a) the repository-scale model and (b) the regional-scale model.*

Table 4-4. Closing balance error for each vault and shoreline position in the repository-scale model.

Shoreline position	1BMA	1BLA	1BTF	2BTF	Silo*
1	–1%	–1%	–2%	–1%	–1%
2	0%	2%	2%	2%	–3%
3	0%	2%	2%	2%	–1%

* Silo results correspond to the waste domain defined in Figure 4-5

In order to compare the calculated driving pressure fields from both models, at least one of the outputs has to be interpolated in the grid of the other model. To this end, it has been decided to evaluate the driving pressure difference in the nodes of the repository-scale model mesh. Thus, the regional hydrogeology model output is imported in COMSOL and interpolated in the repository-scale model nodes. The difference between the two outputs is then evaluated for the three shoreline positions. The volume-averaged difference (VAD) over the repository-scale model domain is presented in Table 4-5. The VAD is lower than 1% for the three computed shoreline positions but increases an order of magnitude from the shoreline position 1 to the shoreline positions 2 and 3. This increase is consistent with the increase in the overall driving pressure gradient over the model domain.

Even though the VAD is lower than 1%, local areas of the model domain present higher pressure differences (Figure 4-7). For the shoreline position 1, areas of driving pressure differences greater than 0.5% are located near the base of the repository-scale model domain without affecting the repository area. For the shoreline position 2, differences higher than the 5% appear at some locations near the boundary between the repository and the rock. These differences could be due to local discrepancies in the definition of the repository geometry. For the shoreline position 3, the extension of the areas of pressure differences greater than the 5% increases compared to the shoreline position 2 although the location of the highest errors coincides, suggesting the same source of discrepancies.

4.2.4 Discussion and conclusions

The pressure field in the repository-scale model reproduces the regional-scale model results with relatively high accuracy (volume average differences are always less than 1%). The computed total flow through the vaults is highly consistent between the repository-scale and regional-scale simulations, despite the differences in geometry and discretization. Therefore, it may be concluded that the benchmark exercise provides a high degree of confidence in the methodology applied to ensure the consistency between the regional-scale and the repository-scale groundwater flow calculations.

Table 4-5. Volume-averaged pressure difference (VAD) between the DarcyTools regional hydrogeology model (subscript DTM) and the COMSOL repository-scale model (subscript CM).

Shoreline position	VAD	Expression
1	0.043%	$100*(P_{CM}^{1}–P_{DTM}^{1})/P_{DTM}^{1}$
2	0.317%	$100*(P_{CM}^{2}–P_{DTM}^{2})/P_{DTM}^{2}$
3	0.687%	$100*(P_{CM}^{3}–P_{DTM}^{3})/P_{DTM}^{3}$

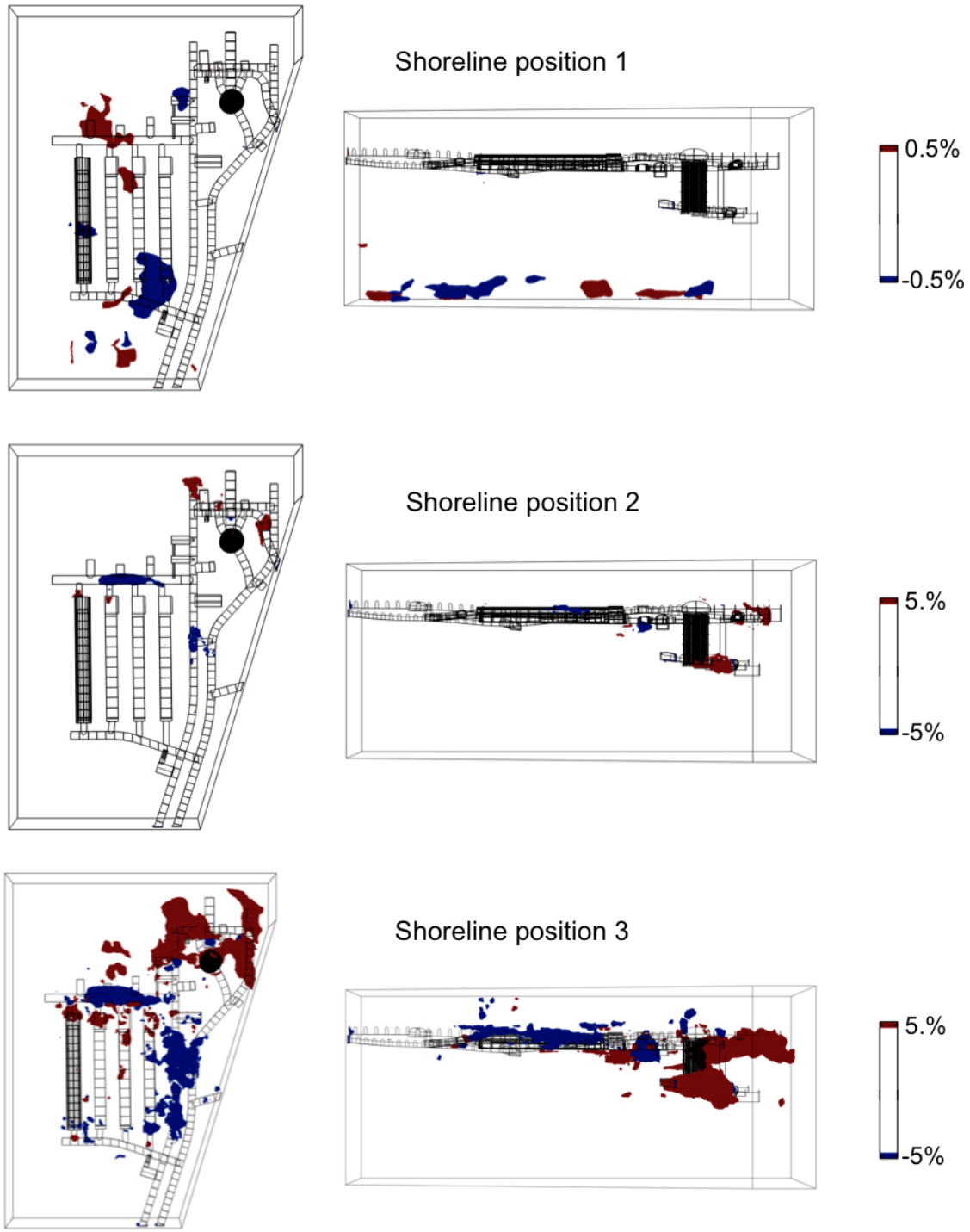

Figure 4-7. *Areas with pressure difference between the repository-scale and regional-scale models greater than the 0.5% for the shoreline position 1 (top) and greater than the 5% for the shoreline position 2 (middle) and shoreline position 2 (bottom) cases. Positive values imply higher pressure in the repository-scale model.*

5 Overview of calculation cases

In order to broaden the system understanding of the SFR 1 and SFR 3, a set of calculation cases have been defined to assess the effects of barrier degradation, repository closure alternatives, permafrost, and the uncertainty in the rock permeability fields on the groundwater flow through the repository near-field. This analysis is particularly relevant to obtain results of groundwater flow through the barriers and waste and to draw conclusions about the impact of different engineering solutions on the near-field hydrogeology. This information can then be used to optimize the design of the barriers and closure materials also from a hydrological perspective.

The calculation cases involve three different shoreline positions, referred to as shoreline position 1, 2, and 3. Each of these shoreline positions corresponds to different boundary conditions for the repository-scale model (see Section 3.6). Furthermore, the different calculation cases consider variations of a Base case (defined in Section 6.1) with regard to the hydraulic conductivity of the vaults, plugs, tunnels, and bedrock.

The complete list of calculation cases simulated in this work is presented in Table 5-1 and Table 5-2 for the SFR 1 and SFR 3 repositories, respectively. These cases have been selected to analyze the effect on groundwater flow due to the following changes in the repository parameterization and/or configuration:

- Degradation of concrete barriers: in the Base case, it is assumed that the concrete barriers are intact. Three additional cases, i.e. moderate, severe, and complete degradation, have been considered, with an increasing hydraulic conductivity assigned to the barriers (see Section 6.2.1 and 7.2.1). In the complete concrete degradation case, it is assumed that the concrete barriers do not provide resistance to flow.
- Degradation of plugs: in the Base case, it is assumed that the structural plugs and the sealed hydraulic bentonite sections are intact. Three additional cases, i.e. moderate, severe, and complete degradation, have been considered with an increasing hydraulic conductivity assigned to the plugs (see Sections 6.2.2 and 7.2.2). In the complete plugs degradation case, it is assumed that the plugs do not provide resistance to flow.
- No barriers: this calculation case is a combination of the completely degraded concrete and the completely degraded plugs cases (see Sections 6.2.3 and 7.2.3). In this case, degradation of the concrete and bentonite barriers is considered simultaneously. In addition, complete degradation of the Silo bentonite walls (top lid, bottom lid, and outer walls) is also assumed.
- Ice lens: this case analyzes the effect of an ice lens formed when the permafrost reaches the Silo depth. The lens is assumed to cause local degradation of the bentonite barrier surrounding the Silo (see Section 6.2.4).
- Closure alternative: the Base case closure of the SFR 1 repository consists of extended sections of bentonite/concrete and structural plugs. In addition, an alternative closure has been considered, in agreement with the designed used in the safety assessment SAR-08 (SKB 2008). In that design, short sections of bentonite with concrete plugs were proposed (see Section 6.3.1).
- Abandoned repository: this case assumes that no additional barriers and structures would be emplaced in the repository after the operational phase is completed (see Sections 6.3.2 and 7.3.1).
- Permafrost: this case analyzes the hydraulic response of the repository to the advance of permafrost. A case of shallow permafrost is considered where the frozen front is located above the vaults and Silo (see Sections 6.4 and 7.4).
- High flow and Low flow: these cases have been proposed to estimate the uncertainty in near-field flow associated with the description of the geosphere hydraulic properties. To this end, two realizations of the rock permeability field have been selected based on previous results of the regional DarcyTools model (Odén et al. 2014). They are considered as representative of two cases that lead to a higher and a lower average tunnel flow with respect to the Base case, respectively (see Sections 6.5 and 7.5).

Table 5-1. List of simulated cases of the SFR 1 repository model.

Simulation Case		Shoreline position	ID
Base case		1	1
		2	2
		3	3
Concrete degradation	Moderate	1	4
		2	5
		3	6
	Severe	1	7
		2	8
		3	9
	Complete	1	10
		2	11
		3	12
Plugs degradation	Moderate	3	13
	Severe	3	14
	Complete	3	15
No barriers		3	16
Ice Lens		1	17
		2	18
		3	19
Closure Alternative		1	20
		2	21
		3	22
Abandoned repository		1	23
		3	24
High flow		1	25
		2	26
		3	27
Low flow		1	28
		2	29
		3	30
Permafrost		Shallow*	31

* Shallow permafrost correspond to a case with the permafrost above the vaults and Silo

Table 5-2. List of simulated cases of the SFR 3 repository model.

CASE		Shoreline position	ID
Base case		1	1
		2	2
		3	3
Concrete degradation	Moderate	1	4
		2	5
		3	6
	Severe	1	7
		2	8
		3	9
	Complete	1	10
		2	11
		3	12
Plugs degradation	Moderate	3	13
	Severe	3	14
	Complete	3	15
No barriers		3	16
Abandoned repository		1	17
		3	18
High flow		1	19
		2	20
		3	21
Low flow		1	22
		2	23
		3	24
Permafrost		Shallow*	25

* Shallow permafrost correspond to a case with the permafrost above the vaults

6 SFR 1 Calculation cases

6.1 Base case: different shoreline positions

This section presents the results of the Base case for three different shoreline positions. The Base case refers to a given set of hydraulic properties (Table 3-3, Figure 3-17 and Figure 3-18) for the different barriers and to a given permeability field for the rock (Figure 6-1). The rock permeability field corresponds with the Base_Case1_DFN_R85 in Odén et al. (2014). Three DarcyTools simulations of the regional hydrogeology, with different top boundary conditions, serve as input to the repository-scale model. These simulations correspond to the different shoreline positions (for more details see Section 3.6).

Streamlines were generated to illustrate the flow field in the vicinity of the repository. The streamline is a curve everywhere tangential to the steady state Darcy velocity field. To calculate the streamlines, COMSOL selects a set of starting points based on the selected origin of the streamlines (surface or each rock vault) and a selected number of initial points (50 points at each surface). The algorithm then finds the Darcy velocity field at these points by interpolation. The algorithm integrates the points along the direction of the Darcy velocity using the integration tolerance using a second-order Runge-Kutta algorithm. At the new positions, the algorithm finds vector values by interpolation and performs another integration. This process stops if it reaches a predetermined number of integration steps, if the points end up outside the geometry, or if the points reach a "stationary point" where the vector field is zero. Finally, the software connects the calculated points for each streamline consecutively with straight lines.

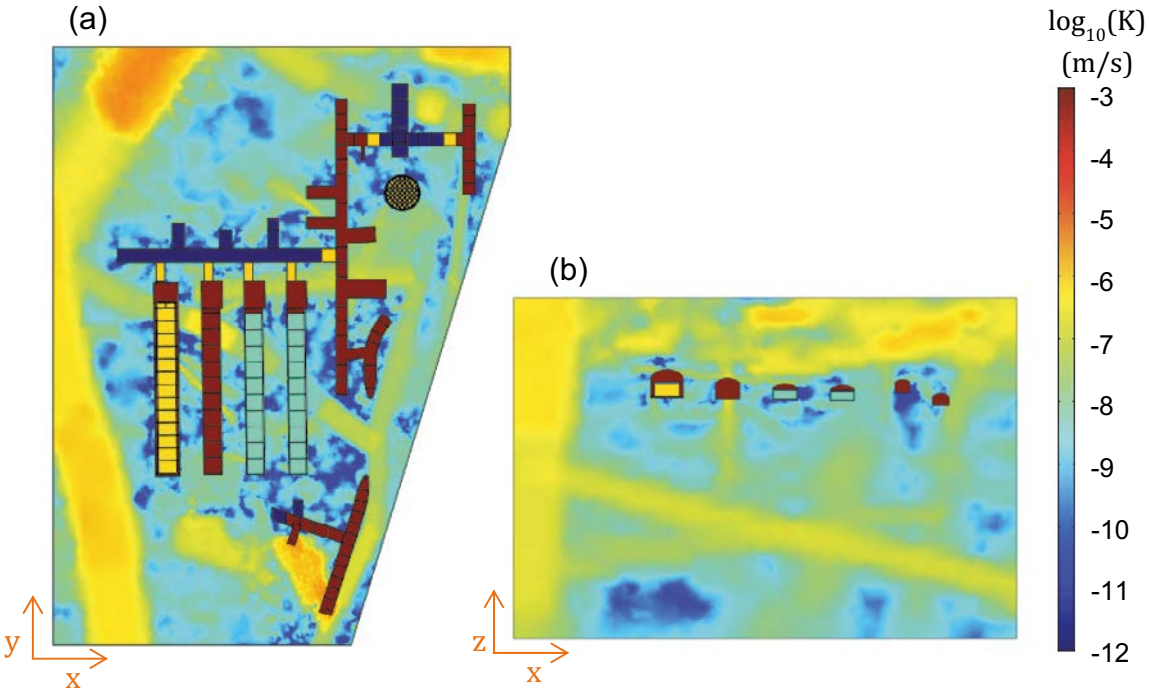

Figure 6-1. *Rock conductivity field (log10, m/s) in two orthogonal of the model domain (z = –82.5 m, and x = 10,050 m), and hydraulic conductivity of the rock vaults and tunnels for the Base Case.*

6.1.1 Shoreline position 1

For this shoreline position, the repository is submerged and situated below the regional groundwater discharge area. The flowpaths followed by the groundwater reaching each individual vault are illustrated in Figure 6-2 (right). The color of the lines represents the destination vault. The water reaching vaults 1BMA, 1BLA, 1BTF and 2BTF is collected in depth by the subhorizontal deformation zone ZFM871 (Figure 3-20) and then moves upwards through the vertical fractures in the rock. Most of the groundwater reaching the Silo arrives through the access tunnels and enters the Silo gravel dome. The flowpaths of the water leaving the vaults are presented in Figure 6-2 (left). It is observed that all the outflowing streamlines present a vertical and distributed flow towards the surface.

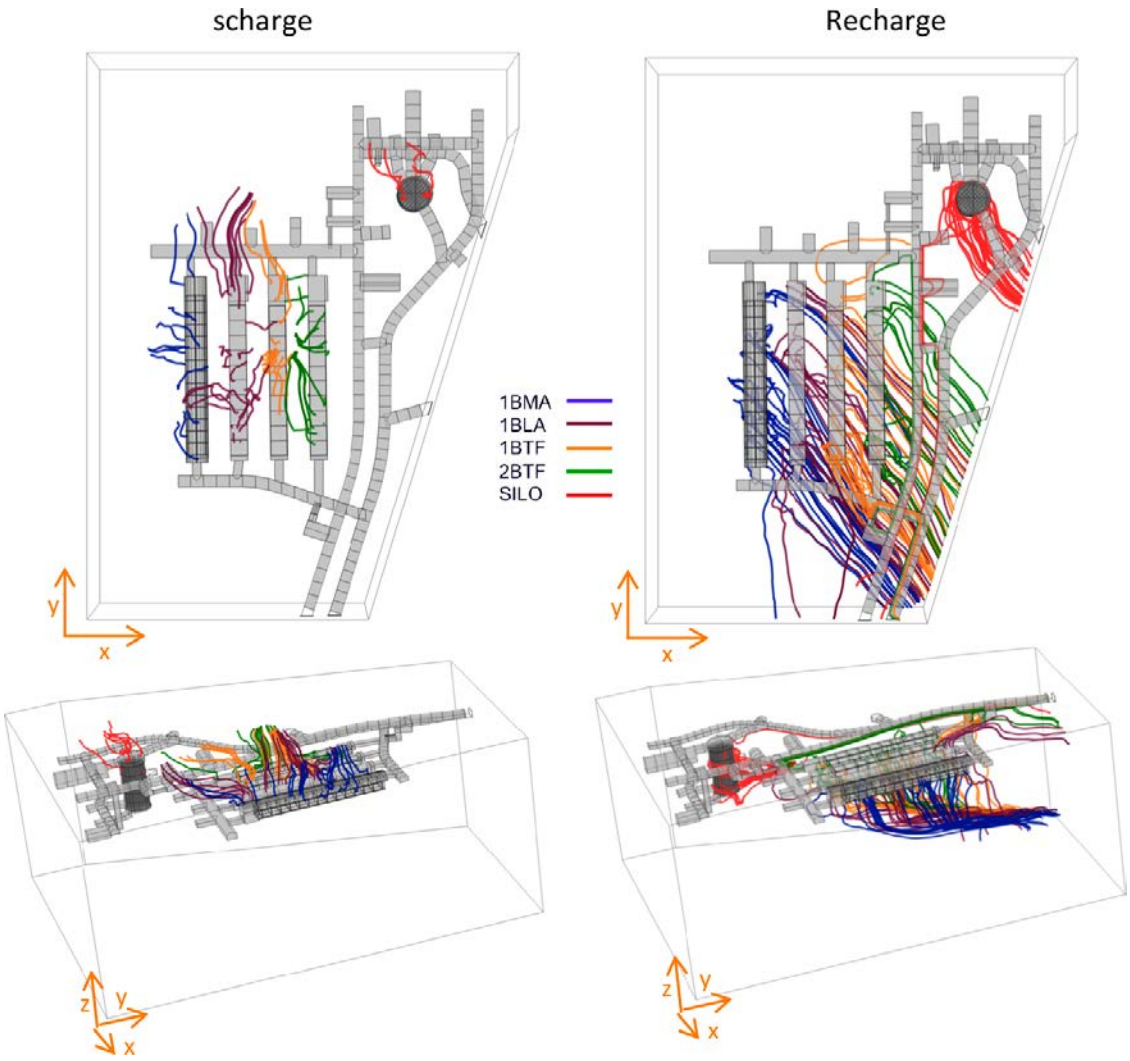

Figure 6-2. *Groundwater streamlines leaving (left) and reaching (right) individual vaults (color tubes) for the Base case and the shoreline position 1.*

6.1.2 Shoreline position 2

Shoreline position 2 shows a more local flow system with recharge-discharge flow cells within the model domain and higher groundwater velocities. The groundwater reaching the vaults originates at the top boundary, south of the repository. The groundwater flowpaths to each individual vault are illustrated in Figure 6-3 (right). The main source of water reaching vaults 1BMA, 1BLA, 1BTF and 2BTF is from the deformation zone ZFMNNW1209 (Figure 3-20). Water flows downwards through ZFMNNW1209 (Figure 6-3c) and reaches the east side of the vaults. 1BMA receives flow mainly through two zones: one at its middle sections and another to north, where the vault crosses the deformation zone ZFMNNW1209. Again, groundwater reaches the Silo dome mainly through the access tunnels. The pathways of the water leaving the vaults are presented in Figure 6-3 (left). Outflow from 1BMA moves west towards ZFMNNE0869. The outflow from the 1BTF and 2BTF vaults is collected by zone ZFM871 and leaves the model domain through north boundaries. North of the repository, within ZFM871, there is a zone of higher permeability which concentrates most of the discharge coming from the repository surroundings. The Silo outflow concentrates north of the vault far from the other vault outflows.

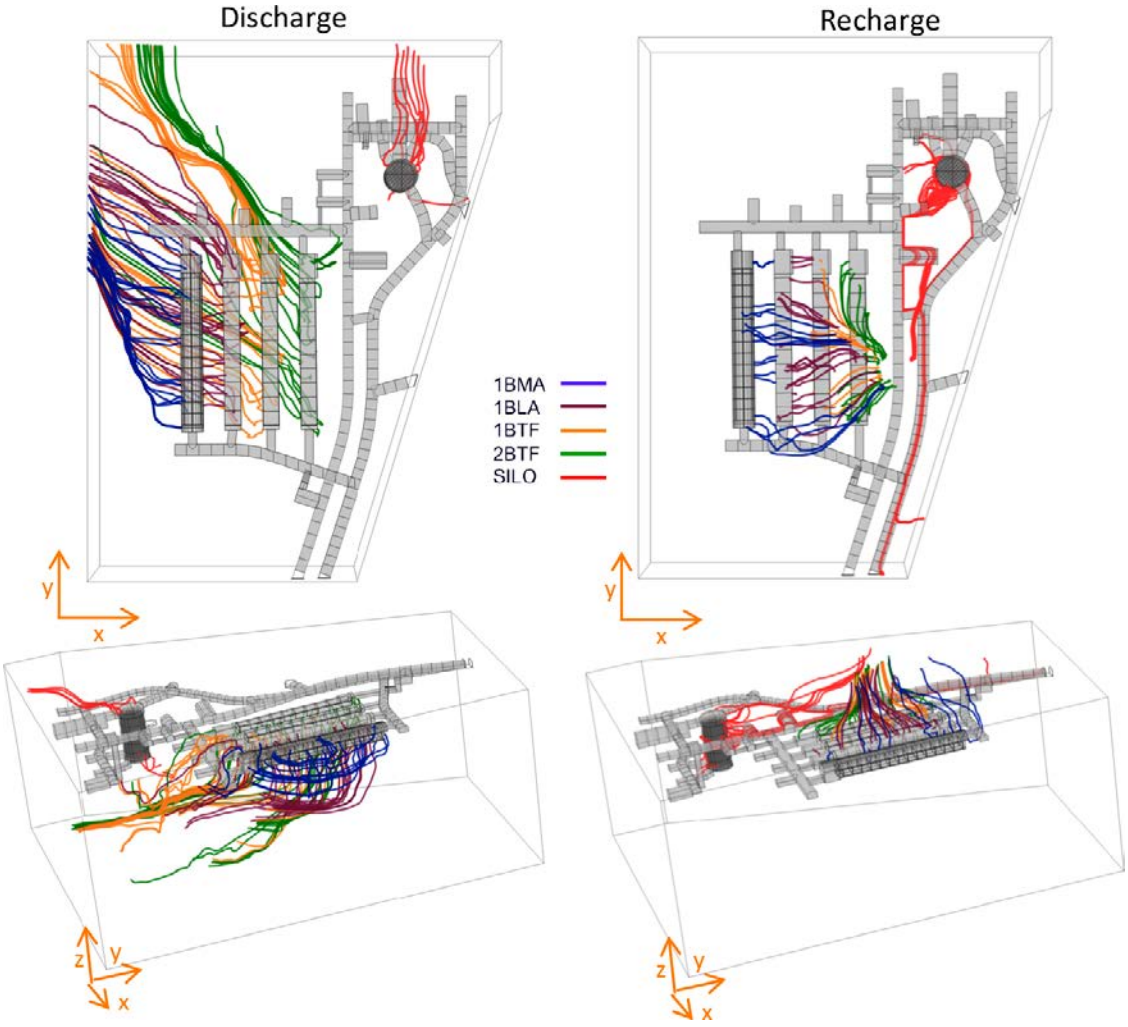

Figure 6-3. *Groundwater streamlines leaving (left) and reaching (right) individual vaults (color tubes) for the Base case and the shoreline position 2.*

6.1.3 Shoreline position 3

The flow system at shoreline position 3 is similar to the one observed for the shoreline position 2. However, in this case the streamlines show deeper and longer pathways within the model domain indicating that the main recharge zone has moved south and the discharge zone is further north. Here, as well, the groundwater reaching the vaults originates at the top boundary, south of the repository. Groundwater flowpaths to each individual vault are illustrated in Figure 6-4 (right). As for the shoreline position 2, the deformation zone ZFMNNW1209 (Figure 3-20) plays an important role delivering water to the vaults. However, in this case, there is an additional inflow to the 1BMA and 1BLA from the southern part of the access tunnels. Both BTF tunnels receive inflow also in its southern sections from minor fractures connecting with the ZFMNNW1209 above. Similar to the previous cases, groundwater reaches the Silo dome through the access tunnels. The pathways of the water leaving the vaults are presented in Figure 6-4 (left). The outflow from all vaults, including the Silo, converges in zone ZFM871, exiting the model domain through its north-west corner.

6.1.4 Total flow through the vaults and waste

One of the results that are computed as a post-process is the total flow through the vaults and through the waste domains. Total flow for a given waste or vault volume (m^3/year) is calculated as the sum of the total flow in each of the surfaces defining the volume:

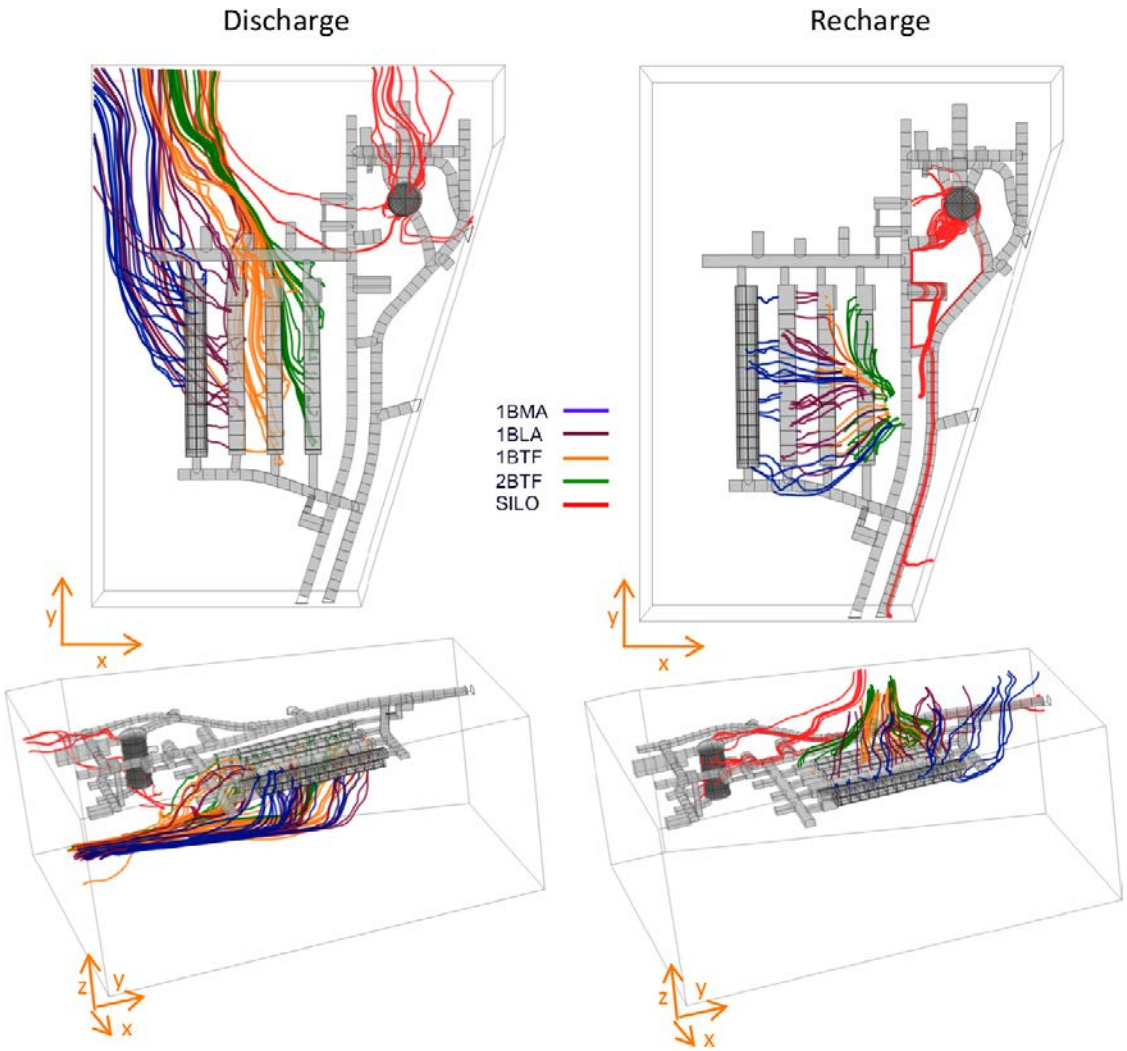

Figure 6-4. *Groundwater streamlines leaving (left) and reaching (right) individual vaults (color tubes) for the Base case and the shoreline position 3.*

$$\text{Total flow}_i = 0.5 \cdot (\text{abs(inflow)} + \text{abs(outflow)}) \qquad \text{Equation 3-7}$$

$$\text{Total flow}_V = \sum_i \text{Total flow}_i \qquad \text{Equation 3-8}$$

Table 6-1 shows the calculated total flow through the vaults and waste domains for the three different shoreline positions. The same information is illustrated in bar plots in Figure 6-5.

As can be observed, the 1BLA has the highest flow. Since this vault has no engineered barriers and the tunnel and waste volumes are very similar, the waste flow represents more than 90% of the tunnel flow. In turn, the 1BMA tunnel flow is less than half the 1BLA flow and only 5% of the tunnel flow enters the waste domain for the shoreline position 2 and shoreline position 3 (17% for the shoreline position 1).

Even though the two BTFs have the same internal configuration the tunnel flow through the 2BTF is more than twice the flow through the 1BTF. The difference lies in the permeability of the surrounding rock (Figure 6-6). The deformation zone ZFMNNW1209 has a higher permeability in the surrounding of 2BTF and connects these vaults with the highly permeable 1BLA. The waste flow is about 10% the tunnel flow in the 2BTF and 20% in the 1BTF.

The Silo has the lowest tunnel and waste flows. The tunnel flow has been divided into the gravel dome domain and the rest of the vault.

The distribution of the flow through the vaults is not homogeneous, as shown in Figure 6-6. The flow in the vicinity of the vaults is controlled by the most permeable structures/features, which are in decreasing order of flow: the access tunnels, main deformation zones (ZFMNNW1209, ZFMNNE0869 and ZFM871), minor fractures and the BLA vault.

Table 6-1. Total flow through the SFR 1 vaults and waste domains (m^3/year) for the Base case.

Total flow (m^3/year)		Shoreline position 1	Shoreline position 2	Shoreline position 3
Vaults	1BMA	0.046	30.385	66.547
	1BLA	0.133	65.220	146.805
	1BTF	0.028	7.801	17.947
	2BTF	0.047	19.891	43.482
	Silo*	0.005	0.741	1.471
	Silo dome	0.008	2.334	3.784
Waste	1BMA	0.008	1.275	3.429
	1BLA	0.123	61.359	138.996
	1BTF	0.009	1.716	3.498
	2BTF	0.009	2.424	4.568
	Silo	0.005	0.682	1.357

* The Silo vault does not include the gravel dome, which is reported separately

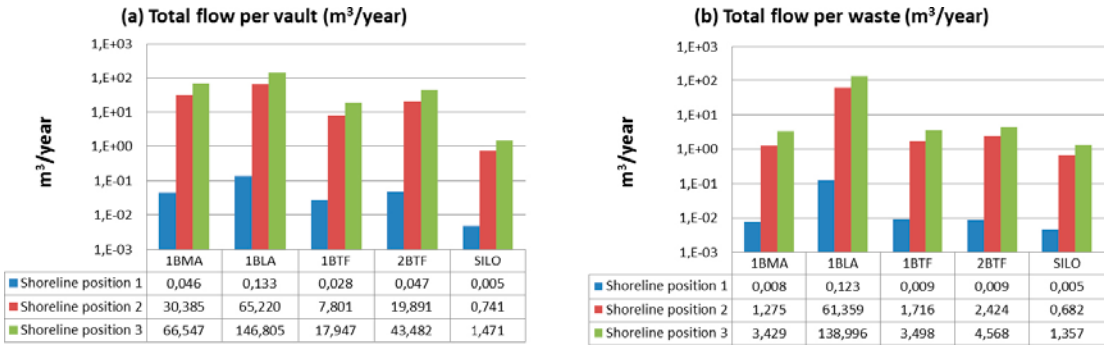

Figure 6-5. *Total flow through the SFR 1 vaults and waste domains (m^3/year) for the Base case. The value for the Silo excludes the flow through the gravel dome, as defined for the radionuclide transport simulations. The vertical axis is logarithmic.*

Figure 6-6. *Color map of the magnitude of the Darcy velocity (m/s) and velocity vectors on a xy plane at z= –82.5 m.*

Using the computed flow rates through the control volumes defined in Section 3.3, the flow in the sections of the longitudinal profile of the vaults has been analyzed to evaluate the spatial distribution of flow within the vaults. Thus, the 1BMA is divided into 15 inner sections so that each of them includes a waste compartment, plus two end backfill sections (Figure 6-7). The 1BLA and 1-2BTF vaults are divided into 10 sections plus two end backfill sections (Figure 6-7 and Figure 6-8) and the Silo is divided into 7 horizontal slices, five of them corresponding to the waste sections plus the bottom and top bentonite sections (Figure 6-9). The Silo dome has not been included in the profiles. In the vaults, each section is composed of one waste control volume (except for the end backfill sections which have none) and by one or several backfill control volumes. Therefore, two flow rates are computed per section: one is the flow through the waste control volume and the other is the result of adding the flow through the different gravel volumes within the section. In the case of the Silo, there is only one flow rate per section, which is the result of adding the total flow through the nine control volumes in which the Silo sections are divided (see Section 3.3). The flow rate profiles are presented in Figure 6-7 (1BMA and 1BLA), Figure 6-8 (1BTF and 2BTF) and Figure 6-9 (Silo) for the three shoreline positions. For the shoreline positions 2 and 3 a flat profile would indicate that most of the flow enters the vault in the most upstream section and flows towards the downstream section without significant lateral inflows in the intermediate sections.

1BMA (Figure 6-7 left): Sections 14 and 15 are half the size of the other sections. Thus, the total flow through these sections is consistently lower than in the rest of the sections.

- For the shoreline position 1, there are two peaks of inflow in the gravel. The first is located in section 9, which is affected by two minor fractures that connect vaults 1BMA and 1BLA (Figure 6-7). The second peak is observed in section 13, affected by the deformation zone ZFMNNW1209. The profile of the flow in the waste follows the flow in the gravel, although the flows are systematically lower. In the waste, the highest and lowest flows are found in section 9 and section 4, respectively.
- The flow profiles of the shoreline positions 2 and 3 show similar patterns, although higher flows are observed compared to shoreline position 1. The flow in the gravel increases continuously from south to north indicating lateral inflow in all sections. There is a clear influence of ZFMNNW1209 in the gravel and waste flow profiles, which present a maximum flow in section 13. In contrast, section 3 has the lowest flow in both cases.

1BLA (right): The gravel in the 1BLA sections is restricted to the 0.2 m-thick bottom layer and the waste occupies the rest of the section (Figure 3-13). For this reason, in the 1BLA plots, the flow through the waste section is higher than the gravel flow.

- For all the shoreline positions, the bottom gravel flow curve presents two local minima in sections 3 and 7 and two maxima in sections 5 and 9. However, the waste flow profile is flat for the shoreline positions 1 and 3. For the shoreline position 2, there is a continuous increase in the waste flow indicating lateral inflow in the middle sections.

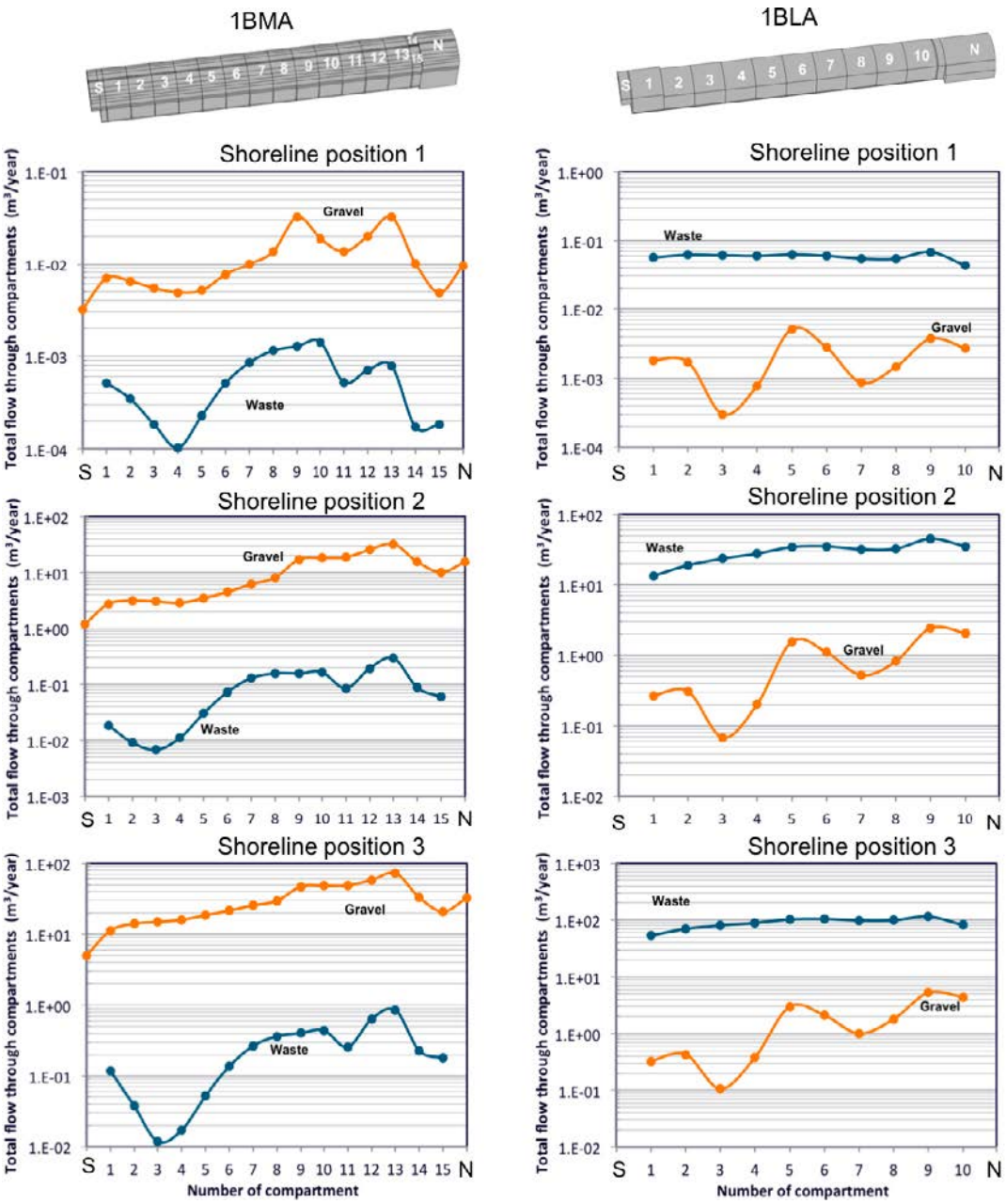

Figure 6-7. *Total flow (m^3/year) along the different gravel and waste sections of the 1BMA (left) and 1BLA (right) for the three shoreline positions. The vertical axis is logarithmic.*

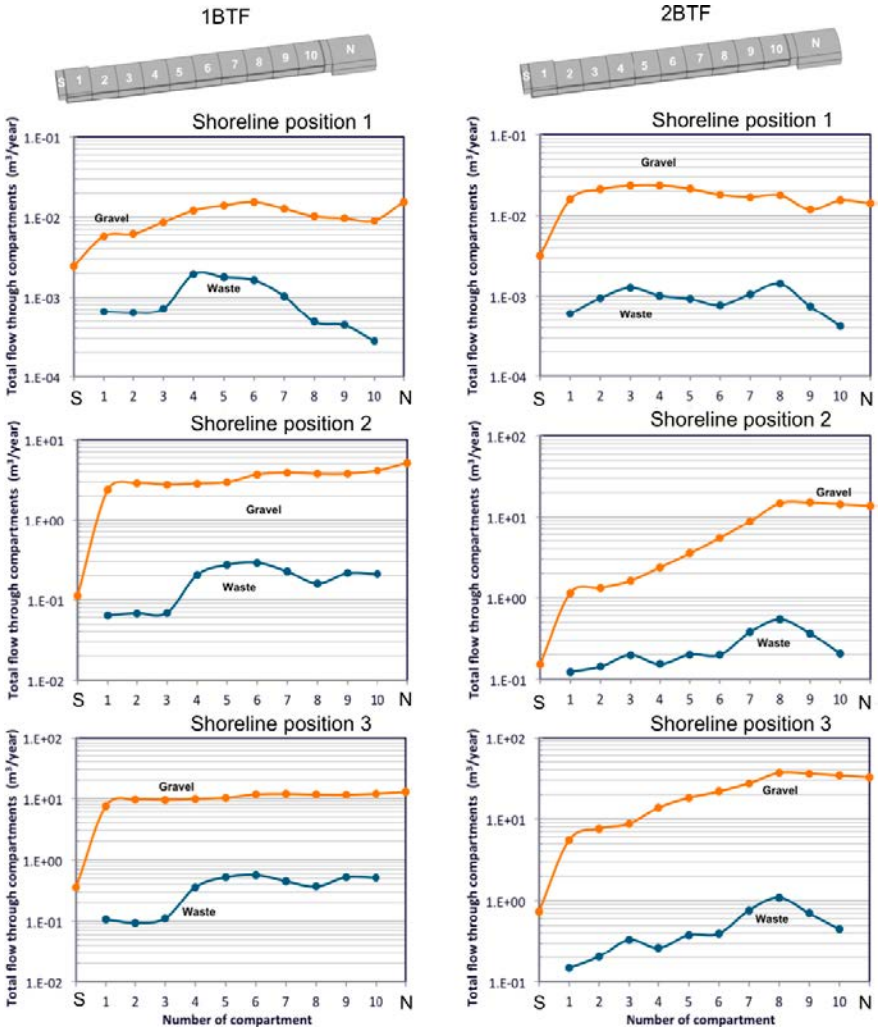

Figure 6-8. *Total flow (m^3/year) along the different gravel and waste sections of the 1BTF (left) and 2BTF (right) for the three shoreline positions. The vertical axis is logarithmic.*

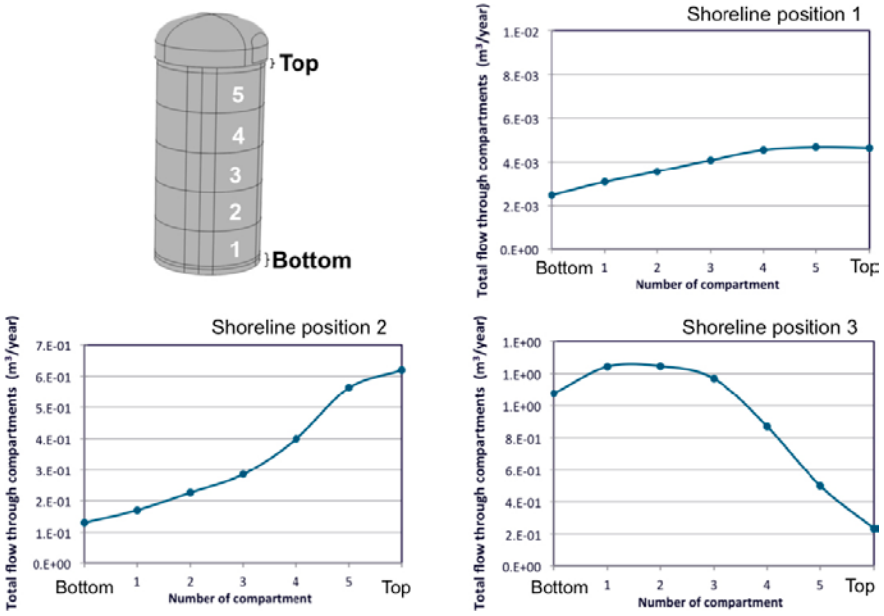

Figure 6-9. *Total flow (m^3/year) along the different waste sections of the Silo for the three shoreline positions.*

1BTF (Figure 6-8 left): The ZFMNNW1209 deformation zone crosses the vault at sections 5-7.

- For the shoreline position 1, the flow through the gravel has a peak in volume 6. The profiles are flatter for the shoreline positions 2 and 3, but with a small increase in section 6.
- The waste flow profile reflects the influence of the deformation zone ZFMNNW1209. In all cases a maximum located between sections 4 and 7 is observed. North of those sections there is a decrease of flow in the waste that is not observed in the gravel for the shoreline positions 2 and 3. This indicates that the higher flow to the waste control volumes affected by the deformation zone ZFMNNW1209 is localized and does not affect the flow to the northern waste control volumes.

2BTF (Figure 6-8 right): Section 8 is intersected by the deformation zone ZFMNNW1209.

- For the shoreline position 1 the **gravel** flow profile is quite flat with a minimum flow in section 9. The waste flow profile shows two maxima in sections 3 and 8.
- For the shoreline positions 2 and 3, the flow through the **gravel** increases from south to north between sections 1 and 8. All the **waste** flow profiles present a higher flow for the sections affected by the deformation zone ZFMNNW1209, with a maximum in section 8.

Silo (Figure 6-9): In the vicinity of the Silo, the flow is upwards for the shoreline position 1 and shoreline position 2 and downwards for the shoreline position 3.

- Shoreline position 1: flow increases smoothly from bottom to top.
- Shoreline position 2: flow increases upwards with a maximum flow in section 5.
- Shoreline position 3: groundwater flows from top to bottom and the flow increases from section 5 to section 3 and stabilizes from sections 3 to 1.

6.2 Barrier degradation

6.2.1 Concrete degradation

This section explores the effect of concrete barrier degradation on the groundwater flow and on the total flow entering the tunnels and waste compartments of the SFR 1 vaults. This effect has been studied with a set of three simulations corresponding to moderate, severe, and complete concrete degradation. The hydraulic conductivities of the different degradation states are defined in Table 6-2. The waste hydraulic conductivity was increased accordingly to retain a contrast in conductivity between the concrete and the waste of three orders of magnitude, until the conductivity threshold of 10^{-3} m/s was reached. The parameterization of the vaults for the different concrete degradation cases is also shown in Figure 6-10.

Table 6-2. Hydraulic conductivity (m/s) for the different materials for all degradation states considered.

Hydraulic conductivity (m/s)	Base case Intact	Concrete Degradation		
		Moderate	Severe	Complete
Concrete	8.30E–10	1.00E–07	1.00E–05	1.00E–03
Concrete Backfill	8.30E–09	1.00E–06	1.00E–04	1.00E–03
BMA concrete beams	8.30E–10	1.00E–07	1.00E–05	1.00E–03
Backfill	1.00E–03	1.00E–03	1.00E–03	1.00E–03
Waste	8.30E–07	1.00E–04	1.00E–03	1.00E–03
Sand Floor	1.00E–07	1.00E–07	1.00E–07	1.00E–07

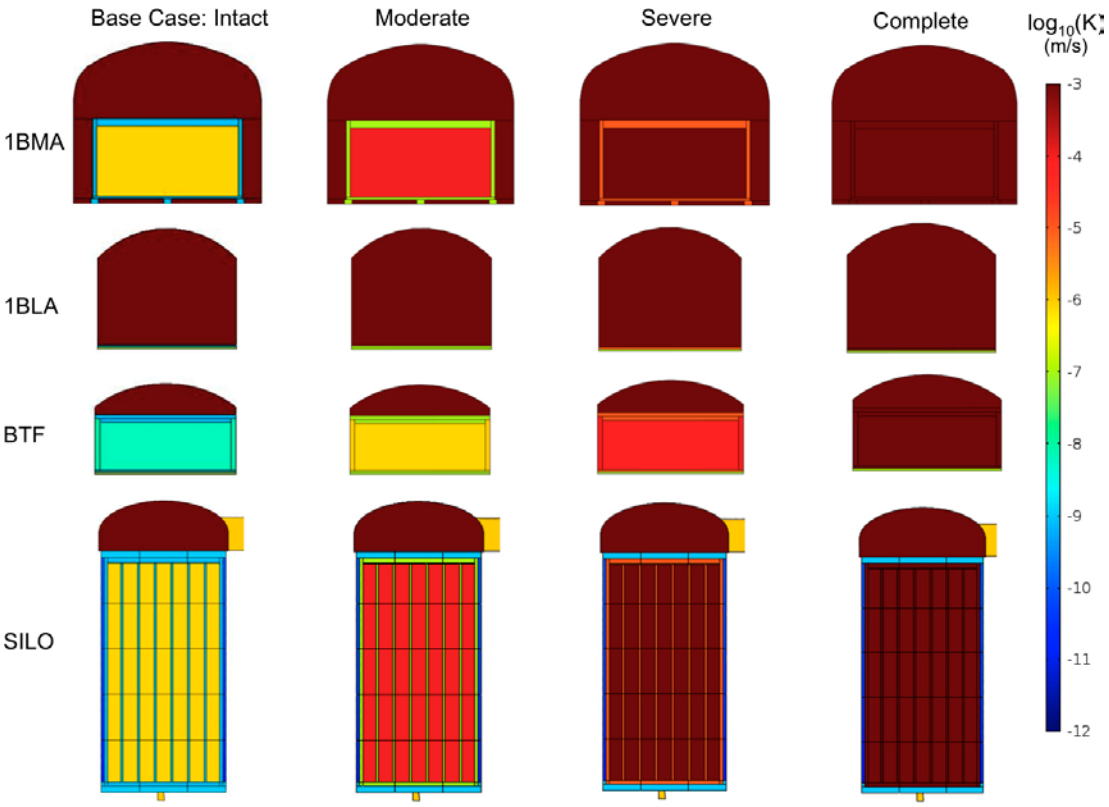

Figure 6-10. *Hydraulic conductivity parameterization for the different concrete degradation cases.*

The total tunnel and waste flows computed for the Base case and the three states of concrete degradation are presented in Table 6-3 and in Figure 6-11. The differences of total flow with respect to the Base case are given in Table 6-4. The comparison of the longitudinal distribution of flow for the three concrete degradation cases and the three shoreline positions is presented in Figure 6-12 (1BMA and 1BLA), Figure 6-13 (1BTF and 2BTF) and Figure 6-14 (Silo). According to the model results, the gravel flow (left panels in Figure 6-11) is not significantly affected by the degradation of the concrete for any of the shoreline positions. The flow distribution along the vaults (Figure 6-12 and Figure 6-13) illustrates the minimal effect of concrete degradation in the gravel flow particularly in the 1BLA and 1BTF vaults. For the 2BTF, there is an increase of flow from the intact to the moderate concrete degradation cases that remains stable for the more advanced degradation cases. The same effect is observed for the 1BMA gravel flow.

Table 6-3. Total flow through the vaults (m^3/year) for the different concrete degradation cases.

		Shoreline position 1			Shoreline position 2			Shoreline position 3		
		Moderate	Severe	Complete	Moderate	Severe	Complete	Moderate	Severe	Complete
Vaults	1BMA	0.04	0.04	0.04	31.11	31.20	31.22	68.37	68.62	68.69
	1BLA	0.13	0.13	0.13	73.06	74.09	74.12	156.17	158.12	158.15
	1BTF	0.03	0.03	0.03	8.83	8.84	8.78	19.85	19.88	19.73
	2BTF	0.05	0.05	0.05	24.57	25.10	24.99	53.12	54.29	54.02
	Silo*	0.006	0.006	0.006	0.85	0.85	0.85	1.80	1.80	1.80
	Silo dome	0.008	0.008	0.008	2.327	2.327	2.327	3.910	3.910	3.910
Waste	1BMA	0.02	0.02	0.03	3.87	7.89	19.89	11.03	16.94	40.90
	1BLA	0.13	0.13	0.13	71.42	73.47	73.68	152.89	156.97	157.39
	1BTF	0.02	0.02	0.02	3.48	3.78	5.81	6.91	7.71	13.78
	2BTF	0.03	0.03	0.04	10.85	13.29	20.81	20.69	26.22	44.26
	Silo	0.006	0.006	0.006	0.80	0.80	0.80	1.74	1.76	1.76

* Silo results correspond to the waste domain defined in Figure 4-5

Table 6-4. Differences in total flow with respect to the Base case (m^3/year) for the different concrete degradation cases.

		Shoreline position 1			Shoreline position 2			Shoreline position 3		
		Moderate	Severe	Complete	Moderate	Severe	Complete	Moderate	Severe	Complete
Vaults	1BMA	–13%	–13%	–13%	2%	3%	3%	3%	3%	3%
	1BLA	–2%	–2%	–2%	12%	14%	14%	6%	8%	8%
	1BTF	7%	7%	7%	13%	13%	13%	11%	11%	10%
	2BTF	6%	6%	6%	24%	26%	26%	22%	25%	24%
	Silo*	20%	20%	20%	15%	15%	15%	22%	22%	22%
	Silo dome	0.0%	0.0%	0.0%	–0.3%	–0.3%	–0.3%	3%	3%	3%
Waste	1BMA	150%	150%	275%	204%	519%	1,460%	222%	394%	1,093%
	1BLA	6%	6%	6%	16%	20%	20%	10%	13%	13%
	1BTF	122%	122%	122%	103%	120%	239%	98%	120%	294%
	2BTF	233%	233%	344%	348%	448%	758%	353%	474%	869%
	Silo	20%	20%	20%	17%	17%	17%	28%	30%	30%

* Silo results correspond to the waste domain defined in Figure 4-5

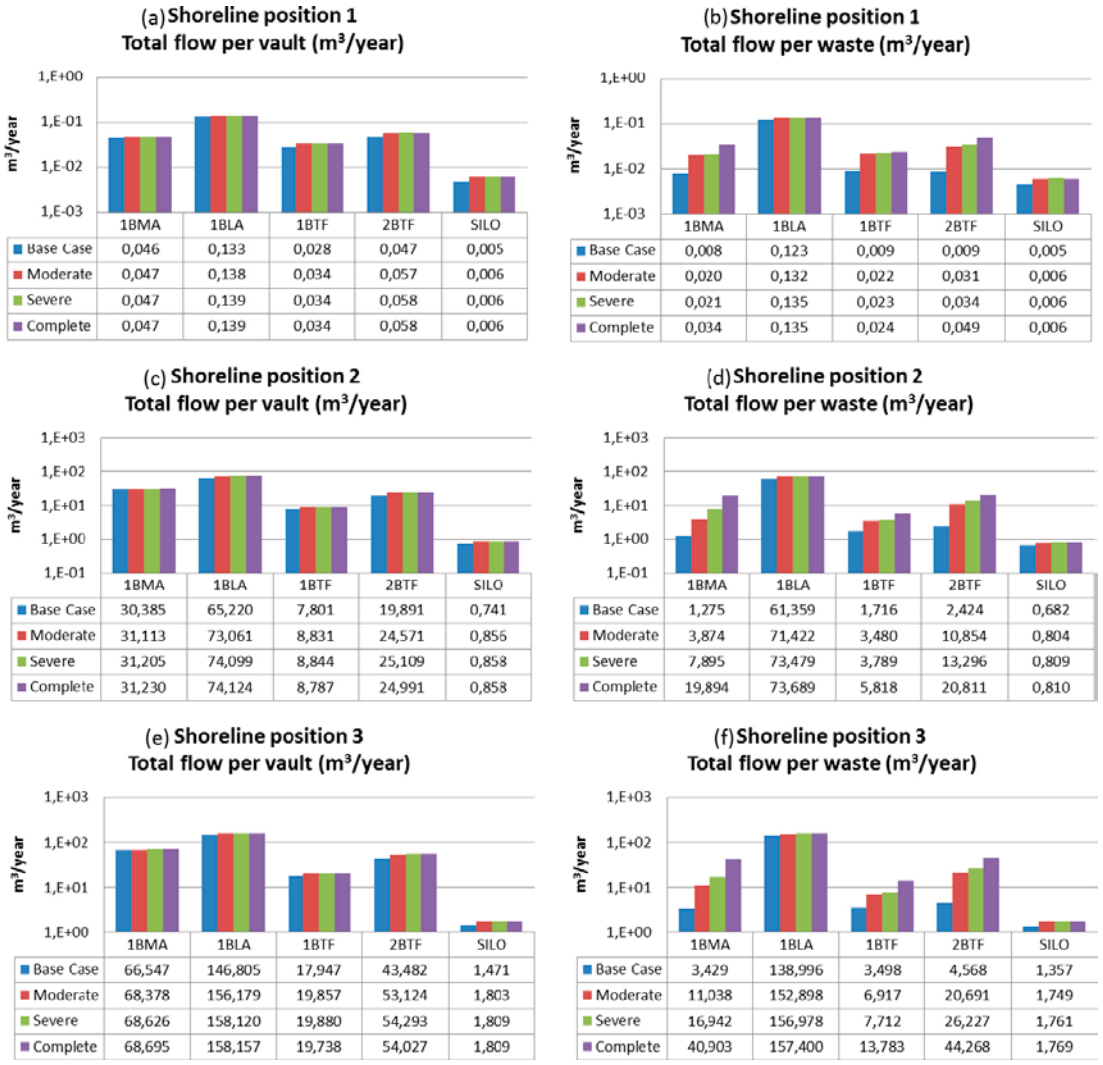

Figure 6-11. *Total flow (m^3/year) through the SFR 1 vaults (left) and waste domains (right) for the different concrete degradation cases and the three shoreline positions. The vertical axis is logarithmic.*

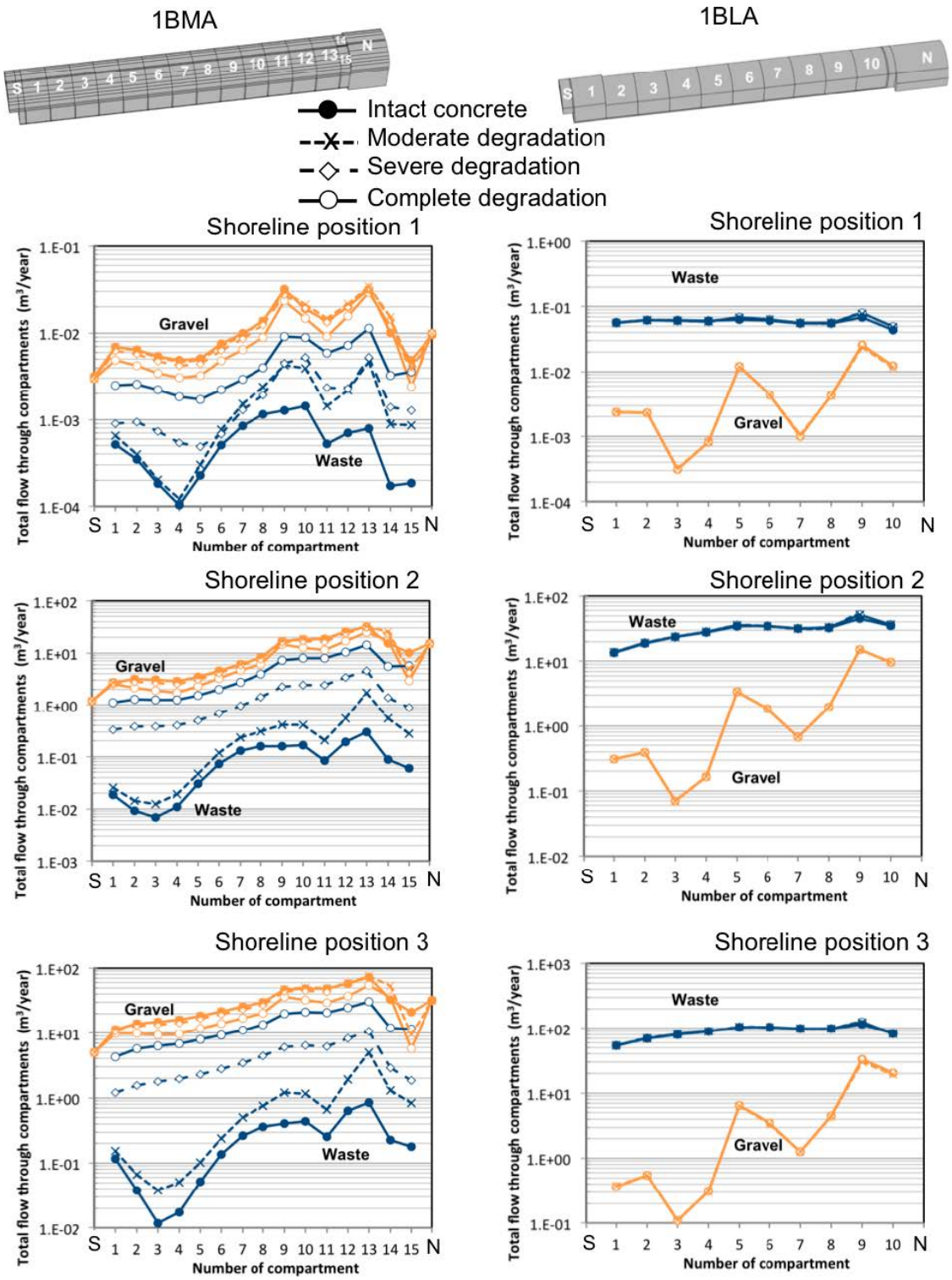

Figure 6-12. *Total flow (m^3/year) along the different gravel and waste sections of the 1BMA (left) and 1BLA (right) for the three shoreline positions. The vertical axis is logarithmic.*

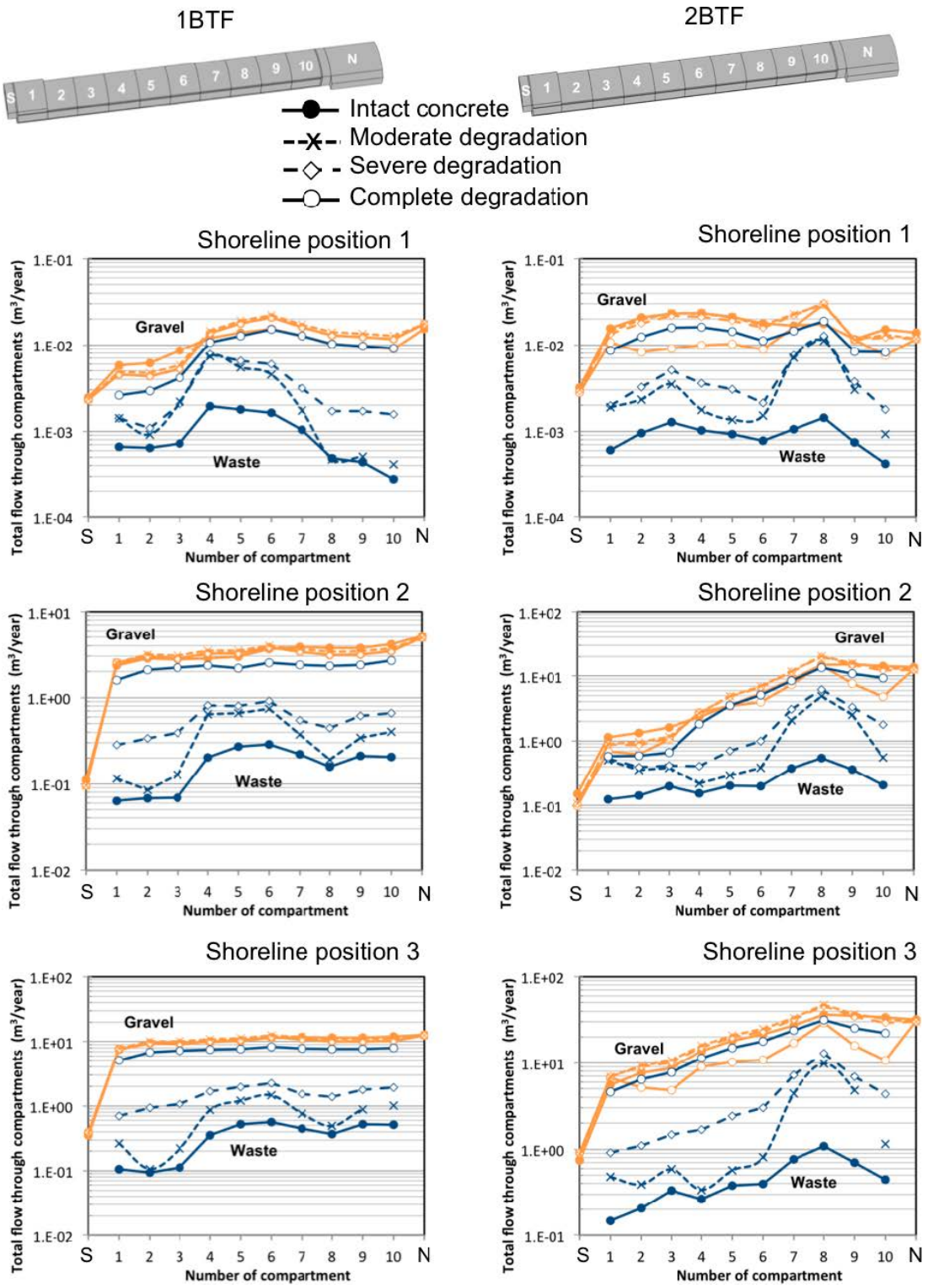

Figure 6-13. *Total flow (m^3/year) along the different gravel and waste sections of the 1BTF (left) and 2BTF (right) for the three shoreline positions. The vertical axis is logarithmic.*

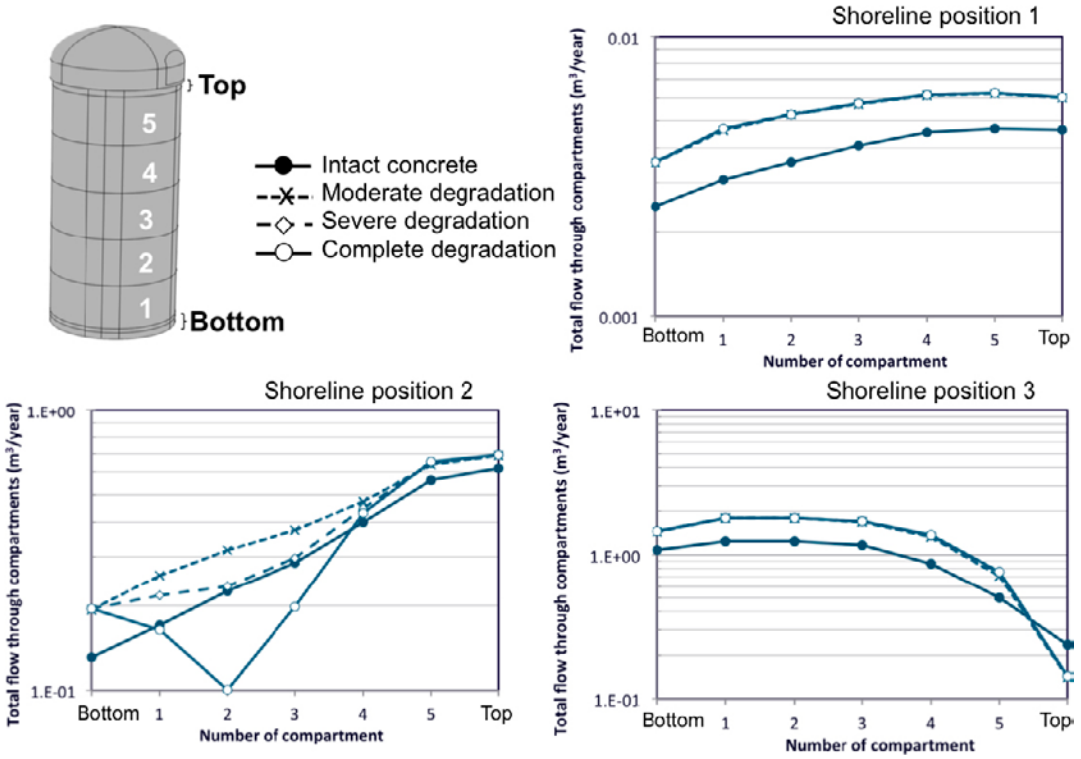

Figure 6-14. *Total flow (m^3/year) along the different waste sections of the Silo for the three shoreline positions. The vertical axis is logarithmic.*

Regarding the effect of the concrete degradation in the waste flow, it is least important for the 1BLA and the Silo. In the 1BLA, the presence of concrete is limited to the 0.2 m-thick concrete slab that separates the gravel floor from the large backfilled waste volume, and therefore the flow is rather insensitive to concrete degradation. On the other hand, the Silo contains a large amount of concrete. However, it is completely surrounded by the external bentonite walls (also on top and bottom of the waste domain, see Figure 6-10), which is not degraded in these cases. For shoreline position 3, there is some redistribution of flow in the lower 1–3 sections of the Silo (Figure 6-14). The other three vaults (i.e. 1BMA, 1BTF, and 2BTF) present an increase in the waste flow of one order of magnitude for the totally degraded concrete case. For the case of moderate concrete degradation, the longitudinal profile of the 1BMA waste flow shows a moderate impact of the concrete degradation in the southern sections (1-5) and a pronounced increase localized in the sections associated with fracture zones (Figure 6-12). Waste flow increases in all sections in the case of severe and complete degradation and shoreline position 1. However, the effect of the deformation zone is still noticeable. For shoreline positions 2 and 3 and for the moderate concrete degradation case the waste flow increases in all sections with a longitudinal profile parallel to the Base case profile. For the severe and complete degradation cases the profile flattens, approaching the gravel flow profiles. The same pattern is observed for the 1BTF and 2BTF vaults (Figure 6-13). The moderate concrete degradation leads to an increase of flow intensified in the sections affected by the deformation zones. For the severe and the complete concrete degradation cases, the flow profiles become more homogeneous, due to a smoothing out effect of the fracture zones.

The effect of the complete concrete degradation in the SFR 1 repository is shown in Figure 6-15 by means of a map of the ratio of the magnitude of the Darcy velocity between the complete degraded concrete cases and the Base case and shoreline position 3. The results show an increase of the flow through the 1 BMA and BTF waste. As expected, the flow through the 1BLA shows a lack of sensitivity to the concrete degradation, as there are no concrete barriers in this vault. With concrete degradation flow decreases in the rock surroundings as water is redirected towards the more conductive vaults. The decrease of flow in the rock is more prominent in the rock between the BTF vaults.

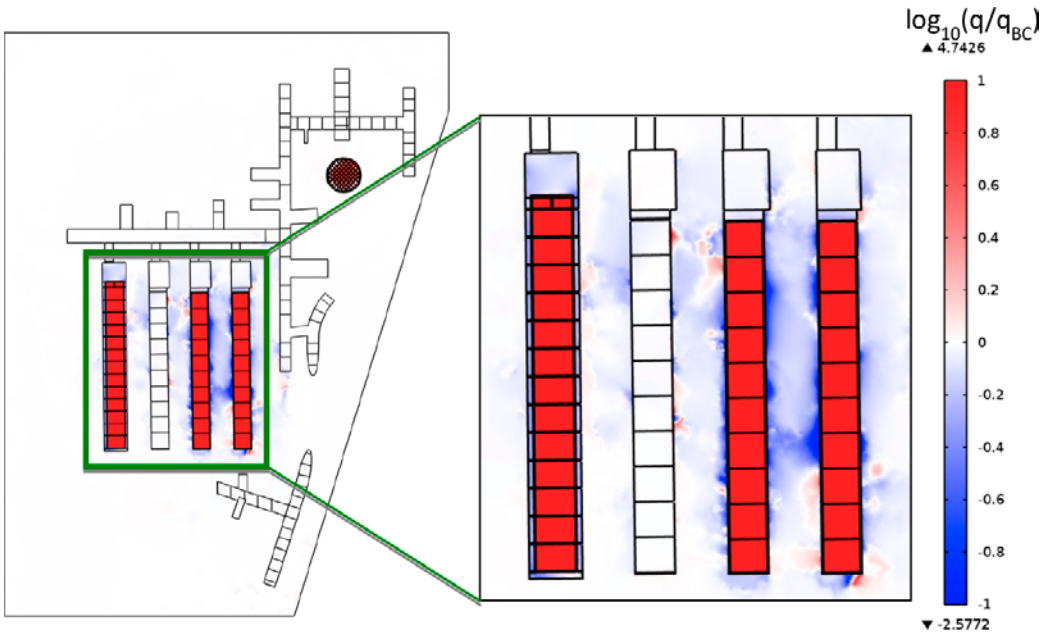

Figure 6-15. *Ratio of the Darcy velocity magnitude between the case of complete degraded concrete and the Base case at the shoreline position 3 in a xy plane at z= –82.5. Values greater than one indicate a higher flow in the alternative closure case.*

The model geometry of the 1BMA includes the concrete beams that support the concrete floor. These beams represent a barrier to groundwater flow and break the continuity of the hydraulic cage surrounding the concrete structure. A set of simulations was set up to analyze the influence of the concrete beams in relation to the flow through the waste during concrete degradation. The model without concrete beams was used to simulate and the four different concrete degradation states (intact, moderate, severe and complete degradation) for the three shoreline positions. Figure 6-16 compares the effect of the concrete degradation of the 1BMA for the Base case and the case with no concrete beams. The flow through the waste in the case of intact concrete and no beams is three orders of magnitude lower than in the case with beams. The reason for this different behavior is the change in the hydraulic cage efficiency. Given the different results for the intact state, the effect of the concrete degradation is much more pronounced for the 1BMA without beams. The results of the sensitivity to the concrete degradation in the case without beams are consistent to those reported by Holmén and Stigsson (2001).

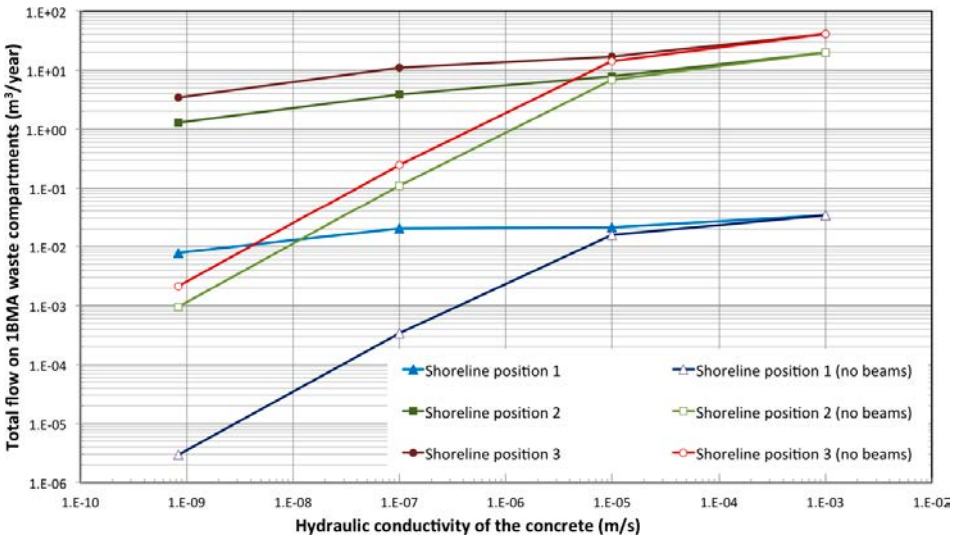

Figure 6-16. *Evolution of the total flow in the waste domain of the 1BMA for an increase in the hydraulic conductivity of the concrete.*

6.2.2 Plug degradation

This section outlines the effect of plug degradation on the groundwater flow and on the total flow entering the tunnels and waste compartments of the SFR 1 vaults. Three different degradation states, in addition to the intact state of the Base case, have been considered for shoreline position 3. The hydraulic conductivity of the plugs for each degradation state is presented in Table 6-5 and Figure 6-17.

The total flow entering the vaults and the encapsulated compartments for each plug degradation state is presented and compared to the Base case in Table 6-6 and Figure 6-18. The comparison of the longitudinal distribution of flow for the three plug degradation cases is presented in Figure 6-19 (1BMA and 1BLA), Figure 6-20 (1BTF and 2BTF) and Figure 6-21 (Silo).

The results show that the impact on flow is small for the moderate plug degradation case and hence that the hydraulic barrier function is maintained at a hydraulic conductivity of 1.00E–09 m/s for the sealed hydraulic bentonite section and 1.00E–05 m/s for the structural plugs. In this case, the plugs still have a higher resistance than the rock surrounding the vaults. The volume-averaged value of the rock hydraulic conductivity within the model domain is of the order of 1e–7 m/s (Table 3-6). Therefore, the rock offers less resistance than the plugs. Even a small reduction in the flow through the Silo is observed (2%) for this plug degradation scenario.

Table 6-5. Hydraulic conductivity (m/s) for the plugs materials for the Base case and the three plug degradation states.

K (m/s)	Intact	Moderate	Severe	Complete
Structural plugs	1.00E–06	1.00E–05	1.00E–04	1.00E–03
Sealed hydraulic bentonite section	1.00E–12	1.00E–09	1.00E–06	1.00E–03

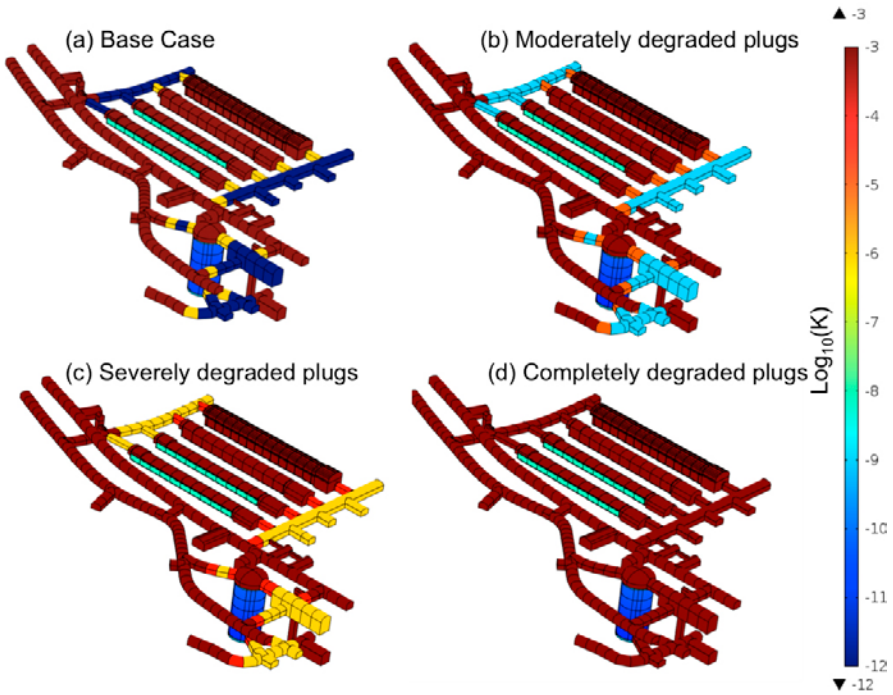

Figure 6-17. *Hydraulic conductivity (log_{10}, m/s) of the repository materials for the different plug degradation cases.*

Table 6-6. Total flow through the vaults (m^3/year) for the different plug degradation cases and comparison with the Base case for the shoreline position 3. Negative percentages indicate a reduction in flow with respect to the Base case.

	Total flow (m^3/year)	Base case Intact	Plugs Degradation Moderate	Severe	Complete	% change Moderate	Severe	Complete
Vaults	1BMA	66.54	66.84	83.31	365.13	0.45%	25.20%	448.74%
	1BLA	146.94	148.93	164.48	540.27	1.35%	11.94%	267.68%
	1BTF	17.95	18.79	36.15	470.75	4.68%	101.39%	2,522.56%
	2BTF	43.48	44.87	70.95	342.77	3.20%	63.18%	688.34%
	Silo	1.47	1.43	2.35	2.83	–2.72%	59.86%	92.52%
	Silo dome	3.79	3.71	2.70	22.25	–2.11%	–28.76%	487.07%
	Silo (Total)	5.26	5.14	5.05	25.08	–2.28%	–3.99%	376.81%
Waste	1BMA	3.42	3.41	4.23	8.45	–0.29%	23.68%	147.08%
	1BLA	141.02	141.02	156.56	516.87	0.00%	11.02%	266.52%
	1BTF	3.43	3.44	2.70	2.80	0.29%	–21.28%	–18.37%
	2BTF	4.51	4.51	3.81	2.96	0.00%	–15.52%	–34.37%
	Silo	1.31	1.32	2.32	2.75	0.76%	77.10%	109.92%

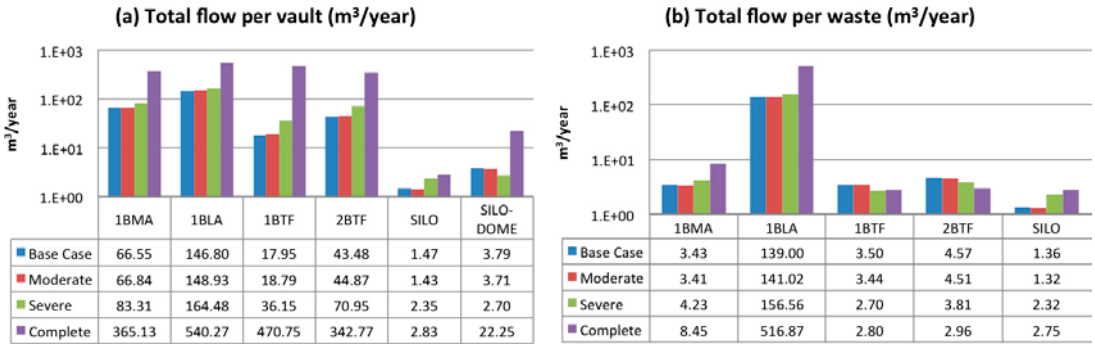

Figure 6-18. *Total flow entering the SFR 1 vaults (a) and waste encapsulated compartments (b). The vertical axis is logarithmic.*

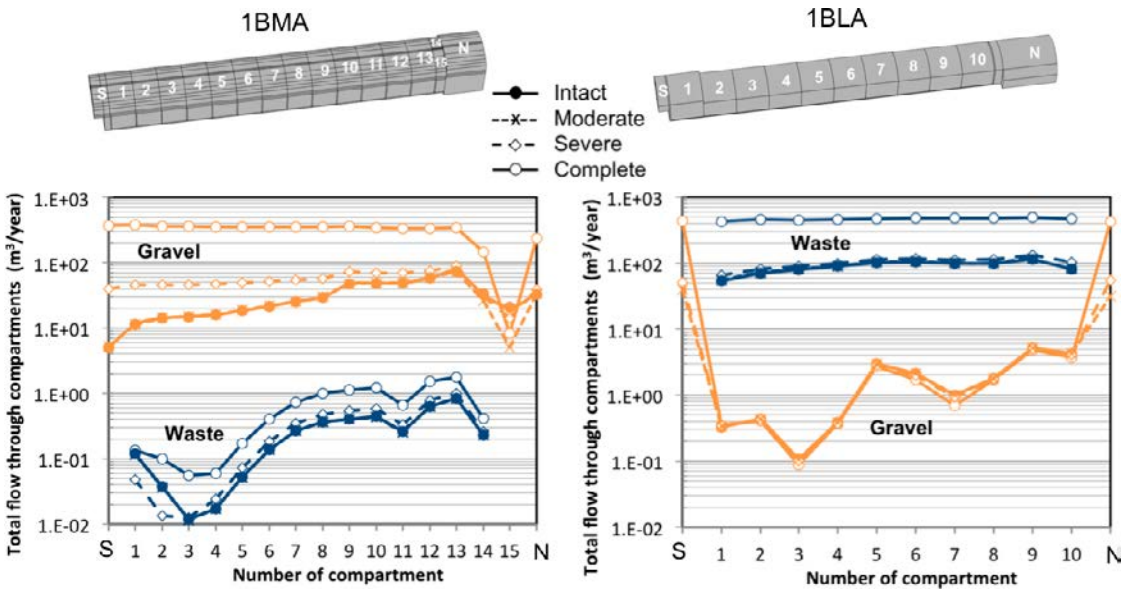

Figure 6-19. *Total flow (m^3/year) along the different gravel and waste sections of the 1BMA (left) and 1BLA (right) for shoreline position 3.*

In the case of severe plug degradation, there is a generalized increase of the flow through all the vaults. The longitudinal profiles of flow distribution (Figure 6-19) show that the increase on flow through the 1BMA (25% increase) gravel affects mainly the southern sections of the vaults. In the case of the 1BLA, the flow increase (12%) corresponds to the increase in the north and south loading areas, without impacting substantially the inner part of the tunnel. The largest impact occurs in the 1BTF (101% increase) and the 2BTF vault (63% increase). The profile of flow distribution shows that the tunnel flow increases homogeneously for all tunnel sections (Figure 6-20). However, even though the tunnel flow increases, there is a reduction in flow through the waste of 15.5% in the 2BTF and of 21% in the 1BTF. In the Silo, a redistribution of the flow is observed. The Silo waste flow increases 77% affecting to a greater extent to the upper sections of the Silo (Figure 6-21), whereas the flow through the gravel dome of the Silo is reduced. This result suggests that, as plugs degrade, part of the water circulating though the Silo dome penetrates into the Silo encapsulation.

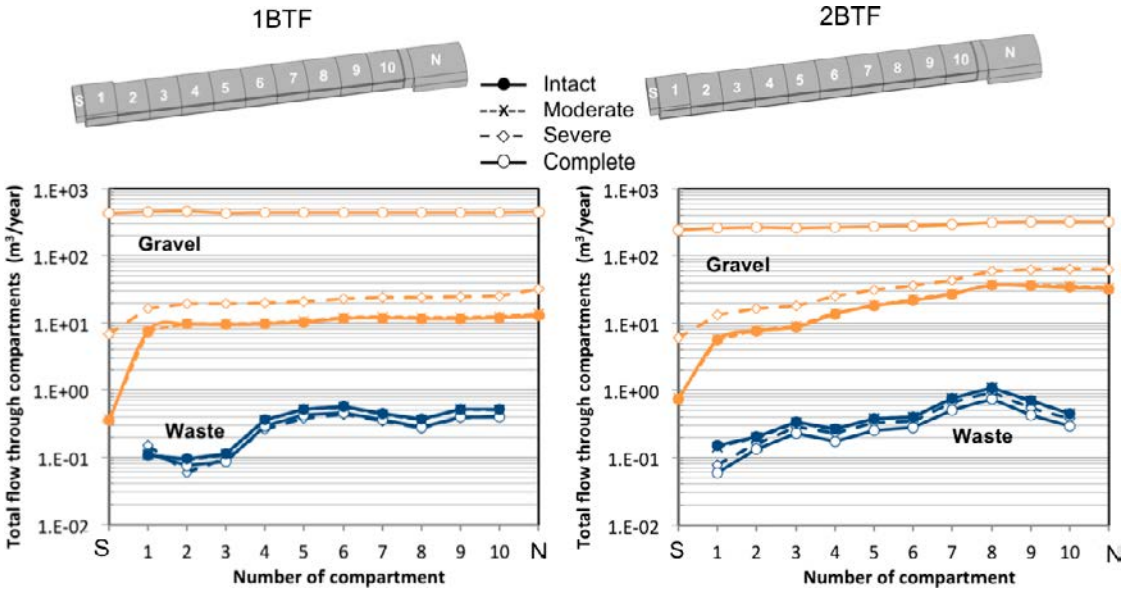

Figure 6-20. *Total flow (m³/year) along the different gravel and waste sections of the 1BTF (left) and 2BTF (right) for the shoreline position 3.*

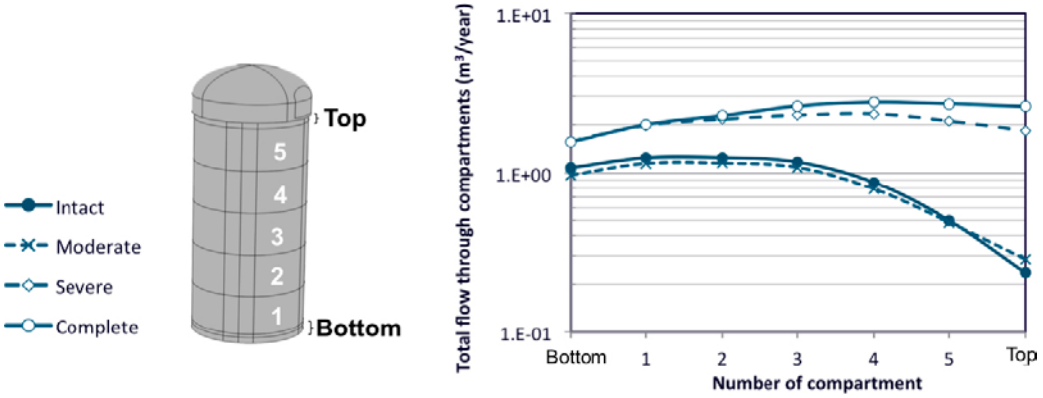

Figure 6-21. *Total flow (m³/year) along the different waste sections of the Silo for the shoreline position 3.*

In the case of a complete degradation of the plugs (conductivity equals the backfill conductivity), the total flow through all vaults substantially increases. The flow profiles show a flat tunnel flow distribution for all tunnel sections (Figure 6-19, Figure 6-20). The maximum effect is again observed in the 1BTF, for which an increase of more than an order of magnitude of the flow through the vault is observed. However, as for the case of severe plug degradation, the waste flow is reduced with respect to the Base case by 18% in the 1BTF and by 34% in the 2BTF. These vaults present an increase in the total vault flow but a decrease in the waste flow. This fact is also evidenced by the differences in the Darcy velocity when the plugs degrade with respect to the Base case (see Figure 6-22 for the complete degradation case, and Appendix C for the remaining cases). These differences show that, for the completely degraded case, most of the flow increase occurs in the backfill areas whereas the flux diminishes in the waste compartments. This result, consistent with the reduction of computed BTF waste flow (Table 6-6) indicates that part of the flow that is forced through the 1-2BTF waste encapsulation when the plugs are intact circumvents the 1-2BTF waste when the plugs degrade. There is a strong lateral component of the flow from East to West in shoreline position 3 that can be observed in Figure 6-23. Therefore, when the plugs are intact some inflow occurs from the East side of the repository and is forced through the 1BTF and 2BTF concrete grouting. It should be mentioned that the BTF vaults do not have high permeability materials surrounding the vault walls and the waste compartments are in direct contact with the surrounding rock. When the plugs degrade, there is better connection between the East and West through the by-pass formed by the South and North ends and the lateral access tunnels. This bypass reduces the pressure gradient between the East and the West sides of the BTF vaults and reducing the lateral flow forced though the BTF waste compartments. Figure 6-22 shows also the consistent groundwater flow reduction in the rock surrounding the BTF vaults.

Finally, the Silo increases the flow through the gravel dome substantially (487%) while the flow through the waste domain shows an increase of 110% with respect to the Base case. In the case of the Silo (without dome), the complete degradation case is not much worse than the severe plug degradation.

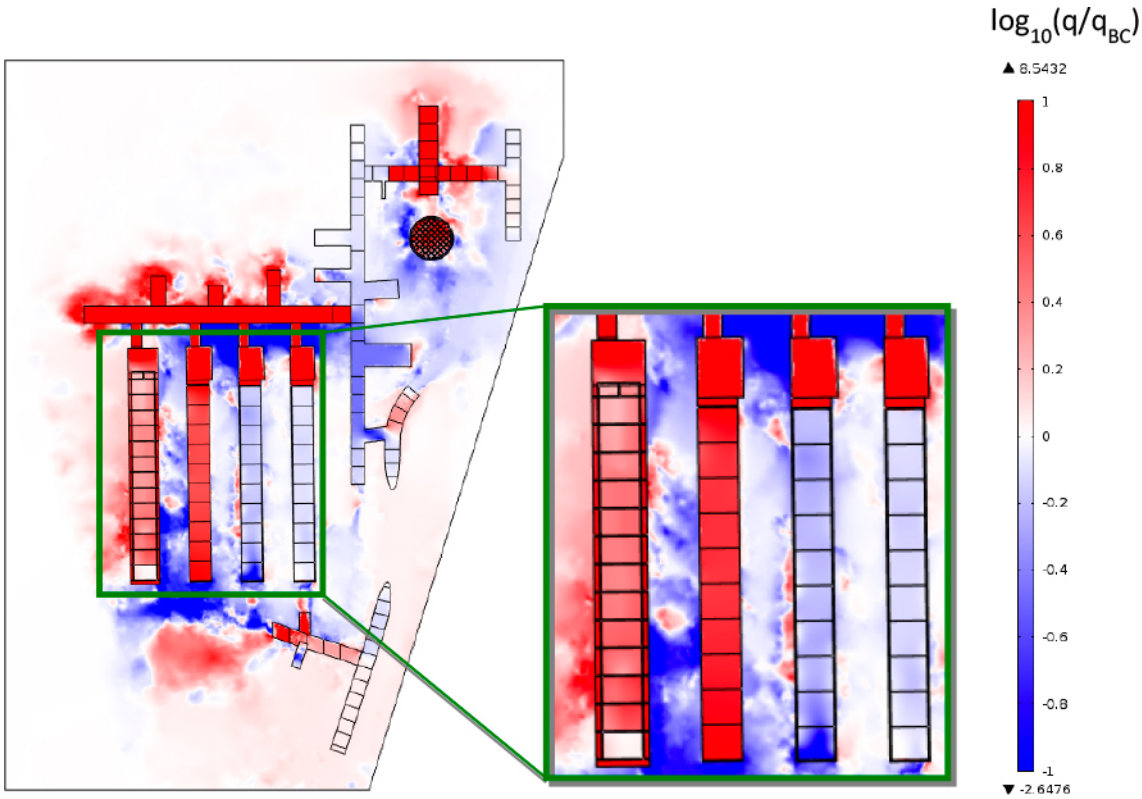

Figure 6-22. *Ratio of the Darcy velocity magnitude between the case of complete degraded plug and the Base case at the shoreline position 3 in a xy plane at z= –82.5. Values greater than one indicate a higher flow in the alternative closure case.*

Figure 6-23 illustrates the changes in the regional groundwater flow due to the plug degradation. It depicts 50 streamlines per vault, which originate at the surface of each vault (shown in different colors). The discharge streamlines (right) indicate discharge pathways of water leaving the vaults. In turn, the streamlines (right) illustrate the pathways of groundwater flowing into the vaults. Note that the streamlines are not proportional to the magnitude of the flow, for clarity. However, zones of converging streamlines indicate high flow areas. The color of the streamlines indicates the vault of origin of the streamlines.

The analysis of the discharge streamlines shows that in the Base case there are two main discharge areas from the vaults. The first one, at the northwest of the model domain is controlled by the combination of the deformation zone ZFMNNW1209 and the sub horizontal deformation zone ZFM871. ZFM871 concentrates the discharging flow from all the vaults, with the exception of the Silo, which has a second distinct discharge area localized north of the Silo. As the bentonite conductivity increases, the contribution of the northwest area to the discharge of the Silo also increases. In the moderately degraded plugs case, part of the Silo discharge of moves west, converging with the discharge from other vaults. Part of the 1BTF discharge moves east as the plugs degrade. In the case of completely degraded plugs, part of the discharge from the 1BTF is redirected through the plugs towards the access tunnels and from there to the discharge area north to the Silo.

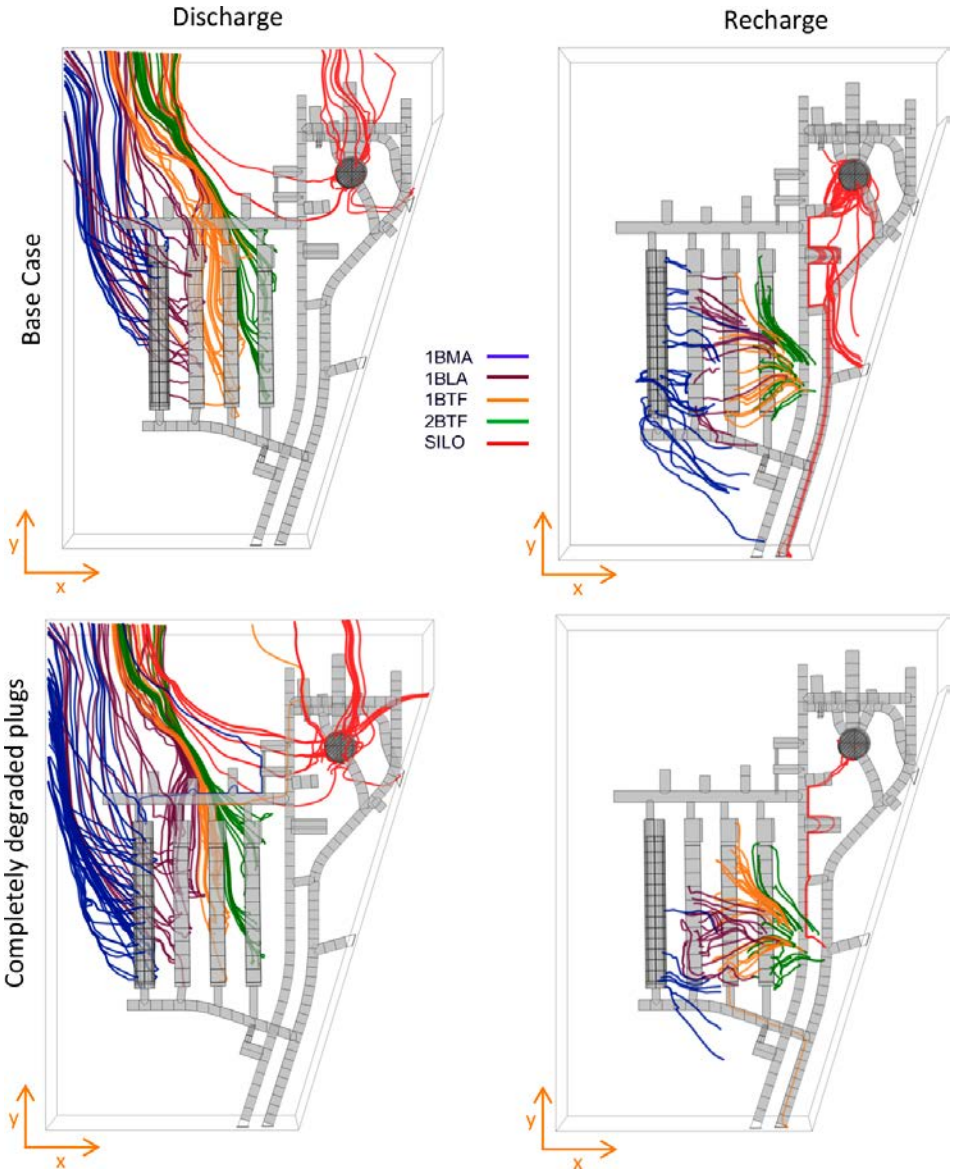

Figure 6-23. *Comparison of the streamlines of the groundwater leaving (left) and reaching (right) the vaults for the Base case (top) and the case of completely degraded plugs (bottom) at shoreline position 3. Each color corresponds to the streamlines originated in a different vault.*

The recharge streamlines (Figure 6-23) are also modified by plug degradation. In the Base case (for shoreline position 3), groundwater flows downwards through the deformation zone ZFMNNW1209 and some other minor vertical fractures. As the plugs degrade, the access tunnels become an important recharge source for all vaults, including the 1BMA (the furthest West vault). In the Base case, the eastern part of the 1BMA has a southern inflow area and a northern discharge area. As the permeability of the plugs increases, the inflow area is reduced, becoming a discharge area in the completely degraded plugs case.

In summary, moderate plug degradation has a limited influence on groundwater flow rates through the vaults and waste. Severe degradation leads to an increase of the waste flow rates through some vaults, with the greatest increase observed for the Silo (+77%). The complete degradation of the plugs leads to significantly larger flow rates in all vaults. The flow through the waste is notably larger for the 1BLA (+230%), 1BMA (+100%), and Silo (+110%), when compared to the Base case. The complete degradation of the plugs leads to an increase of flow through both BTF vaults. However, this is not accompanied by an increase in the waste flow. On the contrary, the flow though the 1-2BTF waste is even reduced by 18–34% in the case of completely degraded plugs.

6.2.3 No barriers

In this calculation case the complete degradation of the concrete barriers and the bentonite barriers is considered simultaneously. This case is a combination of the completely degraded concrete and the completely degraded plugs cases, in addition to the complete degradation of the Silo bentonite walls and the sand-bentonite top and bottom layers. All the concrete and bentonite domains have a conductivity of 10^{-3} m/s. This case has been evaluated for the shoreline position 3. The total vault and waste flow for this case is compared to the Base case and with the complete plug degradation case results in Table 6-7 and Figure 6-24. The most affected vault is the Silo, which flow (vault and waste) is increased three orders of magnitude with respect to the Base case and the complete plug degradation. This is due to the effect of a complete degradation of the bentonite walls and sand-bentonite top and bottom layers. In this situation, there is no flow barrier in the Silo, as opposed to the other cases.

The total flows in each vault are otherwise comparable to the complete plugs degradation case, showing a small reduction for the 1BMA (–11%) and 1BLA (–38%) and an increase in the 1-2BTF vaults (46–65%).

Table 6-7. Total flow through the vaults (m^3/year) for the no barriers case and comparison with the Base case (BC) and complete plug degradation (CPD) case for the shoreline position 3. Negative percentages indicate a reduction in flow with respect to the Base case.

		Total flow (m^3/year)	Difference BC	Difference CPD
Vaults	1BMA	323.30	0.36	–11%
	1BLA	335.15	1.28	–38%
	1BTF	774.54	42.16	65%
	2BTF	501.10	10.52	46%
	Silo*	1,687.52	114,652%	59,530%
	Silo dome	1,614.64	39,356%	7,157%
Waste	1BMA	280.09	8,069%	3,215%
	1BLA	327.10	135%	–37%
	1BTF	625.43	17,780%	22,237%
	2BTF	401.55	8,690%	13,466%
	Silo	1,637.65	120,620%	59,451%

* Silo results correspond to the waste domain defined in Figure 4-5

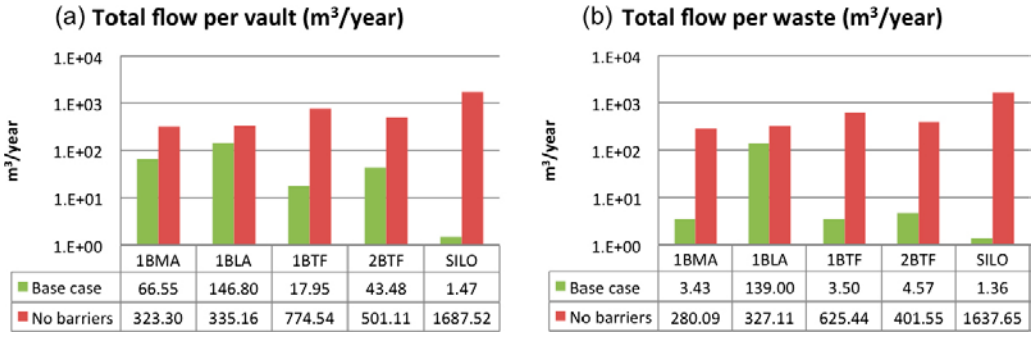

Figure 6-24. *Total flow entering the SFR 1 vaults (a) and waste domains (b) for the no barriers calculation case (shoreline position 3). The vertical axis is logarithmic.*

The flow through the waste domain is at least two orders of magnitude higher than the Base case. An exception is the 1BLA, for which the increase is much smaller (235%), which is due to the flow redistribution between the vaults. Flow from south to north occurs in this case through the completely degraded westernmost BTF vaults, decreasing the flow through the easternmost vaults. The ratio of waste flow to the total vault flow is in the range 80–86% for the 1BMA, 1BTF and 2BTF. For the 1BLA and the Silo, this ratio is as high as 97%, although in these cases the waste domain has a similar volume than the total vault domain. The increase of the flow through all the vaults, the Silo, and waste is also observed in Figure 6-25 in terms of the ratio of the Darcy velocity magnitude between the case of no barriers and the Base case.

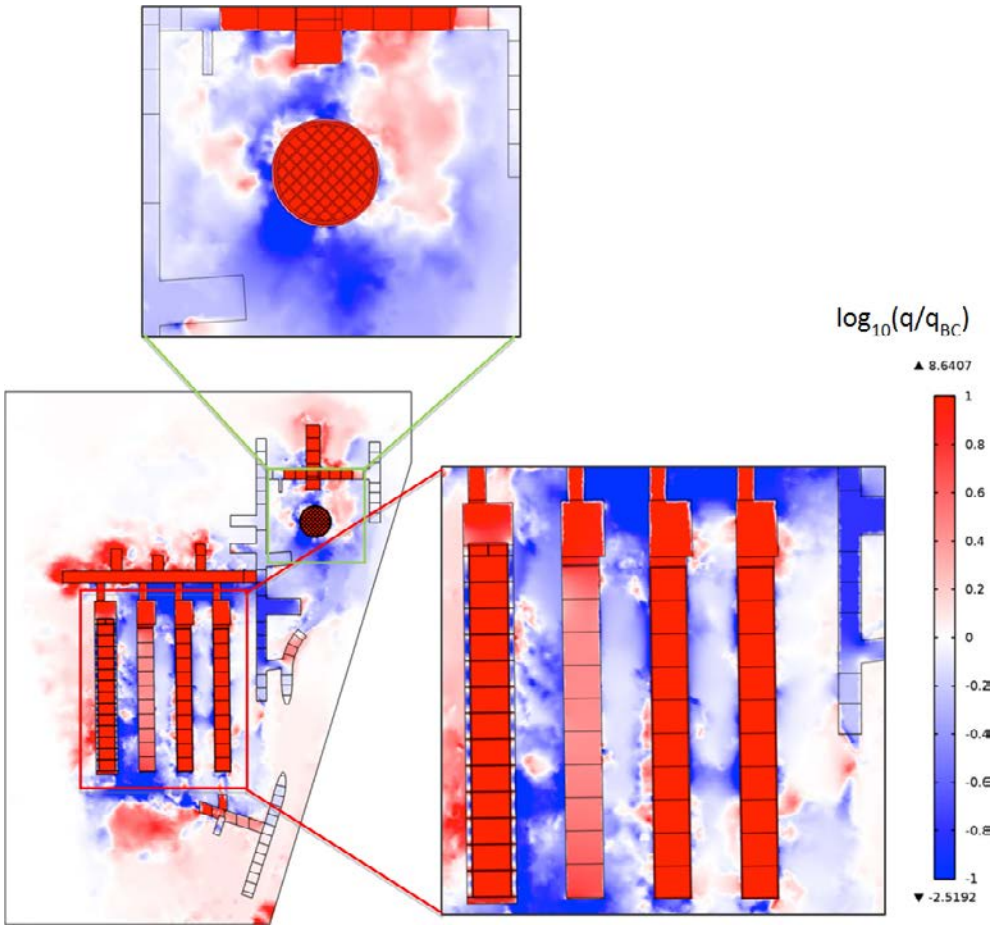

Figure 6-25. *Ratio of the Darcy velocity magnitude between the case of no barriers and the Base case at the shoreline position 3 in a xy plane at z= –82.5. Values greater than one indicate a higher flow in the alternative closure case*

6.2.4 Ice lens

This calculation case explores the effect of an ice lens on the local groundwater flow, formed as permafrost reaches Silo depth. The ice lens is assumed to cause degradation of a section of the outer bentonite wall of the Silo. In the model, the degradation of the bentonite has been simulated by a 10.67 m-thick ring of high hydraulic conductivity (10^{-3} m/s) in the Silo walls (see Figure 6-26), at mid-height of the waste domain. The Silo waste domain has been divided into a top and a bottom lid, and five subdomains with the same height (see Figure 6-26), being subdomain number 3 the degraded one. The rest of the material properties are the same as in the Base case (see Table 3-3).

The degradation of the bentonite ring results in an increase of the total flow through the Silo (Table 6-8) for all the shoreline positions. It is worth noticing that the total flow has been evaluated in a volume that includes the waste domain and the concrete and bentonite walls (see the pink contour in Figure 6-26). A maximum increase of total flow into the waste domain of 350% with respect to the Base case occurs for the shoreline position 2. The flow increase for the shoreline positions 1 and 3 is of 70% and 277%, respectively.

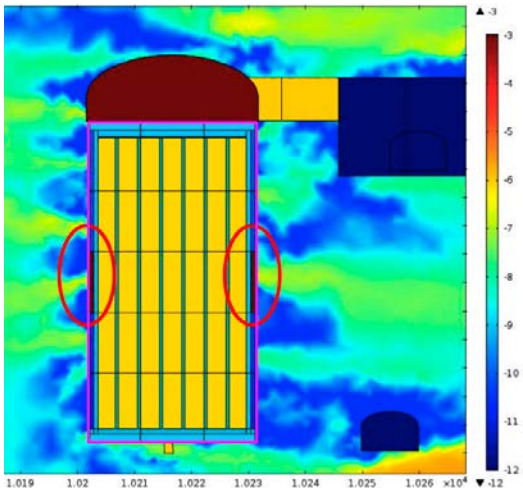

Figure 6-26. *Hydraulic conductivity (log_{10}(K (m/s)) in a yz plane crossing the Silo center (x = 6,537.5 m). Note the high permeability ring in the middle of the outer bentonite walls. The pink contour represents the volume where the total flows are evaluated.*

Table 6-8. Total flow through the Silo sections (m^3/year) and comparison with the Base case (BC). Negative percentages indicate a reduction in the total flow with respect to the Base case.

	Shoreline position 1		Shoreline position 2		Shoreline position 3	
Section	**Total flow (m^3/year)**	**Difference BC**	**Total flow (m^3/year)**	**Difference BC**	**Total flow (m^3/year)**	**Difference BC**
Bottom lid	0.002	–33%	0.341	161%	1.510	40%
1	0.002	–33%	0.405	138%	1.800	45%
2	0.002	–34%	0.416	84%	1.829	47%
3*	0.008	100%	3.331	1,069%	7.485	540%
4	0.006	34%	0.837	110%	0.570	–34%
5	0.006	31%	0.963	71%	0.779	56%
Top lid	0.006	26%	0.991	60%	0.893	280%
Total	**0.032**	**19%**	**7.285**	**204%**	**14.866**	**135%**

* degraded bentonite ring

As expected, the flow increases dramatically in the degraded section whereas the flow increase in the rest of the Silo is moderate, and is even reduced in some cases. Analyzing the flow computed for different vertical sections (Table 6-8 and Figure 6-27), a localized peak of high flow is observed at the section affected by the bentonite degradation (section 3). The increase of flow in this section is 100%, 1,069% and 540% with respect to the Base case for the three shoreline positions, respectively. The flows across the neighboring sections are also affected. For instance, for the shoreline position 1, flow increases around 30% in the sections above the degraded bentonite (sections 4, 5, and top lid) and decrease in a similar magnitude in the sections below. This result suggests an upward movement of the water entering the Silo through the degraded section. For the shoreline position 2, there is an 84% increase of flow in section 2 and a 110% in the above section. For the shoreline position 3, there is an increase of 45% in the flow through the lower two sections (1 and 2) evidencing a downward movement of a portion of the water entering the Silo through the degraded bentonite ring However, there is a flow decrease in the upper section probably due to the concentration of flow towards section 3.

Figure 6-28 presents the velocity vectors in a xy-plane crossing the Silo at the middle of the degraded bentonite ring. The plots for the three different shoreline positions illustrate how groundwater flows within section 3. For the shoreline position 1, water enters the degraded ring at the southern border, flows north within the ring itself and leaves the ring through the northern part. A similar recirculation, but with a SW-NE component, is observed for the shoreline positions 2 and 3. It is important to note that most of the water entering section 3 only recirculates within the degraded zone itself, without penetrating the Silo structure and the waste. Therefore the total amount of water entering section 3 is not a good indicator of the water entering the non-degraded regions of the Silo. The same applies to the total flow across the Silo, which is dominated by the high recirculating flow in section 3. A better indicator of the water infiltrating into the non-degraded Silo is the increase of flow in the neighboring sections 2 and 4. The source of that overflow is the groundwater transmitted from section 3 to the adjoining sections. According to this indicator, the flow in the intact Silo increases by around 5%, 190% and 15% with respect to the Base case for the shoreline positions 1, 2, and 3, respectively. These quantities are much lower than the estimates based on the total or the peak flows.

The presence of an ice lens that degrades a section of the Silo bentonite wall results in an increase in total flow in the Silo. However, most of this water recirculates within the degraded bentonite section without penetrating the waste encapsulation. Considering only the flow increase through the intact sections of the Silo, the increase of flow is minor for the shoreline position 1 (5%) and shoreline position 3 (15%) cases, and it is considerably high in the shoreline position 2 (190%).

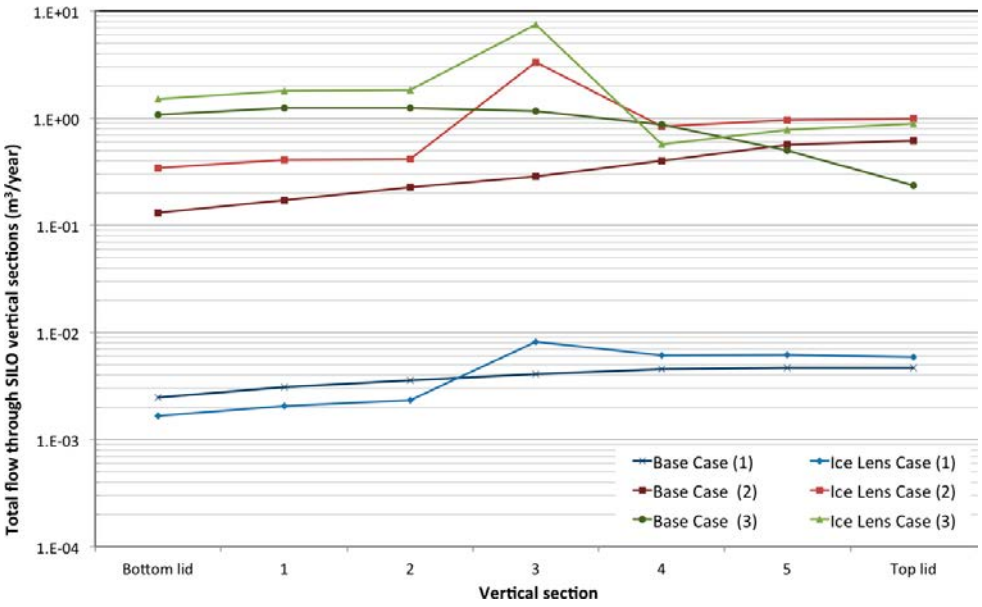

Figure 6-27. *Total flow through the vertical Silo sections of the Base case and the Ice lens case for the three shoreline positions (1, 2 and 3). The vertical axis is logarithmic.*

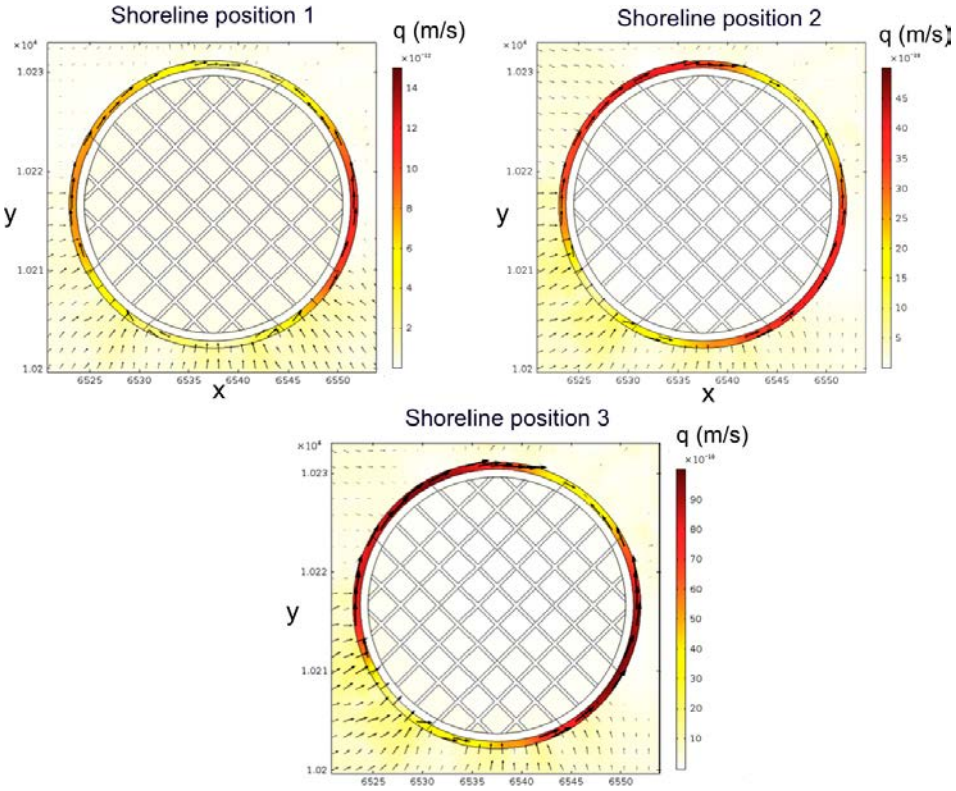

Figure 6-28. *Darcy velocity (m/s) distribution and vectors in a cross section of the Silo traversing the degraded ring (z = –105 m) for the three shoreline positions. For visualization purposes the logarithmic scale of the velocity vectors is different for each plot.*

6.3 Repository closure

6.3.1 Effect of extended bentonite sections

The objective of this section is to assess the effects of two different closure alternatives on the hydrodynamic behavior of the near-field of the repository. Figure 6-29 shows the geometries and main characteristics of the proposed Base case and alternative closures of the repository and Figure 6-30 shows the implementation in the COMSOL model of the two closure layouts. The Base case closure consists of extended sections of bentonite (hydraulic conductivity of 10^{-12} m/s) and structural plugs (hydraulic conductivity of 10^{-6} m/s). The alternative closure considers short sections of bentonite with concrete plugs with a hydraulic conductivity of 5×10^{-10} m/s. This configuration represents a situation where a significantly less bentonite is used to seal the repository.

The total flow rates through the tunnels and waste domains (Table 6-9) of each repository vault for the closure alternative are shown in Figure 6-31 as bar plots for all shoreline positions. It may be observed that both the flow through the vaults and through the waste domains do not differ significantly between the two closure calculation cases, with differences always smaller than 40% (except for the 1BLA for shoreline position 1). The flow rates through the 1BMA, 1BLA, and 2BTF vaults are higher for the alternative closure for the shoreline position 1. The minimum increase occurs for the 1BMA vault. On the other hand, the Silo shows a decrease of the flow with respect to the Base case, while the 1BTF is relatively unaffected by the closure alternatives. Regarding the flow through the waste domains, the trends are similar to the flow in the vaults. The 1BLA seems to be most affected by the closure alternative for the shoreline position 1. In turn, the total flow through the vaults for the shorelines positions 2 and 3 is either unaffected (e.g. in the 1BMA) or lower than for the Base case. The Silo at shoreline position 3 is the only vault that shows an increase in flow in the case of the alternative closure both through the waste and the gravel dome (Table 6-9). The flow through the waste of the 1-2BTF shows an interesting pattern. Even though the total flow through the vault decreases, the waste flow increases for these two vaults for shoreline positions 2 and 3 due to flow redistribution from the gravel (Figure 6-33).

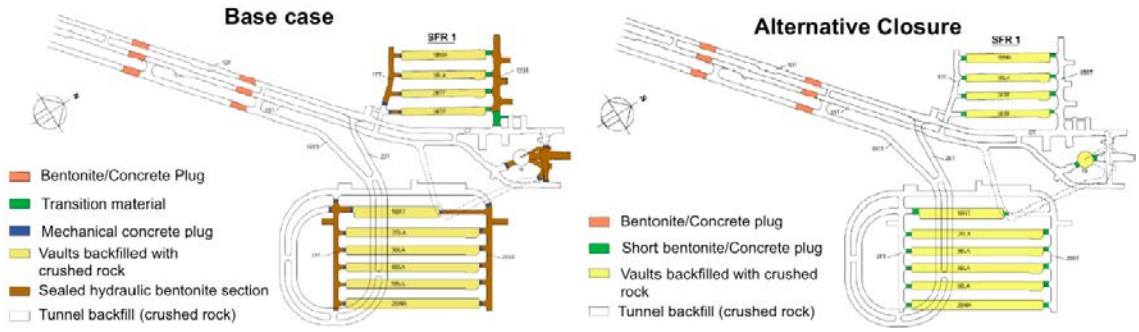

Figure 6-29. *Design of the extended bentonite sections of the Base case (left) and the alternative closure (right).*

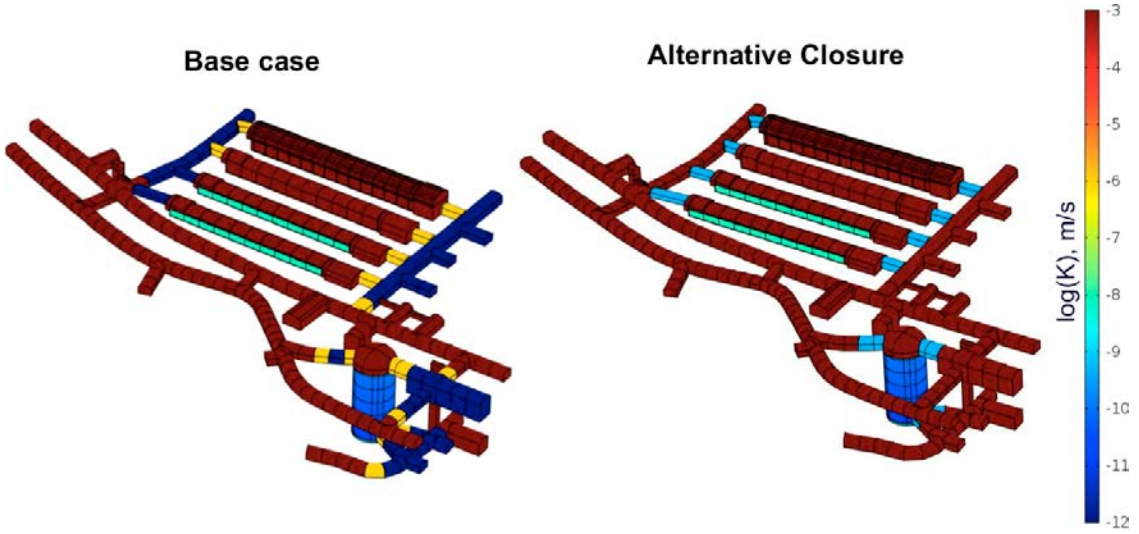

Figure 6-30. *Parameterization in the COMSOL geometry of the Base case closure (left) and the alternative closure (right).*

Table 6-9. Total flow through the SFR 1 vaults (m³/year) for the alternative closure case and comparison with the Base case (BC). Negative percentages indicate a reduction in the total flow with respect to the Base case.

		Shoreline position 1		Shoreline position 2		Shoreline position 3	
		Total flow (m³/year)	Difference BC	Total flow (m³/year)	Difference BC	Total flow (m³/year)	Difference BC
Vaults	1BMA	0.052	14.7%	29.892	–1.6%	64.819	–2.6%
	1BLA	0.222	66.7%	59.306	–9.1%	129.337	–11.9%
	1BTF	0.027	–1.1%	5.907	–24.3%	12.341	–31.2%
	2BTF	0.066	39.6%	16.890	–15.1%	30.286	–30.3%
	Silo*	0.004	–20.6%	0.636	–14.2%	1.507	2.5%
	Silo dome	0.007	–12.5%	2.318	–0.68%	4.131	9.17%
Waste	1BMA	0.008	1.2%	1.297	1.8%	3.432	0.1%
	1BLA	0.198	61.5%	55.629	–9.3%	121.275	–12.7%
	1BTF	0.008	–9.8%	1.865	8.7%	3.905	11.6%
	2BTF	0.008	–3.9%	2.548	5.1%	4.946	8.3%
	Silo*	0.004	–20.4%	0.581	–14.8%	1.473	8.6%

* Silo results correspond to the waste domain defined in Figure 4-5.

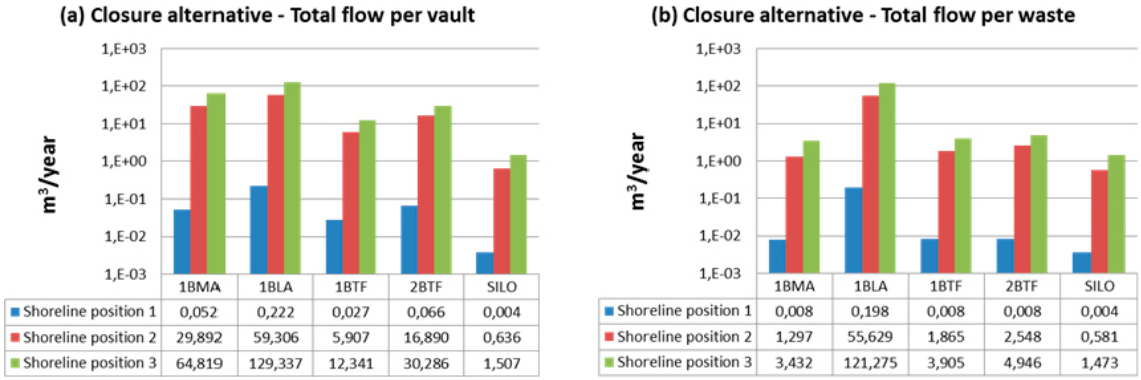

	1BMA	1BLA	1BTF	2BTF	SILO
Shoreline position 1	0,052	0,222	0,027	0,066	0,004
Shoreline position 2	29,892	59,306	5,907	16,890	0,636
Shoreline position 3	64,819	129,337	12,341	30,286	1,507

	1BMA	1BLA	1BTF	2BTF	SILO
Shoreline position 1	0,008	0,198	0,008	0,008	0,004
Shoreline position 2	1,297	55,629	1,865	2,548	0,581
Shoreline position 3	3,432	121,275	3,905	4,946	1,473

Figure 6-31. *Total flow entering the SFR 1 vaults (a) and waste domains (b) for the closure alternative for the three shoreline positions. Negative differences indicate a flow reduction with respect to the Base case. The vertical axis is logarithmic.*

A more detailed analysis of the fluxes is needed to understand the redistribution of flow. To that end, the longitudinal profiles of flow distribution per vault (Figure 6-32, Figure 6-33, and Figure 6-34) and the difference in the Darcy velocity in a horizontal plane crossing the repository waste domains are analyzed. Figure 6-35 shows the ratio between the Darcy velocity of the closure alternative case and the Base case for the shoreline position 3 (the figures for shoreline positions 1 and 2 can be found in Appendix B).

The 1BMA flow profile (Figure 6-32) shows that the flow increase for shoreline position 1 is localized in southern gravel sections, with no appreciable changes in the waste profile. For shoreline positions 2 and 3, the 1BMA gravel and waste profiles for the two closure alternatives are similar. The 1BLA waste profile (Figure 6-32) for the closure alternative shows a larger increase of flow in the southern part of the vault for shoreline position 1. However, the waste flow is reduced in all sections for shoreline positions 2 and 3.

The 1BTF and 2BTF waste profiles for the two closure alternatives are very similar (Figure 6-33). It is worth noticing that, for shoreline positions 2 and 3, the waste flow slightly increases in all sections while the gravel flow diminishes. The increase of flow along the 1BFT and 2BTF waste does not show preferential inflow areas associated with deformation zones, indicating that part of the reduction of the flow through the gravel is due to a redistribution of flow to the waste domain.

In the Silo, the alternative closure case leads to a small homogeneous reduction of the flow through the vault and waste for shoreline position 1. For shoreline position 2, a reduction of the total flow is still observed, although in this case the alternative closure changes the flow pattern through the Silo (Figure 6-34). In the alternative closure case, the flow through the Silo is more homogeneously distributed across its height. For shoreline position 3, the alternative closure leads to a slightly higher total flow through the Silo vault and waste, although differences are smaller than 10%. This increase is homogeneously distributed across the Silo.

There is a trade-off between 1BLA and the 1-2BTF vaults. In all shoreline positions, when the 1BLA waste flow increases, the waste flow of the 1-2BTF vaults decreases and vice versa. This trade-off is illustrated by the groundwater velocity ratio of the two closure cases (Figure 6-35 for shoreline position 3 and Figure B-14 and Figure B-15 in Appendix B for shoreline positions 1 and 2). As observed in the plug degradation analysis, a reduction in the flow from the South to North part of the tunnels leads to an increase in the flow from East to West traversing the 1-2BTF grouted waste. The flow in the rock surrounding the 1-2BTF vaults is modified in the same way. The trade-off between the westernmost vaults absorbs most of the flow, protecting the easternmost vault and the 1BMA waste, whose waste flow remains mostly unaffected.

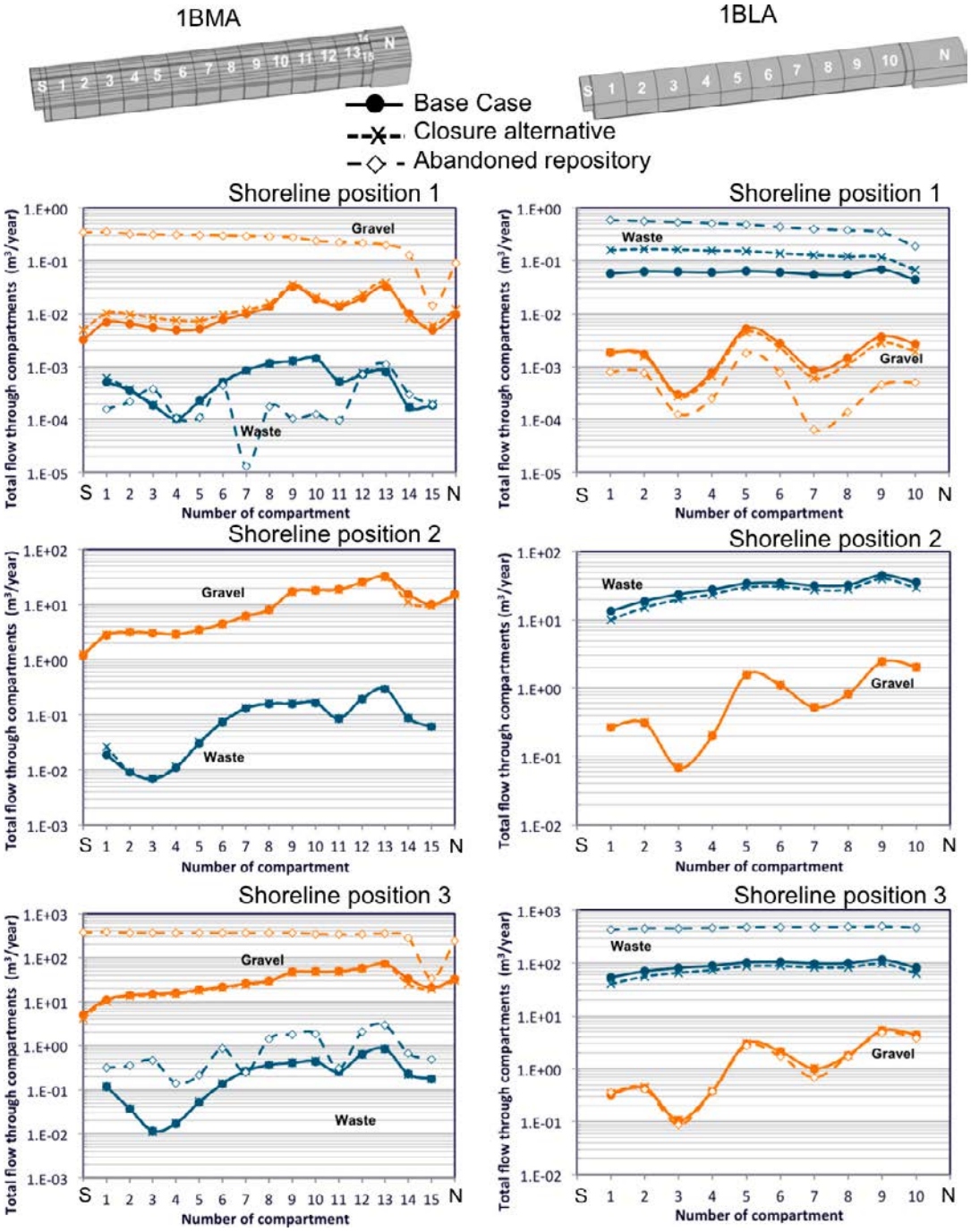

Figure 6-32. *Total flow (m³/year) along the different gravel and waste sections of the 1BMA (left) and 1BLA (right) for the three shoreline positions. The abandoned repository case was simulated for shorelines position 1 and 3. The vertical axis is logarithmic.*

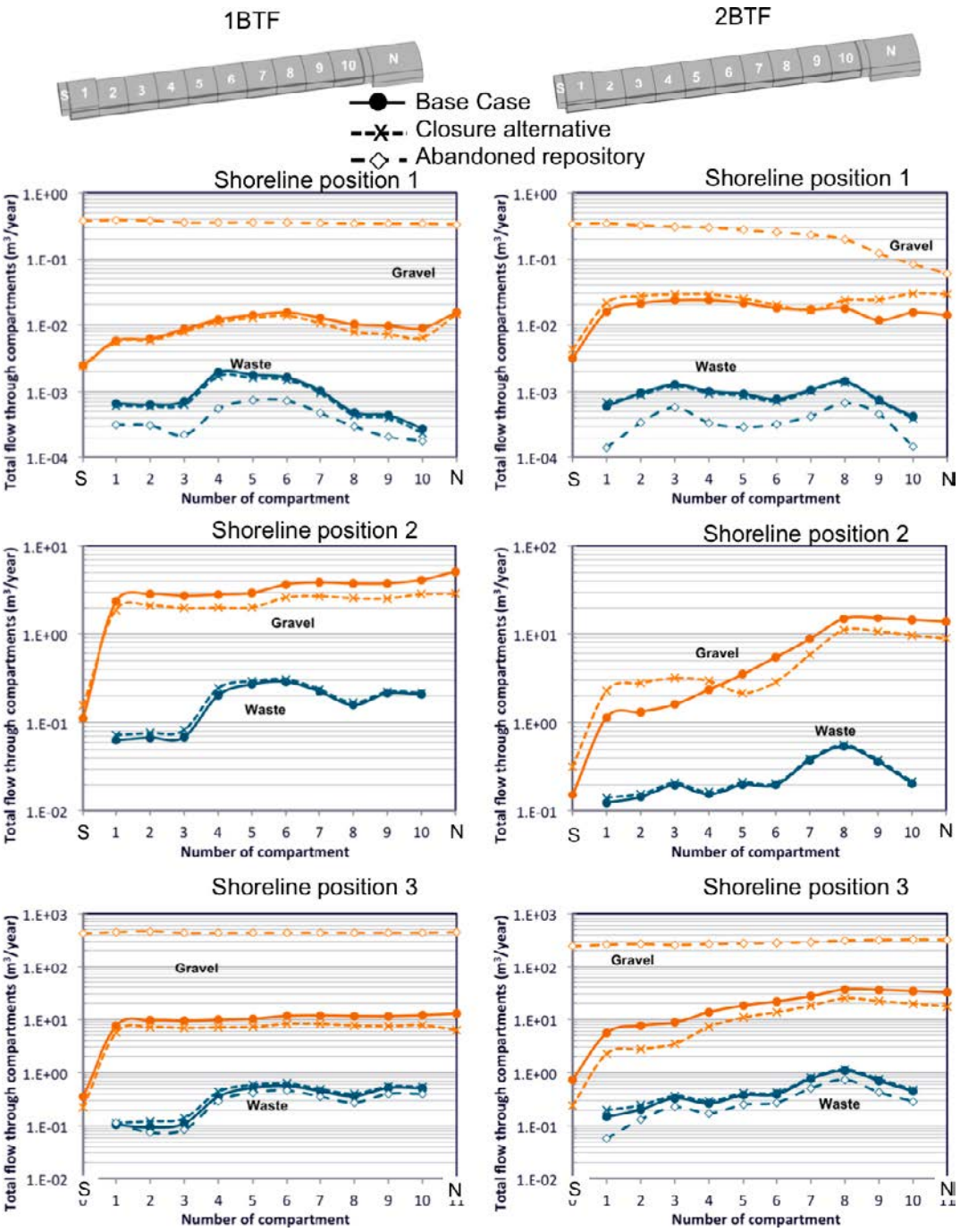

Figure 6-33. *Total flow (m^3/year) along the different gravel and waste sections of the 1BTF (left) and 2BTF (right) for the three shoreline positions. The abandoned repository case was simulated for shorelines position 1 and 3. The vertical axis is logarithmic.*

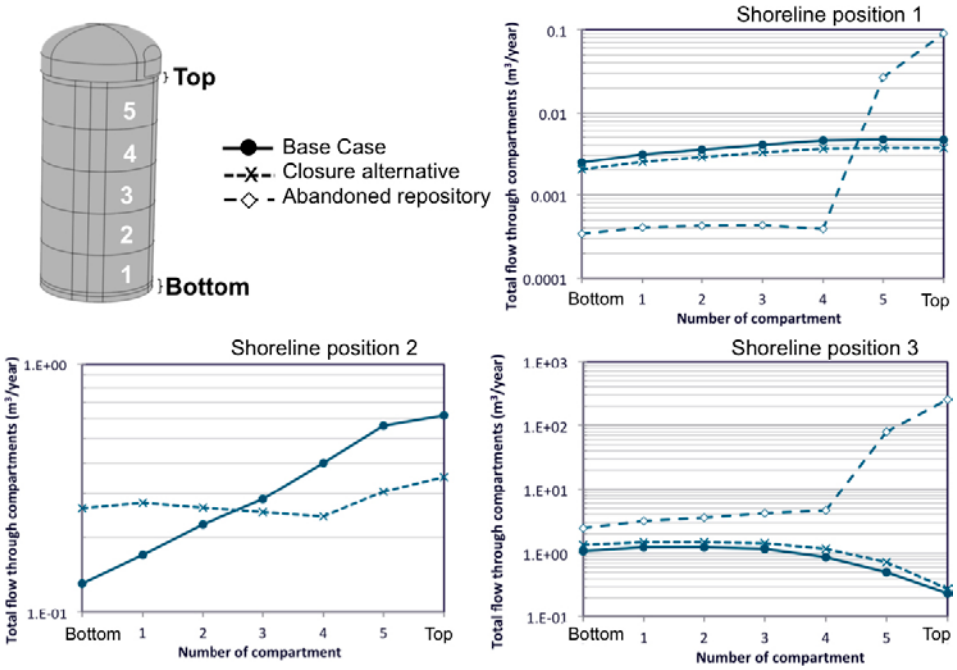

Figure 6-34. *Total flow (m^3/year) along the different waste sections of the Silo for the three shoreline positions. The abandoned repository case was simulated for shorelines position 1 and 3. The vertical axis is logarithmic.*

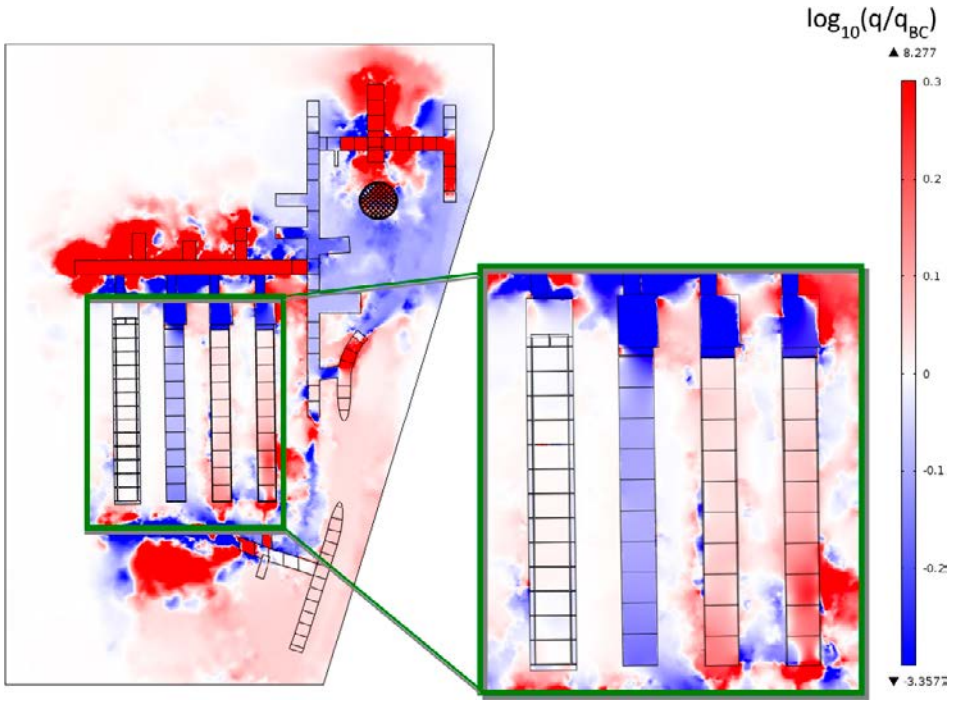

Figure 6-35. *Ratio between the Darcy velocity magnitude for the two closure alternatives at the shoreline position 3 in a xy plane at z= –82.5. Values greater than one indicate a higher flow in the alternative closure case.*

Figure 6-35 also evidences that the largest changes in groundwater velocity are localized in the areas where the material properties change between the two closure layouts, i.e., flux increases in the access tunnels (backfill in the closure alternative) and diminishes in the short bentonite sections. The velocity is also reduced in the north loading areas of the 1BLA, 1BTF, and 2BTF. Shoreline position 2 presents a similar pattern (Figure B-15 in Appendix B), whereas the opposite pattern is observed for shoreline position 2 (Figure B-14 in Appendix B).

The impact of the different closure alternatives in the groundwater paths to and from the vaults is analyzed by comparing the flow streamlines. Figure B-4, Figure B-5 and Figure B-6 in Appendix B show the inflow and outflow streamlines for shoreline positions 1, 2, and 3, respectively. Note that this comparison gives insight into the flow direction but does not contain information on the flow magnitude. Nevertheless, they help to identify the preferential pathways of the water through the repository. In general, the pattern of streamlines reaching and leaving the vaults (Figure 6-36) is similar in both closure alternatives. Only the Silo recharge and discharge areas are significantly modified. The recharge area is larger and the discharge zone is more concentrated to the North of the Silo in the alternative closure case.

Overall, it may be concluded that the hydrodynamic behavior is similar for the Base case and alternative closure options. Depending on the shoreline position, different flow adjustments are observed between the 1BLA and the 1-2BTF vaults while the flow though the 1BMA remains unaltered.

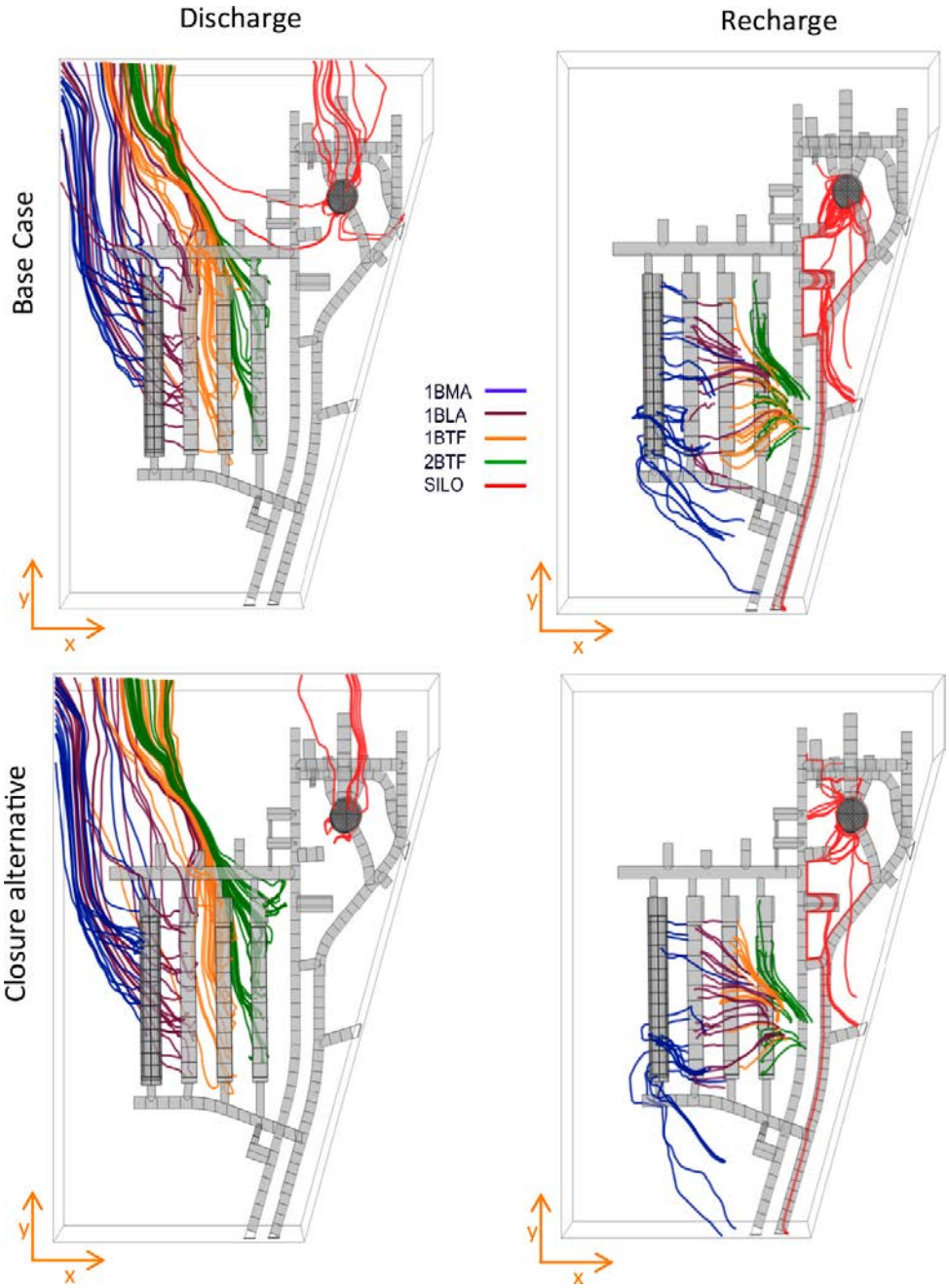

Figure 6-36. *Comparison of the groundwater streamlines leaving (left) and reaching (right) individual vaults (color tubes) for the Base case (top) and the alternative closure case (bottom) for the shoreline position 3.*

6.3.2 Abandoned repository

The abandoned repository calculation case represents a situation in which no additional barriers or structures are emplaced after the operational phase. The repository has not been sealed with bentonite plugs and the lids of the 1BMA and Silo have not been installed. To represent these materials (Figure 6-37) a high hydraulic conductivity of 10^{-3} m/s has been assumed, corresponding to the maximum permeability allowed in the model. This case has been simulated for the shoreline position 1 and shoreline position 3.

The calculated total tunnel and waste flows are presented in Table 6-10 and graphically in Figure 6-38. The tunnel flow increases dramatically with respect to the Base case in all vaults for the two shoreline positions. The highest increase occurs in the Silo for the shoreline position 3. The Silo is located in a low-pressure zone in the shoreline position 3. Thus, in absence of plugs, all water is directed through the access tunnels to the lower pressure zones, such as the Silo.

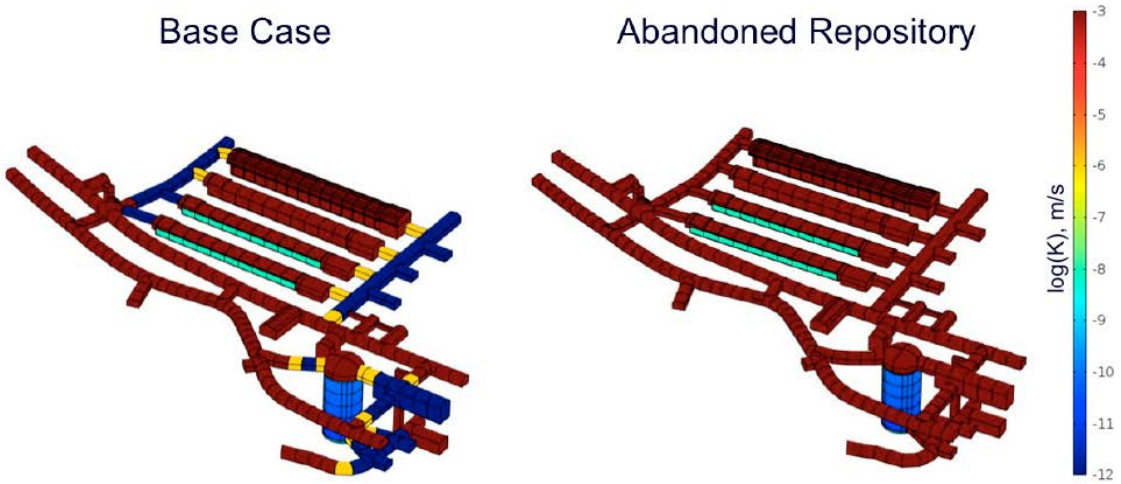

Figure 6-37. Hydraulic conductivity of the vaults and tunnels for the base case (left) and the abandoned repository case (right). The concrete lids are not shown in the figure.

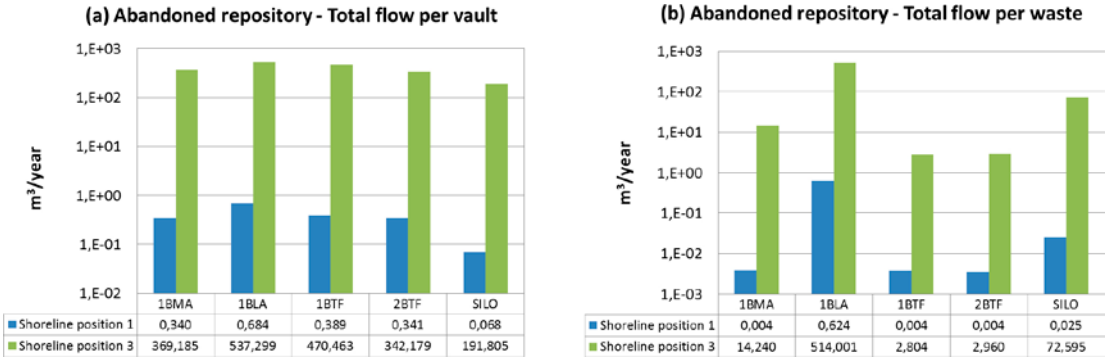

Figure 6-38. Total flow entering the SFR 1 vaults (a) and waste domains (b) for the abandoned repository case for the shoreline positions 1 and 3.

Table 6-10. Total flow through the SFR 1 vaults (m^3/year) for the abandoned repository case and comparison with the Base case (BC). Negative percentages indicate a reduction in the total flow with respect to the Base case.

		Shoreline position 1		Shoreline position 3	
		Total flow (m^3/year)	Difference BC	Total flow (m^3/year)	Difference BC
Vaults	1BMA	0.34	647%	369.18	455%
	1BLA	0.68	413%	537.29	266%
	1BTF	0.38	1,306%	470.46	2,521%
	2BTF	0.34	623%	342.17	687%
	Silo*	0.06	1,347%	191.80	12,943%
	Silo dome	0.003	–62.5%	19.58	417.54%
Waste	1BMA	0.004	–51%	14.24	315%
	1BLA	0.624	409%	514.00	270%
	1BTF	0.004	–58%	2.80	–20%
	2BTF	0.004	–60%	2.96	–35%
	Silo	0.025	451%	72.59	5,251%

To analyze the spatial distribution of the flow, the flow profiles per vault are compared with the Base case and the alternative closure case in Figure 6-32, Figure 6-33, and Figure 6-34. The gravel flow profiles are flat for the 1BMA and BTF vaults with the southern sections yielding a maximum flow increase with respect to the Base Case. The same behavior is observed for the 1BLA waste. The 1BMA waste flow is reduced for shoreline position 1 (vertical upwards flow) but it increases strongly for shoreline position 3 (horizontal flow). The flow decrease in the 1BMA waste in absence of both the plugs and the concrete lids of the 1BMA waste compartments is counterintuitive. Several factors play a roll. First, the vertical upward flow is the most favorable configuration for minimizing the impact of the absent concrete lids. Second, the absence of plugs in all vaults channels the flow from south to north through the vaults themselves therefore reducing the east to west flow between vaults though the fracture zones. This redistribution of flow is clearly depicted by the ratio between the Darcy velocity magnitude for the abandoned repository and the Base case at the shoreline position 1 (Figure 6-39). The flow in the rock between the 1BMA and the 1BLA vaults is reduced (Figure 6-39) and the minor fractures affecting the sections 9 and 10 of the 1BMA are deactivated as is evidenced by the reduction of flow in these sections in the waste flow profile of Figure 6-32. For shoreline position 3, the increase of the 1BMA waste flow is reduced in the sections located upstream of the fracture zones, i.e., in sections 7 and 11 (Figure 6-32). Even though the total flow in the BTFs vaults increases, the waste flow diminishes in the BTF vaults for both shoreline positions (Figure 6-33). This result is consistent with the results observed in the analysis of the plug degradation and closure alternative. In the absence of plugs, there is better connection between the East and West through the by-pass formed by the South and North ends and the lateral access tunnels. This bypass reduces the pressure gradient between the East and the West sides of the BTF vaults and diminishes the lateral flow though the BTF waste compartments. In the case of the Silo, the abandoned repository leads to a vertical redistribution of flow (Figure 6-34). For shoreline position 1, flow decreases in the lower sections of the Silo and increases in the upper sections. For shoreline position 3, flow increases in all sections but the largest increase occurs through the upper section 5 and the absent bentonite lid (top).

In summary, the vault flow increases dramatically in all vaults for shoreline positions 1 and 3. The highest increase occurs in the Silo for the shoreline position 3, located in a low-pressure zone, which gets the water directly from the access tunnels. The 1BMA and the BTF waste flows are reduced. In the absence of plugs, the vaults, specially the 1BLA vault, act as a flow by-pass from south to north of the repository reducing the flow through the rock and through the BTF waste from east to west.

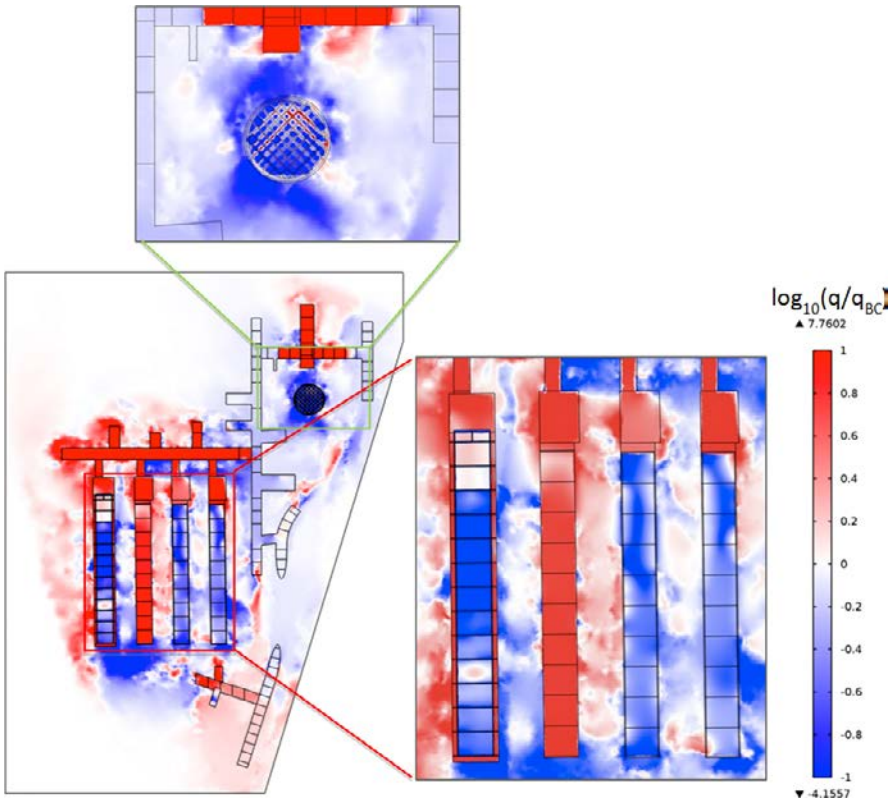

Figure 6-39. *Ratio (in log_{10} scale) of the Darcy velocity magnitude between the abandoned repository and the Base case at the shoreline position 1 in a xy plane at z= –82.5. Positive values indicate a higher flow in the abandoned repository case.*

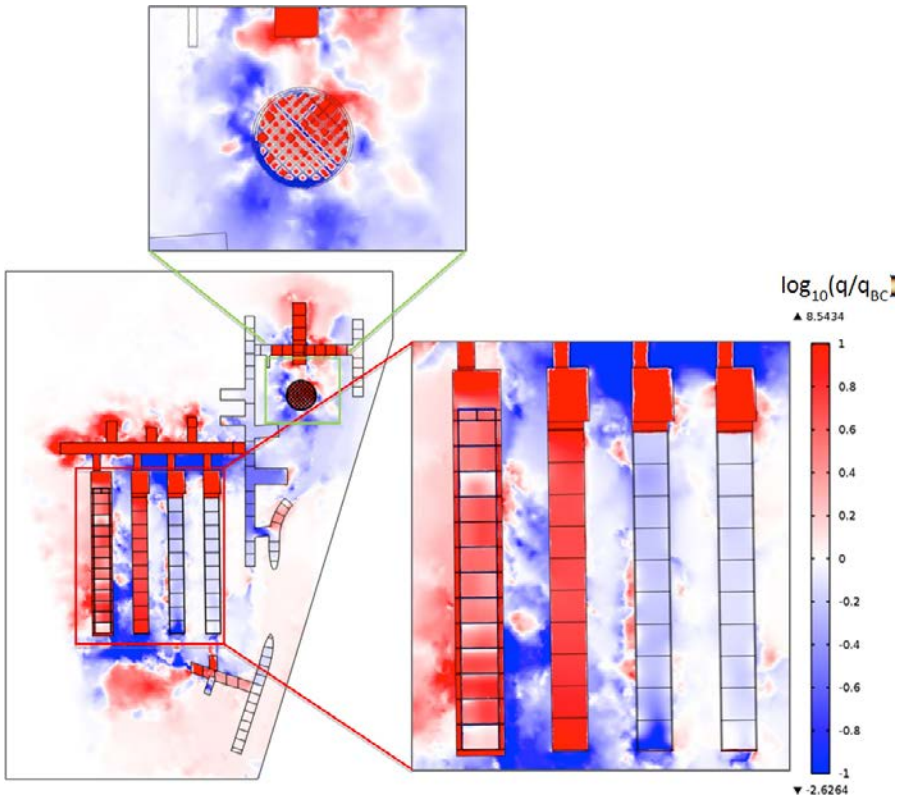

Figure 6-40. *Ratio (in log_{10} scale) of the Darcy velocity magnitude between the abandoned repository and the Base case at the shoreline position 2 in a xy plane at z= –82.5. Positive values indicate a higher flow in the abandoned repository case.*

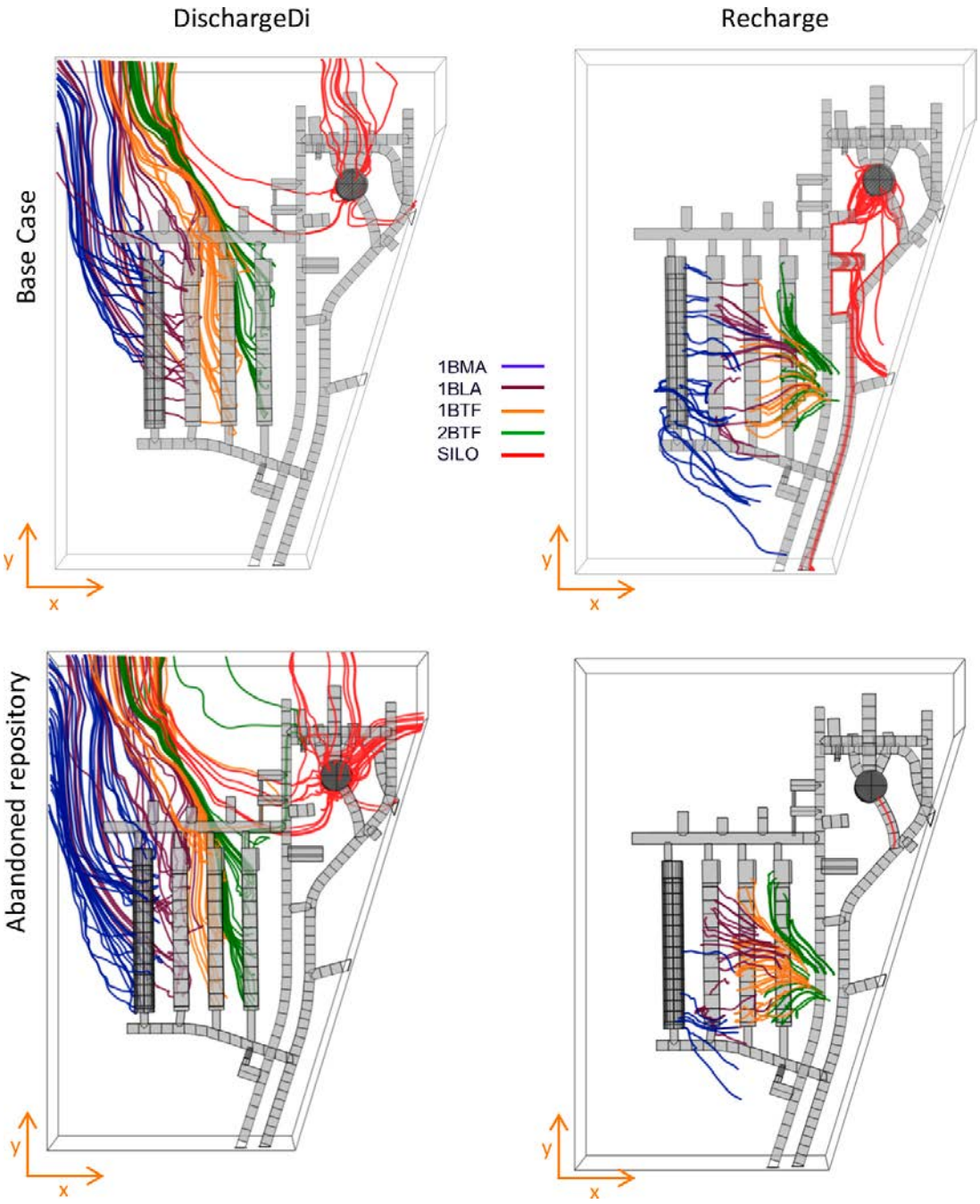

Figure 6-41. *Groundwater streamlines leaving (left) and reaching (right) individual vaults (color tubes) for the Base case (top) and the abandoned repository case (bottom) for the shoreline position 3.*

6.4 Permafrost

This simulation case studies the hydraulic response of the repository to the advance of permafrost. A case of shallow permafrost is considered where the frozen front is located above the vaults and Silo, at a depth of approximately –59 m (Figure 6-42). This case corresponds to the shallow permafrost case in Odén et al. (2014). The host rock realization used for the DarcyTools simulation of the permafrost corresponds to the hydraulic conductivity field of the Base case. The results of the DarcyTools simulation (Shallow permafrost case) that are used in the repository-scale model are the driving pressure field and the Darcy velocity field (from which boundary conditions are extracted) and the hydraulic conductivity field of the rock modified by the permafrost.

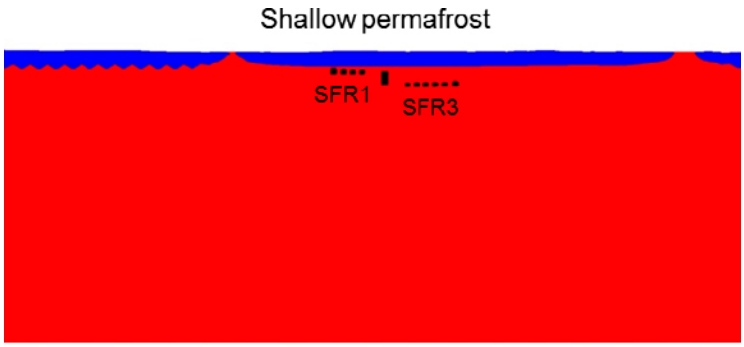

Figure 6-42. *Schematic representation of the Shallow permafrost case with the ice front above the vaults and Silo.*

It is noted that for this simulation it was not possible to consider the bedrock permeability field with the frozen front from DarcyTools prior to the tunnels excavation, as in the rest of simulations (see Section 3.6 for more details). This is due to the fact that the frozen front position is in part dependent on the thermal properties of the domain, which are significantly different in the tunnel and bedrock. For that reason, the permafrost case has been simulated using an alternative rock permeability field constructed by combining two permeability fields: (1) the permafrost permeability field including the repository and the frozen front, and (2) the rock permeability field of the Base Case (i.e., excluding the repository and the frozen front). The procedure is as follows:

- A xy plane is first assumed that approximately divides the permafrost domain from the unaffected rock. The depth of this plane is obtained from the DarcyTools results: –59 m for the shallow permafrost case.
- Above this depth, the rock permeability is equal to the permafrost permeability field.
- Below this depth, rock permeability is equal to the rock permeability of the Base Case.

In this way, the permeability of the rock around the tunnels and vaults of the repository-scale model is not influenced by the DarcyTools repository representation. To account for the influence of the low temperature on the hydraulic properties of the tunnels and vaults it has been assumed that the hydraulic conductivity of the backfill located above the frozen front is reduced by five orders of magnitude (i.e. 10^{-8} m/s). No other modification of the hydraulic conductivity of the repository materials with respect to the Base case is considered.

The hydraulic conductivity field obtained for the permafrost case is shown in Figure 6-43 together with the Base case.

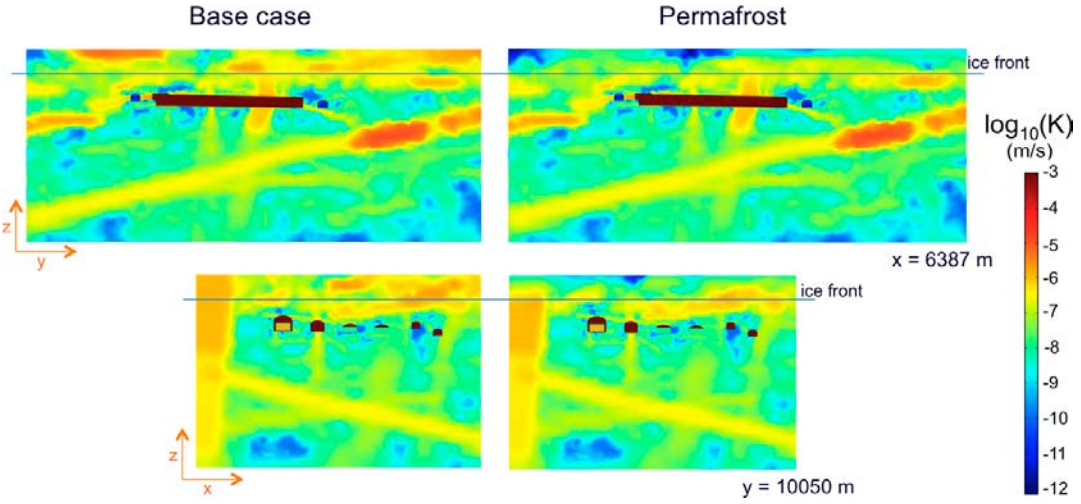

Figure 6-43. *Hydraulic conductivity field used in the simulation of a shallow permafrost case. Cut planes at x = 6,387 m and y = 10,050 m are shown for the Base case (left) and permafrost case (right).*

The calculated total tunnel and waste flow for a shallow permafrost case are presented in Table 6-11 and graphically in Figure 6-44. Both the tunnel and waste flows decrease in all vaults with respect to the Base case situation at shoreline position 3. The average reduction in the flow through the repository structures is about 78%. This value agrees well with the average rock permeability decrease around the frozen front, which is about 75%.

The overall reduction in the water flow around the repository is observed in Figure 6-45, where the distribution of the magnitude of the Darcy velocity is compared with the respective distribution obtained in the Base case. 1BMA, BLA and 2BTF are the most affected vaults (see Table 6-11). These vaults are located below a zone where the permeability of the rock within the permafrost has been considerably reduced (see Figure 6-43).

Table 6-11. Total flow through the SFR 1 vaults (m^3/year) for a shallow permafrost case and comparison with the results of the Base Case (BC) and the shoreline position 3. Negative percentages indicate a reduction in the total flow with respect to the BC.

		Total flow (m^3/year)	% Difference BC
Vaults	1BMA	13.87	–79
	1BLA	30.93	–79
	1BTF	5.21	–71
	2BTF	7.24	–83
	Silo	0.50	–66
Waste	1BMA	0.41	–88
	1BLA	29.20	–79
	1BTF	0.71	–80
	2BTF	0.52	–89
	Silo	0.42	–69

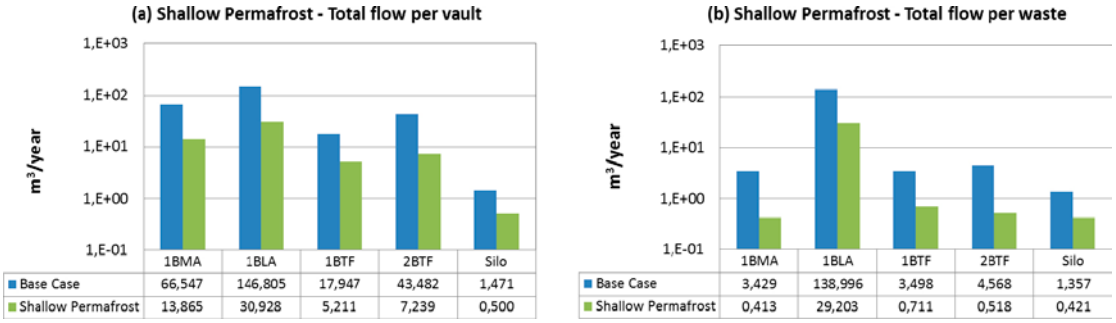

Figure 6-44. *Total flow entering the SFR 1 vaults (a) and waste domains (b) for the Shallow permafrost case compared to the Base Case and the shoreline position 3. The vertical axis is logarithmic.*

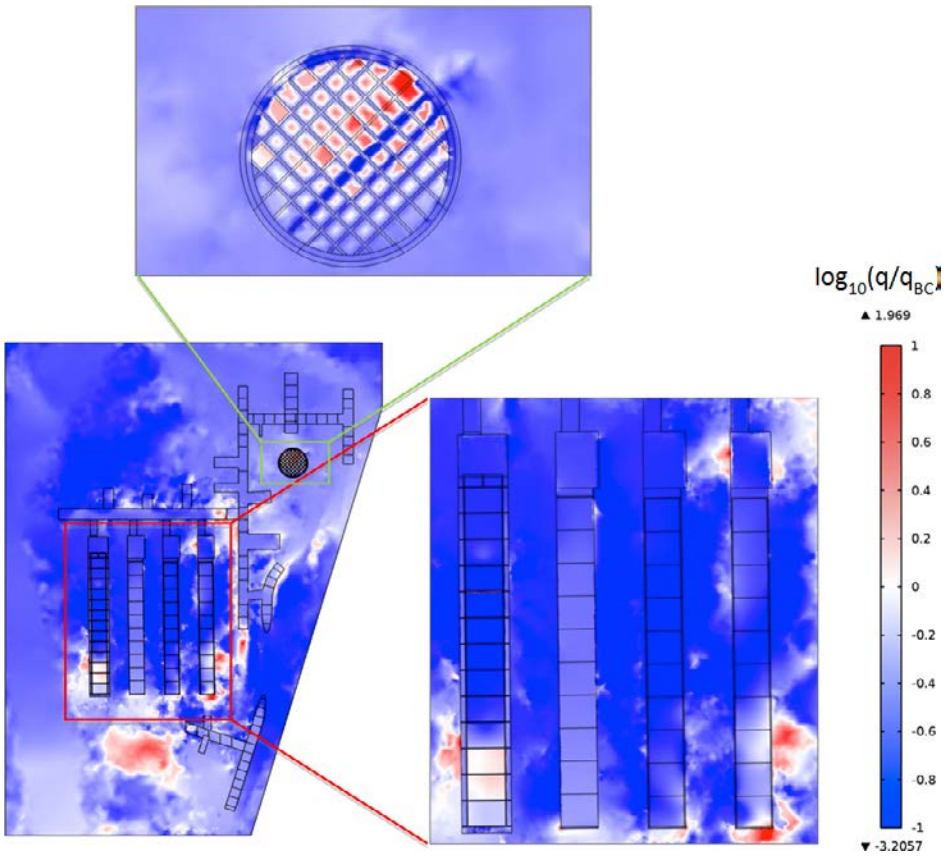

Figure 6-45. *Ratio of the Darcy velocity magnitude between the case of the Shallow permafrost case and the Base case for the shoreline position 3 in a xy plane at z = –82.5 m. Values greater than one indicate a higher flow in the alternative closure case*

In summary, both the tunnel and waste total flows calculated for the shallow permafrost case decrease in all vaults with respect to the Base case for the shoreline position 3. The reduction in the flow through the vaults is consistent with the permeability decrease around the frozen front. The most evident changes in flow are observed for the 1BMA, 1BLA and 2BTF, although all rock vaults follow the same trend. These vaults are located just below a zone within the permafrost where the permeability of the rock is considerably lower than the permeability of the Base case.

6.5 Estimation of uncertainty associated with the geosphere

Two additional realizations of the rock permeability have been used to assess the range of variability in the computed flows due to the uncertainties in the geosphere hydraulic description. These two realizations have been selected based on previous results of the regional DarcyTools model (Odén et al. 2014). They are considered as representative of two cases that lead to a higher and a lower average tunnel flow compared to the Base case, respectively. They will be referred to High and Low flow realizations (see Table 6-12 for correspondence with respective DarcyTools simulations).

Table 6-12. Nomenclature of the three realizations of the rock permeability field in the repository-scale model and the regional-scale model (Odén et al. 2014).

Repository-scale model	Case number in regional-scale model	Regional-scale model
Base case	Case 1	Base_Case1_DFN_R85
High Flow Case	Case 11	nc_DEP_R07_DFN_R85
Flow Flow Case	Case 15	nc_NoD_R01_DFN_R18

The hydraulic conductivity in the vicinity of the SFR 1 repository is presented for two planes (xy and zx) in Figure 6-46 for the three rock permeability realizations. The High Flow case and the Base case share the same discrete fracture network (DFN) realization and thus the location of the minor fractures affecting the vaults. The main difference between these two realizations is the higher connectivity between the deformation zones ZFMNNW1209 and ZFMNNE0869 west of the 1BMA in the High flow case. The Low flow case corresponds to a different DFN realization. The main differences with the Base case are that, in general, the vaults sit in a lower permeability area and are not intersected by the high permeability structures above the vaults. Also, the minor fractures affecting the 1BMA and 1BLA are not present.

The results of the flow through the vaults and the waste domains are presented in Table 6-13 for the High flow case and Table 6-14 for the Low flow case. In turn, the magnitude of the flow (m/s) for the High and Low flow cases is depicted in Figure 6-47 for a xy plane intersecting the rock vaults. Figure 6-48 presents the bar plots of the two same cases in addition to the Base case flow results for the three shoreline positions. It is observed that the High flow case results in an average flow increase through the tunnels with respect to the Base case for all the shoreline positions (Table 6-13 and Figure 6-48 left). The highest flow increase, in relative terms, occurs for the shoreline position 2. Regarding the flow through the waste domain (Table 6-13 and Figure 6-48 right), the increase in tunnel flow does not translate into an increase in waste flow for shoreline position 1. For shoreline positions 2 and 3 there is an overall increase in the total waste flow, which basically reflects the increase in the 1BLA waste flow. For shoreline positions 2 and 3 there is an overall increase in the total waste flow, which basically reflects the increase in the 1BLA waste flow. However, the waste flow through the 1BMA and 2BTF vaults, situated at both sides of the 1BLA, is reduced with respect to the Base case. This result illustrates a trade-off between 1BLA and its neighboring vaults. In the High flow case there is a better connection from the South part of the repository and the deformation zone ZFMNNW1209 through the conductive 1BLA vault. The 1BLA vault acts as a by-pass and leads to a reduction of the lateral flow forced from East to West though the 1-2BTF and the 1BMA waste.

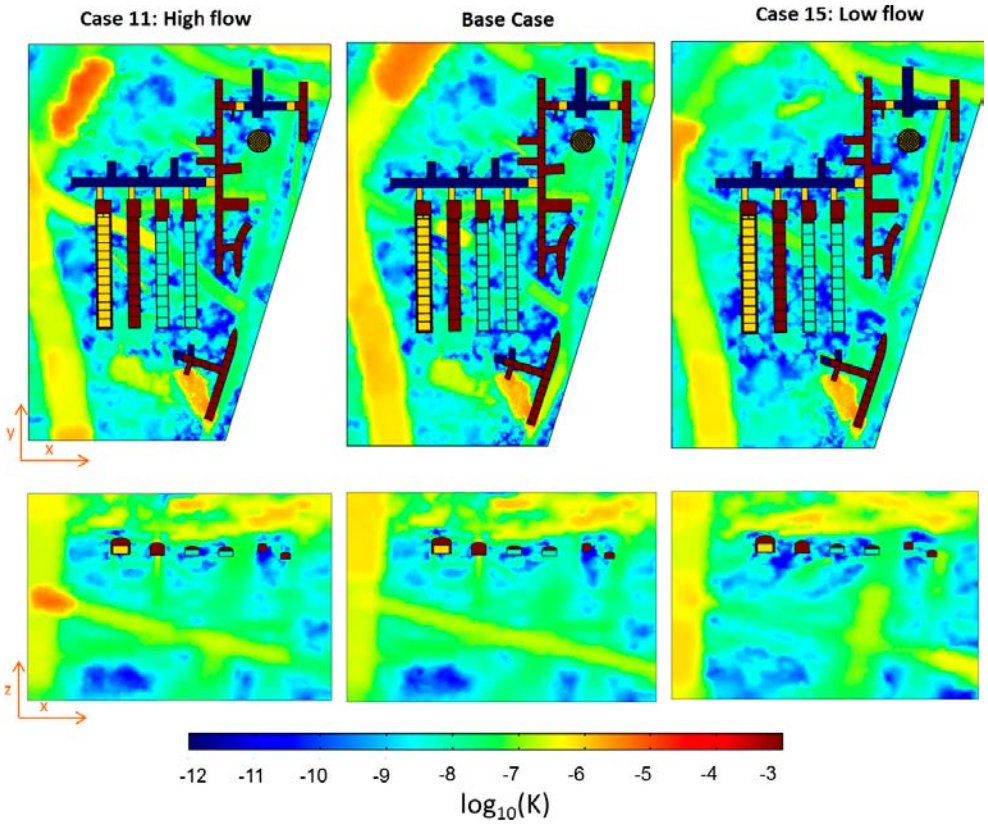

Figure 6-46. *Detail of the hydraulic conductivity (log10, m/s) of the rock around the vaults of the SFR 1 for the three different realizations: High flow, Base case, and Low flow: (top) xy cross section at z = –82.5 m, and (bottom) zx section at y = 10,050 m.*

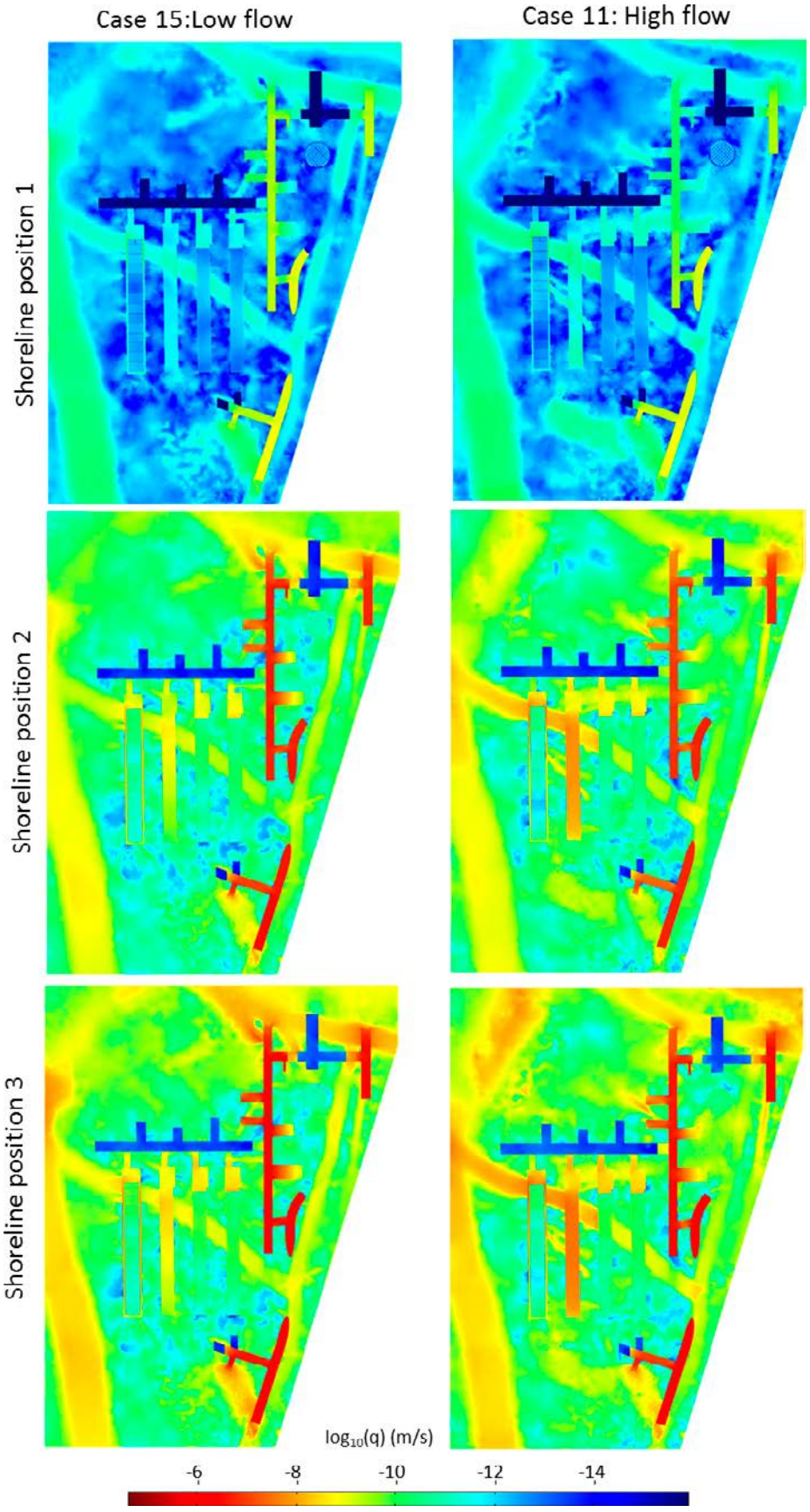

Figure 6-47. *Magnitude of the flow (m/s) for the High and Low flow cases in a xy cross section at z = –82.5 m.*

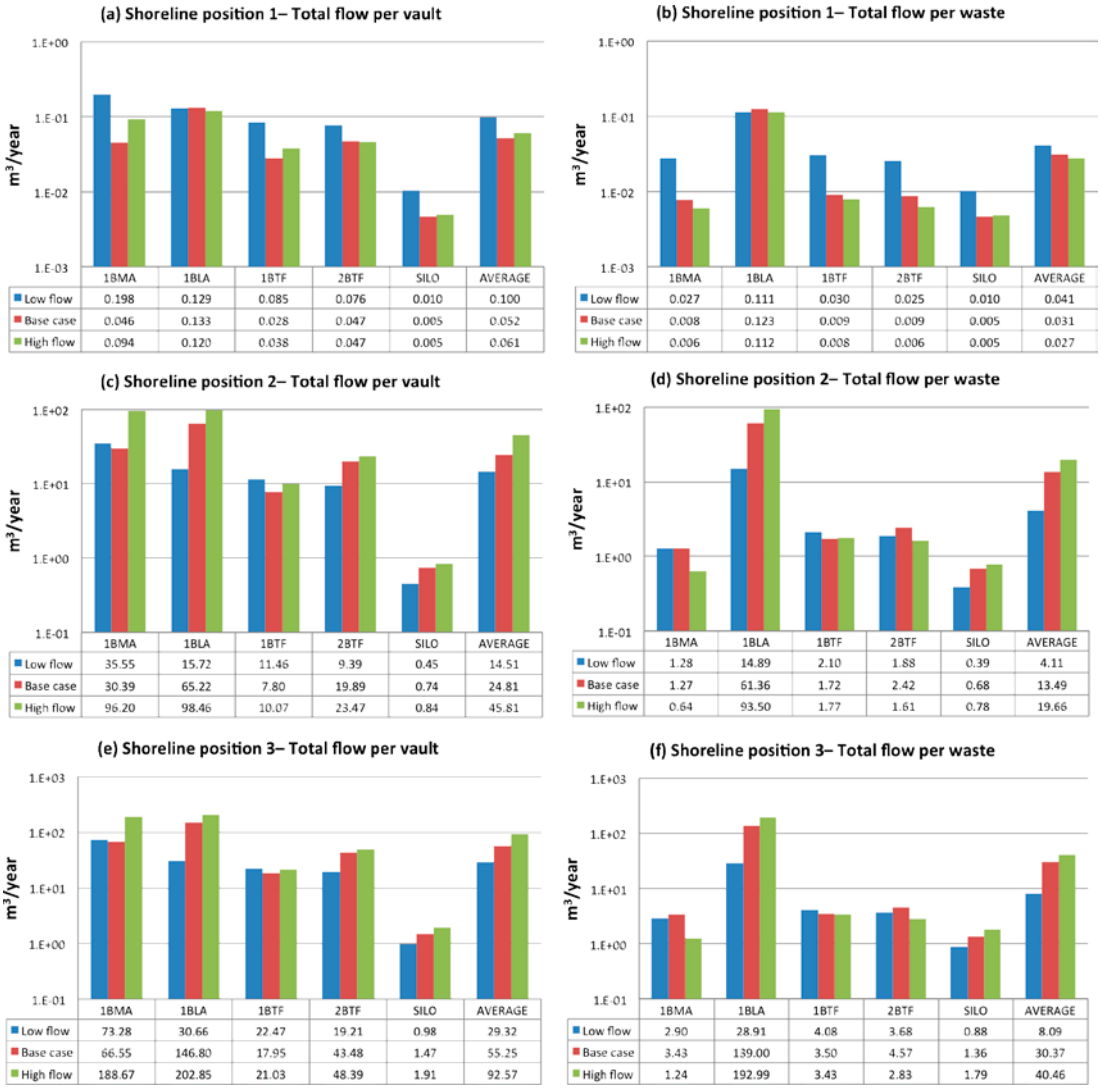

Figure 6-48. *Total flow (m^3/year) through the vaults (left) and waste domains (right) for the three rock permeability cases and the three shoreline positions. The vertical axis is logarithmic.*

Table 6-13. Total flow through the SFR 1 vaults (m^3/year) for the High flow case and comparison with the Base case (BC). Negative percentages indicate a reduction in the total flow with respect to the BC.

		Shoreline position 1		Shoreline position 2		Shoreline position 3	
		Total flow (m^3/year)	Difference BC	Total flow (m^3/year)	Difference BC	Total flow (m^3/year)	Difference BC
Vaults	1BMA	0.094	106%	96.198	217%	188.671	184%
	1BLA	0.120	–10%	98.458	51%	202.851	38%
	1BTF	0.038	37%	10.073	29%	21.027	17%
	2BTF	0.047	–1%	23.466	18%	48.390	11%
	Silo	0.005	5%	0.841	14%	1.907	30%
	Average	**0.061**	**17%**	**45.807**	**85%**	**92.569**	**68%**
Waste	1BMA	0.006	–24%	0.636	–50%	1.244	–64%
	1BLA	0.112	–9%	93.500	52%	192.992	39%
	1BTF	0.008	–13%	1.770	3%	3.430	–2%
	2BTF	0.006	–28%	1.614	–33%	2.831	–38%
	Silo	0.005	5%	0.782	15%	1.791	32%
	Average	**0.027**	**–10%**	**19.660**	**46%**	**40.458**	**33%**

Table 6-14. Total flow through the SFR 1 vaults (m^3/year) for the Low flow case and comparison with the Base case (BC). Negative percentages indicate a reduction in the total flow with respect to the BC.

		Shoreline position 1		Shoreline position 2		Shoreline position 3	
		Total flow (m^3/year)	Difference BC	Total flow (m^3/year)	Difference BC	Total flow (m^3/year)	Difference BC
Vaults	1BMA	0.198	334%	35.55	17%	73.28	10%
	1BLA	0.129	–3%	15.72	–76%	30.66	–79%
	1BTF	0.085	206%	11.46	47%	22.47	25%
	2BTF	0.076	61%	9.39	–53%	19.21	–56%
	Silo	0.010	118%	0.45	–40%	0.98	–33%
	Average	**0.100**	**93%**	**14.51**	**–41%**	**29.32**	**–47%**
Waste	1BMA	0.027	249%	1.284	1%	2.902	–15%
	1BLA	0.111	–9%	14.894	–76%	28.914	–79%
	1BTF	0.030	231%	2.102	22%	4.079	17%
	2BTF	0.025	188%	1.881	–22%	3.676	–20%
	Silo	0.010	121%	0.389	–43%	0.882	–35%
	Average	**0.041**	**33%**	**4.110**	**–70%**	**8.091**	**–73%**

The Low flow case results in an average tunnel flow decrease of more than 40% with respect to the Base case for the shoreline positions 2 and 3, but in an increase of 90% for the shoreline position 1 (Table 6-14). The same is observed for the average waste flow. Note that the behavior of the 1BMA and the 1BTF shows the opposite trend for the shoreline positions 2 and 3. In these cases, the tunnel flow increases for all shoreline positions and so does the 1BTF waste flow.

The comparison of the magnitude of the flow (m/s) for the High and Low flow cases for the three shoreline positions is presented in Figure 6-47 in a xy plane intersecting the vaults. In addition, the comparison of the longitudinal evolution of total flow for the three rock permeability fields is presented in Figure 6-49 for the 1BMA and 1BLA, and Figure 6-50 for the 1BTF and 2BTF. In turn, Figure 6-51 presents the vertical evolution of the flow in the Silo. The following is observed from the figures.

1BMA (Figure 6-49 left):

- The flow through the gravel increases in both realizations, being highest for the Low flow case. Most of the inflow occurs in the sections 12–14 associated with the deformation zone ZFMNNW1209 (also observed in Figure 6-47), indicating a more conductive zone ZFMNNW1209 in the surroundings of the 1BMA.
- The shape of the waste flow profile of the High flow case follows that of the Base case but with higher flow for the shoreline position 1. For the shoreline positions 2 and 3, the small fractures crossing section 9 deliver less inflow, which result into a lower total waste flow. The Low flow case presents the maximum waste flow in sections 11, 12, 13 and a decrease of waste flow in section 9. The larger Darcy velocities in the waste for the Low flow case compared to the High flow case may also be observed in Figure 6-47.

1BLA (Figure 6-49 right):

- In all the shoreline positions, the bottom gravel flow curve of the High flow case is parallel to the Base case curve, but shifted upwards (higher flow) for the shoreline position 1 and downwards for the shoreline positions 2 and 3. These curves present two local minima in sections 3 and 7 and two maxima in sections 5 and 9. In the Low flow case however, the gravel flow increases continuously from south to north evidencing a continuous inflow of water along the bottom gravel.
- For the shoreline position 1, the waste flow profile of the High flow case resembles the flat profile of the Base case. The Low flow case also presents a flat profile but presents an inflow peak in sections 4, 7, 9, and 10, the latter two corresponding to the intersection with ZFMNNW1209 (also observed in Figure 6-47).
- For the shoreline positions 2 and 3, the Base case curve of the waste flow sits between the higher flow and lower flow curves. The Base case and the High flow case profiles are quite flat. In turn, in the Low flow case the flow increases continuously from south to north evidencing a continuous inflow of water along the tunnel. The differences between the Low and High flow cases in the waste domain are also illustrated in Figure 6-47.

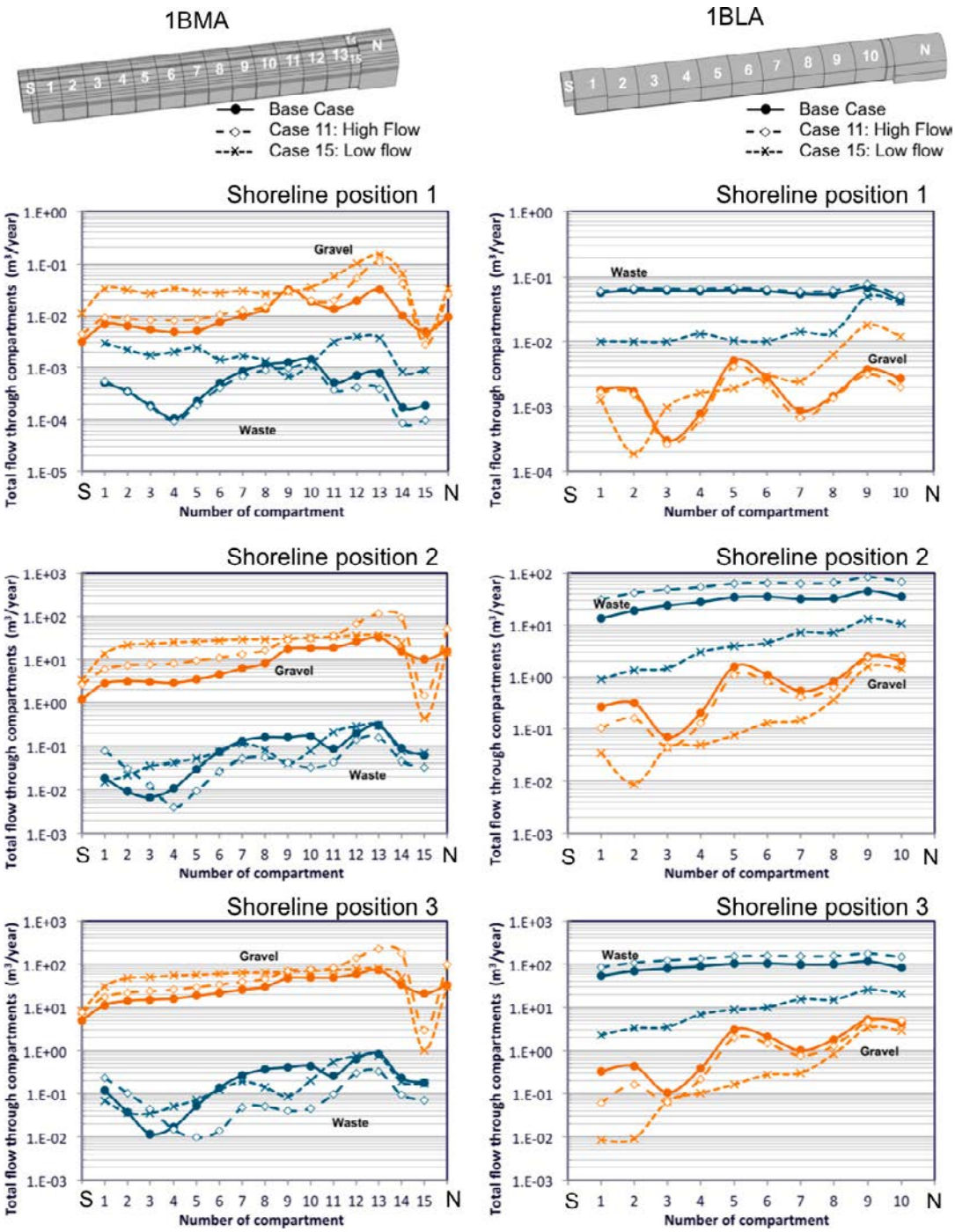

Figure 6-49. *Total flow (m^3/year) along the different sections of the 1BMA (left) and 1BLA (right) for the Base case and the High and Low flow cases. Results for the three shoreline positions. The vertical axis is logarithmic.*

1BTF (Figure 6-50 left):

- For the shoreline position 1, the flow through the gravel has a peak in section 6 for all rock permeability cases. For the shoreline positions 2 and 3, both additional realizations have a lower gravel flow than the Base case in the 1–4 sections. A strong inflow in sections 5–6 increases the flow over the Base case profile, which is due to the effect of ZFMNNW1209. Again, the profiles evidence the higher flow through ZFMNNW1209 in both realizations compared to the Base case. North of those sections, the flat profile indicates that the water infiltrated from ZFMNNW1209 into the tunnel flows towards the north loading area.
- For the shoreline positions 2 and 3, the waste flow profile also reflects the influence of ZFMNNW1209. In all cases the profile shows a maximum located between sections 4 and 7. North of those sections there is a decrease of flow in the waste that is not observed in the gravel. It indicates that the waste areas affected by the deformation zone ZFMNNW1209 are localized and do not affect the water inflow into the northern sections.

2BTF (Figure 6-50 right):

- For the shoreline position 1, the gravel flow curve for the Base case is quite flat, similar to the High flow case. However, for the Low flow case, it presents a maximum located in sections 6–7 (intersected by ZFMNNW1209 at the east) and a minimum in sections 8–9 (intersected by ZFMNNW1209 at the west). This result indicates that there is inflow to the tunnel from the east side of ZFMNNW1209 whereas the west side of ZFMNNW1209 acts as a discharge zone.
- For the shoreline positions 2 and 3, the flow through the gravel increases from south to north. The inflow is more distributed in the Base case and the High flow case, affecting sections 1 to 8. In contrast, the inflow is more concentrated in the Low flow case affecting especially to sections 4 to 6, which are the tunnel sections intersected at the east by ZFMNNW1209.
- For the shoreline position 1, the waste flow is higher than the Base case for Low flow case, while the High flow case leads to a decrease in the flow through sections 4 to 10.
- All the waste flow profiles present a higher flow for the sections affected by ZFMNNW1209 with a maximum in section 8. In both rock permeability realizations, for the shoreline positions 2 and 3, the waste flow in sections south of ZFMNNW1209 is lower than the Base case and very similar to the Base case flow in the area affected by the fractures. For the High flow case, the area affected by the fractures south of ZFMNNW1209 are less conductive than in the Base case.

Silo (Figure 6-51):

- For the shoreline position 1, the two alternative rock permeability realizations result in a higher flow through the Silo sections, although the increase in the High flow case is minimal. Flow increases upwards in all realizations with a maximum flow in section 5 (uppermost waste section).
- For the shoreline position 2, the flow direction changes from one realization to the other. However, a common feature is that the flow is always highest for section 5. In the Base case, the flow increases smoothly from bottom to top. In the High flow case the inflow is oscillatory with two maxima in sections 1 and 5, with values ranging from 0.3 to 0.4 m^3/s. In the Low flow case however, flow increases from bottom to top, although the total flows in sections 1 to 3 are similar. The sections 4 and 5 correspond to an inflow zone.
- For the shoreline position 3, groundwater flows from top to bottom in the Silo and the flow consistently increases from section 5 to section 3 in all the realizations. The three profiles are parallel, with decreasing total flows for the High flow case, Base case, and Low flow case, in that order.

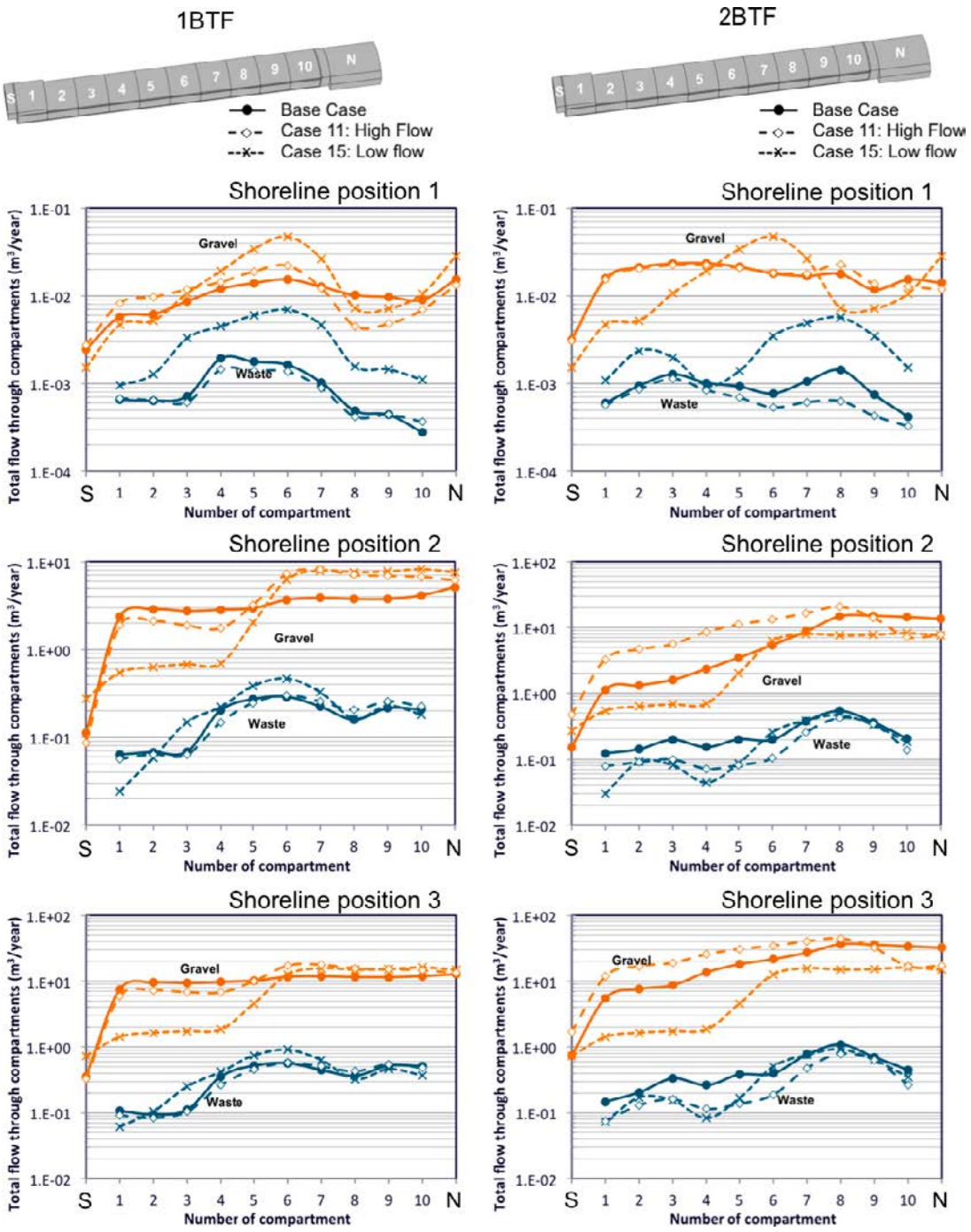

Figure 6-50. *Total flow (m3/year) along the different sections of the 1BTF (left) and 2BTF (right) for the Base case and the High and Low flow cases. Results for the three shoreline positions. The vertical axis is logarithmic.*

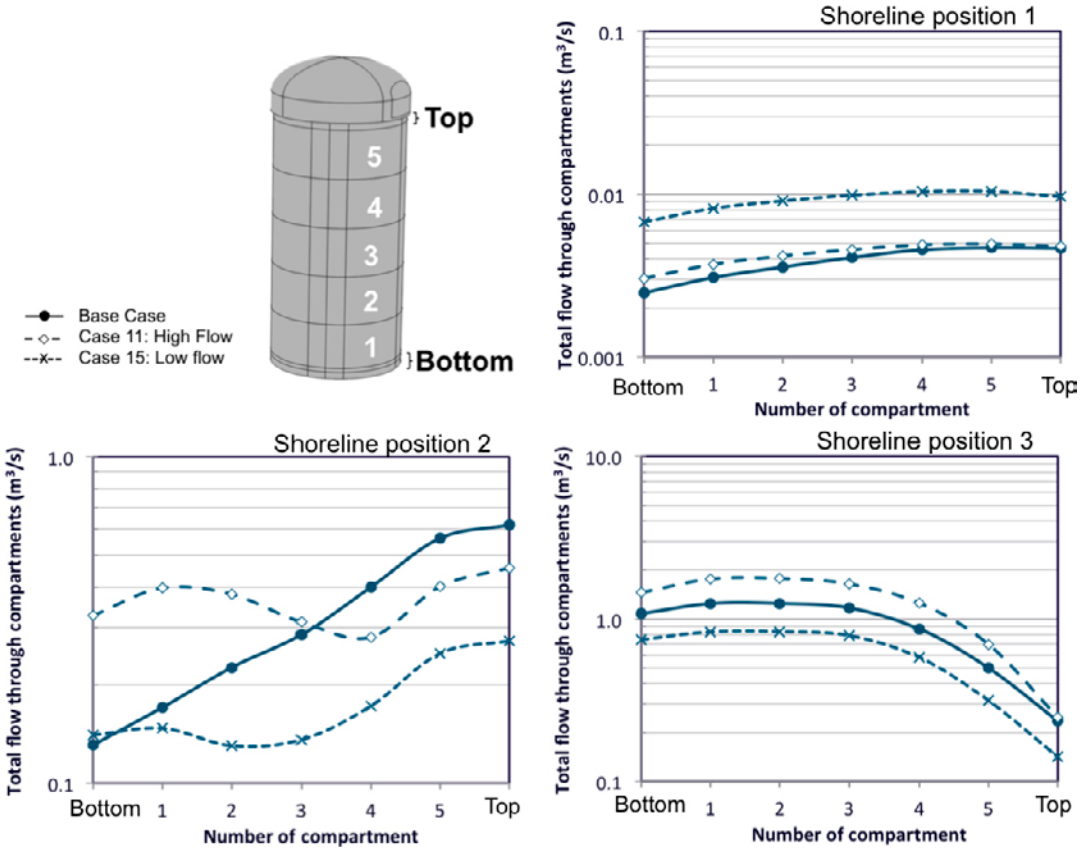

Figure 6-51. *Total flow (m3/year) along the different vertical Silo sections for the Base case and the High and Low flow cases. Results for the three shoreline positions. The vertical axis is logarithmic.*

An analysis has been presented here of the effect of different realizations of the rock permeability field in the modeled domain on the hydraulic behavior of the repository. This may be regarded as a first approximation of the effect of uncertainty in the geosphere hydraulic parameters on the performance of the repository. The variability of the groundwater flow in the different vaults due to different rock permeability fields should be considered to critically analyze and compare the results of different combinations of hydraulic properties of the different materials of the repository. As an example, it could be that the change in the total flow through a given vault due to barriers degradation is smaller than the effect of the rock permeability uncertainty itself. The main conclusions of the study of rock permeability fields are summarized below.

- For the shoreline position 1, the tunnel flow increases with respect of the Base case in both realizations (17% and 93%). Locally, in some vaults, these differences are higher than 100%, (notably the 1BMA). The variability of the results in the waste domain is also notable. The difference in the averages is in the range –10% to 33%, while locally the differences are higher than 100% in some vaults. Results suggest that the 1BMA is more sensitive to rock permeability changes than the other vaults.
- For the shoreline positions 2 and 3, there are variations in the average total flow through all the vaults of between –47% and +85%, compared to the Base case. For the waste domain the difference in the averages range between –73% and + 46%, while locally the differences are in the range of –79% to +52%. It is worth noticing that the increase in waste flow in the 1BLA in the High flow case is accompanied by a reduction in the 1BMA and 2BTF waste flow. This result can be explained by a trade-off between 1BLA and its neighboring vaults. In the High flow case, there is a better connection from the South part of the repository and the through the conductive 1BLA vault and this leads to a reduction of the lateral flow from East to West forced though the 1-2BTF grouted waste and the 1BMA. So, even though, the total flow along the vaults increases, the flow forced through the waste compartments from East to West is reduced. This result is also evidenced in the flow profiles by the flow reduction associated with the small transversal fractures crossing the 1BMA and 2BTF vaults south of the deformation zone ZFMNNW1209.

6.6 Summary of calculation cases

In the Base case, the 1BLA vault has the highest flow rates since it has no concrete barriers. In this case, the waste flow rates represent more than 90% of the tunnel flow. In turn, the 1BMA tunnel flow rate is half the 1BLA flow rate. The 1BMA configuration with low permeability concrete beams that support the concrete floor disrupts the continuity of the hydraulic cage surrounding the concrete structure in an unfavorable way (5% of the tunnel flow rate enters the waste domain at shoreline position 3). A 1BMA configuration with very permeable concrete beams increases the hydraulic cage efficiency substantially, reducing the waste flow by three orders of magnitude compared to the case with impermeable beams. The high permeability of the deformation zone ZFMNNW1209 around the 2BTF results in higher tunnel flow rates through 2BTF than through the 1BTF even though they have the same internal configuration. The waste flow rate is about 10% the tunnel flow rate in the 2BTF and 20% in the 1BTF. The Silo has the lowest tunnel and waste flow rates and the gravel dome concentrates most of the tunnel flow.

The degradation of the concrete barriers has a marginal effect on the tunnel flow rates (less than 26% flow increase) and there is limited impact in the surrounding rock, i.e., there is not obvious redistribution of flow as a consequence of the concrete degradation. The 1BLA and Silo waste flows are also insensitive to concrete degradation (less than 13% flow increase). In the case of the Silo, this apparent independence on concrete degradation is related to the fact that an intact bentonite significantly affects the waste flow rates through the 1BMA and 1-2BTF vaults. The highest increase occurs in the 1BMA and the shoreline position 2 (x15 increase in waste flow). In these vaults, the moderate concrete degradation mainly affects the sections close to deformation zones, while the severe and complete degradation affect the remaining sections, unifying the distribution of waste flow along the vaults. The comparison between the 1BMA configuration with and without concrete beams shows that the waste flow is lower for the 1BMA without beams for all the concrete degradation stages.

Regarding the degradation of the bentonite plugs, the results show that the impact on flow is small for the moderate plug degradation case and hence that the hydraulic barrier function is maintained. Only the complete degradation of the plugs results in an important increase of tunnel flow in the vaults. The results indicate that plugs with lower permeability than the most permeable rock surrounding the rock vaults yield an efficient configuration to restrict flow through the vaults. When the plugs present less resistance to flow than the surrounding rock, the flow distribution changes. The south entrance of the plug becomes the main inflow area to the vaults, and the water circulates mainly through the vaults located at the east side of the SFR 1 repository, close to the access ramp. The vaults situated at the west side of the SFR 1 repository are less affected.

Regarding the degradation of the bentonite plugs, the results show that the impact on flow is small for the moderate plug degradation case and hence that the hydraulic barrier function is maintained at a hydraulic conductivity of 1.00E–09 m/s for the sealed hydraulic bentonite section. In this case, the plugs still have a higher resistance than the rock surrounding the vaults. The severe plug degradation leads to an increase of the waste flow rates through some vaults, with the greatest increase observed for the Silo (+77%). The complete degradation of the plugs leads to significantly larger flow rates in all vaults. The highest flow increase occurs at the BTF vaults (2,522% and 688% for the 1BTF and the 2BTF, respectively). When the plugs present less resistance to flow than the surrounding rock, the flow configuration around the repository changes. Then, the south entrance of the plug becomes the main inflow area to the vaults, and the water circulates primarily through the vaults located at the east side of the SFR 1 repository, close to the access ramp, while the vaults situated at the west side of the repository are less affected.

In case of complete plug degradation the flow through the waste is notably larger for the 1BLA (+230%), 1BMA (+100%), and Silo (+110%), compared to the Base case. However, the flow though the 1-2BTF waste is reduced by 18–34%. Thus, plug degradation has little negative impact in the flow through both BTF waste domains. When the plugs have a higher resistance than the rock surrounding the vaults, there is inflow from the rock at the East side of the repository that is forced through the concrete grouting. When the plugs degrade, there is better connection between the East and West through the by-pass formed by the South and North ends and the lateral access tunnels, which reduces the flow through the BTF waste compartments. The flow through the rock between vaults also decreases due to the redirection of groundwater to the most permeable vaults and tunnels.

The cases above can be compared to the extreme case of no barriers. In that case, the flow through the waste domain is in all cases at least two orders of magnitude higher than the Base case (and even than the complete plug degradation case). An exception is the 1BLA, for which the increase is much smaller (235%), which is due to the flow redistribution between vaults. Flow from south to north occurs in this case through the completely degraded westernmost BTF vaults, decreasing the flow through the easternmost vaults. In the no barriers case the flow that crosses the waste is in the range 80–86% of the total flow through the tunnels for the 1BMA, 1BTF and 2BTF (for the same vaults in the Base case, this range is 5–20%). For the 1BLA and the Silo, this ratio is as high as 97%, although in these cases the waste domain has a similar volume than the total vault domain (the values reported for the Silo do not account for the flow through the Silo gravel dome).

One calculation case has considered the presence of an ice lens that degrades a section of the Silo bentonite. This degradation results in an increase in total flow rate in the Silo. However, most of this water recirculates within the degraded bentonite section without penetrating the waste encapsulation. Considering only the flow increase through the intact sections of the Silo, the increase of flow is minor for the shoreline position 1 (5%) and shoreline position 3 (15%) cases, and it is considerably high in the shoreline position 2 (190%).

Two different closure alternatives have been considered for the SFR 1 repository. The Base case closure consists of extended sections of bentonite/concrete and structural plugs. The alternative closure considers short sections of bentonite with concrete plugs. This configuration represents a situation where a significant lower amount of bentonite is used to seal the repository. Overall, it may be concluded that the hydrodynamic behavior is similar between the Base case and alternative closure options. Depending on the shoreline position, different flow adjustments are observed between the 1BLA and the 1-2BTF vaults while the flow though the 1BMA remains unaltered. There is a trade-off between 1BLA and the 1-2BTF vaults. When the 1BLA waste flow increases, the waste flow of the 1-2BTF vaults decreases and vice versa (Figure 6-52 bottom). As observed in the plug degradation analysis, an increase in the flow from the South to North part of the tunnels through the conductive 1BLA vault leads to an increase in the flow from East to West traversing the 1-2BTF grouted waste. The flow in the rock surrounding the 1-2BTF vaults is also modified the same way. The trade-off between the westernmost vaults absorbs most of the flow protecting the easternmost vault and the 1BMA waste, whose waste flow remains mostly unaffected.

The abandoned repository calculation case represents a situation in which no additional barriers and structures are emplaced after the operational phase. The tunnel flow is 5–7 times larger than the Base case for the easternmost vaults 1BMA, 1BLA, 2BTF and 1 to 2 orders of magnitude higher in the 1BTF and the Silo. The highest increase occurs in the Silo for the shoreline position 3. In absence of plugs, all water is directed through the access tunnels to the lower pressure zones, such as the Silo. Again, the flow in the BTFs tunnels increase but the flow through the waste decreases with respect to the Base case. In the case of shoreline position 1 this effect is also observed in the 1BMA waste flow. Notice that this result for the 1BMA was not evident from the plugs degradation results since that analysis was restricted to shoreline position 3.

In the absence of plugs the vaults act as flow by-pass from the south to north of the repository reducing the flow through the rock and the BTF vaults from East to West. In shoreline position 1, the flow in the rock between the 1BMA and the 1BLA vaults is reduced and the minor fractures affecting the sections 9 and 10 of the 1BMA are deactivated. This flow redistribution is consistent with the results observed in the analysis of the plug degradation and closure alternative.

The hydraulic response of the repository to the advance of permafrost was analyzed under the assumption of a case of shallow permafrost where the frozen front is located above the vaults and Silo, at a depth of about –59 m. In that case, both the tunnel and waste total flows calculated decrease in all vaults with respect to the Base case for the shoreline position 3. The reduction in the flow through the vaults is consistent with the permeability decrease around the frozen front. The most evident changes in flow are observed for the 1BMA, 1BLA, and 2BTF, although all rock vaults follow the same trend. These vaults are located just below a zone within the permafrost where the permeability of the rock is considerably lower than the permeability of the Base case.

An analysis of the effect of different realizations of the rock permeability field in the modeled domain on the hydraulic behavior of the repository was carried out. This may be regarded as a first approximation of the effect of uncertainty in the geosphere hydraulic parameters on the performance of the repository. The variability of the groundwater flow in the different vaults due to different rock permeability fields should be considered to critically analyze and compare the results of different combinations of hydraulic properties of the different materials of the repository.

For the shoreline position 1, the tunnel flow increases with respect of the Base case in both realizations (17% and 93%). Results suggest that the 1BMA is more sensitive to rock permeability changes than the other vaults. For the shoreline positions 2 and 3, there are variations in the average total flow through all the vaults of between –47% and +85%, compared to the Base case. For the waste domain the difference in the averages range between –73% and + 46%, while locally the differences are in the range of –79% to +52%. It is worth noticing that the increase in waste flow in the 1BLA in the High flow case is accompanied by a reduction in the 1BMA and 2BTF waste flow, suggesting a redistribution of flow between these vaults.

The results presented for all the barrier degradation and/or configuration cases are summarized for the shoreline position 3 in Figure 6-52 and Table 6-15. The reason to restrict the analysis to the shoreline position 3 is that some cases have only been calculated with this shoreline position. According to the model predictions, the Silo is the most sensitive structure of the repository to barrier degradation processes. Concrete barriers degradation seems to be not decisive for the total flow in the vaults, although a significant increase of the flow through the waste is predicted, especially for the 1BMA and the BTF vaults. The no barriers case is by far the most unfavorable situation of all the calculation cases considered, with total flow in the waste domains of around two to three orders of magnitude higher than the Base case.

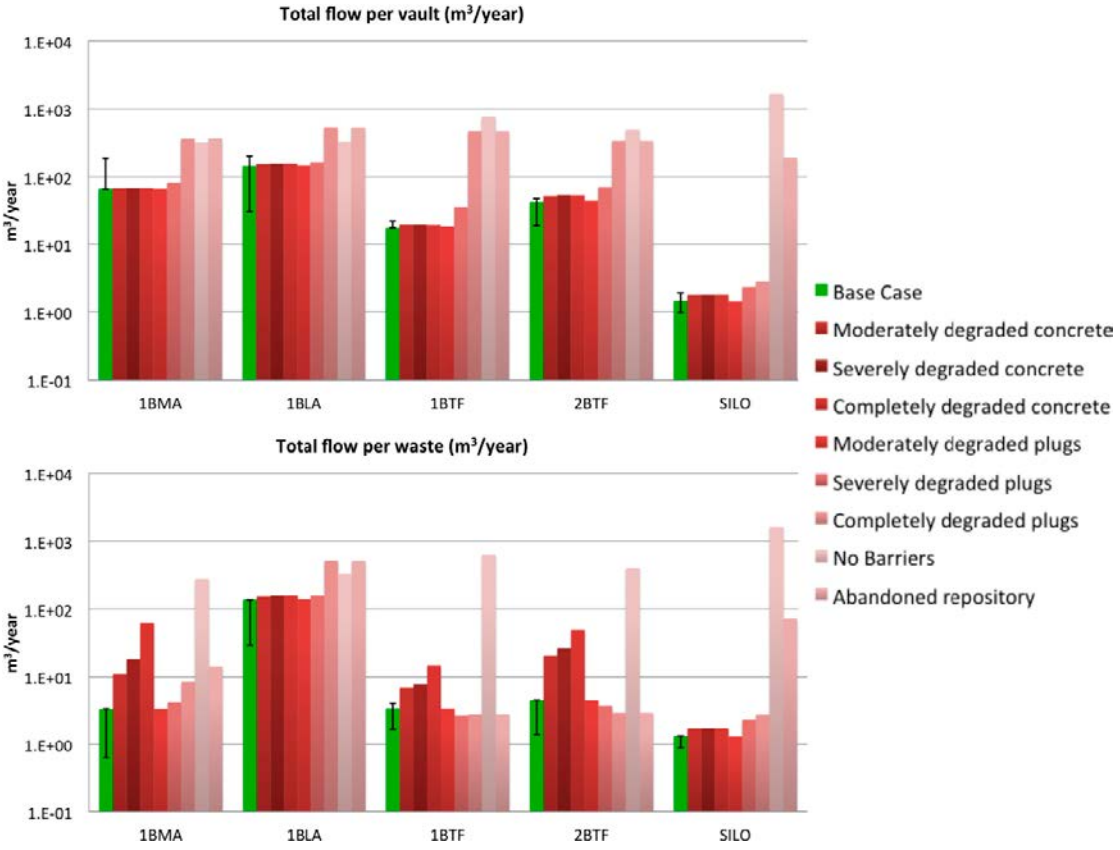

Figure 6-52. *Total flow (m3/year) for the different vaults and waste domains in the SFR 1 repository for the shoreline position 3. The black line accompanying the Base case bar indicates the uncertainty interval for each vault due to the studied variability in the geosphere. The vertical axis is logarithmic.*

Table 6-15. Summary of the results of total flow (m^3/year) in each vault for the different barrier degradation cases for shoreline position 3.

Total flow in vaults and waste (m^3/year)		1BMA	1BLA	1BTF	2BTF	Silo
Vaults	Base case	66.5	146.8	17.9	43.5	1.5
	Moderately degraded concrete	68.4	156.2	19.9	53.1	1.8
	Severely degraded concrete	68.6	158.1	19.9	54.3	1.8
	Completely degraded concrete	68.8	158.2	19.6	54.0	1.8
	Moderately degraded plugs	66.8	148.9	18.8	44.9	1.4
	Severely degraded plugs	83.3	164.5	36.2	70.9	2.4
	Completely degraded plugs	365.1	540.3	470.7	342.8	2.8
	Abandoned repository	369.2	537.3	470.5	342.2	191.8
	No barriers	323.3	335.2	774.5	501.1	1,687.5
Waste	Base case	3.4	139.0	3.5	4.6	1.4
	Moderately degraded concrete	11.0	152.9	6.9	20.7	1.7
	Severely degraded concrete	18.4	157.0	7.7	26.3	1.8
	Completely degraded concrete	63.0	157.3	14.7	49.2	1.8
	Moderately degraded plugs	3.4	141.0	3.4	4.5	1.3
	Severely degraded plugs	4.2	156.6	2.7	3.8	2.3
	Completely degraded plugs	8.4	516.9	2.8	3.0	2.8
	Abandoned repository	14.2	514.0	2.8	3.0	72.6
	No barriers	280.1	327.1	625.4	401.6	1,637.7

7 SFR 3 Calculation cases

7.1 Base case: different shoreline positions

This section presents the results of the Base case for three different shoreline positions relative the SFR 3 repository. The Base case refers to a given set of hydraulic properties for the different barriers and to a given permeability field for the rock. Three DarcyTools simulations of the regional hydrogeology with different top boundary conditions (shoreline positions) serve as input to the repository-scale model (for more details see Section 3.8). As described in Section 3.8, on the outer surfaces of the SFR 3 model domain corresponding to rock materials, a prescribed driving pressure boundary condition was specified and in the intersections of the access tunnels with the model boundaries, a prescribed flux boundary condition was specified.

The rock permeability field in three orthogonal planes in the middle sections of the model domain is presented in Figure 7-1. The high permeability structures of the rock around the SFR 3 repository will determine the main inflow and outflow pathways of the groundwater interacting with the repository.

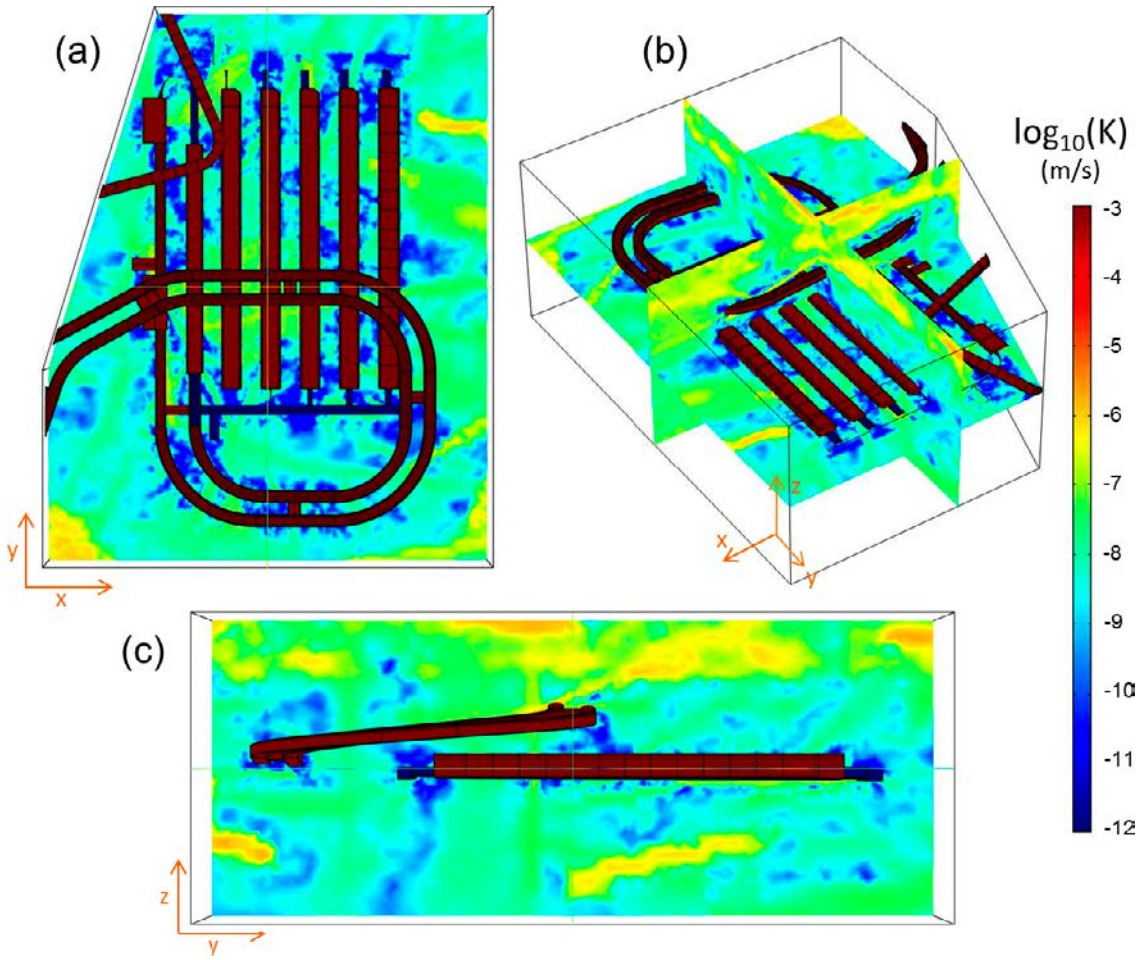

Figure 7-1. *Rock conductivity field (log10, m/s) in three orthogonal planes in the rock in the middle sections of the model domain (z = –127.5 m, below the rock vaults, y = 10,092 m, and x = 6,440 m), and hydraulic conductivity of the rock vaults and tunnels.*

7.1.1 Shoreline position 1

When the repository is submerged, groundwater flows upwards from the south through a deformation zone reaching the southernmost end of the vaults (Figure 7-2 right). Vaults 2BLA and 3BLA get infiltration from a vertical source further north, while 3BLA and 5BLA also receive water at its north extreme. Outflow from the vaults (Figure 7-2 left) can be roughly divided in two zones. At the south end of the vaults there is vertical upward outflow from vaults BRT, 5BLA, 4 BLA and 3BLA. The north part of the vaults has a diffuse outflow, with a NE direction in the case of the 2BMA and NW for the rest of the vaults (2BLA, 3BLA, 4BLA and 5BLA).

7.1.2 Shoreline position 2

For the shoreline position 2, inflow from the top of the domain is localized in the half southern part of the vaults (Figure 7-3 right). Vaults BRT (light blue) and 2BMA (green) get water from the access ramp. The outflow towards the NE is controlled by a deformation zone (ZFM871 in Figure 3-20) (Figure 7-3 left). The vault 2BMA (Dark green) presents a preferential outflow zone at its further north section (section 14). Groundwater flows downwards vertically through a vertical fracture until reaching ZFM871 and then moves NE following a main subhorizontal deformation zone.

7.1.3 Shoreline position 3

For the shoreline position 3, a rather distributed recharge to all vaults form the top boundary is observed (Figure 7-4 right). Groundwater moves horizontally through the most permeable structures at the surface and penetrates vertically through small fracture zones towards the repository. Part of the inflow to 2BMA and 5BLA comes from the access ramp. As for the shoreline position 2, the outflow moves downwards vertically from the vaults until the sub-horizontal deformation zone is reached and then moves north from the repository following mainly two alignments (Figure 7-4 left). The first one, towards the NE corresponds to the outflow from 2BMA, 5BLA and 4BLA and part of the 3BLA. The second deeper alignment towards the NW carries the discharge from 2BLA and 3BLA.

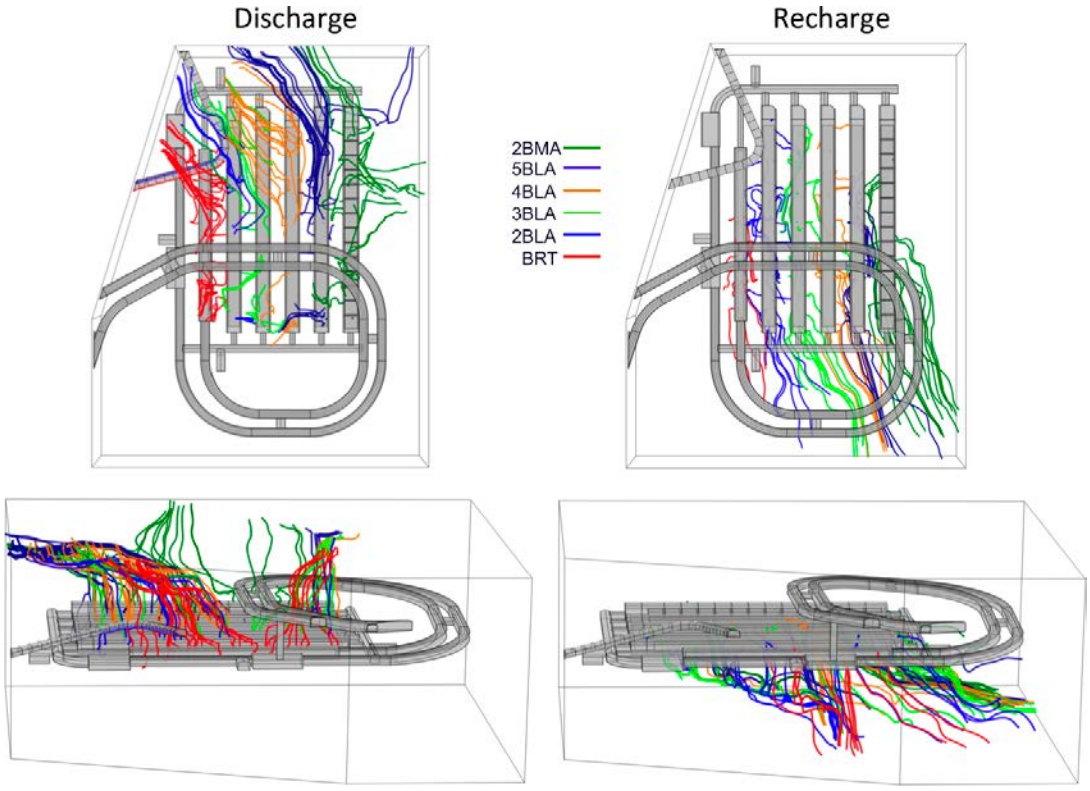

Figure 7-2. *Groundwater streamlines leaving (left) and reaching (right) individual vaults (color tubes) for the Base case and the shoreline position 1. Results are shown for two different views.*

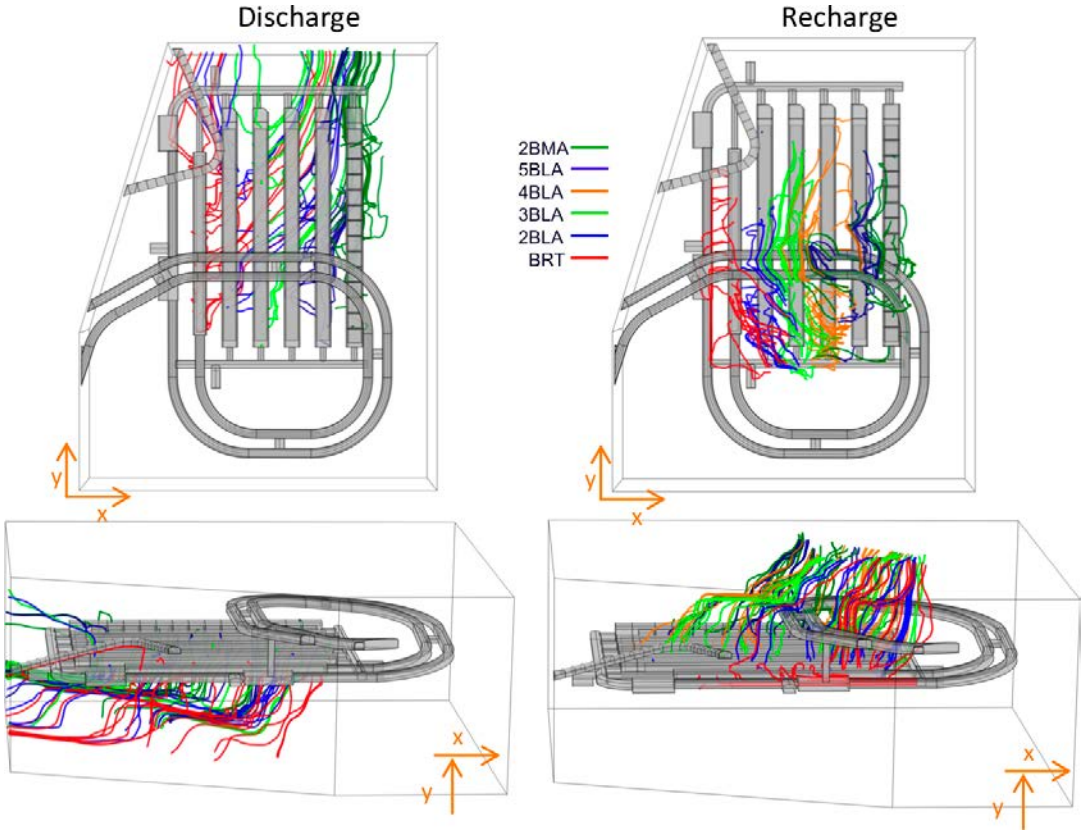

Figure 7-3. *Groundwater streamlines leaving (left) and reaching (right) individual vaults (color tubes) for the Base case and the shoreline position 2. Results are shown for two different views.*

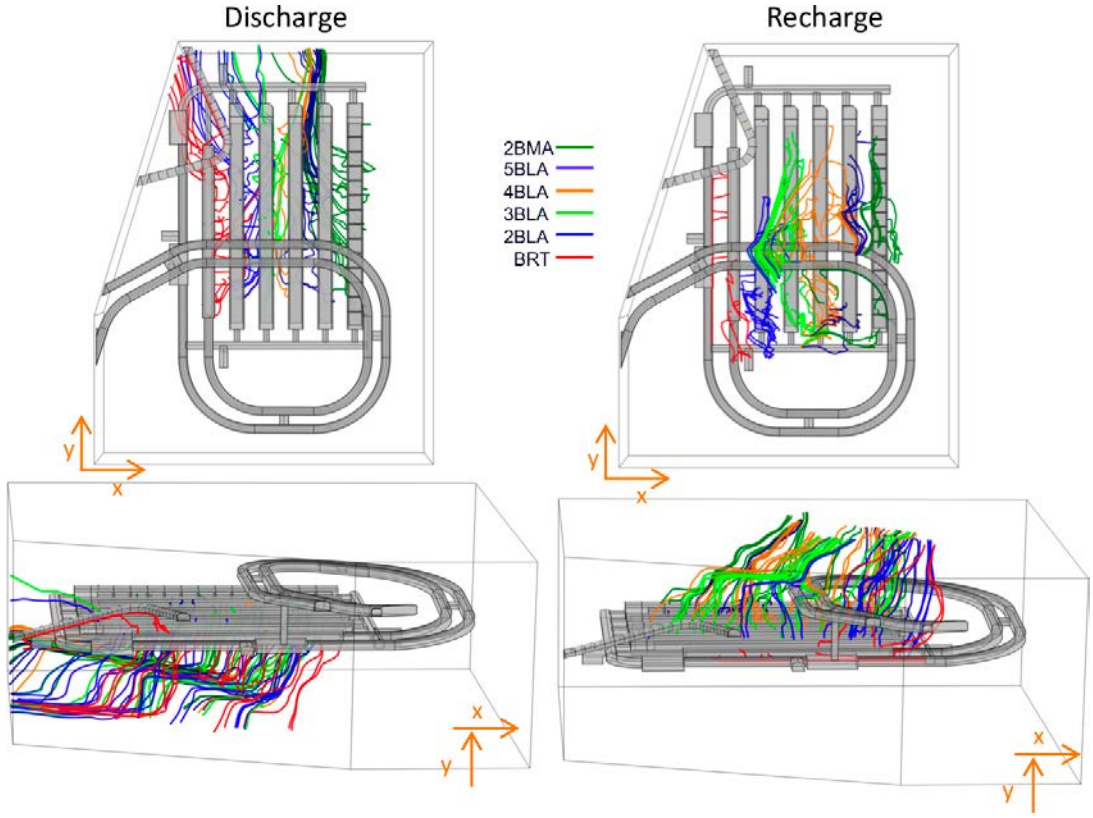

Figure 7-4. *Groundwater streamlines leaving (left) and reaching (right) individual vaults (color tubes) for the Base case and the shoreline position 3. Results are shown for two different views.*

7.1.4 Total flow through the vaults

The total flow through the tunnels and waste domains (calculated as indicated in Section 6.1.4) are presented in Figure 7-5. The 2-5BLA vaults, as the 1BLA in SFR 1, present a waste flow that is very similar to the tunnel flow, which is due to the vault representation. The assigned waste domain nearly equals the tunnel volume. Even though the BRT dimensions are smaller than the 2-5BLA vaults, their tunnel flows are of the same order of magnitude. The flow through the grouted BRT waste corresponds to 18% (shoreline position 1) and 14% (shoreline positions 2 and 3) of the BRT tunnel flow. In the Base case, the 2BMA presents the highest tunnel flow. However, the waste flow is in this case five orders of magnitude smaller than the tunnels flow. For all shoreline positions the waste flow in the 2BMA is the lowest of all vaults in the SFR 3. This is due, on one hand to the effect of the concrete barriers, and on the other hand on the effectiveness of the hydraulic cage design surrounding individual waste compartments. In the 2BMA, each waste compartment is surrounded (and separated from the next waste compartment) by a high permeability backfill material. Unlike the 1BMA, two ways of presenting the total flow per waste are possible for the 2BMA. The first one is results from adding up the flow of the 14 waste packages. This option could lead to a misinterpretation of the results. The second option, which has been used in this report, is to normalize the waste flow with the number of waste compartments (14). The nomenclature 2BMA* is used here to refer to the normalized waste flow in the 2BMA vault. The normalized waste flow of the 2BMA is 0.0008% of the tunnel flow for the shoreline position 1 and 0.0009% of the tunnel flow for the shoreline positions 2 and 3. These small waste flows are a result of the high efficiency of the three-dimensional hydraulic cage in the 2BMA.

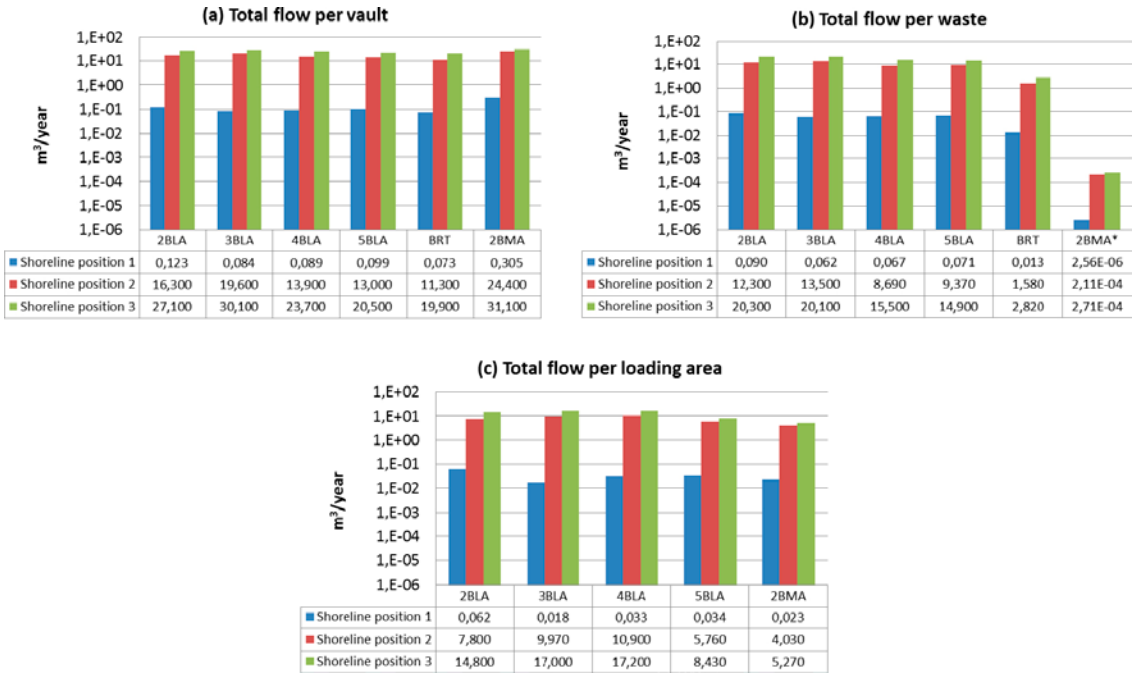

(a) Total flow per vault	2BLA	3BLA	4BLA	5BLA	BRT	2BMA
Shoreline position 1	0,123	0,084	0,089	0,099	0,073	0,305
Shoreline position 2	16,300	19,600	13,900	13,000	11,300	24,400
Shoreline position 3	27,100	30,100	23,700	20,500	19,900	31,100

(b) Total flow per waste	2BLA	3BLA	4BLA	5BLA	BRT	2BMA*
Shoreline position 1	0,090	0,062	0,067	0,071	0,013	2,56E-06
Shoreline position 2	12,300	13,500	8,690	9,370	1,580	2,11E-04
Shoreline position 3	20,300	20,100	15,500	14,900	2,820	2,71E-04

(c) Total flow per loading area	2BLA	3BLA	4BLA	5BLA	2BMA
Shoreline position 1	0,062	0,018	0,033	0,034	0,023
Shoreline position 2	7,800	9,970	10,900	5,760	4,030
Shoreline position 3	14,800	17,000	17,200	8,430	5,270

Figure 7-5. *Total flow through the SFR 3 vaults, waste and loading area domains (m^3/year) for the Base case, for the three shoreline positions. The waste flow for the 2BMA* corresponds to the normalized flow per waste package. The vertical axis is logarithmic.*

The spatial variability of the Darcy velocity along the vaults is illustrated in Figure 7-6 for a xy plane intersecting the waste domains. The 2-5BLA vaults act as the most conductive structures (higher flows) of the system. There is a major deformation zone (ZFMWNW8042) traversing all the vaults at about one third of the vaults length and associated with it there is a high flow zone affecting the rock in between vaults BRT, 2BLA, 3BLA and 4BLA. The 2BMA is crossed by this deformation zone at section 5. Another high conductive zone (ZFMWNW0835) affects sections 11 and 12 of the 2BMA. It is worth noticing the low flow in the inner part of the waste compartments of the 2BMA, evidencing once again the efficiency of the hydraulic cage in this vault. The interaction between the 2BMA and the deformation zones can be also analyzed looking at the flow per waste package and backfill sections (Figure 7-7). The tunnel flow decreases at the north part of the vault, between sections 9 and 14 for the shoreline position 1 and in section 14 for the shoreline positions 2 and 3. The waste flow presents two peaks of flow for all the shoreline positions analyzed; one in section 5 associated to the deformation zone ZFMWNW8042, and another between packages 11 and 13 associated with the wide deformation zone ZFMWNW0835, which affects the northern part of the 2BMA (Figure 7-1).

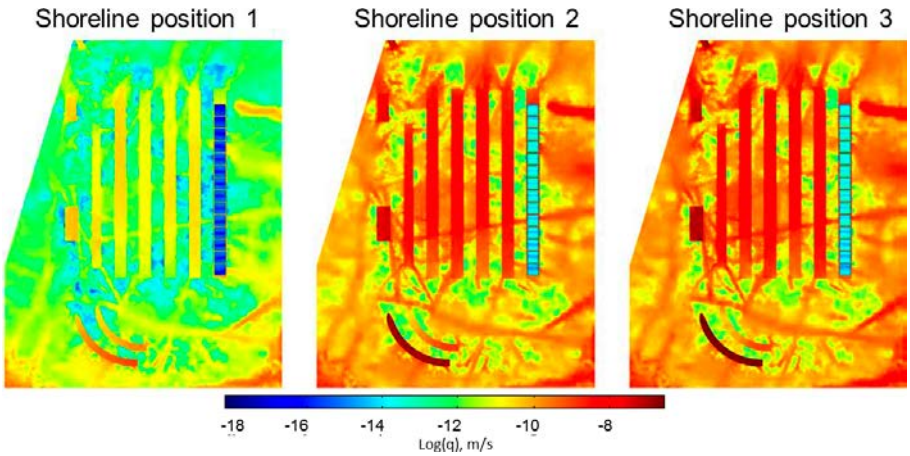

Figure 7-6. *Color map of the magnitude of the Darcy velocity (m/s) for the three shoreline positions.*

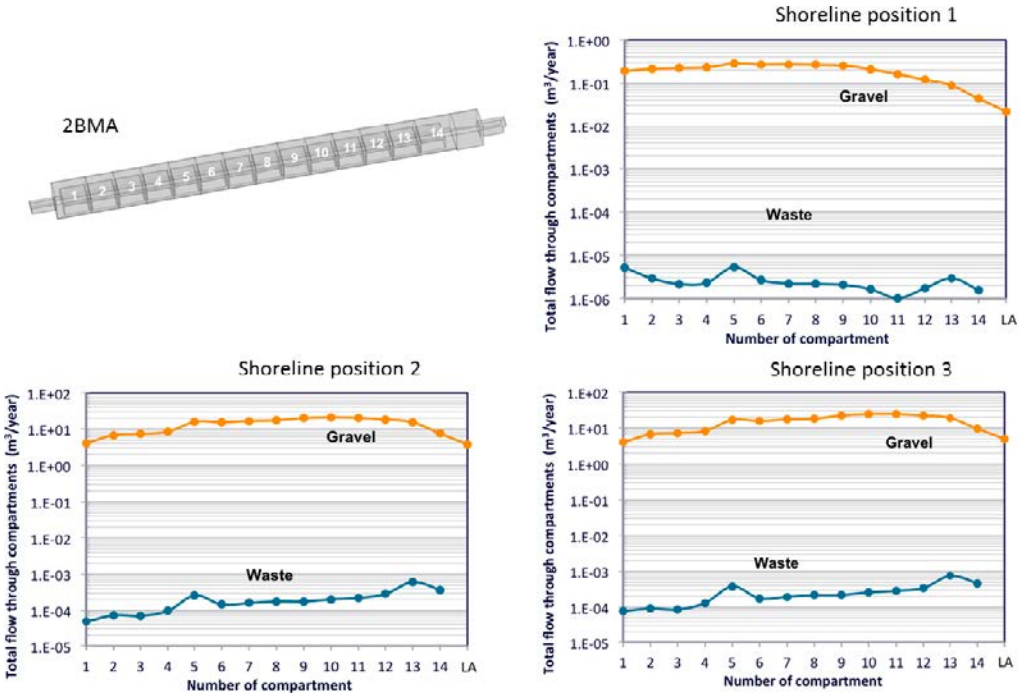

Figure 7-7. *Total tunnel (gravel) and waste flow (m3/year) profiles for the 2BMA for the three shoreline positions. The vertical axis is logarithmic.*

7.2 Barrier degradation

7.2.1 Concrete degradation

This section presents the effect of concrete barriers degradation on the groundwater flow and on the total flow entering the tunnels and waste compartments of the SFR 3 vaults. The effect of the concrete degradation has been studied with a set of 3 simulations corresponding to moderate, severe, and complete concrete degradation states. The Base case represents the intact concrete barrier state. The hydraulic conductivity of the different materials for each degradation state is defined in Table 7-1. The 2BMA waste permeability was assigned to maintain a contrast of permeability between the concrete and the waste by three orders of magnitude, until the conductivity threshold of 10^{-3} m/s was reached. The BRT grouted waste was also consistently degraded assuming an order of magnitude increase between the concrete and the grout permeability.

The calculated tunnel and waste flow for the different concrete degradation stages are presented in Table 7-2 and graphically in Figure 7-8. In all vaults, the change in tunnel flow due to concrete degradation is small for the three shoreline positions studied. On the other hand, the degradation of the concrete yields an important increase of the waste flow in the BRT and especially in the 2BMA vaults. The waste flow increases from 14% of the tunnel flow to 74% in the cases of a complete concrete degradation. For the 2BMA the waste flow increases four orders of magnitude for a total increase in concrete permeability of six orders of magnitude between the intact and completely degraded states (Figure 7-9). The increase of waste flow with respect to the concrete hydraulic conductivity is linear in log-log scale between the intact (concrete conductivity = 8.3e–10 m/s) and severe concrete degradation state (concrete conductivity = 1.0e–5 m/s). For the complete degradation case, the slope of the waste flow versus the concrete permeability decreases. The spatial variability of the Darcy velocity field across the repository is presented in Figure 7-10 for the Base case and the complete degradation case. A significant increase in the 2BMA velocities is observed for the three shoreline positions.

Table 7-1. Hydraulic conductivity (m/s) of the materials of the SFR 3 for the different concrete degradation cases.

K (m/s)	Base case Intact	Concrete Degradation		
		Moderate	Severe	Complete
Concrete	8.30E–10	1.00E–07	1.00E–05	1.00E–03
Backfill	1.00E–03	1.00E–03	1.00E–03	1.00E–03
BRT grouted waste	8.30E–09	1.00E–06	1.00E–04	1.00E–03
2BMA waste	8.30E–07	1.00E–04	1.00E–03	1.00E–03
Material floor	1.00E–07	1.00E–07	1.00E–07	1.00E–07
2BMA sand Floor	1.00E–03	1.00E–03	1.00E–03	1.00E–03

Table 7-2. Total flow through the vaults (m^3/year) for the different concrete degradation cases.

		Shoreline position 1			Shoreline position 2			Shoreline position 3		
		Moderate	Severe	Complete	Moderate	Severe	Complete	Moderate	Severe	Complete
Vaults	2BLA	0.126	0.124	0.125	17.00	16.90	16.94	28.45	28.29	28.34
	3BLA	0.089	0.089	0.089	21.91	21.82	21.85	34.26	34.18	34.19
	4BLA	0.091	0.090	0.091	15.35	15.46	15.44	25.18	25.27	25.29
	5BLA	0.113	0.113	0.113	13.90	13.95	14.00	21.89	21.95	22.04
	BRT	0.091	0.092	0.092	13.14	13.24	13.22	23.13	23.29	23.27
	2BMA	0.301	0.301	0.301	24.37	24.39	24.39	31.07	31.10	31.09
Waste	2BLA	0.094	0.094	0.093	13.02	13.03	13.01	21.34	21.34	21.39
	3BLA	0.073	0.073	0.074	15.00	14.95	15.03	22.59	22.46	22.88
	4BLA	0.070	0.070	0.070	9.61	9.64	9.82	16.63	16.69	16.83
	5BLA	0.083	0.084	0.083	10.18	10.22	10.24	16.32	16.40	16.37
	BRT	0.032	0.033	0.054	3.25	5.09	9.76	5.70	8.89	17.14
	2BMA*	0.0002	0.019	0.092	0.02	1.37	6.54	0.02	1.58	7.40
Loading area	2BLA	0.062	0.062	0.062	7.75	7.77	7.77	14.82	14.83	14.83
	3BLA	0.020	0.021	0.021	10.55	10.63	10.69	18.15	18.35	18.46
	4BLA	0.034	0.034	0.034	11.43	11.48	11.58	18.03	18.11	18.27
	5BLA	0.036	0.036	0.036	6.21	6.18	6.21	9.14	9.10	9.14
	2BMA	0.023	0.023	0.023	4.00	3.99	4.00	5.22	5.22	5.22

* normalized flow per waste package

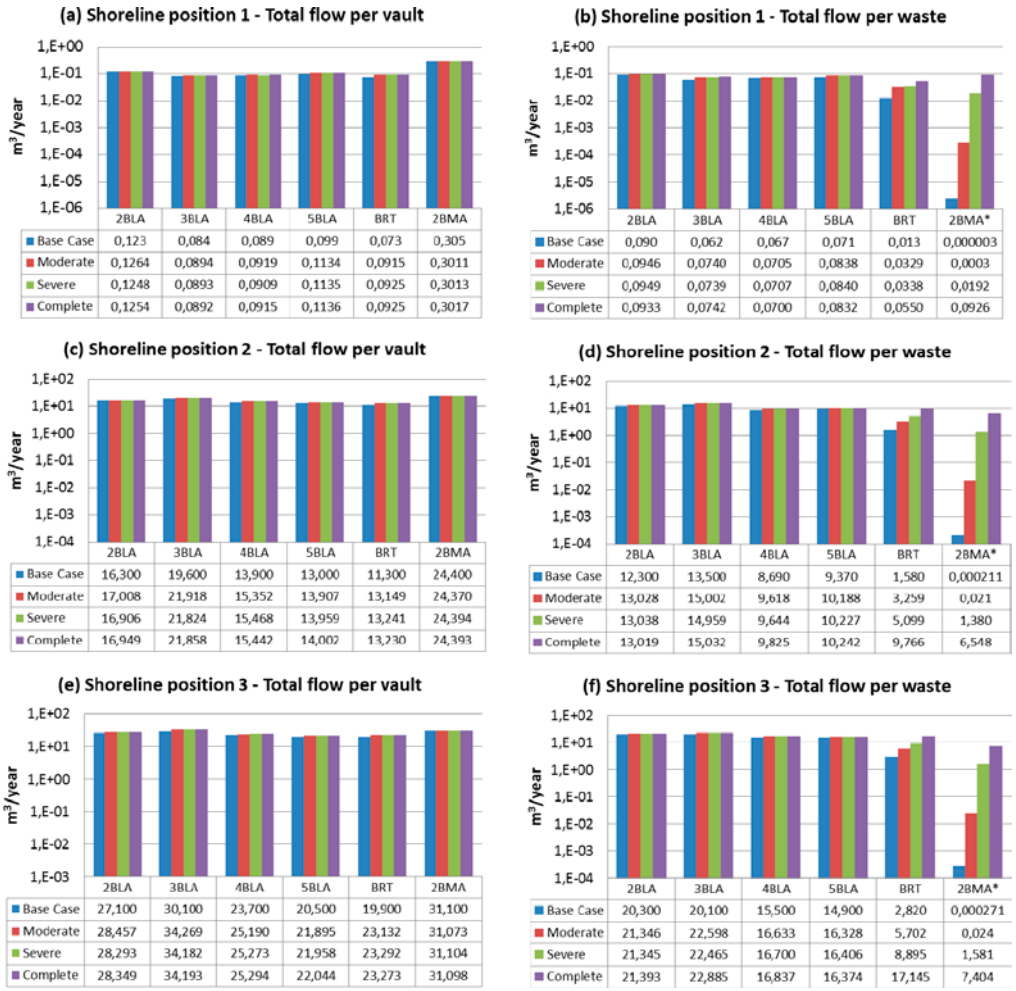

Figure 7-8. *Total flow (m3/year) through the SFR 3 vaults (left) and waste domains (right) for the different concrete degradation cases and the three shoreline positions. The vertical axis is logarithmic.*

Table 7-3. Difference in total flow through the vaults (m^3/year) with respect to the Base case for the different concrete degradation cases. Negative percentages indicate a reduction in flow with respect to the Base case.

		Shoreline position 1			Shoreline position 2			Shoreline position 3		
		Moderate	Severe	Complete	Moderate	Severe	Complete	Moderate	Severe	Complete
Vaults	2BLA	2.7%	1.5%	1.9%	4.3%	3.7%	4.0%	5.0%	4.4%	4.6%
	3BLA	7.1%	6.9%	6.8%	11.8%	11.3%	11.5%	13.9%	13.6%	13.6%
	4BLA	2.8%	1.6%	2.4%	10.4%	11.3%	11.1%	6.3%	6.6%	6.7%
	5BLA	14.3%	14.4%	14.6%	7.0%	7.4%	7.7%	6.8%	7.1%	7.5%
	BRT	26.1%	27.4%	27.4%	16.4%	17.2%	17.1%	16.2%	17.0%	16.9%
	2BMA	–1.3%	–1.2%	–1.1%	–0.1%	0.0%	0.0%	–0.1%	0.0%	0.0%
Waste	2BLA	5.5%	5.8%	4.0%	5.9%	6.0%	5.8%	5.2%	5.1%	5.4%
	3BLA	20.3%	20.2%	20.7%	11.1%	10.8%	11.3%	12.4%	11.8%	13.9%
	4BLA	5.8%	6.0%	5.0%	10.7%	11.0%	13.1%	7.3%	7.7%	8.6%
	5BLA	17.4%	17.7%	16.6%	8.7%	9.1%	9.3%	9.6%	10.1%	9.9%
	BRT	151.2%	157.8%	319.7%	106.3%	222.7%	518.1%	102.2%	215.4%	508.0%
	2BMA*	708.0%	53,335%	257,746%	608.8%	46,509%	221,109%	538.6%	41,604%	195,249%
Loading area	2BLA	1.5%	2.3%	2.3%	–0.5%	–0.3%	–0.3%	0.1%	0.3%	0.2%
	3BLA	15.2%	17.1%	17.9%	5.9%	6.7%	7.2%	6.8%	8.0%	8.6%
	4BLA	4.1%	4.5%	4.7%	4.9%	5.4%	6.3%	4.8%	5.3%	6.2%
	5BLA	6.4%	5.4%	5.6%	8.0%	7.4%	7.8%	8.5%	8.0%	8.5%
	2BMA	–0.4%	–0.7%	–0.6%	–0.7%	–0.7%	–0.7%	–0.8%	–0.9%	–0.8%

* normalized flow per waste package

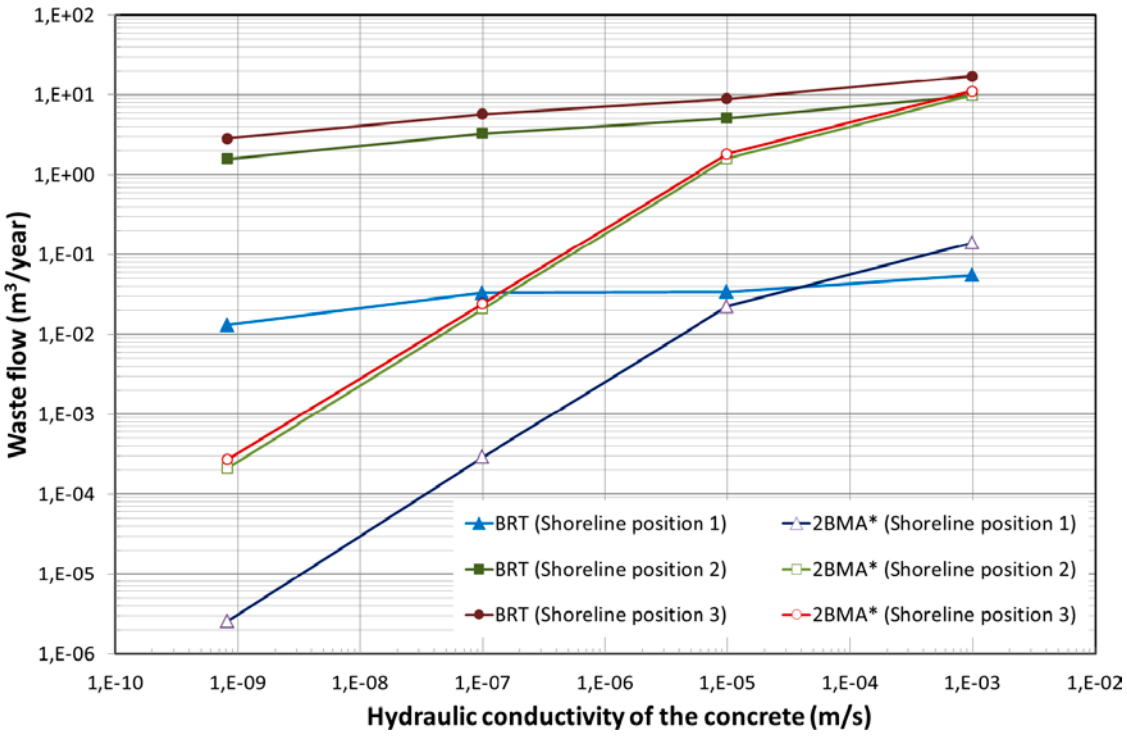

Figure 7-9. *Total flow (m^3/year) in the waste domain as a function of the hydraulic conductivity of the concrete barriers (log_{10}, m/s) for the three shoreline positions: results for BRT and 2BMA vaults. The vertical axis is logarithmic.*

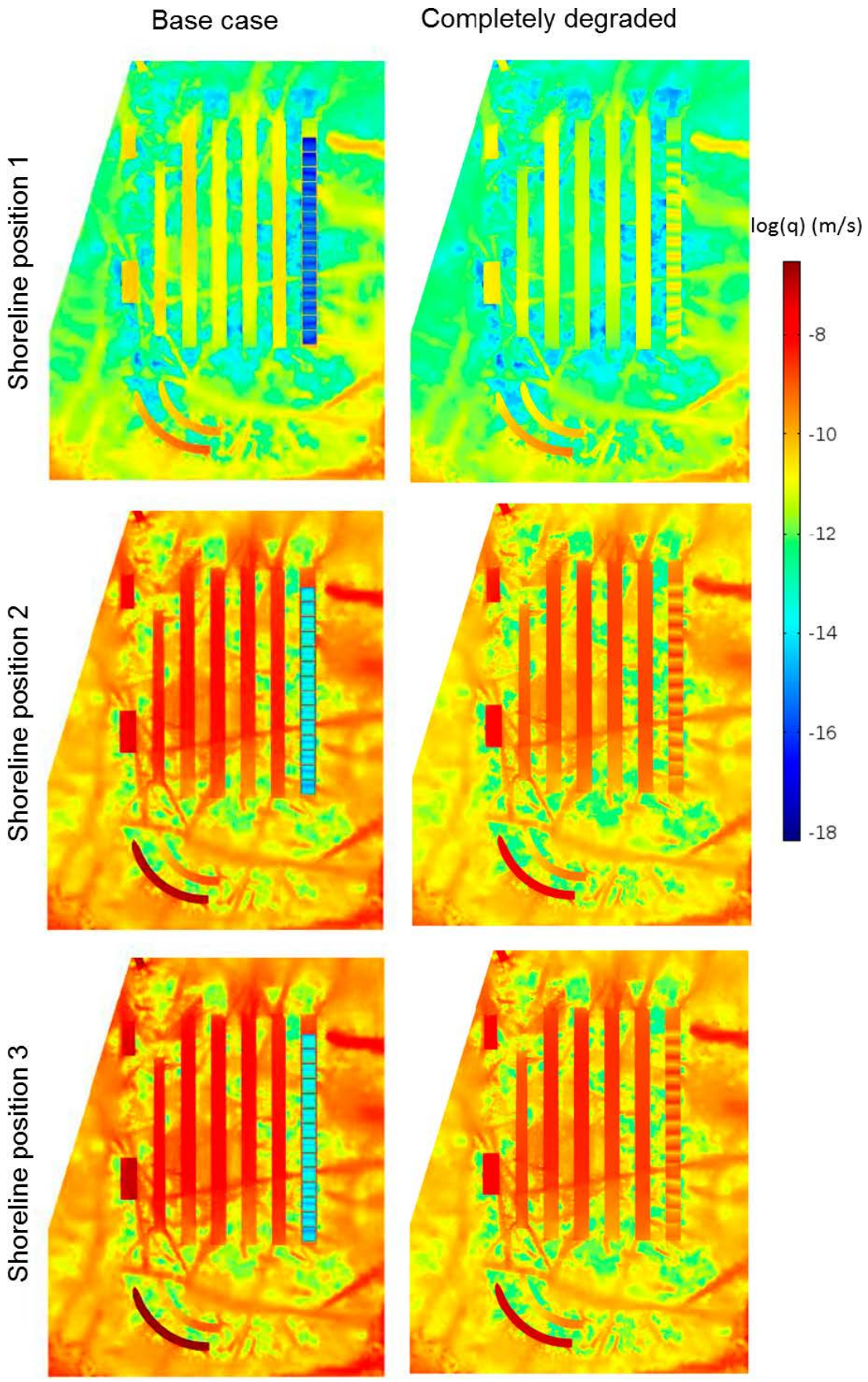

Figure 7-10. *Color map of the magnitude of the Darcy velocity (m/s) in a xy plane at z = –125m for the three shoreline positions.*

The degree of concrete degradation does not affect significantly the flow through the tunnels and loading areas, or the 2-5BLA waste domains. However, it has a strong impact on the BRT and especially the 2BMA waste flow. The BRT waste flow increases up to a 300–500% in the case of a completely degraded concrete. The most critical effects are observed in the 2BMA vault. In this vault the three-dimensional hydraulic cage is very efficient in the Base case and therefore the waste flow is very low. This efficiency is gradually lost as the concrete barriers degrade, with an increase of several orders of magnitude for the severe and complete degradation states.

7.2.2 Plug degradation

The effect of plug degradation was evaluated with a set of simulations where an increasing permeability was assigned to the bentonite sections. Moderate, severe, and complete degradation states were assigned hydraulic conductivities of 10^{-9} m/s, 10^{-6} m/s, and 10^{-3} m/s, respectively. Simulations were performed only for shoreline position 3. The computed tunnel and waste flows (Table 7-4 and graphically in Figure 7-11) show that there is little effect in the case of moderate plug degradation In the case of a severe plug degradation, tunnel flows increase by 18–26% (Figure 7-11c) compared to the Base case. This difference increases to 30–200% in the case of complete plug degradation. The BRT, which is the vault closer to the West access tunnels, presents the highest tunnel flow increase (208%). A decreased effect is observed for 2BLA, 3BLA, 4BLA, 5BLA, and 2BMA, in that order.

The 2-5BLA waste flow (Figure 7-11) increases consistently with the tunnel flow. Again, the BLA vaults located at the west of the repository suffer a higher increase of waste flow. The BRT waste flow rate does not change more than 4% despite the important increase in tunnel flow rates in the case of complete plug degradation. The 2BMA waste flow decreases for the cases of moderate and severe plug degradation. Figure 7-12 shows the 2BMA tunnel (gravel) and waste flows along a longitudinal profile of the 2BMA. The intact case presents two clear peaks associated with the two fractures intersecting sections 5 and 13. Those peaks are reduced for the moderate and severe plug degradation case, indicating a reduction in the flow associated with those fractures in those cases. In the complete degraded case however, the tunnel and waste flow south of the fracture increases with respect to the other cases. In this case there is a shift in the main inflow source to the 2BMA. Water enters the 2BMA vault through the south plug instead of through the deformation zone.

Table 7-4. Total flow through the vaults (m^3/year) for the different plug degradation cases and comparison with the Base case for the shoreline position 3. Negative percentages indicate a reduction in flow with respect to the Base case.

	Total flow (m^3/year)	Base case Intact	Plugs Degradation			% change		
			Moderate	Severe	Complete	Moderate	Severe	Complete
Vaults	2BLA	27.1	27.21	32.14	74.92	0%	19%	176%
	3BLA	30.1	30.36	35.65	59.56	1%	18%	98%
	4BLA	23.7	23.83	28.67	44.24	1%	21%	87%
	5BLA	20.5	20.52	25.91	32.70	0%	26%	60%
	BRT	19.9	19.96	23.27	61.32	0%	17%	208%
	2BMA	31.1	31.12	35.80	40.47	0%	15%	30%
Waste	2BLA	20.3	20.38	23.24	47.94	0%	15%	136%
	3BLA	20.1	20.17	23.85	39.79	0%	19%	98%
	4BLA	15.5	15.48	17.42	29.08	0%	12%	88%
	5BLA	14.9	14.97	17.28	21.16	0%	16%	42%
	BRT	2.82	2.81	3.02	2.94	0%	7%	4%
	2BMA*	0.0002	0.0002	0.0002	0.0003	–25%	–15%	14%
Loading area	2BLA	14.8	14.87	17.35	53.99	0%	17%	265%
	3BLA	17	17.10	20.31	27.98	1%	19%	65%
	4BLA	17.2	17.58	24.43	24.87	2%	42%	45%
	5BLA	8.43	8.61	17.27	17.85	2%	105%	112%
	2BMA	5.27	5.35	14.14	8.34	2%	168%	58%

* normalized flow per waste package

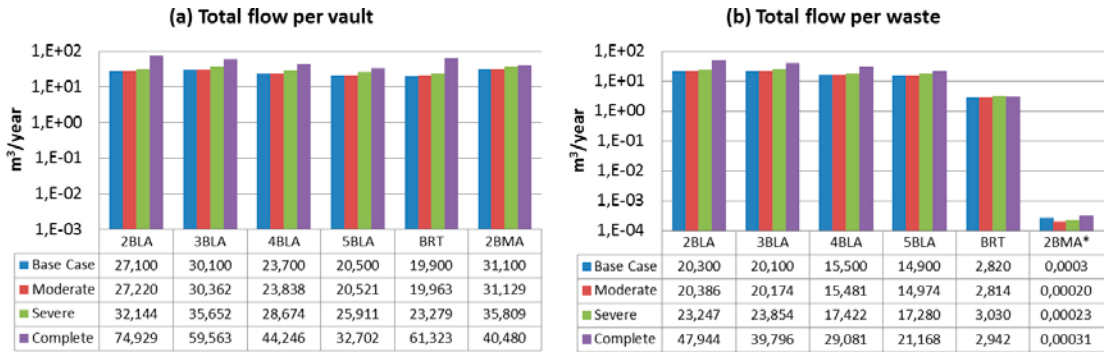

	2BLA	3BLA	4BLA	5BLA	BRT	2BMA
Base Case	27,100	30,100	23,700	20,500	19,900	31,100
Moderate	27,220	30,362	23,838	20,521	19,963	31,129
Severe	32,144	35,652	28,674	25,911	23,279	35,809
Complete	74,929	59,563	44,246	32,702	61,323	40,480

	2BLA	3BLA	4BLA	5BLA	BRT	2BMA*
Base Case	20,300	20,100	15,500	14,900	2,820	0,0003
Moderate	20,386	20,174	15,481	14,974	2,814	0,00020
Severe	23,247	23,854	17,422	17,280	3,030	0,00023
Complete	47,944	39,796	29,081	21,168	2,942	0,00031

Figure 7-11. *Total flow (m3/year) through the SFR 3 vaults (left) and waste domains (right) for the different plug degradation cases and the shoreline position 3. The vertical axis is logarithmic.*

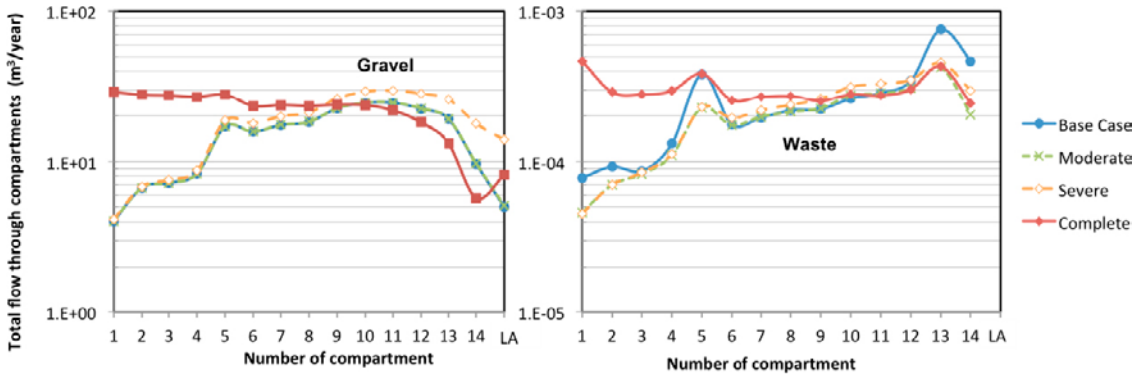

Figure 7-12. *Total flow (m^3/year) along the different gravel (left) and waste (right) control volumes of the 2BMA.*

The change in the main pathways is also illustrated in Figure 7-13. The increase in the plugs hydraulic conductivity leads to an increase in the magnitude of flow through the BLA vaults and a decrease in the rock structures intersecting the vaults (Figure 7-13). The flow in the high permeability vaults between vaults BRT and 4BLA is reduced and so it is the flow in the two deformation zones affecting the 2BMA. There is a reduction of the vaults interconnection through the deformation zone as the plugs permeability increases. Note the low flow within the BLA vaults south of the main fracture crossing the vaults in the moderate and severe degradation cases. That low flow area disappears in the case of complete degraded plugs, indicating the change in inflow to the vaults from the fracture to the south entrance of the tunnels.

Only the complete degradation of the plugs results in an important increase of tunnel and waste flows. The impact of the plug degradation increases towards the west part of the repository, where the access tunnels are located. Completely degraded plugs change the location of the main groundwater inflow to the vaults. In the Base case (and moderate and severe plug degradation cases) water enters the vaults mainly through the main fracture crossing all vaults, but in the case of completely degraded plugs, the south entrance of the tunnel (plug) becomes the main inflow area to the vaults. Interestingly, the flow in the 2BMA waste decreases in the case of a moderately and severe plug degradation. This reduction in flow is the consequence of the redirection of flow from the fractures affecting the 2BMA to the permeable BLA vaults.

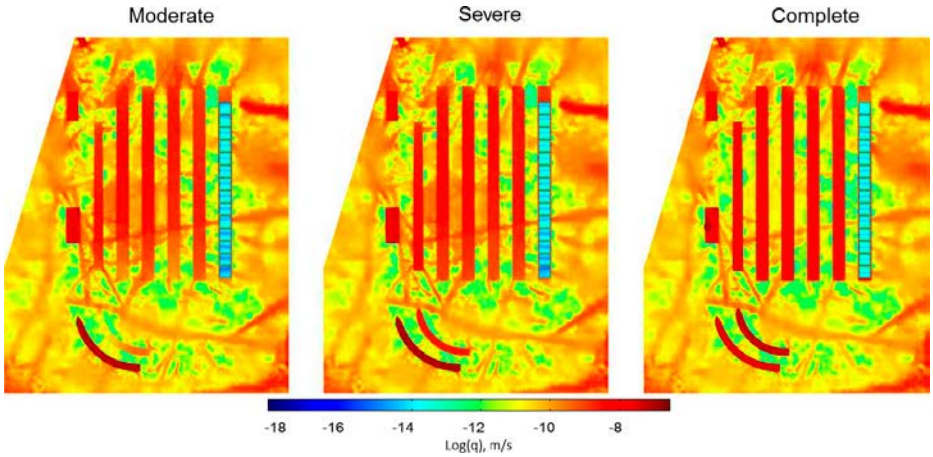

Figure 7-13. *Color map of the magnitude of the Darcy velocity (m/s) for three different states of plug degradation and the shoreline position 3.*

7.2.3 No barriers

The case of no barriers corresponds to the simultaneous degradation of both the concrete structures and the bentonite plugs. All the concrete and bentonite domains are here assigned a conductivity of 10^{-3} m/s. Therefore, this case is the combination of the complete concrete degradation and the completely degraded plugs. This case was analyzed for the shoreline position 3. The computed tunnel and waste flows are presented in Table 7-5 and graphically in Figure 7-15. The tunnel flow increases in all vaults with respect to the base case. As in the cases of the completely degraded plugs, the flow increases especially in the west vaults of the repository. The BRT vault, the closest to the access tunnels, sees an increased flow by 275%. The 2BMA vault, located further east, increases its tunnel flow by 25%. In fact, it is interesting that the BRT vault is the only vault whose tunnel flow increases compared to the completely degraded plugs case. This is reasonable since the waste grout of the BFT is also degraded in this case. What is not so evident is the fact that the 2-5BLA and 2BMA vaults decrease their tunnel flow compared to the completely degraded plugs case. Part of the water reaching the access tunnels flow through the BRT (which increases its flow) redirecting water from the vaults further east through the access tunnels.

The increase in waste flow in the 2-5BLA vaults is consistent with the increase in the tunnel flow. It affects predominantly the vaults in the West side of the repository. The waste-to-vault flow ratio is 60–65% in all SFR 3 BLA vaults. The BRT waste flow increases one order of magnitude compared to the Base case (Table 7-5 and Figure 7-14), and doubles the value of the completely degraded concrete case (see Section 7.2.1, Table 7-2). In turn, the BRT waste-to-tunnel flow ratio is around 50%. The 2BMA is by far the most affected vault. Even though the increase in the tunnel flow is modest (25%), the impact on the waste total flow is very large. From an efficient three-dimensional hydraulic cage of the Base case, in the case of no barriers the 2BMA becomes a groundwater flow pipe (resembling the behavior of the 2-5BLA vaults). The waste-to-tunnel total flow ratio increases substantially (32%). The smaller percentage with respect to the 2-5BLA vaults is due to the smaller waste volume of the 2BMA.

The spatial distribution of flow on a plane across the repository (Figure 7-15) shows that, as seen in the completely degraded plugs case (see Section 7.2.2), the flow increases in all the vaults and access tunnels and decreases in the rock structures perpendicular to the vaults. There is an increase of flow in the southern part of the vaults (south of the main fracture crossing all vaults), indicating that the inflow of water occurs mainly through the southern plug. The flow within the 2BMA waste compartments increases greatly and the 2BMA behaves as a BLA vault.

In summary, the no barriers case has important implications for the BRT vault, leading to an increase of both the tunnel flow (275%) and the waste flow (more than one order of magnitude). For the BLA vaults, the influence is reduced compared to the completely degraded plugs case. The BRT vault acts as a flow by-pass, reducing the flow towards the BLA vaults. The 2BMA, located at the east side of the repository, and benefits the most from this redirection of flow. Its tunnel flow increases only by 25% with respect to the Base case. However, the effect on the waste flow is severe, and increases approximately 5 orders of magnitude.

Table 7-5. Total flow through the vaults (m^3/year) for the no barrier case and comparison with the Base case (BC) for the shoreline position 3. Negative percentages indicate a reduction in flow with respect to the Base case.

		Shoreline position 3	
		Total flow (m^3/year)	Difference BC
Vaults	2BLA	71.51	164%
	3BLA	57.25	90%
	4BLA	42.03	77%
	5BLA	30.37	48%
	BRT	74.60	275%
	2BMA	38.93	25%
Waste	2BLA	45.15	122%
	3BLA	39.42	96%
	4BLA	27.72	79%
	5BLA	19.71	32%
	BRT	35.34	1,154%
	2BMA*	12.36	4,567,947%
Loading area	2BLA	51.03	245%
	3BLA	23.39	38%
	4BLA	22.77	32%
	5BLA	14.92	77%
	2BMA	4.33	-18%

* normalized flow per waste package

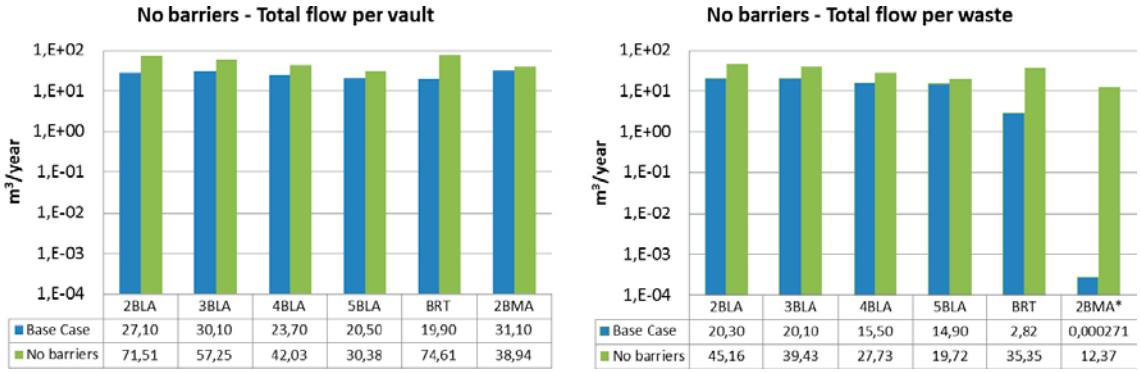

Figure 7-14. *Total flow (m3/year) through the SFR 3 vaults (left) and waste domains (right) for the different plug degradation cases and the shoreline position 3. The vertical axis is logarithmic.*

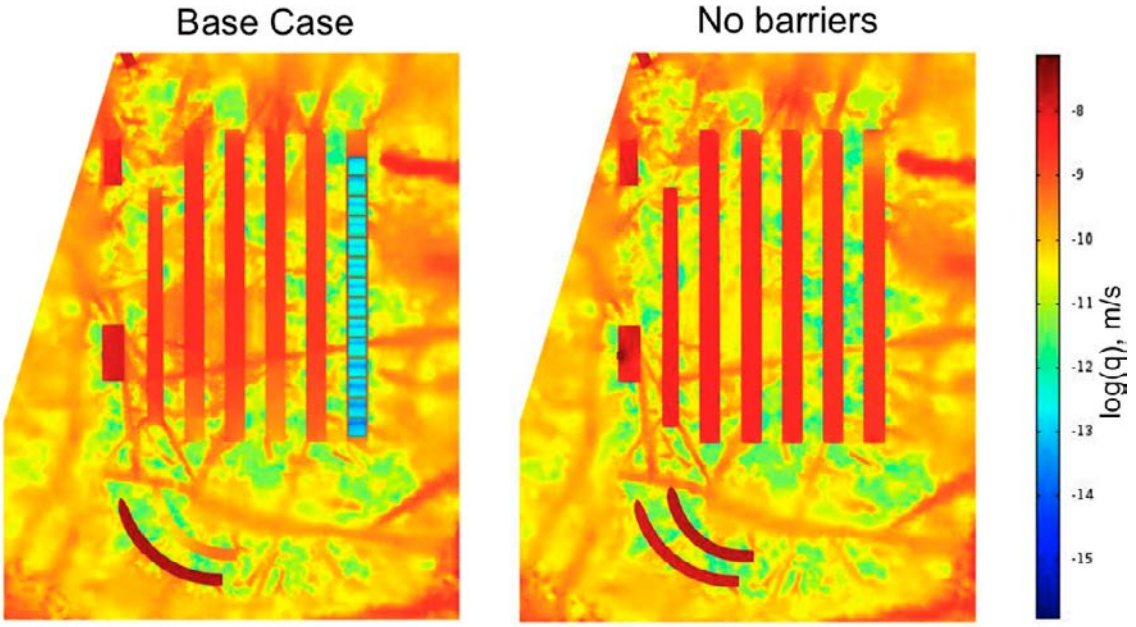

Figure 7-15. *Color map of the magnitude of the Darcy velocity (m/s) in a xy– plane at z = –125 m of the SFR 3 repository for the Base case and the no barriers case. Results for the shoreline position 3.*

7.3 Repository closure

7.3.1 Abandoned repository

The abandoned repository case represents a situation where no additional barriers and structures are emplaced after the operational phase. In this case, the concrete lids of the 2BMA waste compartments are not in place, the BRT waste is not grouted, and the repository is not sealed with bentonite plugs. The hydraulic conductivity of the absent elements is set to 10^{-3} m/s, the maximum value of conductivity considered in the model. This calculation case resembles the no barriers case except for the presence of the intact concrete walls and floor of the 2BMA waste compartments. The computed tunnel and waste flows are presented in Table 7-6 and Figure 7-16 for the shoreline positions 1 and 3. The results of the tunnel flows are similar to the no barrier case. The flow in the tunnels increase substantially with respect to the Base case with a maximum increase in the BRT located at the west side of the repository. The impact in the other vaults decreases towards the east, and in the 2BMA is the least affected. The increase in the waste flow follows a similar pattern in the BLA vaults; the impact increases towards the west. In the BRT, the waste flow is of the same order of magnitude as in the no barrier case. The absence of the concrete lids in the 2BMA waste compartments result in one order of magnitude higher flow through the waste compared to the base case.

The distribution of flow in the repository near-field (Figure 7-17) shows the pattern observed for the completely degraded plugs and the no barrier case. The absence of plugs increases the flow though the vaults and decreases the flow in the rock permeable structures perpendicular to the vaults.

The results of the abandoned repository case are similar to the no barriers case for the tunnel flows and the BLA and BRT waste flows. The BRT tunnel flow increases by 260% and the waste flow one order of magnitude compared to the Base case. The 2BMA waste flow increases one order of magnitude compared to the Base case, due to the absence of the concrete lids on the compartments.

Table 7-6. Total flow through the vaults (m^3/year) for the abandoned repository case and comparison with the Base case for the shoreline positions 1 and 3. Negative percentages indicate a reduction in flow with respect to the Base case.

		Shoreline position 1		Shoreline position 3	
		Total flow (m^3/year)	Difference BC	Total flow (m^3/year)	Difference BC
Vaults	2BLA	0.24	101%	71.52	164%
	3BLA	0.19	130%	57.76	92%
	4BLA	0.15	78%	43.26	83%
	5BLA	0.16	63%	31.98	56%
	BRT	0.21	191%	71.89	261%
	2BMA	0.27	-11%	40.51	30%
Waste	2BLA	0.15	73%	45.98	127%
	3BLA	0.12	105%	38.74	93%
	4BLA	0.10	57%	28.49	84%
	5BLA	0.10	50%	20.77	39%
	BRT	0.11	752%	35.20	1,148%
	2BMA*	0.00002	745%	0.0059	2,115%
Loading area	2BLA	0.15	147%	50.65	242%
	3BLA	0.12	616%	26.23	54%
	4BLA	0.09	181%	23.95	39%
	5BLA	0.12	255%	17.11	103%
	2BMA	0.04	97%	8.46	61%

* normalized flow per waste package

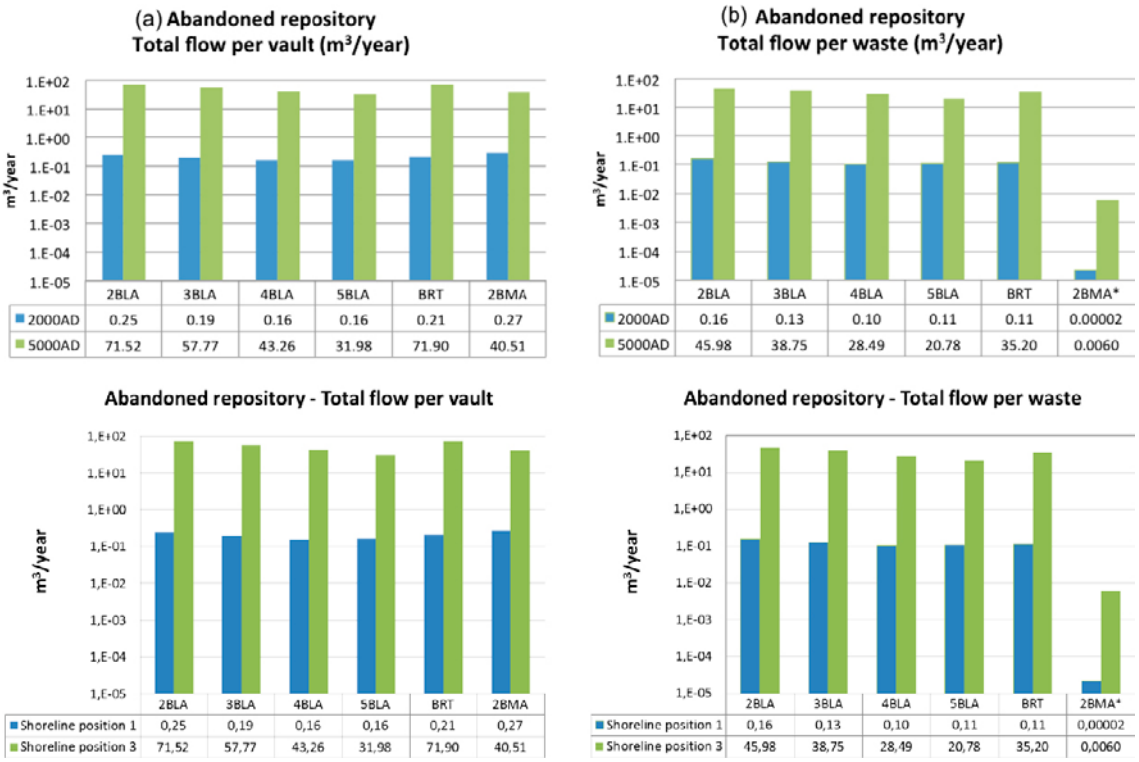

Figure 7-16. *Total flow (m3/year) through the SFR 3 vaults (left) and waste domains (right) for the abandoned repository case and the shoreline positions 1 and 3. The vertical axis is logarithmic.*

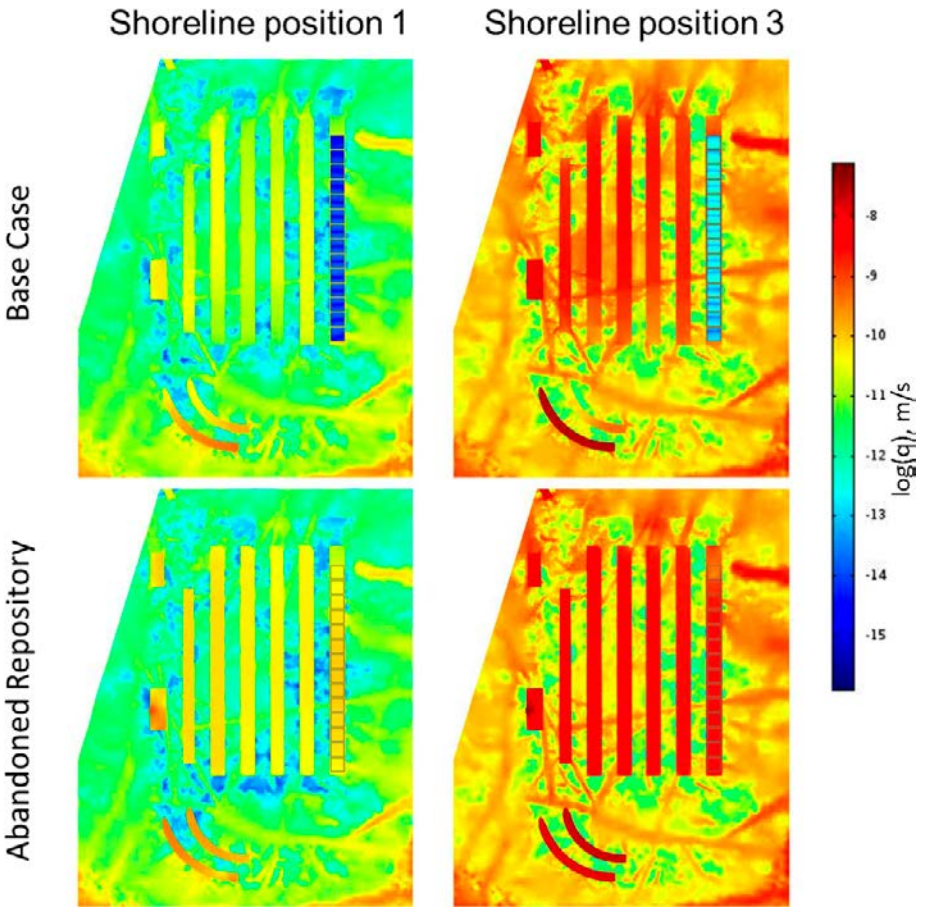

Figure 7-17. *Color map of the magnitude of the Darcy velocity (m/s) on a horizontal xy plane at z = –125 m of the SFR 3 repository for the Base case (top) and the abandoned repository case (bottom). Results for the shoreline positions 1 and 3.*

7.4 Permafrost

The permafrost case described in section 6.4 for the SFR 1 repository (see Figure 6-42) was also simulated for SFR 3. Figure 7-18 show the conductivity field used in the simulation for the shallow permafrost case and the comparison with the conductivity field of the Base case.

The calculated total tunnel and waste flow for a shallow permafrost case are presented in Table 7-7 and graphically in Figure 7-19. Both the tunnel and waste flows decrease in all vaults with respect to the Base case situation for the shoreline position 3, except for the 2BMA for which an increase of 6% is observed. The average reduction in the flow through the repository structures is ~40%, a value that is lower than the average rock permeability decrease around the frozen front (~58%).

Figure 7-20 shows the comparison between the Darcy velocity magnitude at the level of the repository resulting from the permafrost simulation with that obtained for the Base case for the shoreline position 3. As it was found in the permafrost simulation of SFR 1, the water flow around the SFR 3 repository is generally lower than the flow in the Base case. A higher flow is developed in one of the access tunnels. This is also confirmed by comparing the recharge streamlines of the vaults shown in Figure 7-4 (Base case for the shoreline position 3) and Figure 7-21 (permafrost of SFR 3). The comparison between the streamlines for the Base case and the shoreline position 3 (Figure 7-4), with the permafrost shorelines (Figure 7-21 and Figure 7-22) shows that in the Base case groundwater recharge flow is vertical and comes from the media above the access tunnels of the repository (Figure 7-4). On the contrary, permafrost induces a horizontal recharge flow (Figure 7-21 through the access tunnels. In addition, unlike the SFR 1 repository, the horizontal flow discharge flow pattern of SFR 3 is also changed. In particular, more intense discharge streamlines follow the East direction (see Figure 7-22).

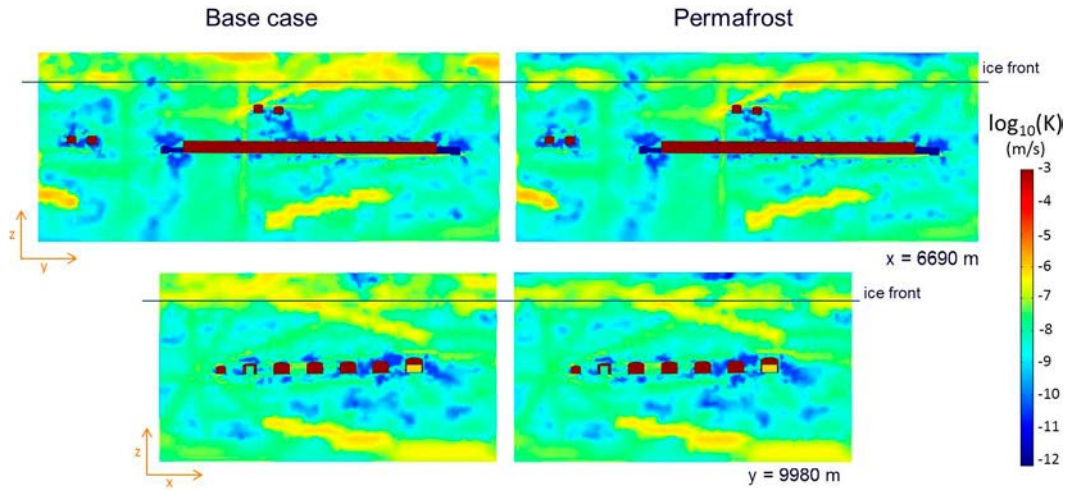

Figure 7-18. *Hydraulic conductivity field used in the simulation of a shallow permafrost case. Cut planes at x = 6,690 m and y = 9,980 m are shown for the Base case (left) and permafrost case (right).*

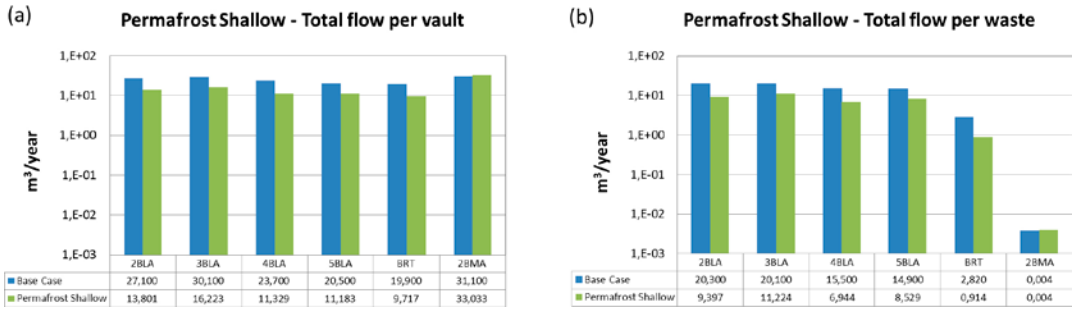

Figure 7-19. *Total flow entering the SFR 3 vaults (a) and waste domains (b) for the Shallow permafrost case compared with the Base Case for the shoreline position 3. The vertical axis is logarithmic.*

Table 7-7. Total flow through the vaults (m^3/year) for the Shallow permafrost case and comparison with the Base Case (BC) for the shoreline position 3. Negative percentages indicate a reduction in flow with respect to the BC.

		Total flow (m^3/year)	Difference BC, %
Vaults	2BLA	13.80	–49
	3BLA	16.22	–46
	4BLA	11.33	–52
	5BLA	11.18	–45
	BRT	9.72	–51
	2BMA	33.03	6
Waste	2BLA	9.40	–54
	3BLA	11.22	–44
	4BLA	6.94	–55
	5BLA	8.53	–43
	BRT	0.91	–68
	2BMA*	0.004	6
Loading area	2BLA	8.96	–39
	3BLA	9.02	–47
	4BLA	10.16	–41
	5BLA	6.49	–23
	2BMA	4.56	–13

* normalized flow per waste package

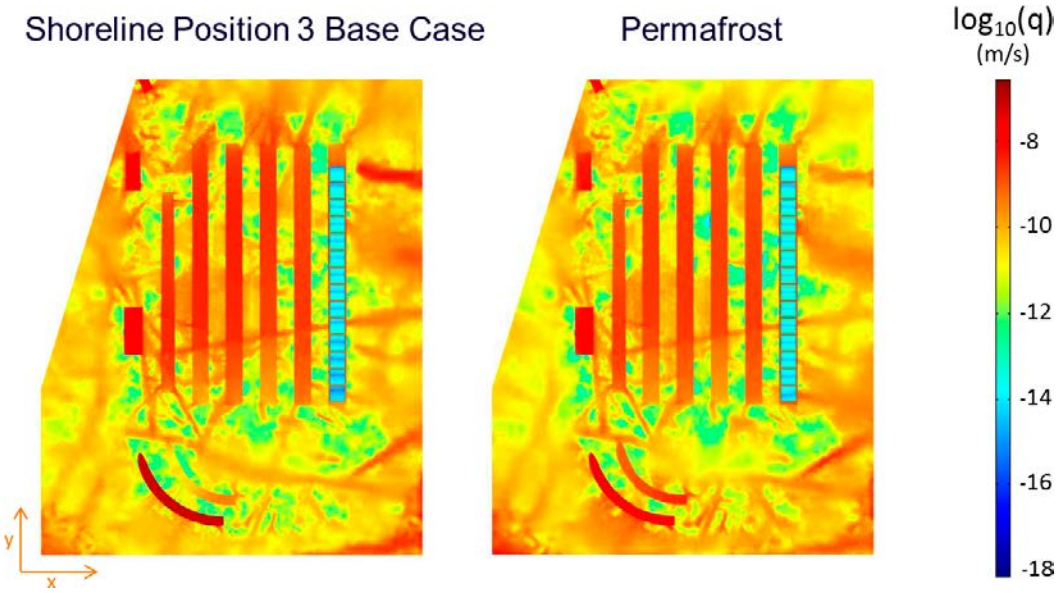

Figure 7-20. *Comparison of the Darcy velocity (m/s) for the Shallow permafrost case (right) and the Base case for the shoreline position 3 (left) in a xy plane at z = –125 m*

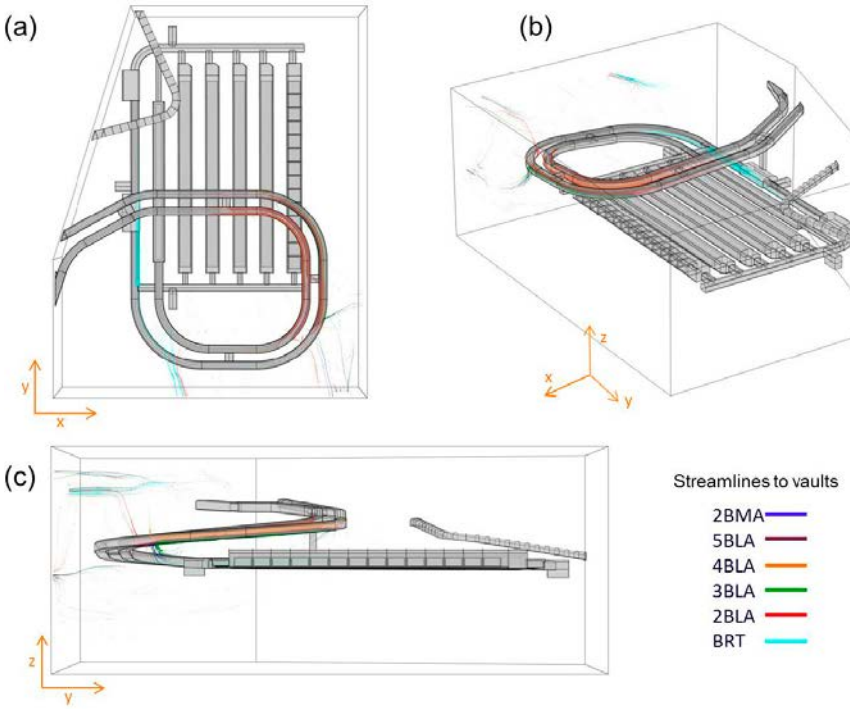

Figure 7-21. *Groundwater streamlines reaching individual vaults (color tubes) for the Shallow permafrost case: results shown from three different angles. The streamline thickness is proportional to the magnitude of the flow.*

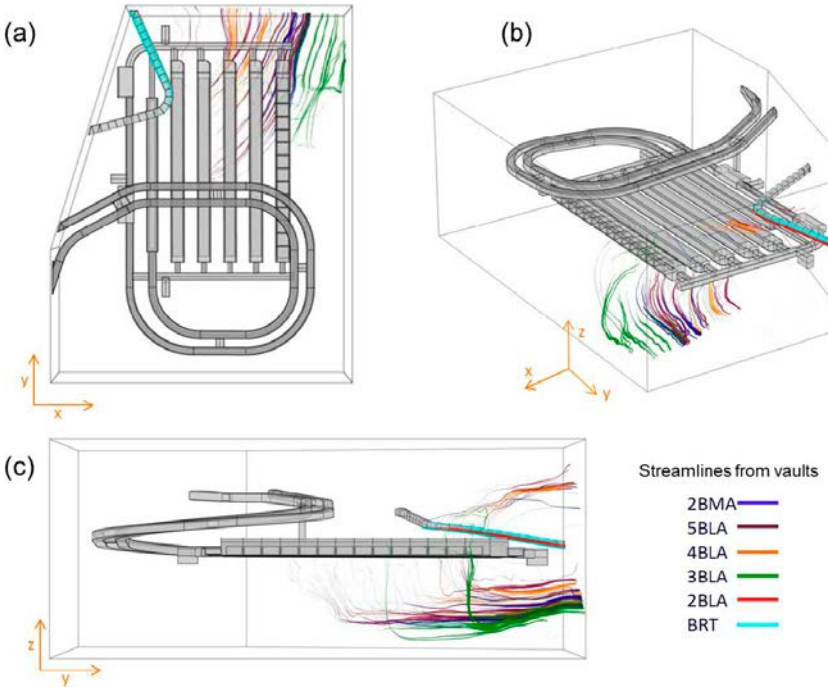

Figure 7-22. *Groundwater streamlines leaving individual vaults (color tubes) for the Shallow permafrost case: results shown from three different angles. The streamline thickness is proportional to the magnitude of the flow.*

Both the vault and waste flows calculated for the Shallow permafrost case decrease in all vaults with respect to the Base case at shoreline position 3, except for the 2BMA vault where a slight increase is observed. The flow behavior displayed in the permafrost case is more horizontal than the respective flow pattern of the Base case. A more intense discharge from the vaults is also observed and the direction of flow is displaced to the East, whereas in the Base case the streamlines are more parallel to the vaults.

7.5 Estimation of uncertainty associated with the geosphere

Two realizations of the rock permeability field have been used to assess the range of variability in the computed flow due to uncertainties in the description of the hydraulic properties in the geosphere. The realizations are considered as representative of cases that lead to higher and lower average tunnel flow compared to the Base case. They are here referred to as the High and Low flow realization (see Table 6-12 for correspondence with respective DarcyTools simulations). The hydraulic conductivity field of the surrounding rock of the SFR 3 repository is illustrated in Figure 7-23. The Base case and the High flow realization present the same structures affecting the repository. There are basically three high permeability zones. The first is the deformation zone ZFMWNW8042, a thin fracture zone crossing all the vaults and 2BMA at section 5. The second is an extensive, rounded high permeability zone, affecting the rock between vaults BRT and 5BLA. The third structure is the deformation zone ZFMWNW0835, a thick deformation zone crossing the 2BMA at sections 10–13, which also affects the 4BLA and 5BLA vaults. All these structures have a higher permeability in the High flow realization. There is also an increased presence of high permeability vertical structures in the High flow realization. The Low flow realization is characterized by a lower permeability zone in the areas of the access tunnels and the BRT and by thinner and less permeable fractures crossing the repository. The main two deformation zones crossing the 2BMA (ZFMWNW0835 and ZFMWNW8042) are present but are less permeable than for the base case. A zone of higher permeability exists between the BRT and 5BLA. There is a fourth permeable structure in the Low flow realization that crosses the 2BMA between sections 7 and 8 and extends west affecting all the SFR 3 vaults.

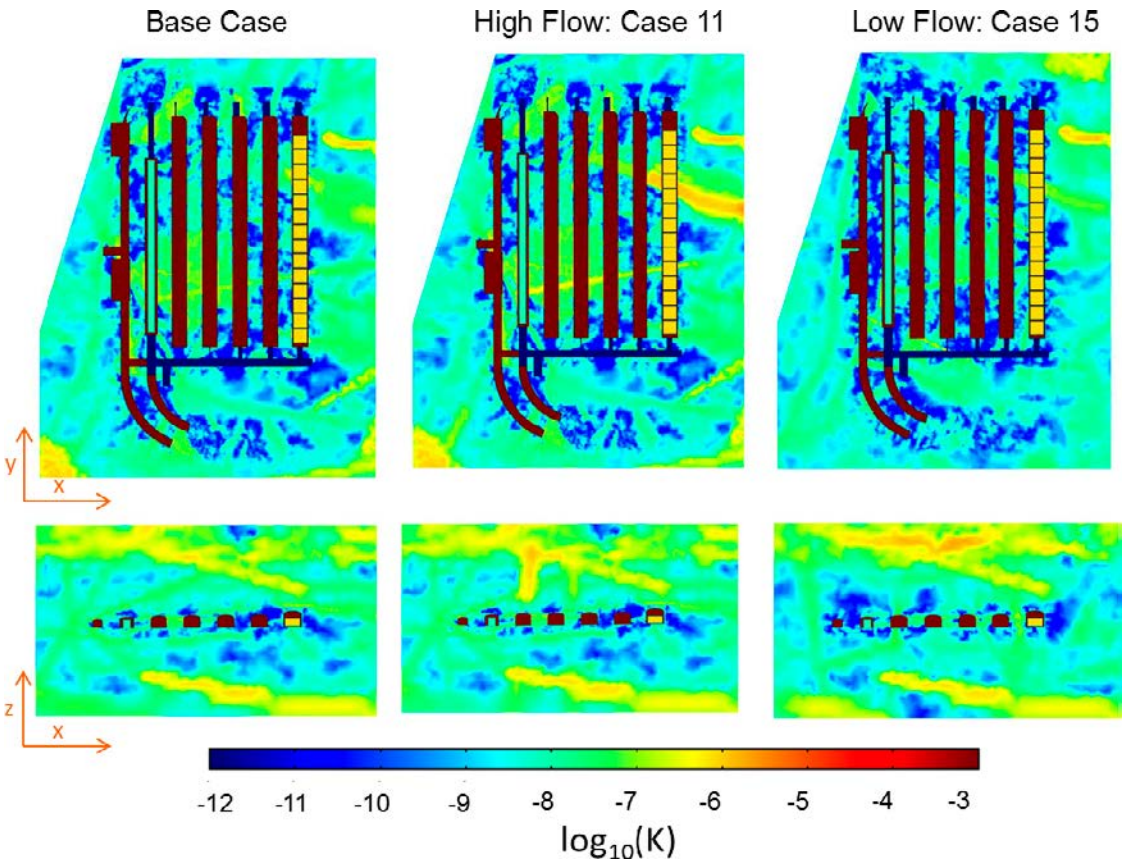

Figure 7-23. *Hydraulic conductivity of the rock on two planes traversing the SFR 3 repository: horizontal plane at z =–127.5 m (top) and y =10,000 m (bottom).*

The magnitude of the flow (m/s) in a horizontal plane at z = –125 m (Figure 7-24) clearly demarks the most conductive deformation zone in each realization. In the vertical cross section (Figure 7-23 bottom), a vertical fracture between the 5BLA and the 2BMA vaults is observed.

The calculated tunnel and waste flow for the High flow and Low flow realizations are presented in Table 7-8 and Table 7-9 and graphically in Figure 7-25. The vault with the highest flow is the 2BMA vault. The results show that:

- For the shoreline position 1, the 2BMA doubles its flow in the High flow realization and it is reduced to 2/3 in the Low flow realization. The BRT flow increases a 60% in the High flow realization and it is not altered in the case of the Low flow case. The BLA vaults present the lowest flow at the base case, but they seem quite insensitive to the permeability realization. The waste flow, however, does not follow the same criterion. In the BLA and BRT vaults, the waste flow is reduced between a 35–52% in the Low flow realization. The waste flow increases in the High flow realization affecting mostly to the vaults located at the east side of the repository. The 2BMA vault increases its waste flow a 70% and the 5BLA a 56% whereas it only increases a 1% in the BRT and it is even reduced in the 2BLA.
- The shoreline positions 2 and 3 yield similar behavior of the tunnel and waste flows but flows are higher for the shoreline position 3. The 2BMA tunnel flow increases in both alternative realizations; more than 200% in the high flow case and a 30–40% in the Low flow realization. The 5BLA vault, located west of the 2BMA shows a similar behavior. Its flow increases in both realizations between a 25–50%. The flow variation in the other vaults is small and the follow the expected result; flow is reduced in the Low flow realization and increased in the High flow realization. Regarding the waste flow, the BRT vaults present the highest flow in the base case and it is the only vault not following the criterion of decreasing flow in the Low flow cases and increasing it in the High flow case.

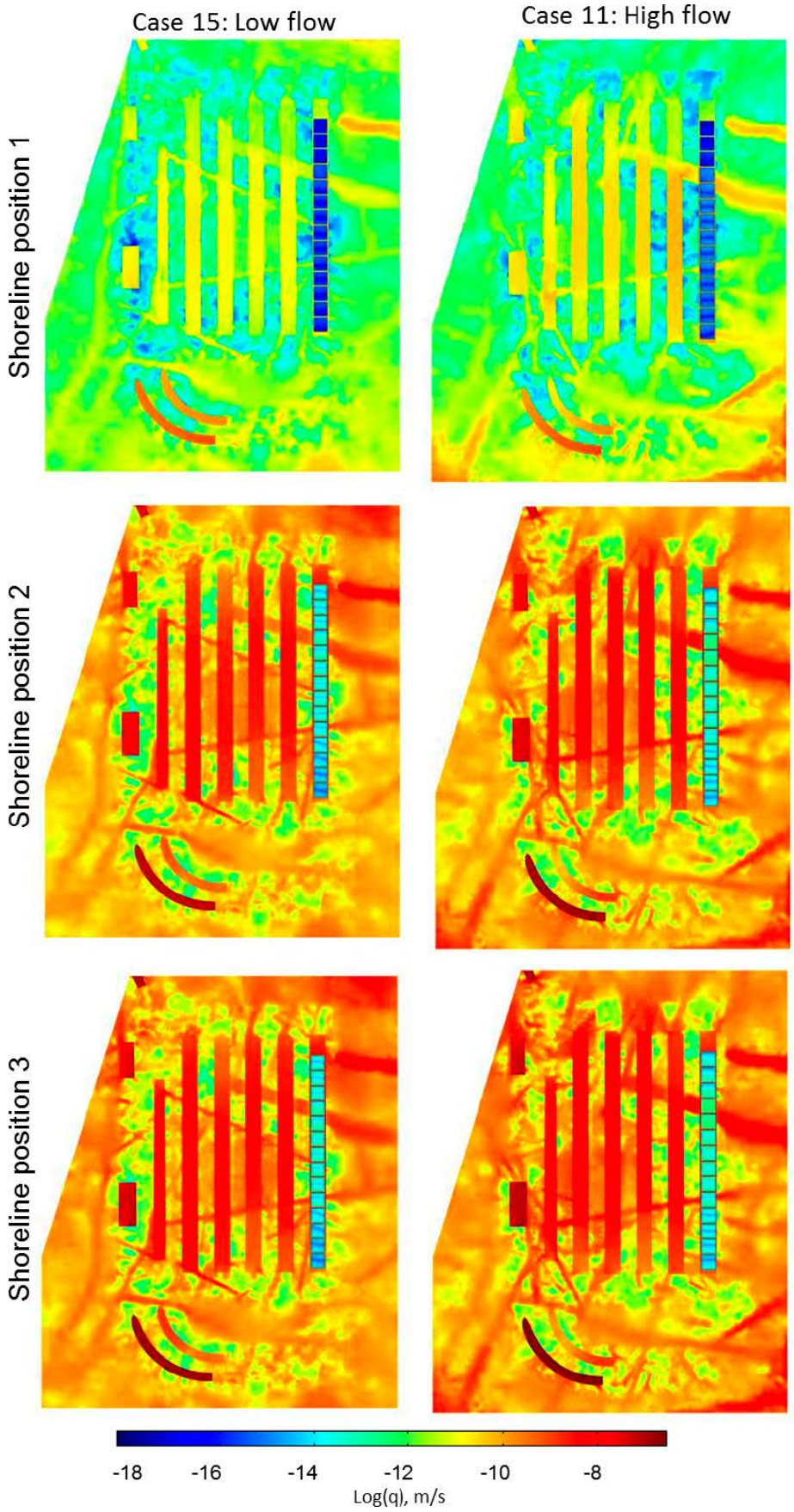

Figure 7-24. *Color map of the magnitude of the Darcy velocity (m/s) on a horizontal xy plane at z = –125 m of the SFR 3 repository for three rock permeability realizations and the three shoreline positions.*

Table 7-8. Total flow through the SFR 1 vaults (m^3/year) for the High flow case and comparison with the Base case (BC). Negative percentages indicate a reduction in the total flow with respect to the BC.

		Shoreline position 1		Shoreline position 2		Shoreline position 3	
		Total flow (m^3/year)	Difference BC	Total flow (m^3/year)	Difference BC	Total flow (m^3/year)	Difference BC
Vault.	2BLA	0.11	–8%	19.07	17%	29.21	8%
	3BLA	0.09	19%	23.82	22%	33.63	12%
	4BLA	0.11	28%	20.47	47%	34.94	47%
	5BLA	0.13	34%	20.67	59%	29.92	46%
	BRT	0.11	62%	13.79	22%	22.48	13%
	2BMA	0.71	134%	81.59	234%	116.83	276%
Waste	2BLA	0.08	–9%	14.90	21%	22.34	10%
	3BLA	0.07	16%	17.43	29%	23.48	17%
	4BLA	0.08	27%	13.09	51%	23.25	50%
	5BLA	0.11	56%	14.39	54%	20.55	38%
	BRT	0.01	1%	1.39	–11%	2.38	–15%
	2BMA*	0.000004	70%	0.0004	96%	0.0005	98%
Loading area	2BLA	0.05	–13%	8.66	11%	16.58	12%
	3BLA	0.01	–11%	8.50	–15%	14.81	–13%
	4BLA	0.02	–39%	11.74	8%	19.30	12%
	5BLA	0.01	–67%	2.82	–51%	4.40	–48%
	2BMA	0.01	–56%	3.51	–13%	4.71	–11%

* normalized flow per waste package

Table 7-9. Total flow through the SFR 1 vaults (m^3/year) for the Low flow case and comparison with the Base case (BC). Negative percentages indicate a reduction in the total flow with respect to the BC.

		Shoreline position 1		Shoreline position 2		Shoreline position 3	
		Total flow (m^3/year)	Difference BC	Total flow (m^3/year)	Difference BC	Total flow (m^3/year)	Difference BC
Vault	2BLA	0.13	11%	14.38	–12%	23.34	–14%
	3BLA	0.10	25%	11.12	–43%	17.60	–42%
	4BLA	0.11	30%	13.16	–5%	21.55	–9%
	5BLA	0.12	24%	16.30	25%	24.57	20%
	BRT	0.07	10%	7.48	–34%	12.92	–35%
	2BMA	0.20	–32%	32.13	32%	44.96	45%
Waste	2BLA	0.043	–52%	5.30	–57%	8.53	–58%
	3BLA	0.037	–40%	4.39	–67%	6.83	–66%
	4BLA	0.041	–37%	4.60	–47%	7.48	–52%
	5BLA	0.043	–40%	5.73	–39%	8.58	–42%
	BRT	0.008	–35%	0.61	–61%	1.08	–61%
	2BMA*	0.0000005	–78%	0.00009	–55%	0.0001	–55%
Loading area	2BLA	0.012	–80%	2.06	–78%	4.04	–73%
	3BLA	0.002	–87%	0.58	–94%	0.93	–95%
	4BLA	0.007	–77%	3.62	–67%	5.43	–68%
	5BLA	0.011	–68%	3.08	–46%	4.30	–49%
	2BMA	0.025	9%	7.28	81%	9.53	81%

* normalized flow per waste package

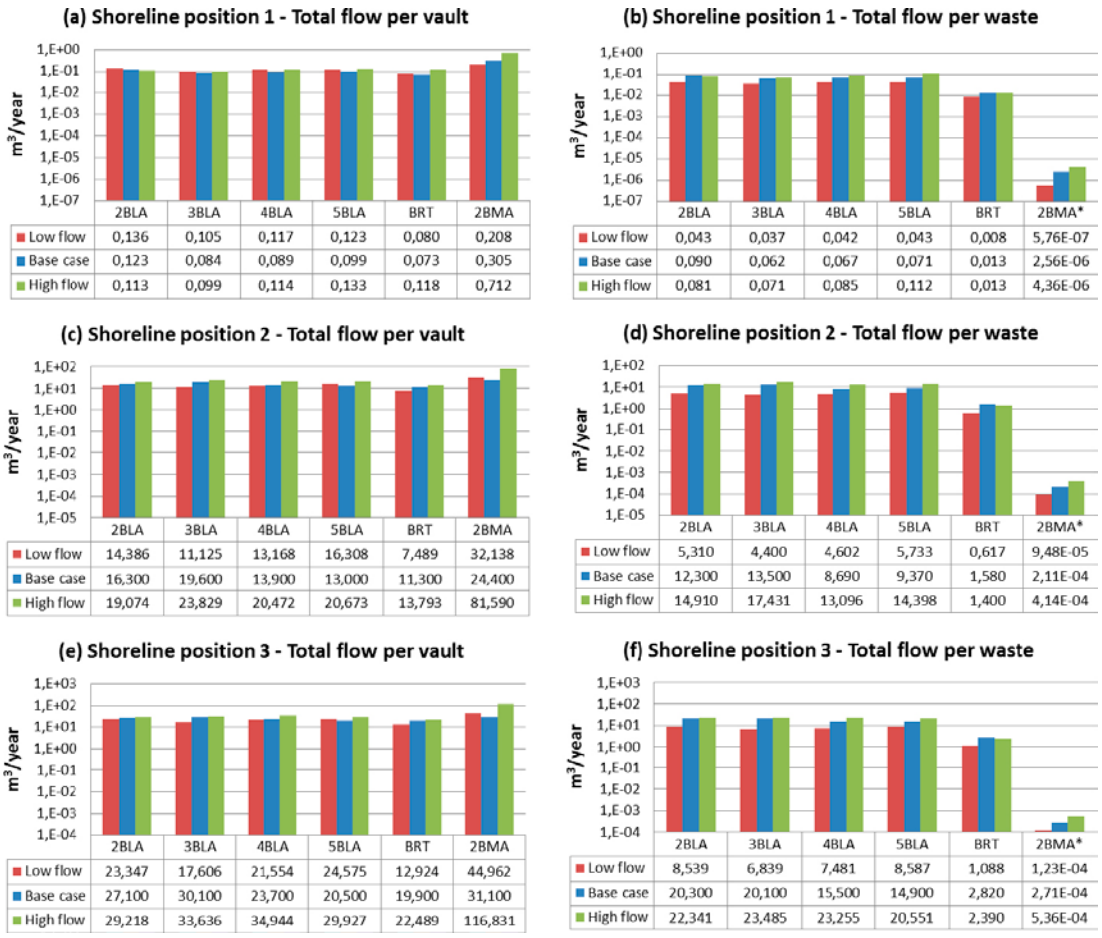

Figure 7-25. *Total flow (m^3/year) through the vaults (left) and waste domains (right) for the three rock permeability cases and the three shoreline positions. The vertical axis is logarithmic.*

The distribution of the tunnel and waste flow along the 2BMA is illustrated in Figure 7-26 for the three rock realizations. For the shoreline position 1, the gravel and waste flow profiles for the Base case lie between the curves of the High flow and the Low flow cases except at the north end of the vaults (sections 12–14 and loading area). In those sections, the Base case presents the highest flow. Both alternative realizations result in higher flow in the section 11, which is affected by the deformation zone ZFMWNW0835, and lower flow north of that deformation zone. The profiles for the shoreline positions 2 and 3 present similar patterns. The tunnel (gravel) flow profiles for the Low flow case and the Base case look alike. The flow between sections 4–11 is higher in the High flow case. Both alternative realizations yield higher flow in sections 10 and 11, indicating that the higher conductivity of the ZFMWNW0835 fracture zone affects the waste flow. Per contra, the waste flow diminishes in sections 13 and 14 and the effect of the fracture crossing section 5 fades away.

For the shoreline position 1, the average tunnel flow varies with respect of the Base from –6% to +66% and the waste flow from –43% to +16%. For the shoreline positions 2 and 3, there are variations in the average total flow through all the vaults of between –4% and +82%, compared to the Base case. For the 2BMA waste domain the difference in the averages range between –56% and +35%, while locally the differences are in the range of –78% to +98%. The comparatively high uncertainty in the waste flow in percentage actually corresponds to a small absolute change due to the very low values of the 2BMA waste flow.

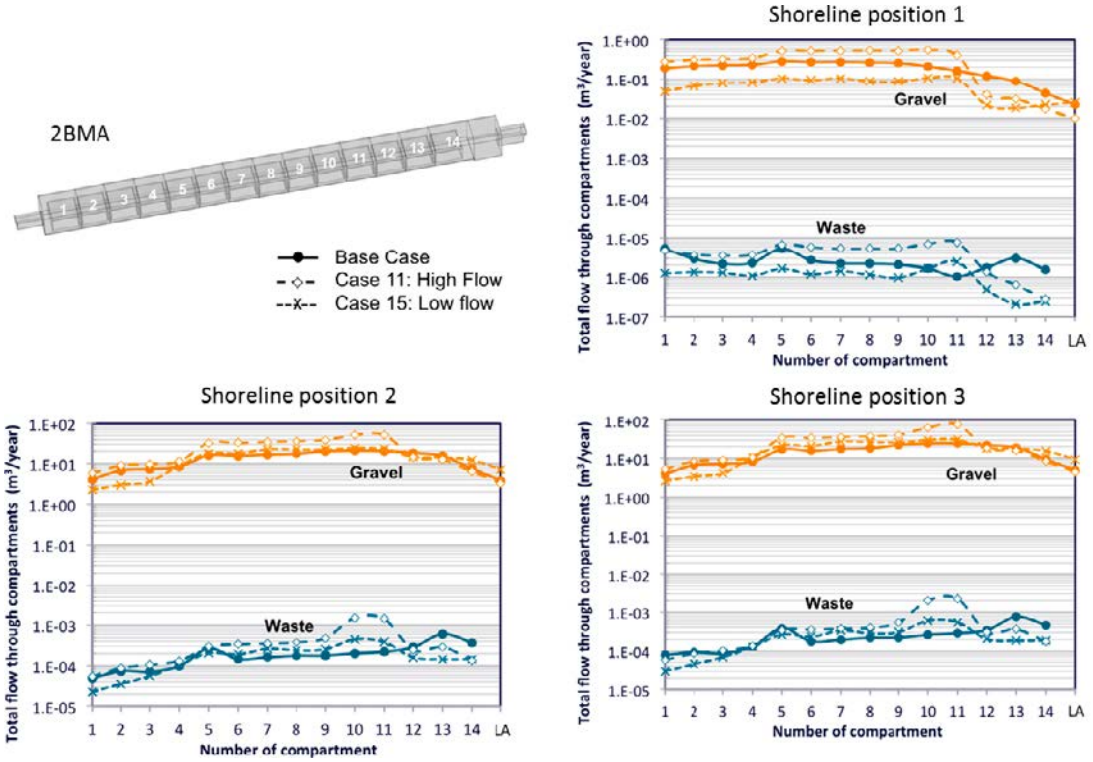

Figure 7-26. *Flow through gravel and waste packages of the 2BMA for the three rock permeability realizations and the three shoreline positions. LA stands for the loading area section.*

7.6 Summary of calculation cases

The results presented for all the barrier degradation cases are summarized in Figure 7-27 and Table 7-10 for the shoreline position 3, the only set of boundary conditions for which all the calculation cases have been simulated. In Figure 7-27, together with the Base case, a black line indicates the variability in the flow associated with the uncertainty in the geosphere, as reported in Section 7.4. According to the model predictions, the most unfavorable cases are the completely degraded plugs case, the no barriers case and the abandoned repository case. The impact in the tunnel flow of those cases is greatest for the vaults located at the west side of the repository, close to the access ramp. The most unfavorable case for the BRT is the no barriers case. Most of the water circulates through this vault and prevents the increase of flow in the vaults situated east from the BRT. Thus, the worst case for the rest of the vaults corresponds to the completely degraded plug case. In that case, the BRT with grouted waste does not act as an efficient by-pass and the water from the tunnels penetrates further east increasing significantly the tunnel flow in the BLA vaults and the 2BMA. The abandoned repository case is almost as unfavorable as the no barriers case, with the difference that the absence of lids in the 2BMA waste compartments results in an increase of flow in the 2BMA that extends to the vaults in the east and reduces the flow in the west vaults (with respect to the no barriers case). In the absence of plugs, there seems to be a tunnel flow trade-off between the east and west side of the repository. The impact of those three cases (no barriers, completely degraded plugs and the abandoned repository cases) is greater than the interval of variability due to the changes in the geosphere defined in Section 7.4, except for the 2BMA vault. The latter vault is extremely sensitive to the permeability of the different fracture zones intersecting it. The geosphere properties have a higher impact in the tunnel flow than the absence of plugs in the repository.

Regarding the waste flow, the worst cases for the BLA vaults are also the three no plugs cases and the impact is greater than the interval associated to the geosphere variability. However, for the BRT and 2BMA, the critical cases are all the degraded concrete or no barrier cases. The concrete degradation impact is greater than the uncertainty interval associated with the geosphere variability, which is very small in the BRT and 2BMA waste flow. The most critical cases for the BRT waste flow are the no barriers and abandoned repository cases while for the 2BMA these are the complete concrete degradation and the no barriers cases.

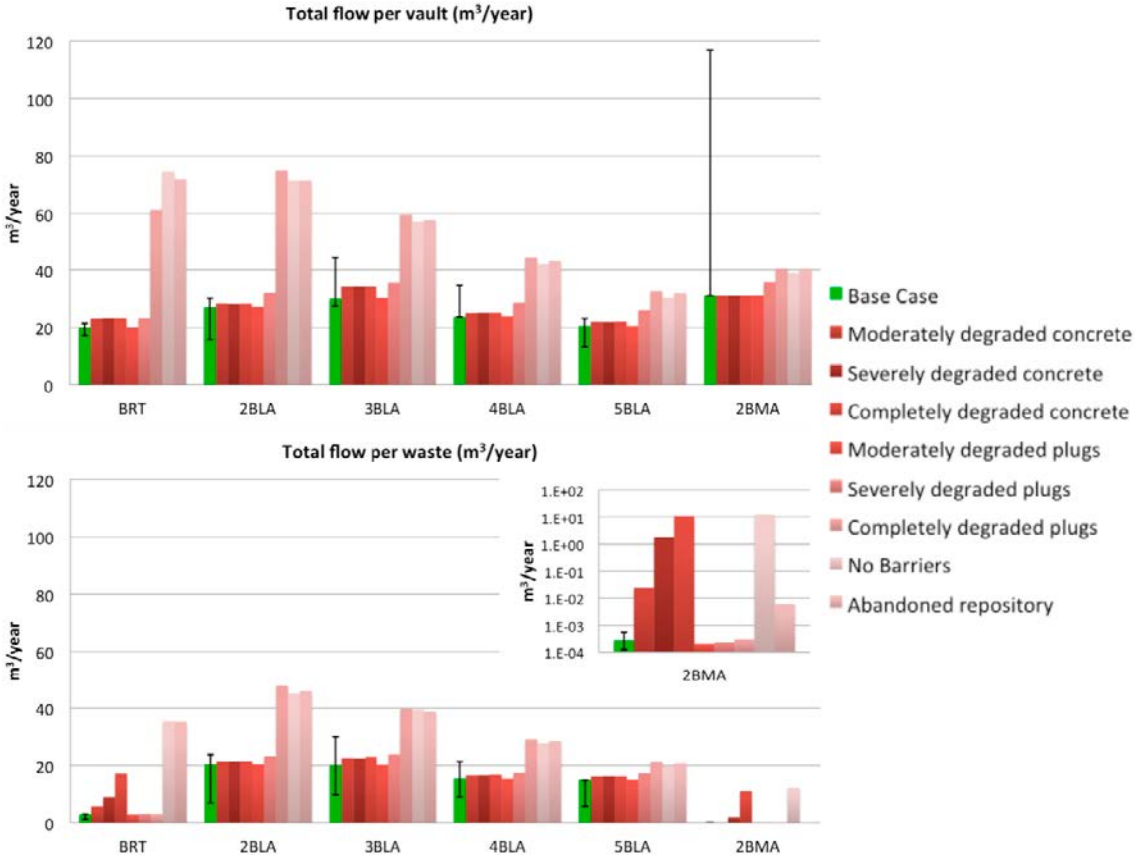

Figure 7-27. *Total flow (m3/year) for the different vaults and waste domains in the SFR 3 repository for all the simulated cases for the shoreline position 3. The black line accompanying the Base case bar indicates the uncertainty interval for each vault due to the studied variability in the geosphere. The vertical axis is logarithmic.*

Table 7-10. Summary of the results of total flow (m³/year) in each vault for the different barrier degradation cases.

		BRT	2BLA	3BLA	4BLA	5BLA	2BMA
Vaults	Base case	19.90	27.10	30.10	23.70	20.50	31.10
	Moderately degraded concrete	23.13	28.46	34.27	25.19	21.90	31.07
	Severely degraded concrete	23.28	28.35	34.29	25.27	21.86	31.09
	Completely degraded concrete	23.25	28.41	34.29	25.30	21.94	31.09
	Moderately degraded plugs	19.96	27.22	30.36	23.84	20.52	31.13
	Severely degraded plugs	23.28	32.14	35.65	28.67	25.91	35.81
	Completely degraded plugs	61.32	74.93	59.56	44.25	32.70	40.48
	No Barriers	74.61	71.51	57.25	42.03	30.38	38.94
	Abandoned repository	71.90	71.52	57.77	43.26	31.98	40.51
Waste	Base case	2.82	20.30	20.10	15.50	14.90	2.71E–04
	Moderately degraded concrete	5.70	21.35	22.60	16.63	16.33	0.024
	Severely degraded concrete	8.89	21.37	22.51	16.67	16.38	1.823
	Completely degraded concrete	17.13	21.42	22.93	16.81	16.35	11.036
	Moderately degraded plugs	2.81	20.39	20.17	15.48	14.97	2.04E–04
	Severely degraded plugs	3.03	23.25	23.85	17.42	17.28	2.29E–04
	Completely degraded plugs	2.94	47.94	39.80	29.08	21.17	3.08E–04
	No Barriers	35.35	45.16	39.43	27.73	19.72	12.366
	Abandoned repository	35.20	45.98	38.75	28.49	20.78	0.006

8 Summary and Conclusions

The work presented here is a part of the long-term safety assessment for the SFR extension application, and concerns the future hydrogeological conditions in the near-field of the SFR 1 (the existing facility) and the SFR 3 (the planned extension). The present study has two main objectives. The first is to estimate groundwater flows in the repository under saturated and steady-state conditions. These flows serve as input to the radionuclide transport model that is performed in order to show compliance. The second objective is to deepen the system understanding of the SFR 1 and SFR 3 from a hydrogeological perspective, focusing on the effects of barrier degradation, closure alternatives, permafrost, and the uncertainty related to the rock permeability fields on the groundwater flow through the repository. Knowledge gained allows for the evaluation of proposed engineering solutions with increased confidence.

The methodology is based on three dimensional finite element models of both the SFR 1 and SFR 3. The commercial software COMSOL Multiphysics is used in the simulations. The repository-scale model is connected to a larger model for the regional flow that is set up and solved in the software DarcyTools. The regional flow model supplies (1) driving pressure and/or fluxes boundary conditions to the repository-scale model, as well as (2) the hydraulic conductivity field of the bedrock that is considered in the repository-scale model.

A benchmark exercise has been successfully implemented to verify that the interface DarcyTools to COMSOL (iDC, see Appendix A) works properly, and that the regional-scale model in DarcyTools and the repository-scale model in COMSOL are consistently connected. The repository-scale model reproduces the DarcyTools driving pressure field with high accuracy (volume average differences are always less than 1%) and the total flow rates computed through the tunnels are highly consistent between COMSOL and DarcyTools simulations, despite the differences in geometry and discretization.

Different boundary conditions for the SFR 1 and SFR 3 steady-state models have been defined based on the results of the regional hydrogeology model in DarcyTools. The simulations outline the time-evolution of the groundwater flow and correspond to three different positions of the repository relative the shoreline of the sea:

- Shoreline position 1 (2000 AD): corresponds to a submerged repository scenario
- Shoreline position 2 (3000 AD): corresponds to an intermediate case in which the shoreline is above the repository and
- Shoreline position 3 (5000 AD): corresponds to a retreating shoreline position, well removed from the repository.

Total flow through the vaults and waste

The total flow rates through the tunnels and waste domains of the two repository facilities have been evaluated for a Base case at three the different shoreline positions. In SFR 1, the 1BLA vault has the highest flow rates since it has no concrete barriers. In this case, the waste flow rates represent more than 90% of the tunnel flow. In turn, the 1BMA tunnel flow rate is half the 1BLA flow rate. The 1BMA configuration with low permeability concrete beams that support the concrete floor results in the break of the continuity of the hydraulic cage surrounding the concrete structure and low efficiency (5% of the tunnel flow rate enters the waste domain at shoreline position 3). A 1BMA configuration with very permeable concrete beams increases the hydraulic cage efficiency substantially, reducing in three orders of magnitude the waste flow with respect to the case with impermeable beams. The high permeability of the deformation zone ZFMNNW1209 around the 2BTF results in higher tunnel flow rates through 2BTF than through the 1BTF even though they have the same internal configuration. The waste flow rate is about 10% the tunnel flow rate in the 2BTF and 20% in the 1BTF.The Silo has the lowest tunnel and waste flow rates and the gravel dome concentrates most of the tunnel flow rate.

In SFR 3, the BLA vaults, as in SFR 1, present a waste flow rate that is very similar to the tunnel flow rate, which is due to the vault structure. The volume of the waste domain is very close to the tunnel volume. Even though the BRT dimensions are smaller than the BLA volume, its tunnel flow rate has the same order of magnitude as the BLA vaults. The flow rate through the grouted BRT waste corresponds to 14–18% of the BRT tunnel flow rate. In the Base case the 2BMA presents the highest tunnel flow rates. However, the waste flow rate is in this case five orders of magnitude smaller than the tunnels flow rate. This is due, on one hand to the effect of the concrete barriers, and on the other hand on the effectiveness of the hydraulic cage surrounding the individual waste compartments.

In addition to the base case, a set of cases investigating different hydraulic properties of repository components have been simulated to assess the impact on groundwater flow in the repository. The results have pointed out a number of important features of the repository. Some of these are listed below.

Concrete degradation

The degradation of the concrete barriers has a marginal effect on the tunnel flow rates (less than 26% flow increase) and there is limited impact in the surrounding rock, i.e., there is not obvious redistribution of flow as a consequence of the concrete degradation. The 1BLA and Silo waste flows are also insensitive to concrete degradation (less than 13% flow increase). In the case of the Silo, this apparent independence on concrete degradation is related to the fact that a bentonite layer is placed between the rock and the concrete barriers, which is not degraded in the simulations as concrete degrades. The comparison between the 1BMA configuration with and without concrete beams shows that the waste flow is lower for the 1BMA without beams for all the concrete degradation stages. The most critical effects are observed in the 2BMA vault. In this vault the three-dimensional hydraulic cage is very efficient in the Base case and therefore, the waste flow rates are very low. That efficiency rapidly vanishes as the concrete barriers degrade.

Plug degradation

Regarding the degradation of the bentonite plugs, no significant effect is observed when the plugs maintain a higher resistance than the rock surrounding the rock vaults. Only the complete degradation of the plugs results in an important increase of tunnel flow in the repository (SFR 1 and SFR 3). The results indicate that plugs with lower permeability than the most permeable rock surrounding the rock vaults yield an efficient configuration to restrain the flow rates through the vaults. However, when the plugs present less resistance to flow than the surrounding rock, the flow configuration around the repository changes. Then, the south entrance of the plug becomes the main inflow area to the vaults, and the water circulates mainly through the vaults located at the east side of the SFR 1 repository and the west side of the SFR 3 repository, close to the access ramp. The vaults situated in the west side of the SFR 1 repository and on the east side of the SFR 3 repository are less affected in case of complete plug degradation.

The complete degradation of the plugs increases substantially the waste flow rate of the BLA vaults, which have no concrete barriers. However, the impact on the waste flow through the vaults with concrete barriers is diverse. The flow increase is considerable in the 1BMA and the Silo but it is minor in the 2BMA. In the case of both 1-2BTF vaults, on the contrary, a waste flow decrease of 18–34% is observed. When the plugs maintain a higher resistance than the rock surrounding the rock vaults water flows from East to West primarily through the main deformation zones traversing the vaults and is forced through the 1BTF and 2BTF concrete grouting. When the plugs degrade, there is better connection between the East and West through the by-pass formed by the South and North ends and the lateral access tunnels. This bypass reduces the pressure gradient between the East and the West sides of the BTF vaults and diminishes the lateral flow though the BTF waste compartments.The flow through the rock between vaults also decreases due to the redirection of groundwater towards the most permeable vaults and tunnels.

One calculation case has considered the presence of an ice lens that degrades a section of the Silo bentonite. This degradation results in an increase in total flow rate in the Silo. However, most of this water recirculates within the degraded bentonite section without penetrating the waste encapsulation.

No barriers case

The cases above can be compared with the extreme case of no barriers. For the SFR 1 repository, the no barrier case leads to a waste flow that is at least two orders of magnitude higher than the rest of the cases. An exception is the 1BLA, for which the increase is much smaller due to the flow redistribution between vaults. In this case, groundwater flows from south to north occurs in this case through the completely degraded westernmost BTF vaults, decreasing the flow through the easternmost vaults. In the no barriers cases, the flow that crosses the waste is in the range 80–86% of the total flow through the vaults for the 1BMA, 1BTF and 2BTF (for the same vaults in the Base case, this range is 5–20%). For the 1BLA and the Silo, this ratio is as high as 97%, although in these cases the waste domain has a similar volume than the total vault domain (the values reported for the Silo do not account for the flow through the Silo gravel dome). In the SFR 3 repository, the absence of engineered barriers is critical for the BRT vault. However, for the BLA vaults in SFR 3, this case is not as critical as the completely degraded plugs case. The BRT acts as a flow by-pass, reducing the flow past the BLA vaults that are located further away from the access tunnels. The 2BMA, located at the east side of the repository is the furthest from the access tunnels. As in the case of no plugs, the access tunnels become the main inflow area to the westernmost vaults. Only a small fraction of that flow reaches the 2BMA. However, it is noteworthy that the effect on the 2BMA waste flow rates is critical, increasing approximately 5 orders of magnitude. Therefore, the combined effect of the concrete barriers and bentonite plugs degradation turns this case into the most unfavorable one for the 2BMA vault.

Repository closure

Two different closure alternatives have been considered for the SFR 1 repository. The Base case closure consists of extended sections of bentonite/concrete and structural plugs. The alternative closure considers short sections of bentonite with concrete plugs. This configuration represents a situation where a significant lower amount of bentonite is used to seal the repository. Overall, it may be concluded that the hydrodynamic behavior is similar between the Base case and alternative closure options. Depending on the shoreline position, different flow adjustments are observed between the 1BLA and the 1-2BTF vaults while the flow though the 1BMA remains unaltered. There is a trade-off between 1BLA and the 1-2BTF vaults. When the 1BLA waste flow increases, the waste flow of the 1-2BTF vaults decreases and vice versa. As observed in the plug degradation analysis, a reduction in the flow from the South to North part of the tunnels leads to an increase in the flow from East to West traversing the 1-2BTF grouted waste. The flow in the rock surrounding the 1-2BTF vaults is also modified analogously. The trade-off between the westernmost vaults absorbs most of the flow protecting the easternmost vault, the 1BMA waste, whose waste flow remains mostly unaffected.

Abandoned repository case

This calculation case represents a situation in which no additional barriers and structures are emplaced after the operational phase. The tunnel flow is 5–7 times larger than the Base case for the easternmost vaults 1BMA, 1BLA, 2BTF and 1 to 2 orders of magnitude higher in the 1BTF and the Silo. The highest increase in the SFR 1 repository occurs in the Silo, which receives all the water directly from the access tunnels. The flow in the BTFs tunnels increases but the flow through the waste decreases with respect to the Base case. In the case of shoreline position 1 this effect is also observed in the 1BMA waste flow. Notice that this 1BMA result was not evident from the plugs degradation results since that analysis was restricted to shoreline position 3. In the absence of plugs the vaults act as flow by-pass from the south to north of the repository reducing the flow through the rock and the BTF vaults from East to West. In shoreline position 1, the flow in the rock between the 1BMA and the 1BLA vaults is reduced and the minor fractures affecting the sections 9 and 10 of the 1BMA are deactivated. This flow redistribution is consistent with the results observed in the analysis of the plug degradation and closure alternative.

For the SFR 3, the results are similar to the no barriers case for the tunnel flow rates and the 2-5BLA and BRT waste flow rates. The waste flow rates of the BRT and the 2BMA vaults increase one order of magnitude with respect to the Base case, due to the absence of grout and the concrete top lids, respectively.

Shallow permafrost case

The hydraulic response of the repository to the advance of permafrost was analyzed under the assumption of a case of shallow permafrost where the frozen front is located above the repositories, at a depth of about –59 m. In that case, both the tunnel and waste total flows calculated decrease in all vaults with respect to the Base case for the shoreline position 3. The reduction in the flow through the vaults is consistent with the permeability decrease around the frozen front. For the SFR 1, the most evident changes in flow are observed for the 1BMA, 1BLA, and 2BTF, although all rock vaults follow the same trend. These vaults are located just below a zone within the permafrost where the permeability of the rock is considerably lower than the permeability of the Base case. For the SFR 3, both the vault and waste flows calculated for the Shallow permafrost case decrease in all vaults with respect to the Base case at shoreline position 3, except for the 2BMA vault where a slight increase is observed. The flow behavior displayed in the permafrost case is more horizontal than the respective flow pattern of the Base case.

Estimation of uncertainty associated with the geosphere

An analysis of the effect of different realizations of the rock permeability field in the modeled domain on the hydraulic behavior of the repository has been conducted. This study may be regarded as a first assessment of the effect of uncertainty in the geosphere hydraulic parameters on the performance of the repository. The variability of the flow rates in the SFR 1 and SFR 3 vaults due to different rock permeability fields should be considered in order to critically assess and compare the results of different combinations of hydraulic properties of the repository. The variability of groundwater flow rates for different rock permeability fields seems to be highest for the 1BMA and 2BMA vaults. For the tunnel flow rates, only the impact of the three no plug cases (i.e. no barriers, completely degraded plugs and the abandoned repository cases) is greater that the interval of variability due to the uncertainty of the rock permeability description. The same applies to the waste flow rates in the BLA vaults. In the vaults with concrete barriers, the effect of the concrete degradation on the waste flow rates is greater than the uncertainty interval associated with the rock permeability field. The uncertainties associated with the rock permeability field have a small impact in the flow rates through encapsulated waste.

References

SKB's (Svensk Kärnbränslehantering AB) publications can be found at www.skb.se/publications. References to SKB's unpublished documents are listed separately at the end of the reference list. Unpublished documents will be submitted upon request to document@skb.se.

COMSOL, 2012a. COMSOL Multiphysics 4.3a. Burlington, MA: COMSOL Inc.

COMSOL, 2012b. COMSOL Subsurface Flow Module. User's guide. Version 4.3a. Burlington, MA: COMSOL Inc.

Curtis P, Markström I, Petersson, J, Triumf C-A, Isaksson H, Mattsson H, 2011. Site investigation SFR. Bedrock geology. SKB R-10-49, Svensk Kärnbränslehantering AB.

Holmén J G, Stigsson M, 2001. Modelling of future hydrogeological conditions at SFR. SKB R-01-02, Svensk Kärnbränslehantering AB.

Luterkort D, Gylling B, Johansson R, 2012. Closure of the Spent Fuel Repository in Forsmark. Studies of alternative concepts for sealing of ramp, shafts and investigation boreholes. SKB TR-12-08, Svensk Kärnbränslehantering AB.

Odén M, Follin S, Öhmans J, Vidstrand P, 2014. SR-PSU Bedrock hydrogeology. Groundwater flow modelling methodology, setup and results. SKB R-13-25, Svensk Kärnbränslehantering AB.

SKB, 2008. Safety analysis SFR 1. Long-term safety. SKB R-08-130, Svensk Kärnbränslehantering AB.

SKB, 2013. Site description of the SFR area at Forsmark at completion of the site investigation phase. SDM-PSU Forsmark. SKB TR-11-04, Svensk Kärnbränslehantering AB.

SKB, 2014a. Radionuclide transport and dose calculations for the safety assessment SR-PSU. SKB TR-14-09, Svensk Kärnbränslehantering AB.

SKB, 2014b. Model summary report for the safety assessment SR-PSU. SKB TR-14-11, Svensk Kärnbränslehantering AB.

SKB, 2014c. Initial state report for the safety assessment SR-PSU. SKB TR-14-02, Svensk Kärnbränslehantering AB.

SKB, 2014d. Climate and climate related issues for the safety assessment SR-PSU. SKB TR-13-05, Svensk Kärnbränslehantering AB.

Svensson U, 2010. DarcyTools, version 3.4. Verification, validation and demonstration. SKB R-10-71, Svensk Kärnbränslehantering AB.

Svensson U, Ferry M, 2010. Darcy Tools version 3.4. User's guide. SKB R-10-72, Svensk Kärnbränslehantering AB.

Öhman J, 2010. Site investigation SFR. Hydrogeologic modelling of SFR v 0.1. Influence of the ridge on the flow fields for different target volumes. SKB R-09-43, Svensk Kärnbränslehantering AB.

Unpublished documents

SKBdoc id	Title	Issuer, year
1395214 ver 1.0	TD08- SFR 3 effect on the performance of the existing SFR 1	SKB, 2013
1395217 ver 1.0	TD11- Temperate climate conditions	SKB, 2013

Appendix A

iDC interface

Introduction

The program connecting DarcyTools with COMSOL is called *iDC (interface DarcyTools to COMSOL)*. The program reads the output files from the regional hydrogeology model, extracts the necessary information for the repository-scale model, and writes it to text files.

These files can be read by COMSOL and used as interpolation function fields.

System Architecture

This interface has been designed to be easily extended with additional functionalities by decoupling the different processes of the program in several modules. Different options like cell filtering and requesting specific variables are set in a configuration file that is read by the program.

Configuration File

The configuration file is a text file used by the *iDC* interface to define the data to be extracted.

Table A-1 gives an overview of the configuration file structure. Reserved keywords are written in capital letters.

Table A-1. Configuration file example.

Row	Description	Configuration file command example
1	Title of the run	iDC Test case input data file
2	Choose a FILTER: BOX or MARKER In BOX mode coordinates of two point must be set using POINT1 and POINT2 (see example) In MARKER mode the number of the marker must be supplied	FILTER BOX POINT1 6316.0 10166.0 -98.0 POINT2 6378.0 9964.0 -60.0
3	The ROF file can contain several time steps. With TIMESTEP a specific time step is requested.	TIMESTEP 607
4	MESH INPUT specifies the DarcyTools mesh file. OUTPUT specifies file to write the mesh details for the cells in the filtered area.	MESH INPUT xyz OUTPUT meshFiltered.out
5	This row can be repeated to extract multiple variables. VARIABLE specifies the rquested variable.	VARIABLE CELL pressure INPUT DTCOMSOLRofPressure.rof OUTPUT DTCOMSOLRofPressure.txt
..	In can extract the following types of variables: CELL, XFACE, YFACE and ZFACE). INPUT specifies the DarcyTools ROF input file.	VARIABLE XFACE darcy-u INPUT DTCOMSOLRofDarcyU.rof OUTPUT DTCOMSOLRofDarcyU.txt
..	OUTPUT specifies the text output file to be extracted.	VARIABLE YFACE darcy-v INPUT DTCOMSOLRofDarcyV.rof OUTPUT DTCOMSOLRofDarcyV.txt
n		VARIABLE ZFACE darcy-w INPUT DTCOMSOLRofDarcyW.rof OUTPUT DTCOMSOLRofDarcyW.txt
n+1	END tag to advertise to the program that no more information must be read	END

Filter option

The filter option is used to select how the area to be extracted from the DarcyTools model is specified. Two cell filtering options criteria are available:

- Marker filter retrieves the values of the variables in the cells (or their faces) that are set with a Marker in the DarcyTools simulation. The marker information is retrieved from the DarcyTools mesh file (normally called xyz).
- Box filter retrieves the values of the variables in cells enclosed in a block domain which contains the near-field, specified by two corner points.

Technical Details

iDC has been programmed in Fortran. Because of its dependency on the DarcyTools libraries, the Intel Fortran compiler is required to compile it. The interface has been designed for ROF files generated by DarcyTools version 3.4.

Although iDC is designed to be multi-platform, in the framework of this project it has only been tested on Microsoft Windows.

Appendix B

Figures SFR 1

Streamlines plug degradation

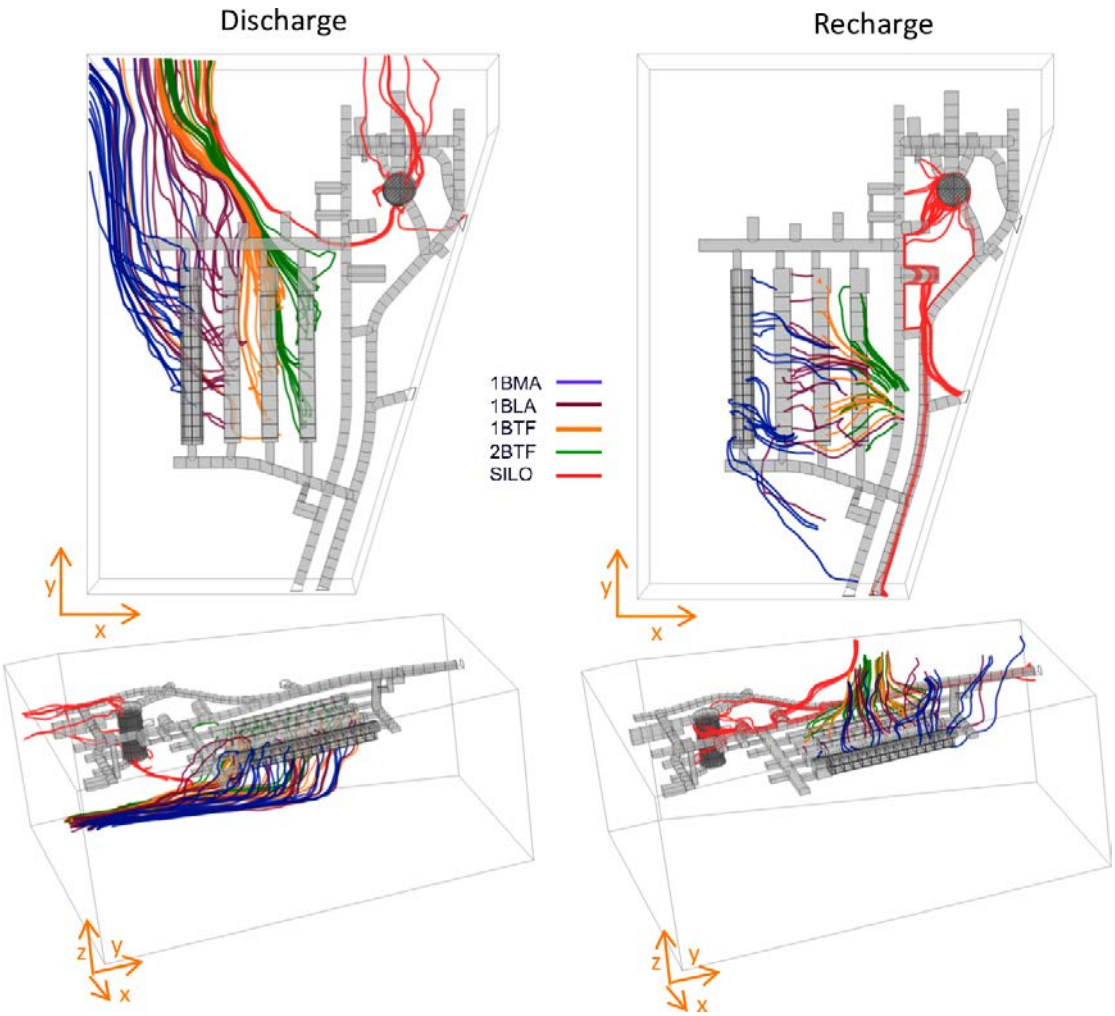

Figure B-1. *Groundwater streamlines leaving (left) and reaching (right) individual SFR 1 vaults (color tubes) for the moderately degraded plugs and the shoreline position 3.*

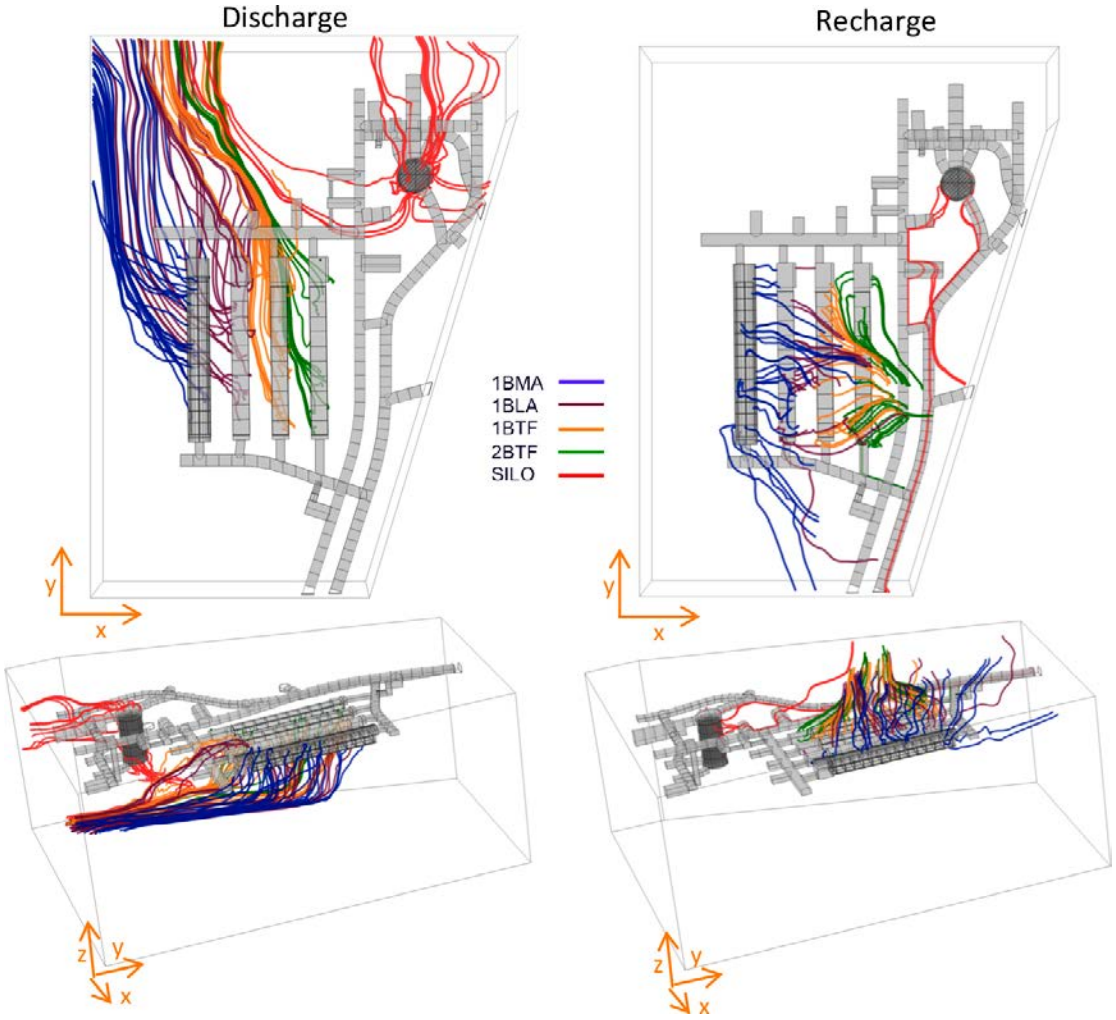

Figure B-2. *Groundwater streamlines leaving (left) and reaching (right) individual SFR 1 vaults (color tubes) for the severely degraded plugs and the shoreline position 3.*

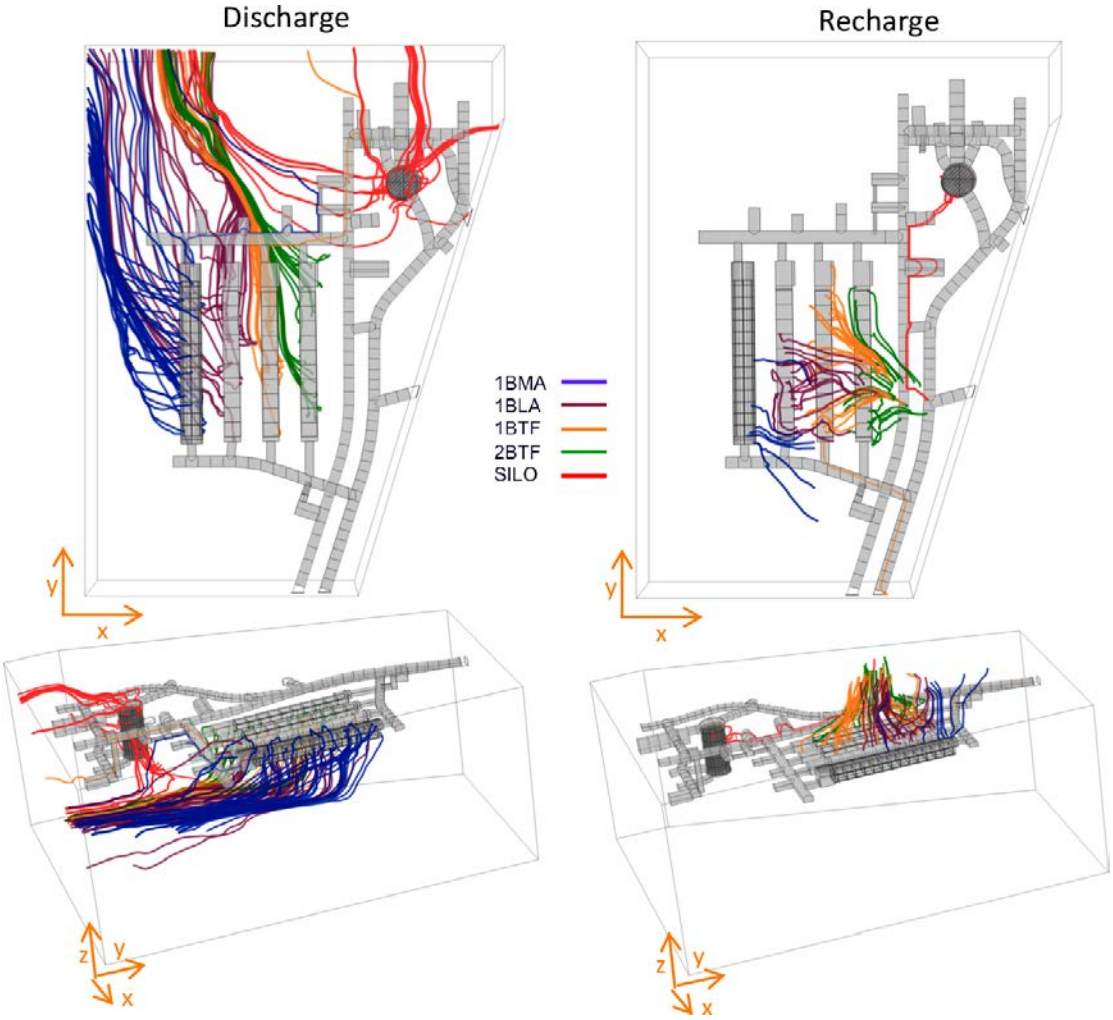

Figure B-3. *Groundwater streamlines leaving (left) and reaching (right) individual SFR 1 vaults (color tubes) for the completely degraded plugs and the shoreline position 3.*

Streamlines closure alternative

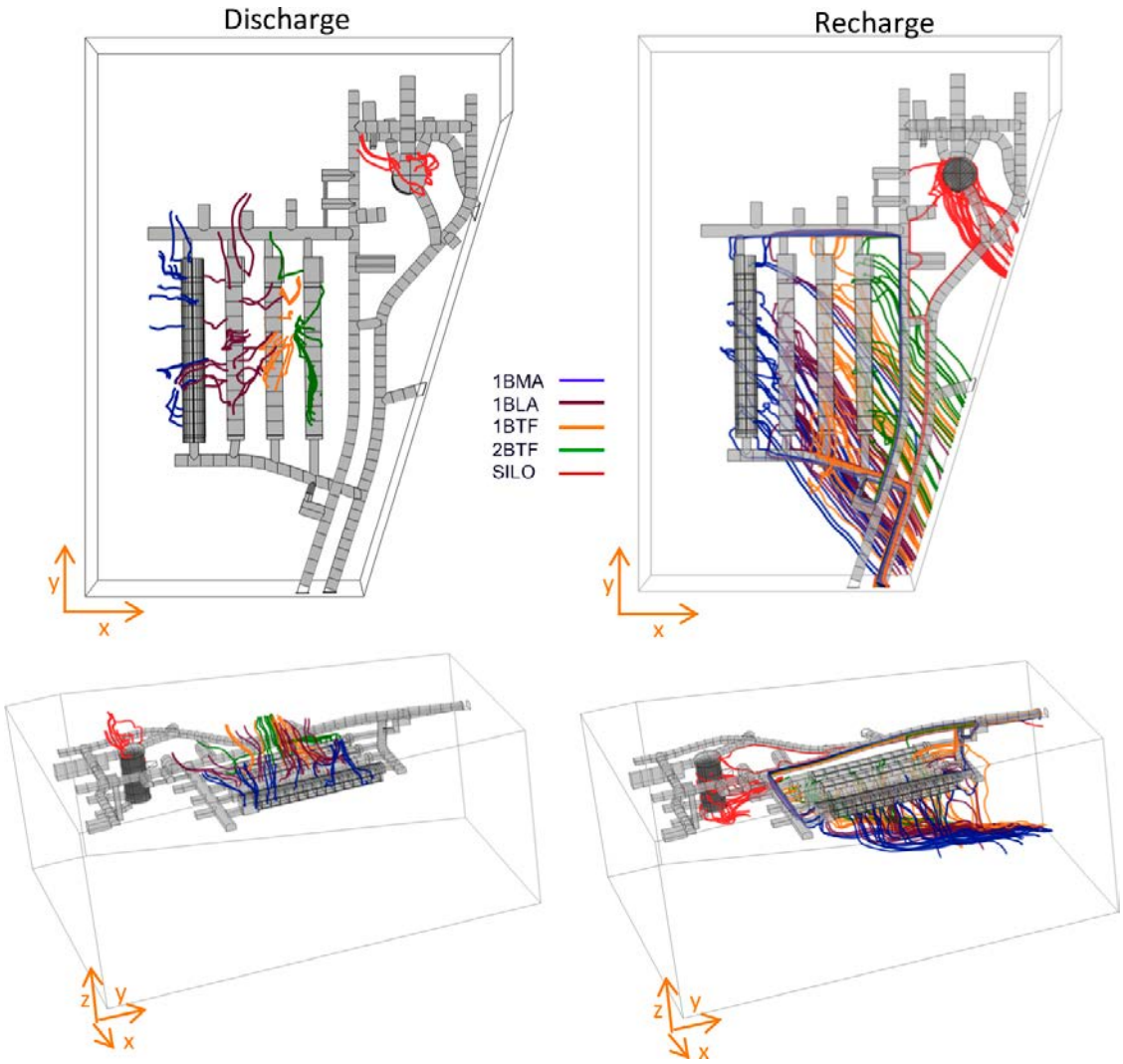

Figure B-4. *Groundwater streamlines leaving (left) and reaching (right) individual SFR 1 vaults (color tubes) for the closure alternative case and the shoreline position 1.*

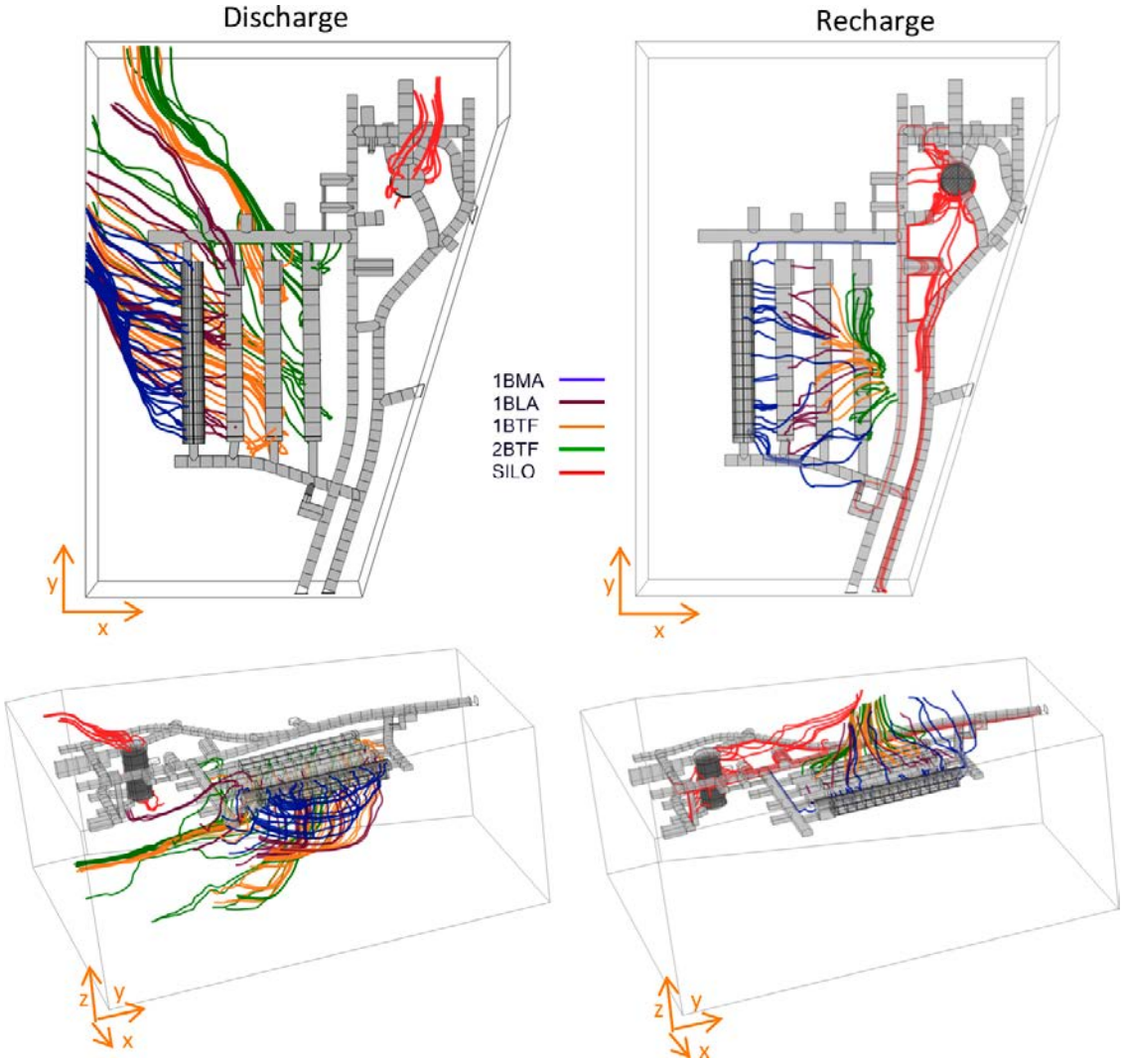

Figure B-5. *Groundwater streamlines leaving (left) and reaching (right) individual SFR 1 vaults (color tubes) for the closure alternative case and the shoreline position 2.*

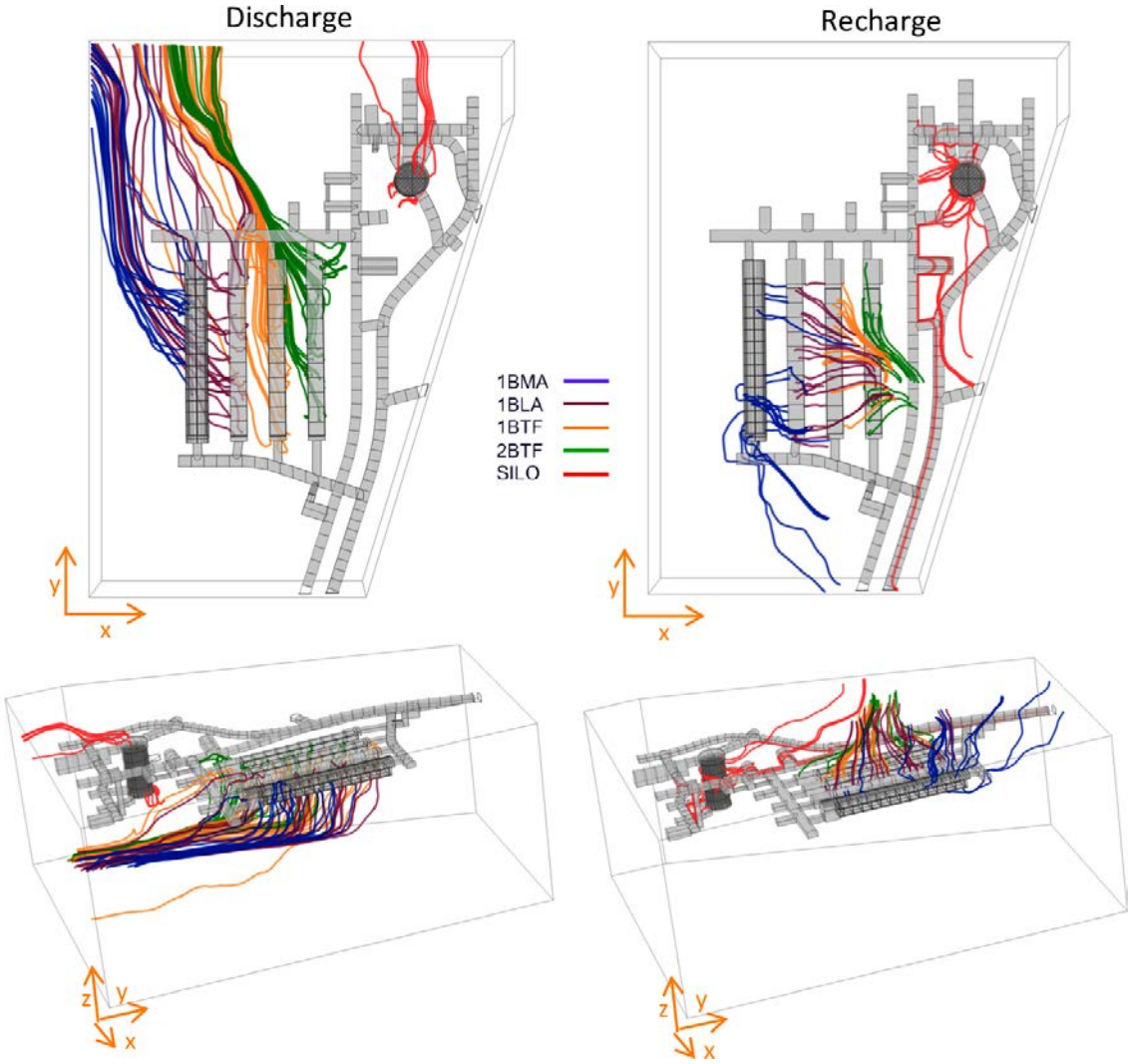

Figure B-6. *Groundwater streamlines leaving (left) and reaching (right) individual SFR 1 vaults (color tubes) for the closure alternative case and the shoreline position 3.*

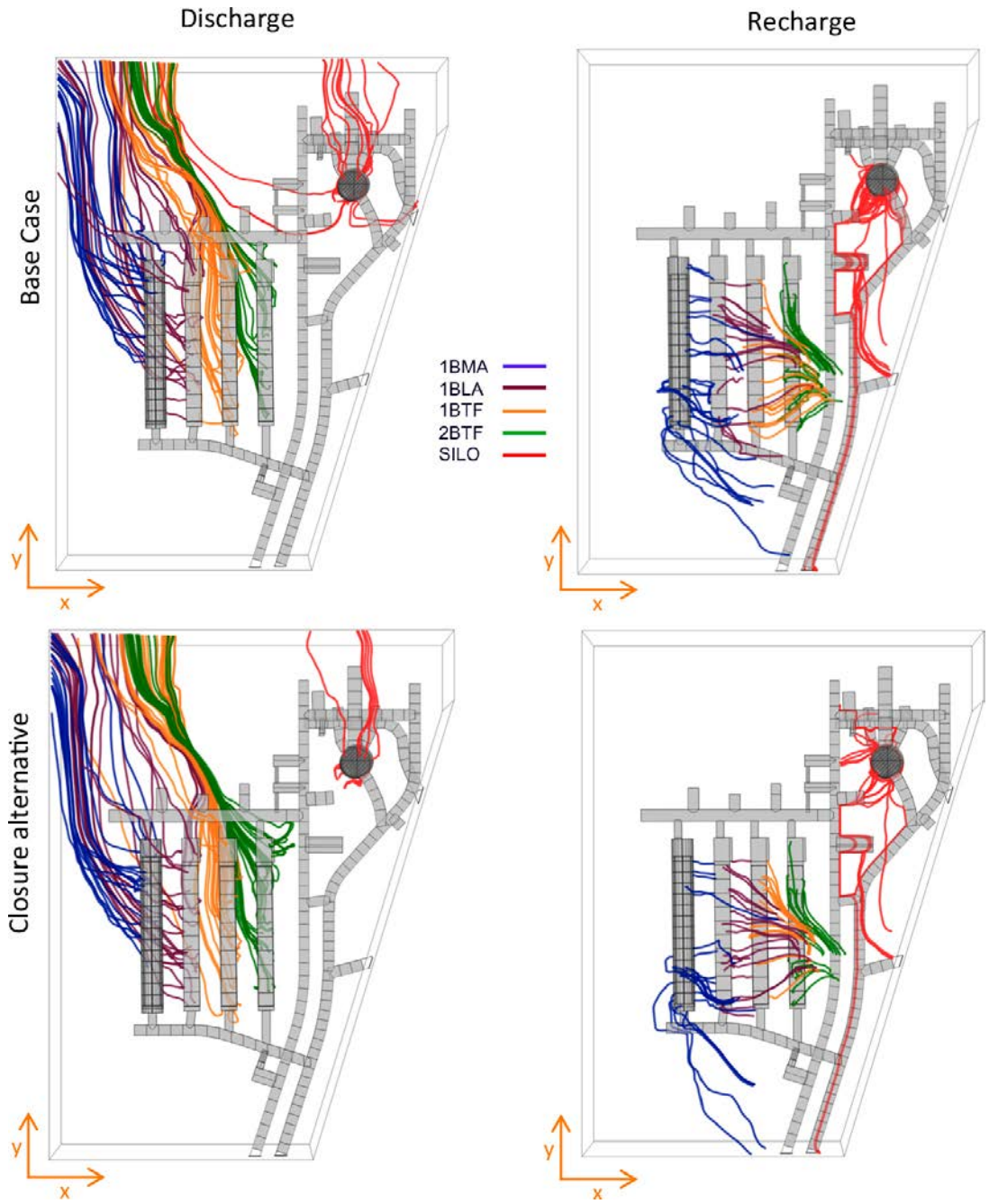

Figure B-7. *Comparison of the groundwater streamlines leaving (left) and reaching (right) individual SFR 1 vaults (color tubes) for the Base case (top) and the closure alternative case (bottom) for the shoreline position 3.*

Streamlines abandoned repository

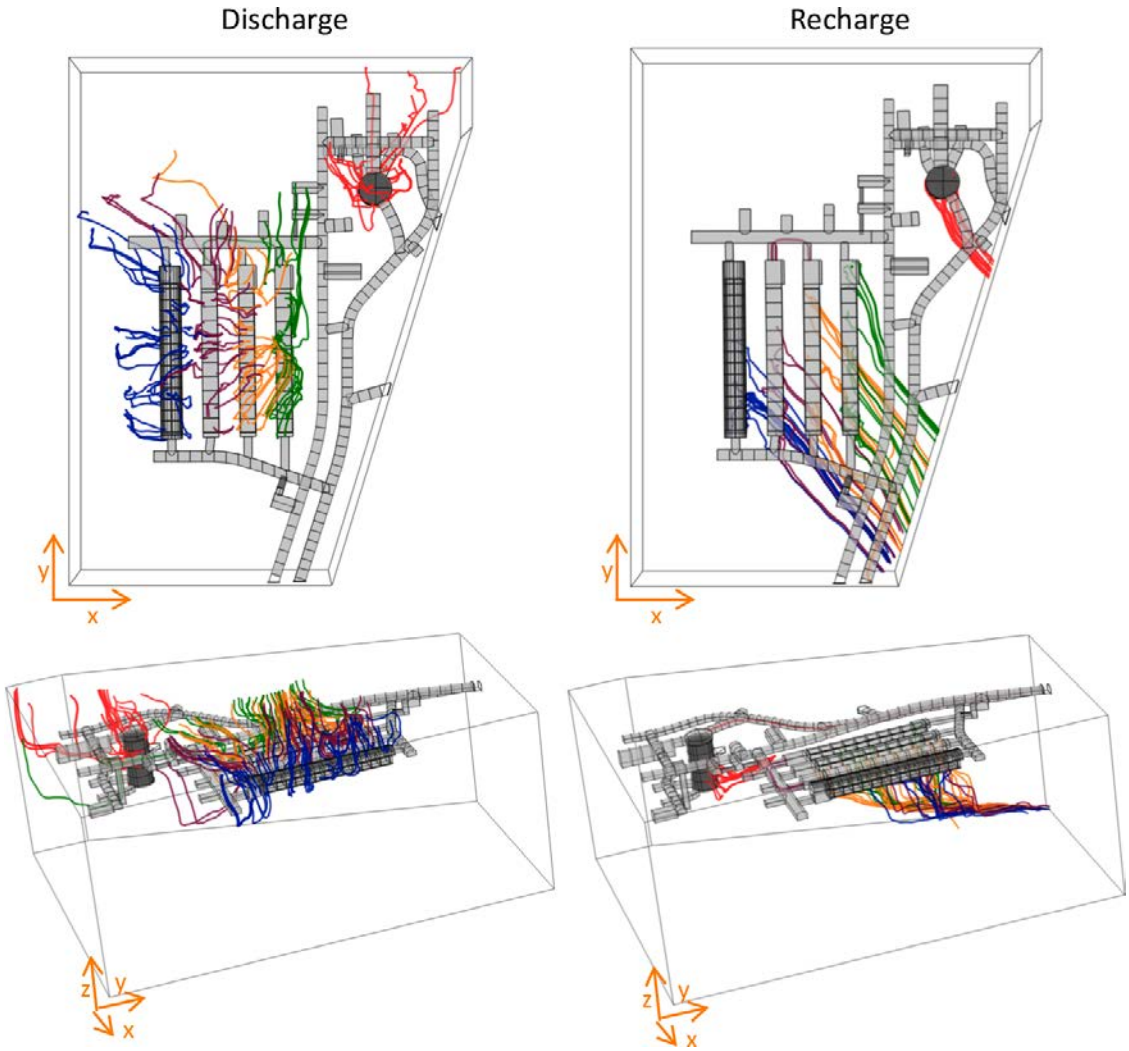

Figure B-8. *Groundwater streamlines leaving (left) and reaching (right) individual SFR 1 vaults (color tubes) for the abandoned repository case and the shoreline position 1.*

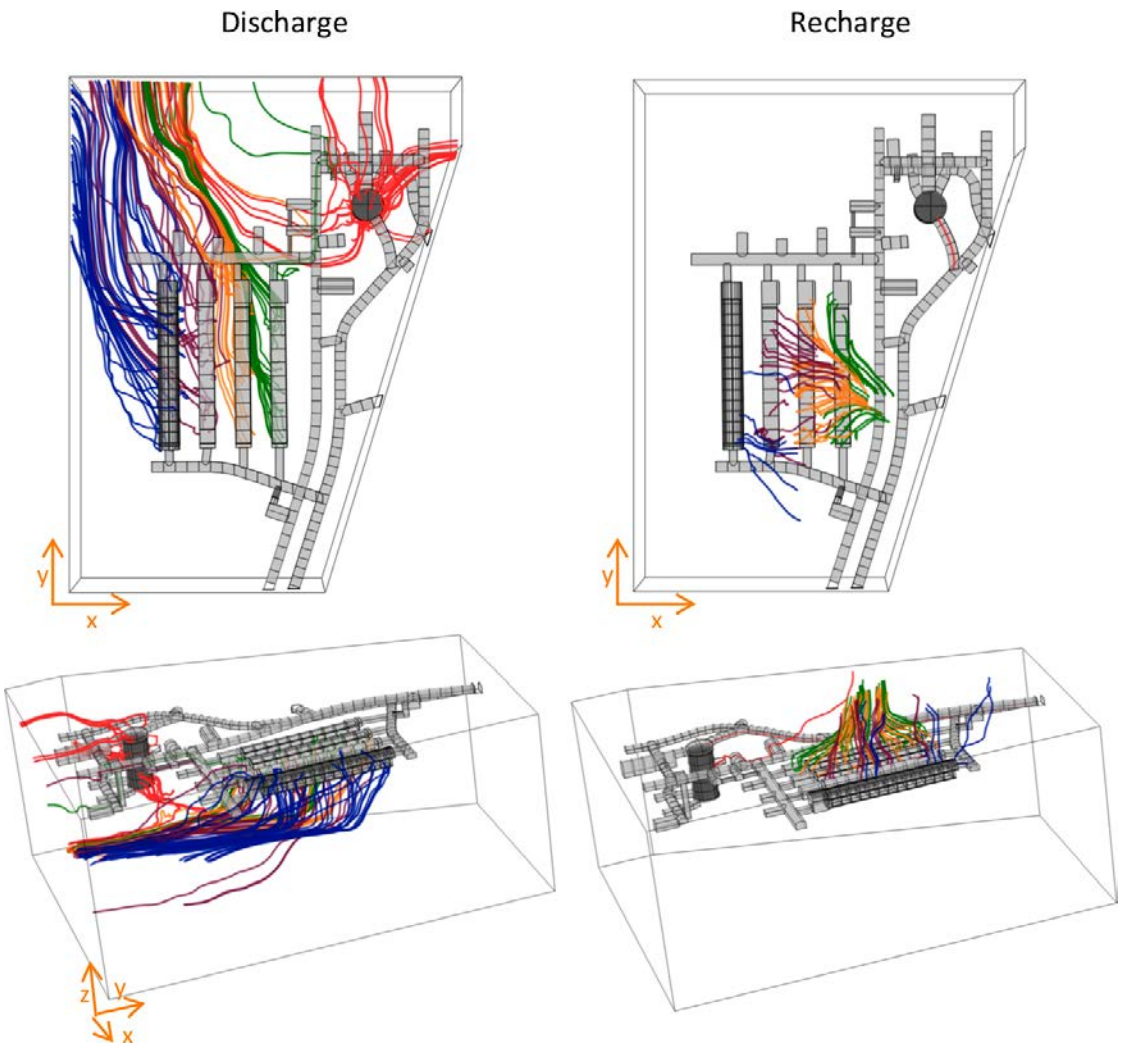

Figure B-9. *Groundwater streamlines leaving (left) and reaching (right) individual SFR 1 vaults (color tubes) for the abandoned repository case and the shoreline position 3.*

Darcy velocity differences for concrete degradation cases

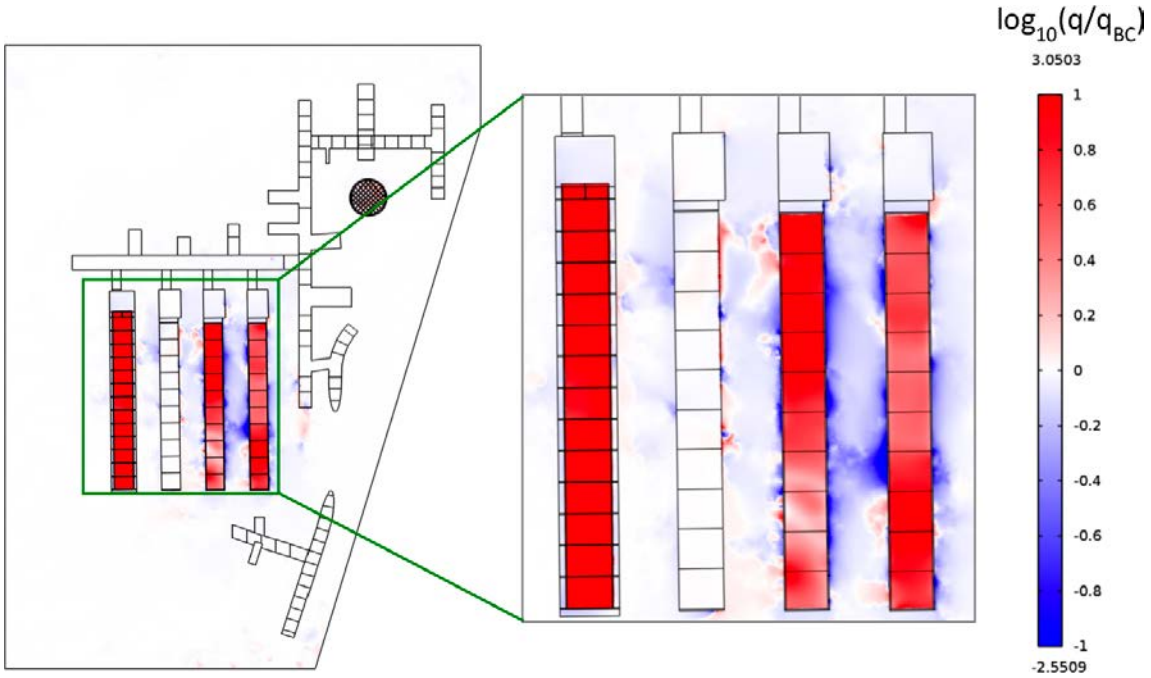

Figure B-10. *Ratio (in log_{10} scale) of the Darcy velocity magnitude between the case of severely degraded concrete and the Base case at the shoreline position 2 in a xy plane at z= –82.5. Positive values indicate a higher flow in the severely degraded concrete.*

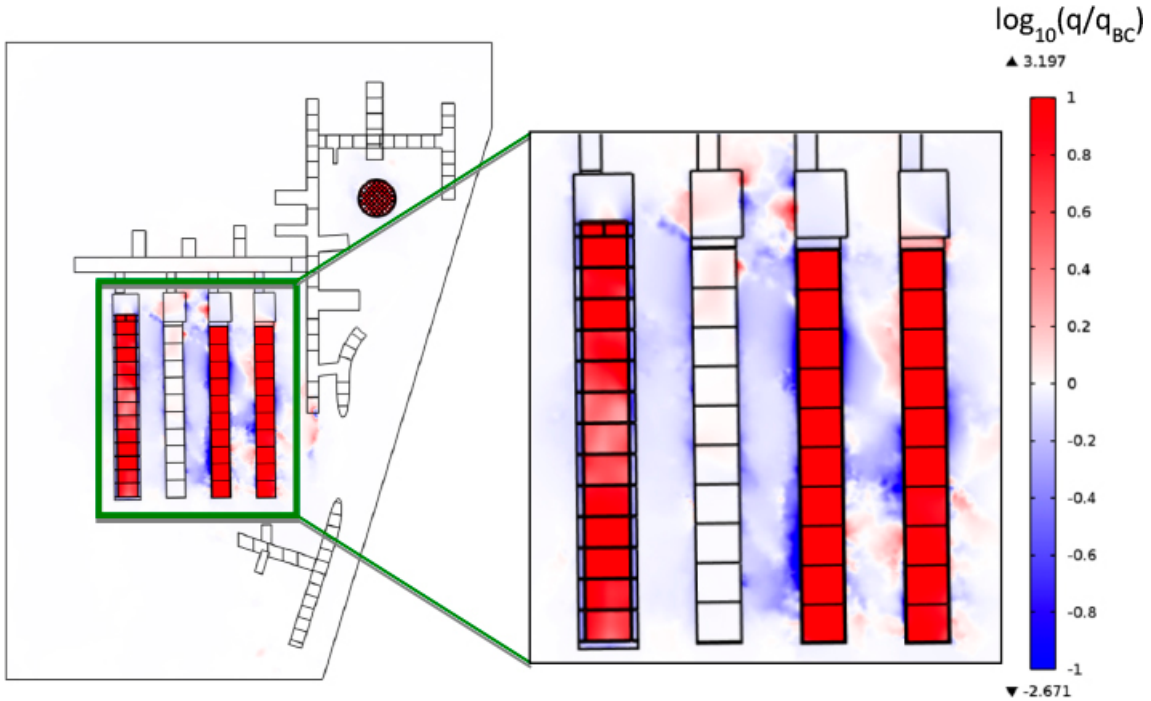

Figure B-11. *Ratio (in log_{10} scale) of the Darcy velocity magnitude between the case of completely degraded concrete and the Base case at the shoreline position 1 in a xy plane at z= –82.5. Positive values indicate a higher flow in the completely degraded concrete.*

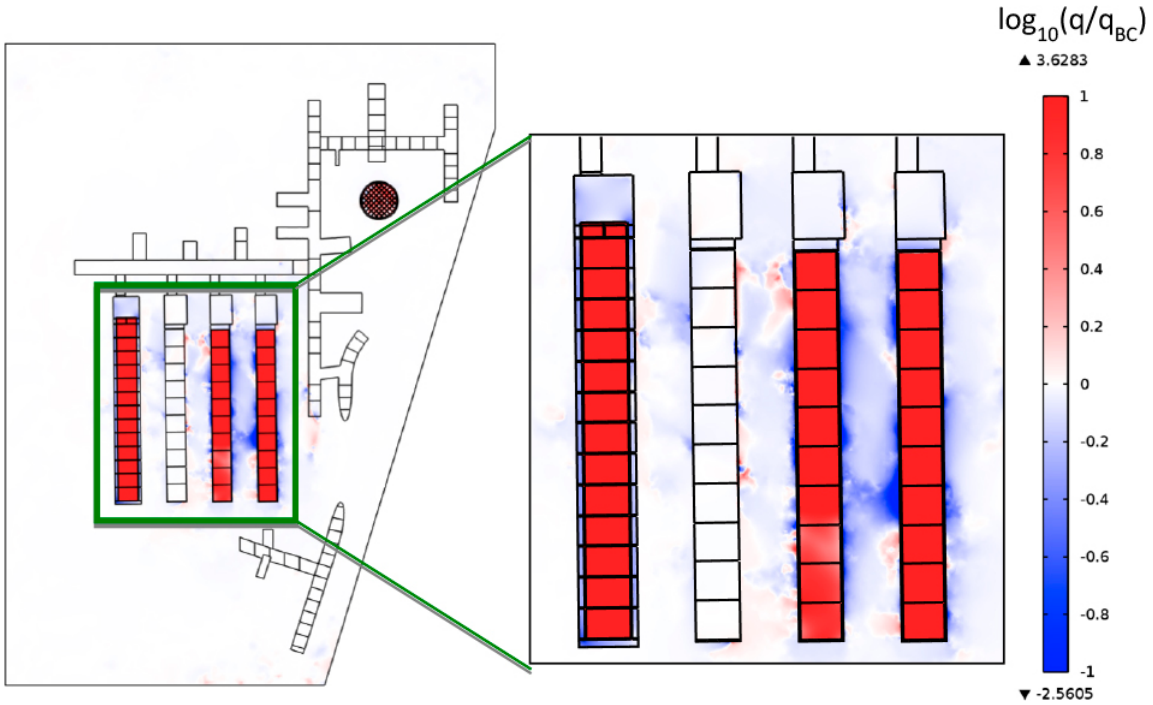

Figure B-12. *Ratio (in log_{10} scale) of the Darcy velocity magnitude between the case of completely degraded concrete and the Base case at the shoreline position 2 in a xy plane at z= –82.5. Positive values indicate a higher flow in the completely degraded concrete.*

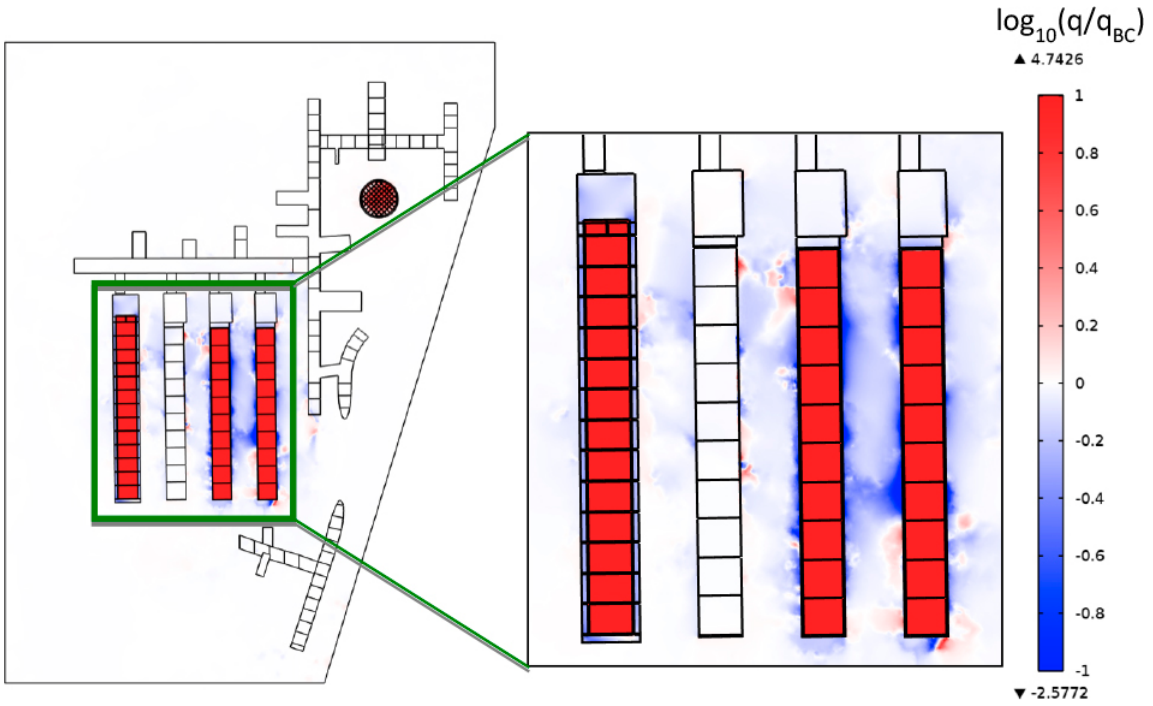

Figure B-13. *Ratio (in log_{10} scale) of the Darcy velocity magnitude between the case of completely degraded concrete and the Base case at the shoreline position 3 in a xy plane at z= –82.5. Positive values indicate a higher flow in the completely degraded concrete.*

Darcy velocity differences for the closure alternative

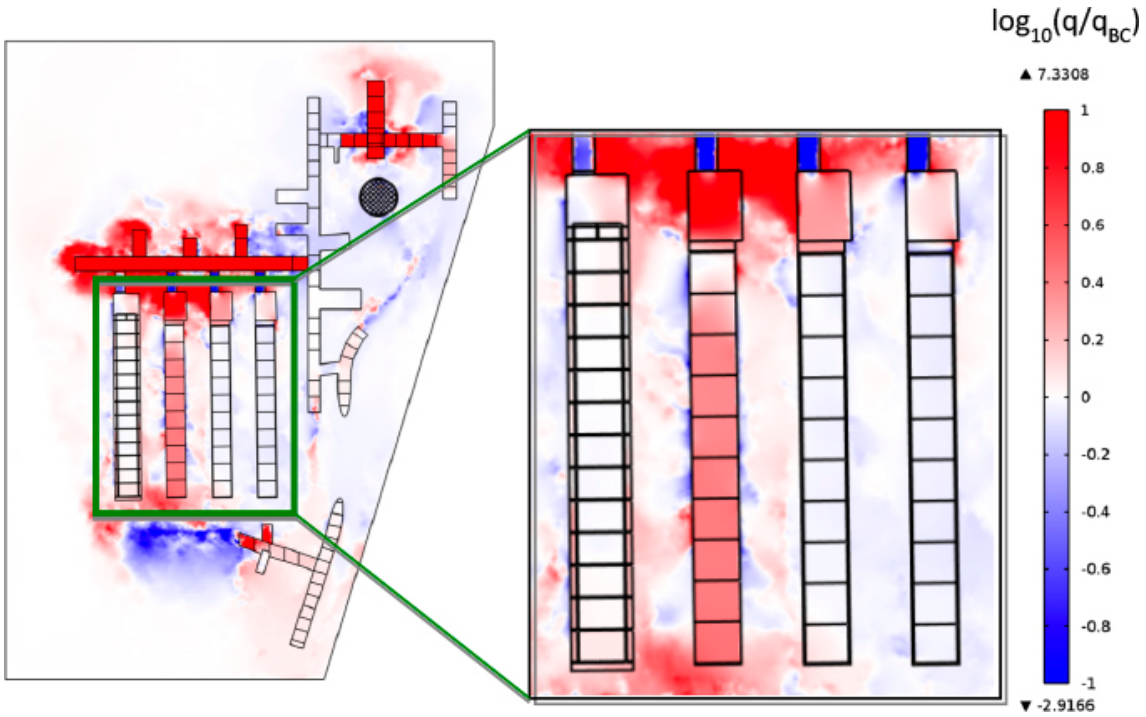

Figure B-14. *Ratio (in log_{10} scale) of the Darcy velocity magnitude between the alternative closure case and the Base case at the shoreline position 1 in a xy plane at z= –82.5. Positive values indicate a higher flow in the alternative closure case.*

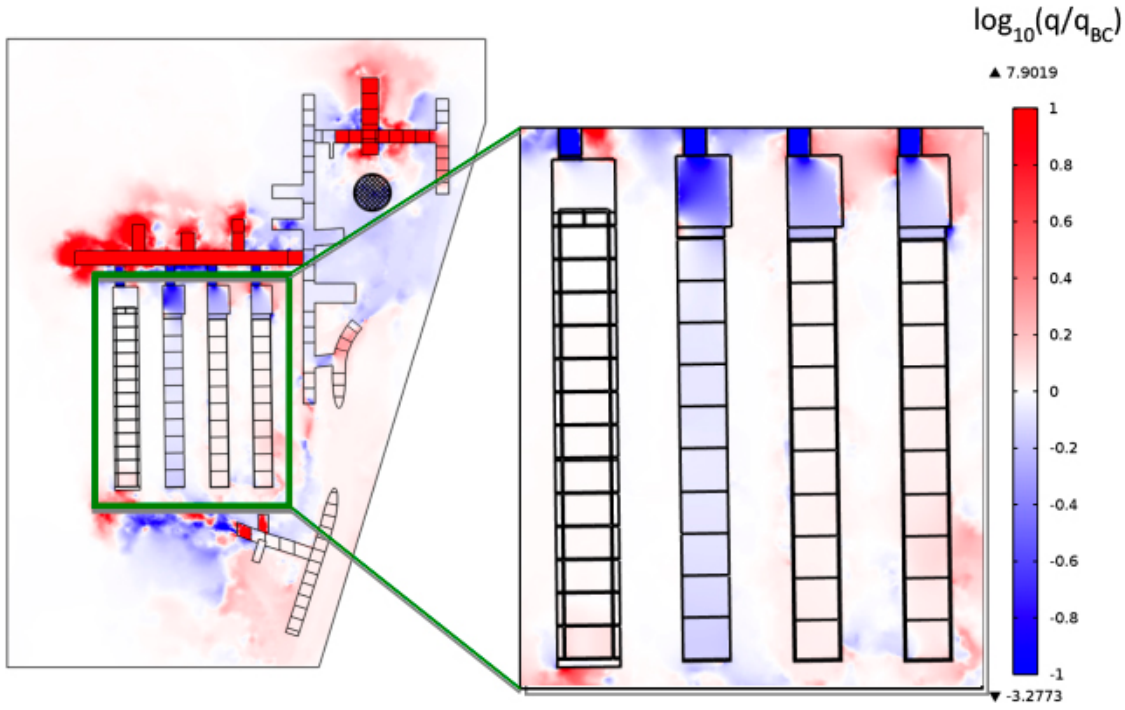

Figure B-15. *Ratio (in log_{10} scale) of the Darcy velocity magnitude between the alternative closure case and the Base case at the shoreline position 2 in a xy plane at z= –82.5. Positive values indicate a higher flow in the alternative closure case.*

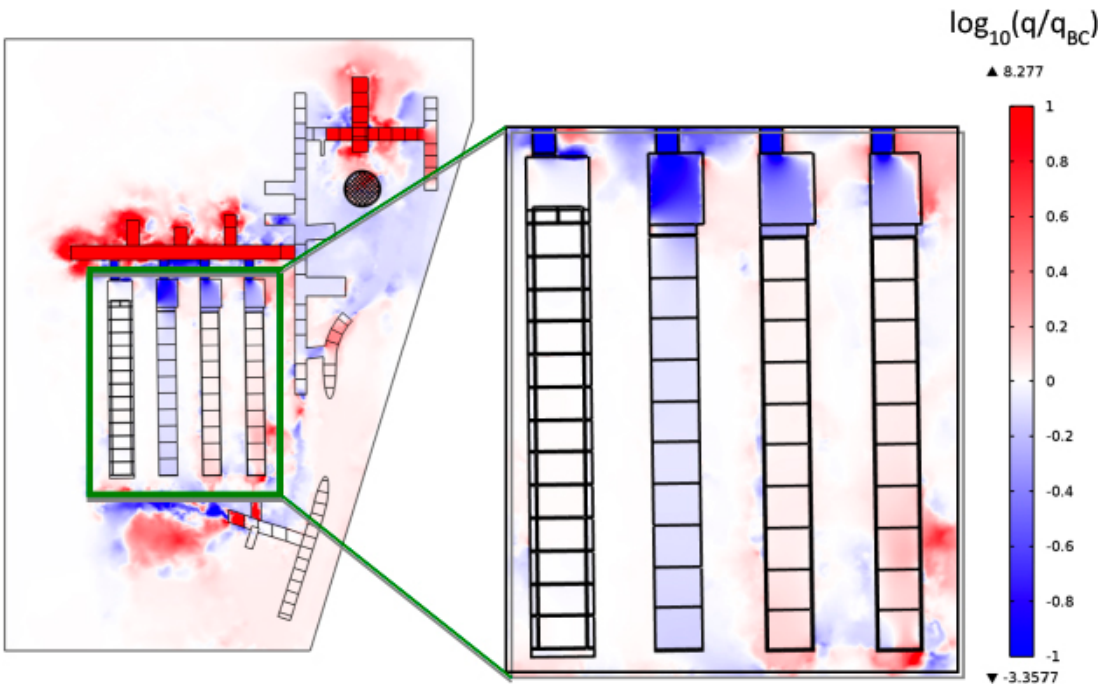

Figure B-16. *Ratio (in log_{10} scale) of the Darcy velocity magnitude between the alternative closure case and the Base case at the shoreline position 3 in a xy plane at z= –82.5. Positive values indicate a higher flow in the alternative closure case.*

Appendix C

Figures SFR 3

Streamlines plug degradation

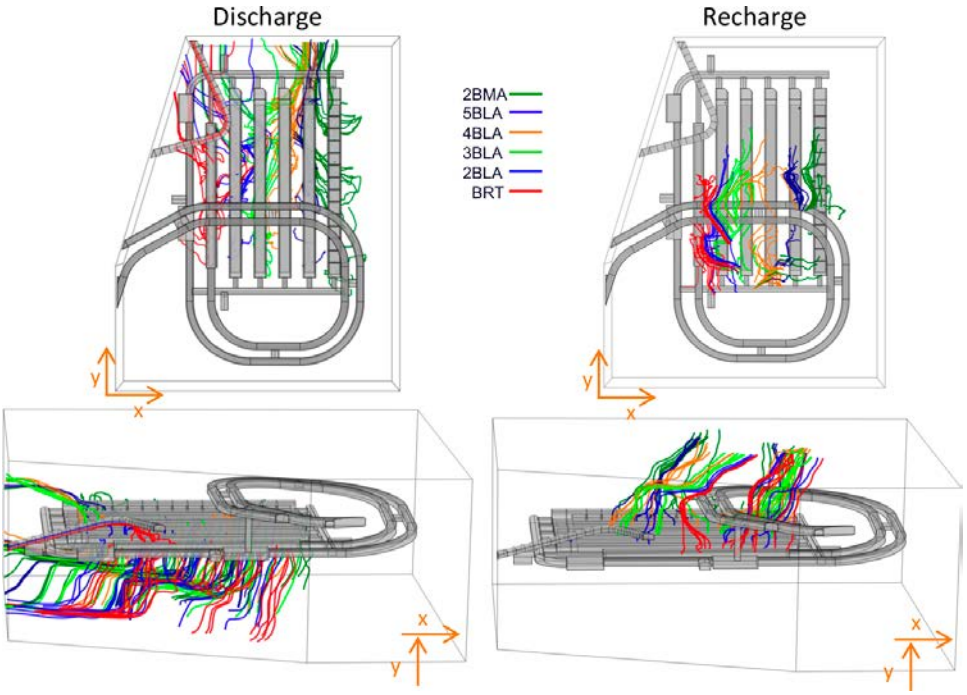

Figure C-1. *Groundwater streamlines leaving (left) and reaching (right) individual SFR 3 vaults (color tubes) for the moderately degraded plugs and the shoreline position 1.*

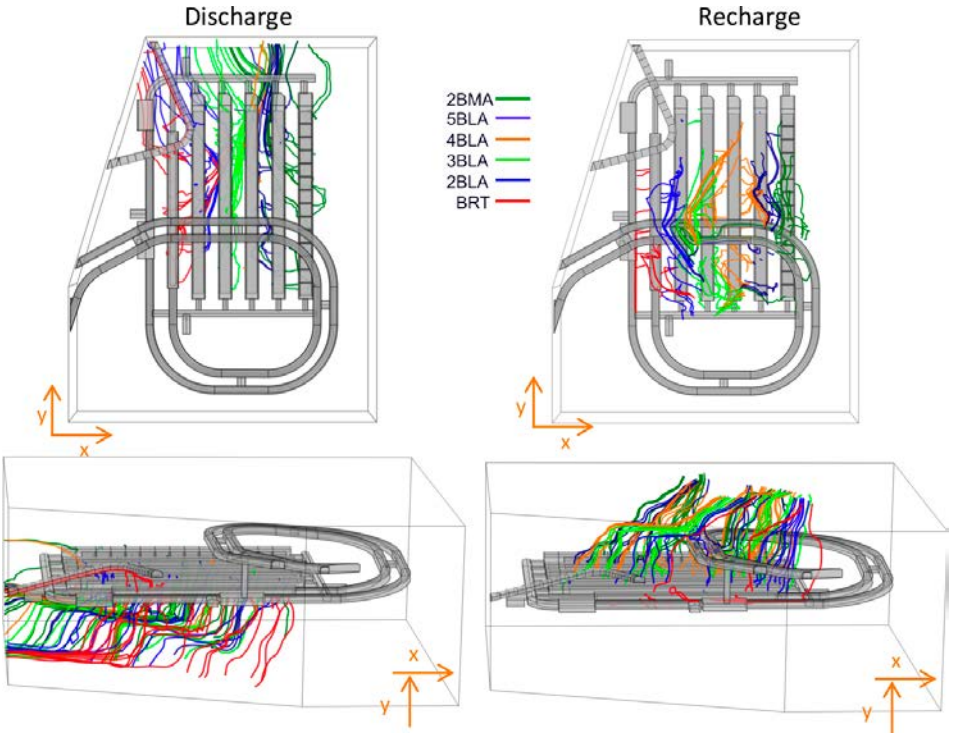

Figure C-2. *Groundwater streamlines leaving (left) and reaching (right) individual SFR 3 vaults (color tubes) for the severely degraded plugs and the shoreline position 2.*

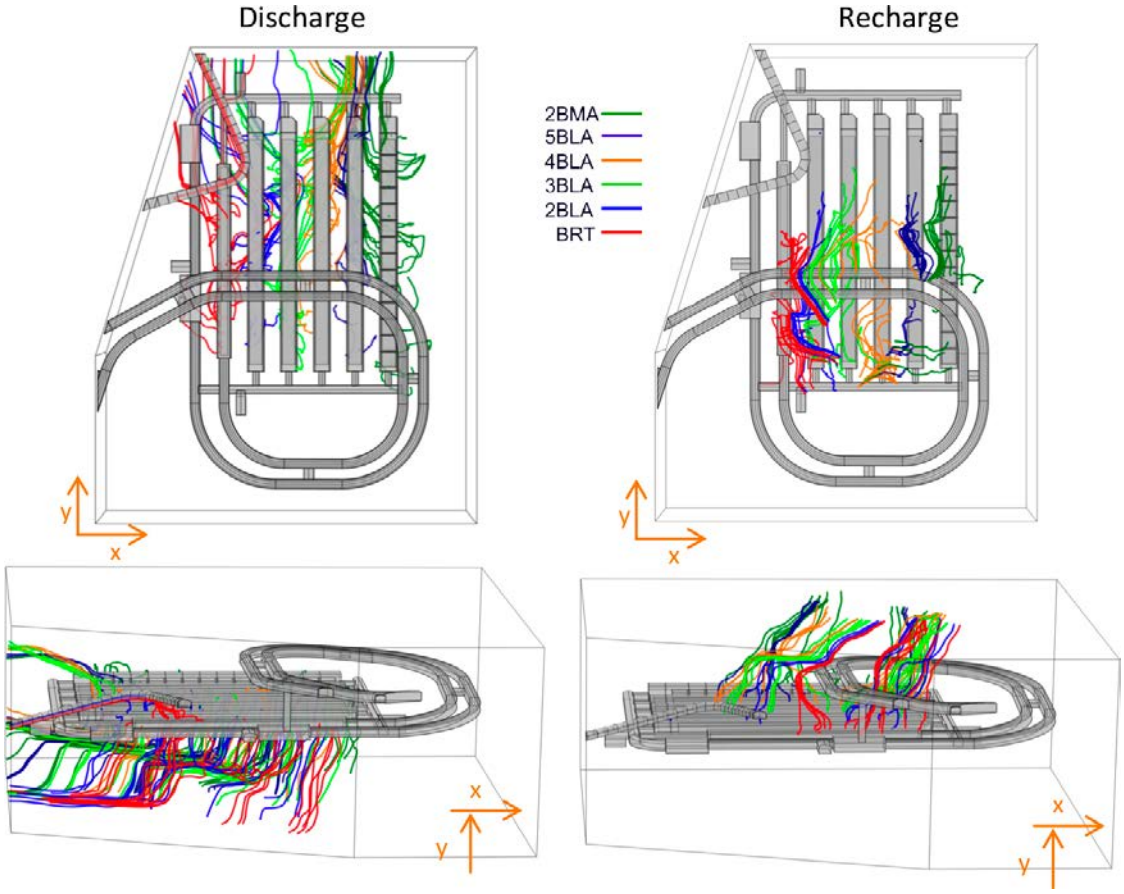

Figure C-3. *Groundwater streamlines leaving (left) and reaching (right) individual SFR 3 vaults (color tubes) for the completely degraded plugs and the shoreline position 3.*

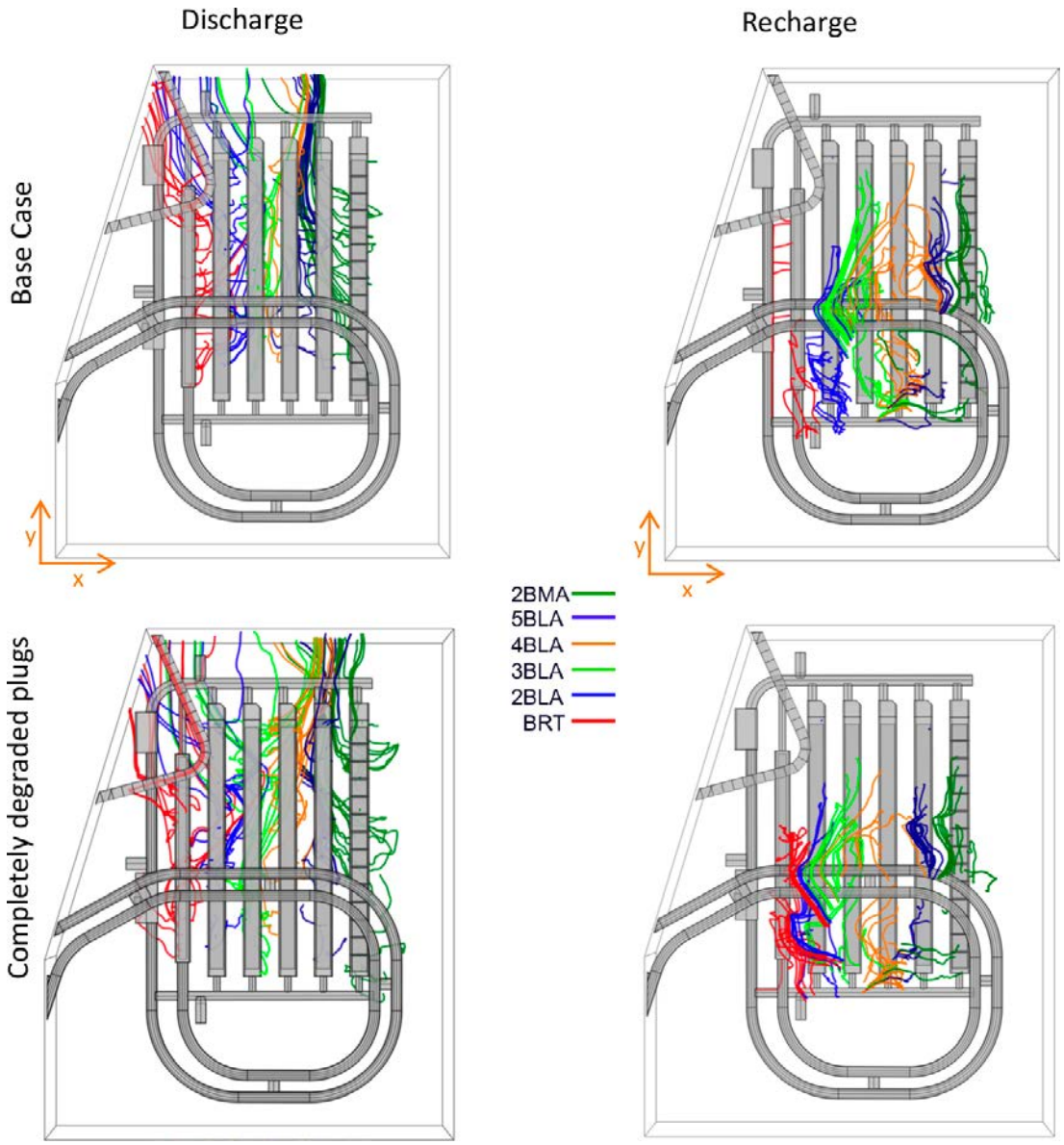

Figure C-4. *Comparison of the streamlines of the groundwater leaving (left) and reaching (right) the vaults for the Base case (top) and the case of completely degraded plugs (bottom) at shoreline position 3. Each color corresponds to the streamlines originated in a different vault.*

Streamlines no barriers

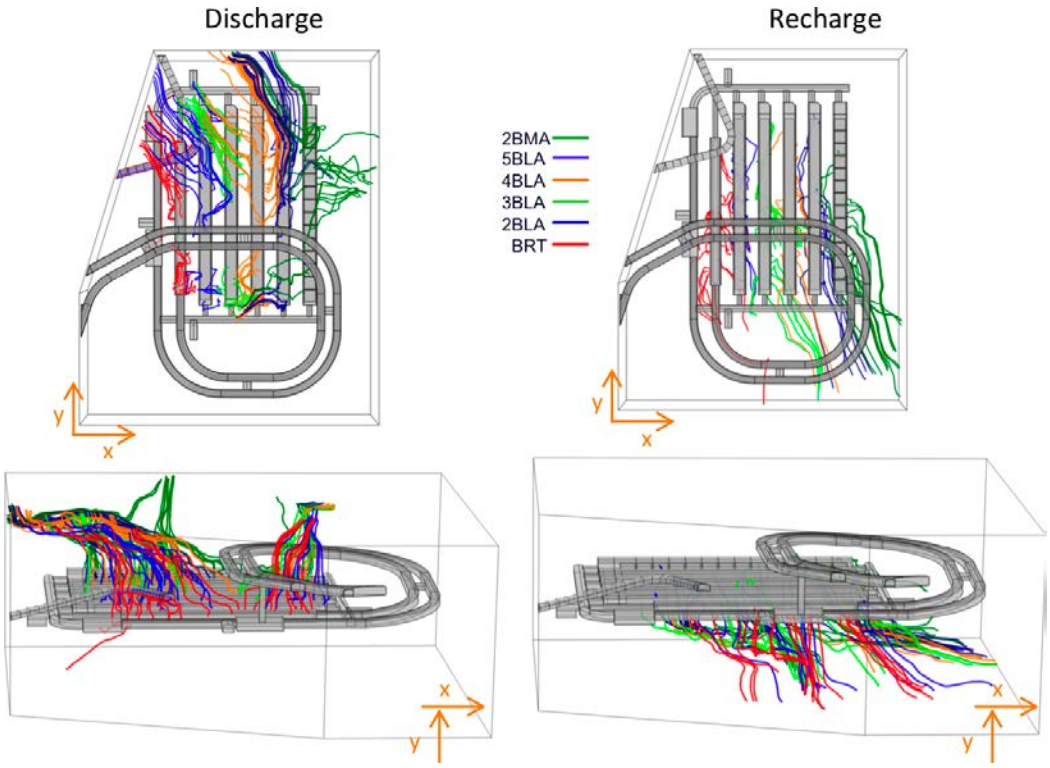

Figure C-5. *Groundwater streamlines leaving (left) and reaching (right) individual SFR 3 vaults (color tubes) for the no barriers case and the shoreline position 1.*

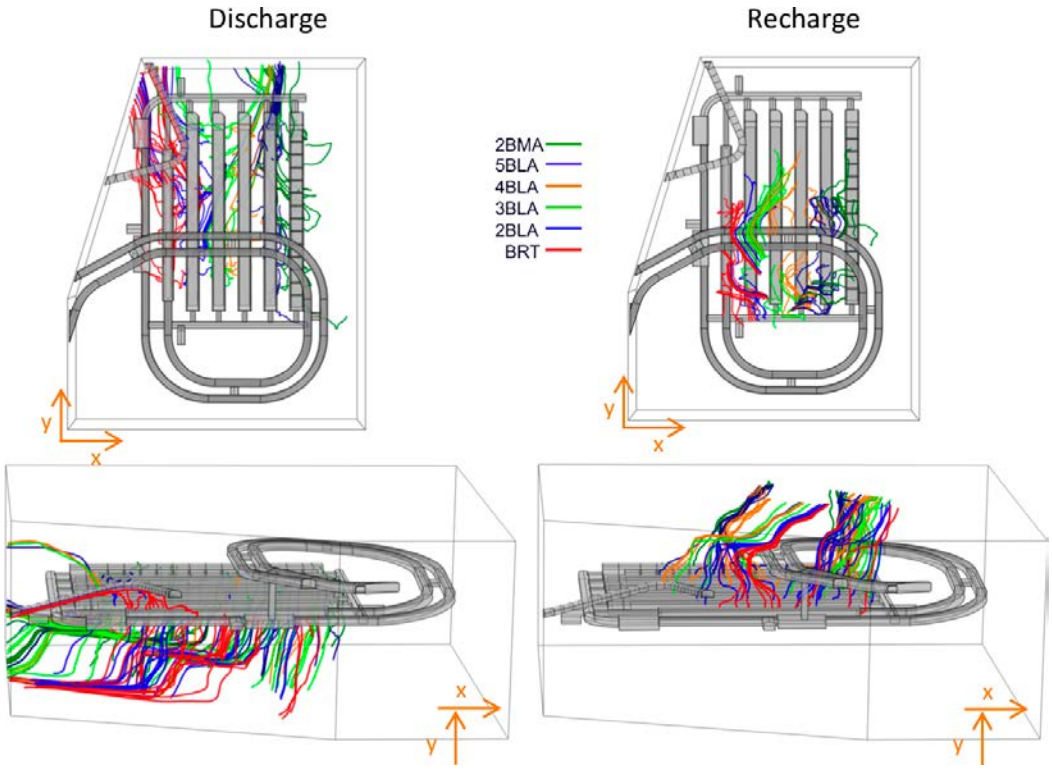

Figure C-6. *Groundwater streamlines leaving (left) and reaching (right) individual SFR 3 vaults (color tubes) for the no barriers case and the shoreline position 3.*